APEX-23

[redacted]

DOCUMENTATION REMOVED BY AUTHORITY
OF IDM APPENDIX 2105.
DATE NOV. 18 1968 BY

DECLASSIFIED

APEX-23
COPY 37
MARCH 1957

This document consists of 143 pages No. 37 of 278 copies, Series

AIRCRAFT NUCLEAR PROPULSION DEPARTMENT

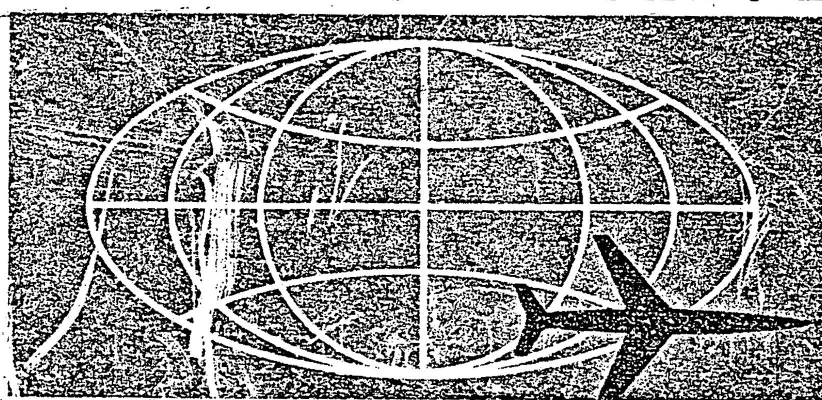

ENGINEERING PROGRESS REPORT
No. 23

Classification cancelled (or changed to CONFIDENTIAL
By authority of TID-1366 10-31-64
by 2-15-65

Classification cancelled, or changed to UNCLASSIFIED
By authority of TID
By

ATOMIC PRODUCTS DIVISION
GENERAL ELECTRIC

This Document/Material Has Been Reviewed
And determined to Contain
NO CLASSIFIED OR SENSITIVE INFORMATION
Classification Reviewer: K.C. Gerard
Signature Date 6-6-12

DECLASSIFIED

[redacted]

[redacted]

CONFIDENTIAL CANCELLED [redacted]

Cy 1

Reactors - Aircraft Nuclear Propulsion Systems
(M-3679, 19th Edition)

APEX-23

This Document consists of
143 Pages No. 37
of 274 Series

AIRCRAFT NUCLEAR PROPULSION DEPARTMENT

ENGINEERING PROGRESS REPORT No. 23

January 1, 1957 - March 31, 1957

classification cancelled (or changed to CONFIDENTIAL
by authority of TID-1306 10-31-64
By Connie Erickson 3-15-65

United States Air Force	Contract No. AF 33(038)-21102
United States Atomic Energy Commission	Contract No. AT (11-1)-171

GENERAL ELECTRIC
ATOMIC PRODUCTS DIVISION
Cincinnati 15, Ohio

Published by
Technical Publications Sub-Section

[redacted] RESTRICTED DATA [redacted]

CONFIDENTIAL CANCELLED

[redacted]

CANCELLED

DISTRIBUTION

STANDARD DISTRIBUTION

1	AF Plant Representative, Baltimore
2	AF Plant Representative, Burbank
3	AF Plant Representative, Clifton
4	AF Plant Representative, Long Beach
5	AF Plant Representative, Marietta
6 - 8	AF Plant Representative, Santa Monica
9 - 10	AF Plant Representative, Seattle
11	AF Plant Representative, Wichita
12	Air Research and Development Command (RDGN)
13	Air Technical Intelligence Center
14	Air University Library
15 - 17	ANP Project Office, Fort Worth
18	Argonne National Laboratory
19	Armed Forces Special Weapons Project, Sandia
20	Armed Forces Special Weapons Project, Washington
21	Assistant Secretary of the Air Force, R&D
22 - 27	Atomic Energy Commission, Washington
28	Bureau of Aeronautics
29	Bureau of Aeronautics General Representative
30	Chicago Operations Office
31	Chicago Patent Group
32	Chief of Naval Research
33	Convair-General Dynamics Corporation
34	Curtiss-Wright Corporation
35	Hartford Area Office
36	Headquarters, Air Force Special Weapons Center
37	Idaho Operations Office
38	Lockland Area Office
39	Los Alamos Scientific Laboratory
40	Marquardt Aircraft Company
41	National Advisory Committee for Aeronautics, Cleveland
42	National Advisory Committee for Aeronautics, Washington
43 - 45	Naval Air Development and Material Center
46	Naval Research Laboratory
47	North American Aviation, Inc. (Missile Development Division)
48	Nuclear Development Corporation of America
49	Office of the Chief of Naval Operations (OP-361)
50	Patent Branch, Washington
51 - 54	Pratt and Whitney Aircraft Division (Fox Project)

[redacted]

CANCELLED

[redacted]

CANCELLED

55 San Francisco Operations Office
56 Sandia Corporation
57 Sandia Corporation, Livermore
58 School of Aviation Medicine
59 - 66 Union Carbide Nuclear Company (ORNL)
67 USAF Headquarters
68 USAF Project RAND
69 University of California Radiation Laboratory, Livermore
70 - 87 Wright Air Development Center (WCOSI-3)
88 - 97 Technical Information Service Extension, Oak Ridge

SPECIAL DISTRIBUTION

98 Aircraft Reactors Branch
99 Lockland Area Office
100 Lockland Area Office Field Operation, Idaho Falls
101 Air Materiel Command Contracting Officer
102 Air Research and Development Command (RDZN)
103 Air Force Plant Representative
104 Oklahoma City Air Materiel Area (OCMW)
105 Battelle Memorial Institute
106 - 107 Phillips Petroleum Company (NRTS)
108 General Electric Company (APED)
109 - 111 Hanford Atomic Products Operation
112 - 114 Knolls Atomic Power Laboratory
115 Mr. S. W. Ahrends
116 Dr. F. A. Aschenbrenner
117 Mr. E. M. Ashley
118 Mr. E. L. Auyer
119 Mr. R. A. Averitt
120 Mr. E. A. Bage
121 Mr. J. H. Barnwell
122 Mr. M. L. Barron
123 Mr. D. T. Barry
124 Mr. W. G. Baxter
125 Mr. N. J. Bifano
126 Mr. J. C. Blake
127 Mr. B. Blumberg
128 Mr. E. R. Bogle
129 Mr. B. Bonini
130 Mr. B. W. Bruckman
131 Dr. V. P. Calkins
132 Mr. R. W. Carr
133 Mr. D. Cochran
134 Mr. J. Colley
135 Mr. C. G. Collins
136 Mr. E. S. Collins
137 Mr. E. M. Coleman
138 Dr. J. B. Conway
139 Dr. W. C. Cooley
140 Mr. M. P. Coover
141 Mr. A. Corbin
142 Mr. V. Cornett
143 Mr. C. H. Crandall
144 Mr. F. E. Crever
145 Mr. A. R. Crocker
146 Mr. W. F. Cronin
147 Mr. J. M. Crook
148 Mr. S. E. Cumpston
149 Mr. H. S. Daniel
150 Mr. J. W. Darley
151 Mr. E. B. Delson
152 Mr. T. A. DeRosier
153 Mr. F. C. Domina
154 Mr. P. W. Dwyer
155 Dr. H. S. Edwards
156 Dr. A. E. Focke
157 Mr. D. L. Francis
158 Dr. C. C. Gamertsfelder
159 Mr. R. L. Gartner
160 Mr. D. L. Gilliland
161 Mr. G. E. Gorker
162 Mr. M. S. Harned
163 Mr. C. F. Heddleson
164 Mr. E. L. Hill
165 Mr. A. S. Hintze
166 Mr. J. I. Hope
167 Mr. C. R. Horner
168 Mr. S. A. Huffman

[redacted]

CANCELLED

169 Mr. T. M. Hunter
170 Mr. W. B. Hunter
171 Mr. D. E. Irons
172 Col. N. P. Jackson
173 Mr. W. A. Jensen
174 Mr. D. P. Johnson
175 Mr. L. D. Jordan
176 Mr. G. P. Kerr
177 Mr. N. L. Kincaid
178 Mr. W. J. Koshuba
179 Mr. C. S. Lankton
180 Mr. M. E. Lapides
181 Mr. G. G. Leeth
182 Mr. J. I. Lerom
183 Mr. J. R. Lewis
184 Dr. M. C. Leverett
185 Mr. S. J. Levine
186 Mr. F. C. Linn
187 Mr. W. H. Long
188 Mr. P. E. Lowe
189 Mr. R. F. Lutz
190 Mr. L. E. MacFadden
191 Mr. R. R. McCready
192 Mr. F. K. McCune
193 Mr. J. A. McGurty
194 Mr. L. B. Mackey
195 Mr. R. C. Mann
196 Mr. H. F. Matthiesen
197 Mr. A. F. Mentink
198 Mr. K. F. Merten
199 Mr. F. W. Mezger
200 Mr. H. Miller
201 Mr. S. H. Minnich
202 Mr. T. R. Mitchell
203 Dr. J. W. Morfitt
204 Mr. J. Moteff
205 Mr. H. O. Nay
206 Mr. J. J. Neely
207 Mr. G. Neumann
208 Mr. G. W. Newton
209 Mr. J. R. Osgood
210 Mr. W. H. Perry
211 Mr. R. L. Potter
212 Mr. E. Price
213 Mr. S. Proffitt
214 Mr. J. D. Provost
215 Mr. C. L. Ridgeway
216 Mr. W. C. Schmill
217 Mr. R. E. Scott
218 Dr. D. S. Selengut
219 Mr. B. J. Sevold
220 Mr. W. D. Shadduck
221 Mr. D. R. Shoults
222 Mr. J. D. Simpson
223 Mr. G. L. Smith
224 Mr. H. P. Smith
225 Mr. E. J. Specht
226 Mr. N. P. Spofford
227 Mr. R. K. Steele
228 Mr. H. R. Stephan
229 Mr. C. L. Storrs
230 Mr. R. M. Strock
231 Mr. W. B. Thomson
232 Mr. G. Thornton
233 Mr. J. I. Trussell
234 Mr. L. M. Tupman
235 Mr. E. R. Ur
236 Mr. R. E. VanAusdal
237 Mr. P. R. Webb
238 Mr. G. L. Wheeler
239 Mr. J. F. White
240 Dr. E. P. Wigner
241 Mr. R. E. Wood
242 Mr. J. O. Woodbridge
243 Mr. L. F. Yost
244 - 248 Library (Idaho)
249 - 274 Library (Evendale)

REPORTS PREVIOUSLY ISSUED IN THE SERIES

DC 51-9-36	Period ending September 30, 1951
DC 51-12-25	Period ending December 31, 1951
DC52-3-54	Period ending March 31, 1952
APEX-4	Period ending June 30, 1952
APEX-5	Period ending September 30, 1952
APEX-6	Period ending December 31, 1952
APEX-7	Period ending March 31, 1953
APEX-8	Period ending June 30, 1953
APEX-9	Period ending September 30, 1953
APEX-10	Period ending December 31, 1953
APEX-11	Period ending March 31, 1954
APEX-12	Period ending June 30, 1954
APEX-13	Period ending September 30, 1954
APEX-14	Period ending December 31, 1954
APEX-15	Period ending March 31, 1955
APEX-16	Period ending June 30, 1955
APEX-17	Period ending September 30, 1955
APEX-18	Period ending December 31, 1955
APEX-19	Period ending March 31, 1956
APEX-20	Period ending June 30, 1956
APEX-21	Period ending September 30, 1956
APEX-22	Period ending December 31, 1956

[redacted]

CONTENTS

[redacted]

USE OF THIS REPORT

This report, prepared in accordance with provisions of contracts of the Aircraft Nuclear Propulsion Department of the General Electric Company with the United States Atomic Energy Commission and the United States Air Force, is intended to give a comprehensive, but not necessarily detailed, picture of the status of the technical aspects of the work of the Department at the close of the quarter. It is not intended that information contained herein should be used in aircraft design studies by other organizations. Information intended for such use is explicitly so designated and is transmitted separately in other reports and memoranda.

[redacted]

1. INTRODUCTION AND SUMMARY

The long-range research and development program of the General Electric Aircraft Nuclear Propulsion Department continued with the submission of a program report for Fiscal and Contract years 1957, 1958, and 1959 to the government at the end of the quarter.

The GE-ANPD program presented in this report continues to have as its basic objective the early development of a militarily useful nuclear propulsion system for aircraft. The program objective, however, is not primarily associated with the requirements of any formalized and specific military flight mission profile. The emphasis in the program is directed toward the development, design, fabrication, and preparation for all-nuclear flight of a promising nuclear power plant, currently designated the XMA-1. The major steps in the power plant development program leading to the XMA-1 are:

1. Heat Transfer Reactor Experiment No. 1 - the first operation of aircraft-type turbomachinery by the energy from a direct cycle, liquid moderated, metallic fuel element reactor. This test has been successfully concluded, but the data obtained are currently being analyzed.
2. Heat Transfer Reactor Experiment No. 2 - continued operation of an HTRE No. 1 type core modified to enable testing portions of reactors using various solid moderator and advanced fuel element materials. Initial criticality experiments on two nuclear mockup inserts were performed during the quarter.
3. Heat Transfer Reactor Experiment No. 3 - test of a flight-size solid moderated core in a shield of more advanced configuration.

PROJECTS

HTRE No. 1

With the termination of the third series of power tests at the end of the past quarter, the test phase of HTRE No. 1 was completed. Postoperational analyses were conducted during this quarter. The increase in fission-product release observed near the conclusion of the test series resulted from small blisters on the fuel sheet. Although the cause of the blisters has not yet been determined, they are believed to be the result of a metallurgical process variable which presumably can be corrected when discovered. After the fuel was unloaded and the core was cleaned of contaminants, inspection revealed that the core was in excellent condition. The improved spiral-wound insulation liners which were used in the third test series proved satisfactory, and no redesign seems necessary.

Comparison of the second series of power tests with the third indicates little aerothermodynamic difference, although the over-all performance of the third was much better on the basis of full-nuclear operation, number of hours of operation before fission-product release, and the temperature rise across the reactor.

Effects on power distribution of control rod insertion were determined experimentally and found to be in good agreement with values from critical experiments. Three independent methods of determining power profiles yielded fair agreement with critical experiment data.

[redacted]

Prior to removal of fuel elements from the A3 core, relative degree of fission fragment release from each cartridge was inferred from radiochemical analyses of the solids deposited on stainless steel and paper filters located in the air-sampling tubes at the exit of each fuel tube. No consistent correlation was found between control rod positions and the predictions. In general, good agreement existed between the radiochemical analyses and the cartridge examination.

HTRE No. 2

The HTRE No. 2 A4 reactor assembly was completed early in the quarter and was installed in the IET facility at ITS. Initial criticality of the A4 was accomplished using nuclear mockups of both Inserts No. 1 and No. 2. Power mapping and reactivity experiments were begun and were about 40 percent complete by the end of the quarter. Data thus far indicate that calculations had predicted the excess reactivity of Insert No. 1 to within the experimental error and had under-predicted the excess reactivity for Insert No. 2 by approximately 1 percent. With the exception of gamma flux, experimental values of power distribution and reactivity were well within the limits of the calculated values. Thus power operation with Insert No. 1 should proceed without complications.

Fifty parent-core fuel cartridges were completed during the quarter, bringing the total number of cartridges available for the A4 and A5 cores to 66.

Instrumentation for the ceramic insert will be quite different from that for Insert No. 1 because of the nature of the ceramic material and because of the higher operating temperature. Assembly of the instrumentation is expected to begin early next quarter.

The necessary changes in the control and instrumentation wiring on the CTF and in the IET facility have been made to accommodate HTRE No. 2.

HTRE No. 3

All HTRE No. 3 final design layouts have been completed except those for the moderator, reflector, aft plug, and auxiliary shields. Orders are being placed for the fabrication of components.

Preliminary measurements, including power mapping, rod worth, and core gamma heating rate were made on the HTRE No. 3 nuclear mockup. The results of reactivity measurements on the nuclear mockup indicated a need for additional fuel in the operational core in order to provide sufficient excess reactivity for 100 hours of operation under X39-5 conditions. Accordingly, a 19th stage was added to each fuel cartridge of the design reactor to add a total of 20 pounds of U^{235} to the inventory.

Recent progress in hydriding techniques has made it possible to increase the N_H specifications for the outer 42 moderator cells to 4.10 ± 0.05. Efforts continued to be directed toward obtaining a metallurgical bond between the outside cladding and the hydrided zirconium. At present the cladding process involves heating the moderator segment in a die block to around $1600^{\circ}F$ and swaging internally to effect a bond.

A fuel element configuration has been proposed for HTRE No. 3 on the basis of performance in burner rig and MTR tests. This fuel element differs from the HTRE No. 1 element in that the front support consists entirely of comb ribs and there is no rear hardware.

The X39-5 development engines are being assembled, and the major components for the turbine-scroll test loop and the single-engine test loop have been shipped to the Idaho Test Station. Results of a test on the prototype of the automatic engine control system indicated that the planned temperature control system was unstable. The system was redesigned to a speed control system with temperature trim.

During the quarter tests were conducted with the 1/4-scale flow model using inlet scroll and transition ducting. The results indicated that the presence of the scroll had no measurable effect on core tube-to-tube weight flow distribution with either 1- or 2-engine flow conditions.

XMA-1 Power Plant

The fuel tube selected for the XMA-1 power plant is a conventional constant-diameter tube. A tapered tube design had been proposed, but investigation indicated problems in power distribution that more than offset the aerodynamic advantages.

A full-scale mockup has been completed of the turbomachinery components. Design of all components for the first series of development X211 engines has been finalized and detailed for manufacture and procurement.

Progress was made in the development of XMA-1 fuel ribbon by the successful use of wrought Fe-Cr-Al frames for fabrication of niobium fuel billets. Tests have shown that the wrought alloy offers greater resistance to nitriding at high temperatures than does the standard Fe-Cr frame.

Fuel ribbon has been subjected to 2200°F under a stress of 1000 psi for 500 hours without failure, and more stringent tests will be conducted next quarter.

Major progress was made in edge sealing of fuel ribbon by brazing. One ferrous-base alloy used as an edge-sealing sample for oxidation testing was tested successfully for 100 hours at 2300°F. Until testing of the ferrous-base alloys, the test edge-seal life obtained was 4 hours at 2300°F. Specimens sealed by cover caps seam-welded over cut edges were also tested during the quarter and withstood exposure at 2300°F for 100 hours; indicating that this method has merit.

Much of the work on actuator and thermocouple development for HTRE No. 3 is expected to be directly applicable to the needs of the first development model of the XMA-1 power plant. Progress has been made in determining the feasibility of pneumatic actuation for dynamic rods, in identifying the problems associated with high-temperature hydraulic actuation, and in the development program for nuclear sensors. Provisions for safety action have been modified. Neutron flux, fuel element temperature, reactor unit temperature, and engine speed have been chosen as parameters to initiate action to prevent power increase and to decrease power demand.

Design of the 1/4-scale model of the primary-flow circuit of the XMA-1 power plant was completed, and construction is under way. Testing should begin next quarter.

Nuclear analyses of shielding for the XMA-1 power plant have been extended to account for the nonhomogeneity of the power plant core. Previous analyses were based on the assumption of a homogeneous core, disregarding the air passages that run longitudinally through the core. Studies to determine the extent of error entailed in such calculations indicate that calculated neutron and gamma dose rates increase by factors of 10 and 5, respectively, at the front of the reactor, and by factors of 8 and 4 at the rear.

Studies were conducted to determine the shielding effects of engine components in the power plant. It is estimated that these components cause reductions in the calculated radiation beam by factors as high as 40 and 250 for neutrons and gamma rays, respectively.

Materials for the mockups of the three porous-plug-type XMA-1 power plant shields were specified during the quarter. The material selected is an unborated, lead-loaded plastic that will be uniform in density within approximately 1 percent.

Work is nearly complete on a new wavy-plate shield configuration from which a nuclear-shield test model will be constructed for future testing.

not produce significant N_H increases. Sections of extruded moderator components have been hydrided to N_H values as high as 5.6 without loss of integrity.

Cladding techniques have been developed using gas to apply the pressure required to bond molybdenum to zirconium or hydrided zirconium and to 446 stainless steel.

The ductile, metallic nature of hydrided yttrium at elevated temperatures was established with the successful extrusion at $1650^{\circ}F$ of two hydrided yttrium moderator billets, clad with 446 stainless steel and niobium.

A test program to obtain thermal and radiation stability data on promising fluids in support of high-temperature hydraulic system development was completed during the quarter. Results of tests show all of the materials tested during the quarter to be potentially useful to dosages of about 3×10^7 rads if the high-temperature exposure is restricted to short periods such as might occur in cruise-sprint-cruise missions. For extended periods of high-temperature exposure the best of the materials tested are MLO-8200 and Esstic-45.

Results of tests on electric motors in the Systems Panel Test No. 2 at Convair demonstrated excellent radiation stability for Alkanex insulated electric motors at temperatures in the range from 250° to $400^{\circ}F$.

An investigation of techniques for the measurement of nuclear heating was begun, and studies were conducted to determine what instruments are most effective for dose measurements. Comparison of photographic film, silver-phosphate glass needles, and chemical dosimeters indicates that chemical dosimeters offer distinct advantages for this application. Microcalorimetric techniques for direct measurement of heating effects are also being investigated.

The experimental phase of the 2π shield tests at the Oak Ridge National Laboratory Tower Shielding Facility was concluded this quarter. Preliminary analysis of the data indicates that one of the objectives, independent measurements of the primary and secondary gamma radiations reaching the crew position, has been achieved. When no 2π covers are used, the effects of the ground on all dose rate measurements is still apparent at the maximum altitude available (195 feet). The gross effect of the 2π covers is a flattening of the altitude traverses. The effect is more pronounced when both crew shield and reactor covers are used. The analysis of the test results is continuing.

Feasibility studies of transistorized reactor control equipment have proved encouraging enough to warrant placing contracts for transistorized circuitry to be used for test and evaluation.

Several assemblies were subjected to approximately 500 hours of reactor flux generated at reactor powers of 100 kilowatts and above in the Convair Systems Panel Test No. 2. The most severely affected unit was a television camera. Postexposure examination showed that the television lens was almost opaque.

A developmental fission chamber was successfully operated at elevated temperatures. Fabrication methods for high-temperature chambers are being investigated in an effort to obtain hermetically sealed assemblies that will operate at $700^{\circ}C$ without deleterious effects on the lead and the chamber-leakage resistances. Two conceptual designs for the development of high-temperature ionization chambers were submitted to component manufacturers for evaluation of fabrication problems.

Design of experimental equipment for the ETR irradiation facility is nearly complete. Orders have been placed for much of the equipment, and specifications have been completed for most of the remaining components. It is expected that the ETR will be completed late in the next quarter and that reactor tests will extend two months from that time.

Design of nearly all of the basic solid moderator reactor structure was completed for the high-temperature critical experiment facility.

An outline of test program objectives for the Ground Test Prototype facility was developed.

Drawings for the 2000°F ducting loop were issued during the quarter, and fabrication is under way. Two phases of testing are proposed: a checkout of the loop, followed by insertion of the test component and performance of endurance-type tests.

2. PROJECTS

2.1 HTRE No.1

2.11 GENERAL STATUS

The conclusion of IET No. 6 at the end of the previous quarter marked the successful completion of the test phase of HTRE No. 1 with full realization of test objectives. Overall operation of HTRE No. 1 was as originally expected, and the system as a whole is considered to be basically sound.

Operation was terminated because of positive identification of fission products in the exhaust air. Figure 1 indicates the particulate activity as a function of time for the final stages of operation. During this transfer to full-nuclear power, the activity at 75 to 80 percent full-nuclear power was observed to be 17 curies per hour. As the reactor power was increased to 90 percent full-nuclear power, the activity as determined by the stack monitor increased to 25 curies per hour and then rapidly decreased to about 0.4 curies per hour after transfer to full-nuclear power.

In order to verify the high rate of activity observed prior to transfer, smoke was released into the stack for a short period of time. The activity under these conditions and a

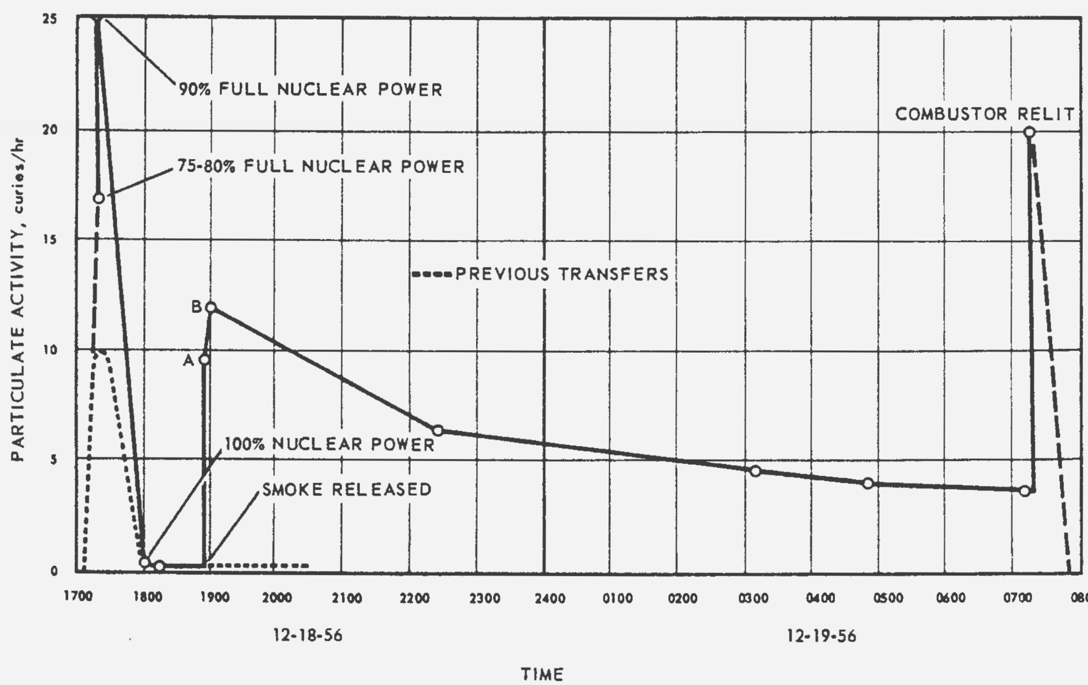

Fig. 1 – Particulate activity vs. a function of time during the final stages of HTRE No. 1 operation.

core discharge temperature of 1280°F was 9.5 curies per hour. When the core discharge temperature was increased to 1380°F, the activity increased to 12.5 curies per hour. The activity decreased along the line shown in Figure 1 for 12 hours, reaching a low of about 3.5 curies per hour. At this time the engine was relit on chemical fuel, and the activity jumped to 20 curies per hour. The dotted curve at the left on Figure 1 indicates a typical curve of observed activity during previous transfers.

Although the 3.5 curies per hour appeared to be only slightly above background, the decision was made to discontinue operation so that the fuel elements could be removed from the reactor for inspection to determine the mechanism of fission fragment release in its initial stages. Table 1 shows the status of IET No. 6 at the time of shutdown. The difference between peak and average recorded fuel element temperature was 150°F; and metallurgical evidence, although not complete, has indicated that this value must be substantially correct.

TABLE 1

IET NO. 6 PERFORMANCE DATA

Time above 200 kilowatts	257.6 hr
Time on full nuclear power [a]	105.82 hr
Time on full nuclear power [b]	38.95 hr
No. transfers to full nuclear power	40
Total operation	3092.20 mw-hr
Maximum power	20.2 mw
Maximum fuel element temperature [a]	1750°F
Maximum fuel element temperature [b]	1860°F

[a] Reactor exit air temperature = 1280°F
[b] Reactor exit air temperature = 1380°F

The A3 core was removed from the cocoon at the beginning of the quarter for inspection and unloading. Large, thick deposits of boric acid were on the lower section of the core shell as a result of shield water leaking into the cocoon. Coolant was circulated throughout the core during fuel unloading operations. The core was successfully unloaded without apparent damage to fuel cartridges; however, several web assemblies were damaged because the upper limit switch of the tube loading machine failed to function. As the core was unloaded, components were examined, photographed, and prepared for further detailed examination.

At the end of fuel unloading operations, the core was flushed and cleaned of boric acid and other contaminants. The core was then closely inspected and monitored, and was found to be in excellent condition.

The A3 core is being prepared for possible future operations by replacing the damaged web assemblies, securing the bottom-face insulation sheet, and revising the circuits for compatability with HTRE No. 2.

Examination of the fuel elements revealed that small blisters had formed in the fuel sheet. The examination has not progressed to the point that the cause of the blisters has been determined, but it is known that they were not caused by over-temperature. Although the basic cause of the blisters is still unknown and much work remains to be done, it is felt that the difficulty is a metallurgical process variable that can be corrected when discovered.

The amount of bent, dented, and broken rails, as well as the wrinkling of liners, is so markedly less than on any previous run that no mechanical redesign of elements and liners seems necessary at the present time. The improved spiral-wound insulation sleeves were used in IET No. 6. These observations together with the satisfactory performance of the reactor during the test indicate that mechanical difficulties with insulation sleeves caused the fuel element failures in previous tests.

Thermodynamic analysis of IET No. 6 data is continuing. Temperature perturbations, including gross radial and fine radial temperature patterns; effects of control rod position; local power distributions; and reactor aftercooling were investigated.

The net result of the testing was that, although some minor difficulties remain to be ironed out, the HTRE No. 1 system operated successfully as predicted in almost every respect. No basic unforeseen difficulties were encountered.

2.12 POSTOPERATIONAL ANALYSIS

Aerothermodynamic Analysis of IET No. 6 Data

An increase in the required fuel-plate and core-discharge-air temperature for a given engine speed was noted after about 100 hours of operation. The locations of the airflow stations designated as 3.54, 3.65, etc., in the following discussion are shown on Figure 2. A plot of core ($T_{3.53}$) and hot-torus exit ($T_{3.65}$) air temperature and turbine inlet temperature (T_4) versus engine speed for operation with engine 5011 is presented in Figure 3. It is seen from the graph that a temperature rise of between 30° and 40°F is recorded at stations 3.53 and 3.65, although there is no increase in the turbine-inlet temperature requirements. From other system measurements the following temperature correlations were observed between data taken before and data taken after 100 hours of operation with engine 5011.

1. No change in temperature parameters was observed between stations 3.15 and 3.49.
2. A 30° to 40°F temperature increase was recorded at stations 3.53, 3.54, 3.62, and 3.65 and in the average 11th- and 18th-stage fuel plates.
3. Little if any temperature increase was recorded at station 3.8 while the temperature requirements at station 4.0 remained constant.

The flow resistance factor across the core was calculated to determine whether an increase was apparent for the later runs; however, no change was evident.

While only thermodynamic data using engine 5011 are presented in Figure 3, data obtained for a run using engine 5012 show a discharge air temperature increase comparable to that obtained using engine 5011. Later the fuel cartridge tail assembly missing after IET No. 4 was found wedged in the inlet of the combustor unit in the loop with engine 5012. The obstruction prevented full movement of the bypass valve and also reduced the air passage area.

The magnitude of the increase in core-discharge-air temperature with engine 5012 was the same as that noted with engine 5011; however, with engine 5012 the air temperatures at stations 3.8 and 4.0 also increased slightly. Since the turbine inlet temperature increased, the temperature rise through the core results not only from whatever affected reactor performance using engine 5011, but also from the fact that the reduced flow area in the unit combustor increased the system pressure drop and required a higher internal energy input.

The test results are inconclusive as to exactly what caused the change in reactor performance since it is not known whether operation using both engines was affected in the same manner. A possible explanation, however, is that the bypass valves were not fully closed.

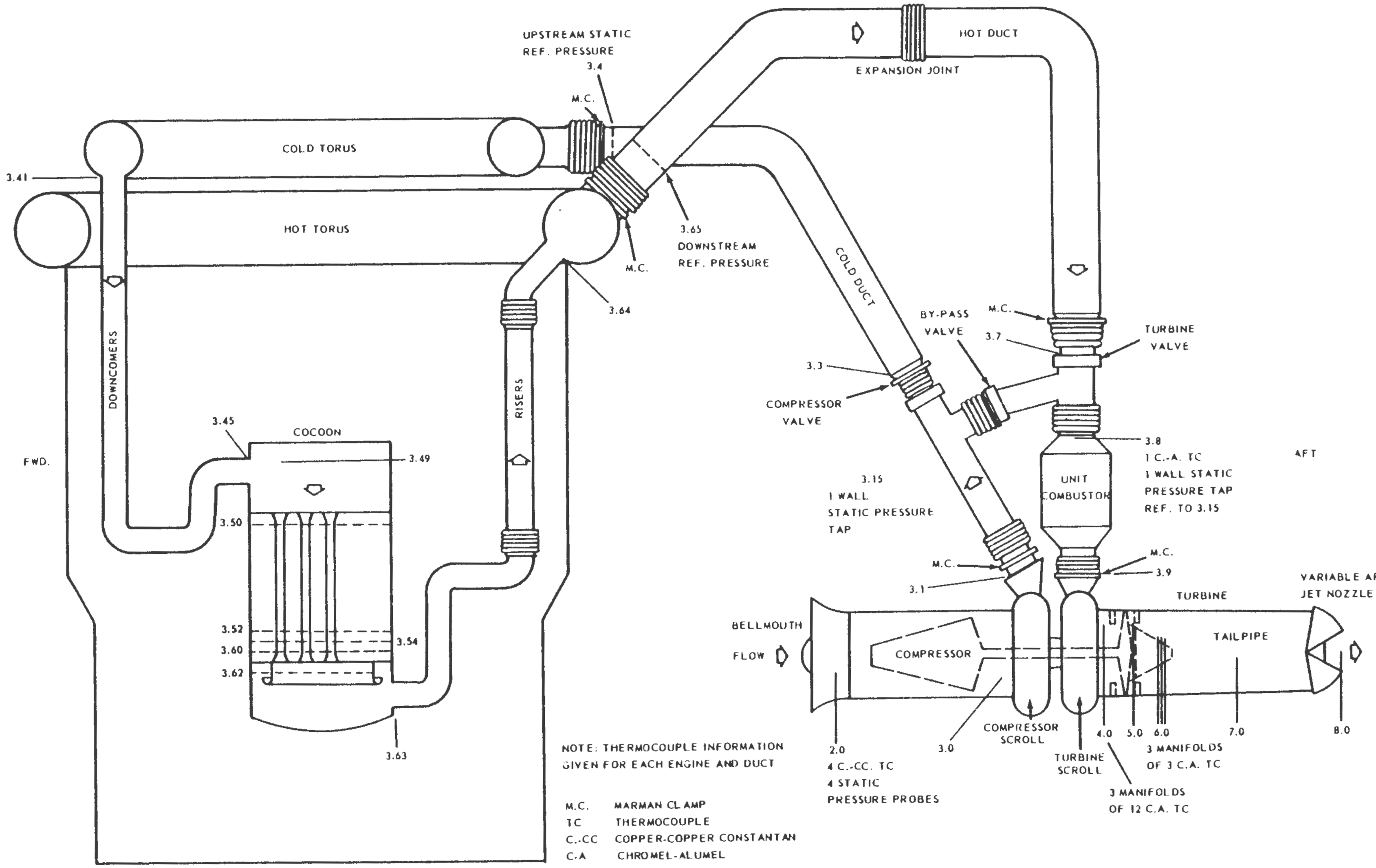

Fig. 2 – Station designations, HTRE No. 1

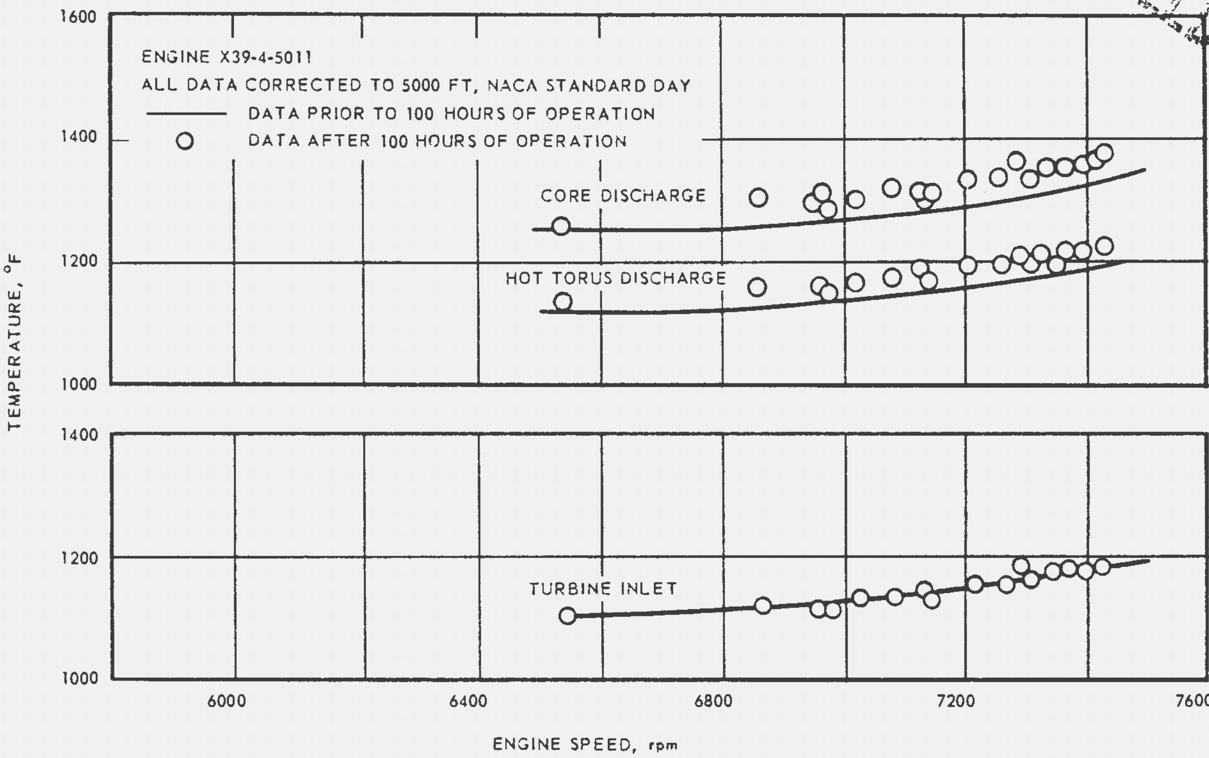

Fig. 3 – Reactor system temperature versus engine speed at full-nuclear power

Comparison of the data obtained from the A2 and A3 cores (HTRE No. 1) during IET No. 3, No. 4, and No. 6 have indicated that the measured values of core-outlet-air temperature ($T_{3.53}$, $T_{3.54}$) are in doubt by a significant amount. The location and number of thermocouples measuring core discharge temperature does not guarantee measurement of a true mixed-air temperature. Differences among the three operations which may influence the air temperature measurements include:

1. Improvement in the annular flow configuration between the outside of the fuel cartridge and the insulation liner.
2. Loss of thermocouples during the IET No. 3 and No. 4 operations.
3. Change in the instrumentation between tests IET No. 4 and No. 6. This change was primarily the addition of radiation shields to the 3.54 thermocouples and the addition of 3.53 thermocouples (platinum - platinum/rhodium thermocouples, immediately downstream of stage 18).

These temperatures, therefore, may not be valid for reactor performance comparisons among the three tests (see Figure 4). The fact that the temperature drop between the core discharge and torus exit varies widely among the three operations indicates that the measured core-discharge temperature may not be correct (assuming no change in ducting heat losses).

Attempts to define a temperature such that comparisons could be made have met with a reasonable degree of success. The temperature that permits a reasonable comparison of performance is defined as $T_{3.60}$, which is determined empirically from $T_{3.65}$ (outlet of the hot torus) based upon heat loss in the ducting back to the downstream face of the reactor. The relationship determined is $T_{3.60} = 1.16(T_{3.65}) - 60$ (all corrected to 5000 feet, NACA Standard Day).

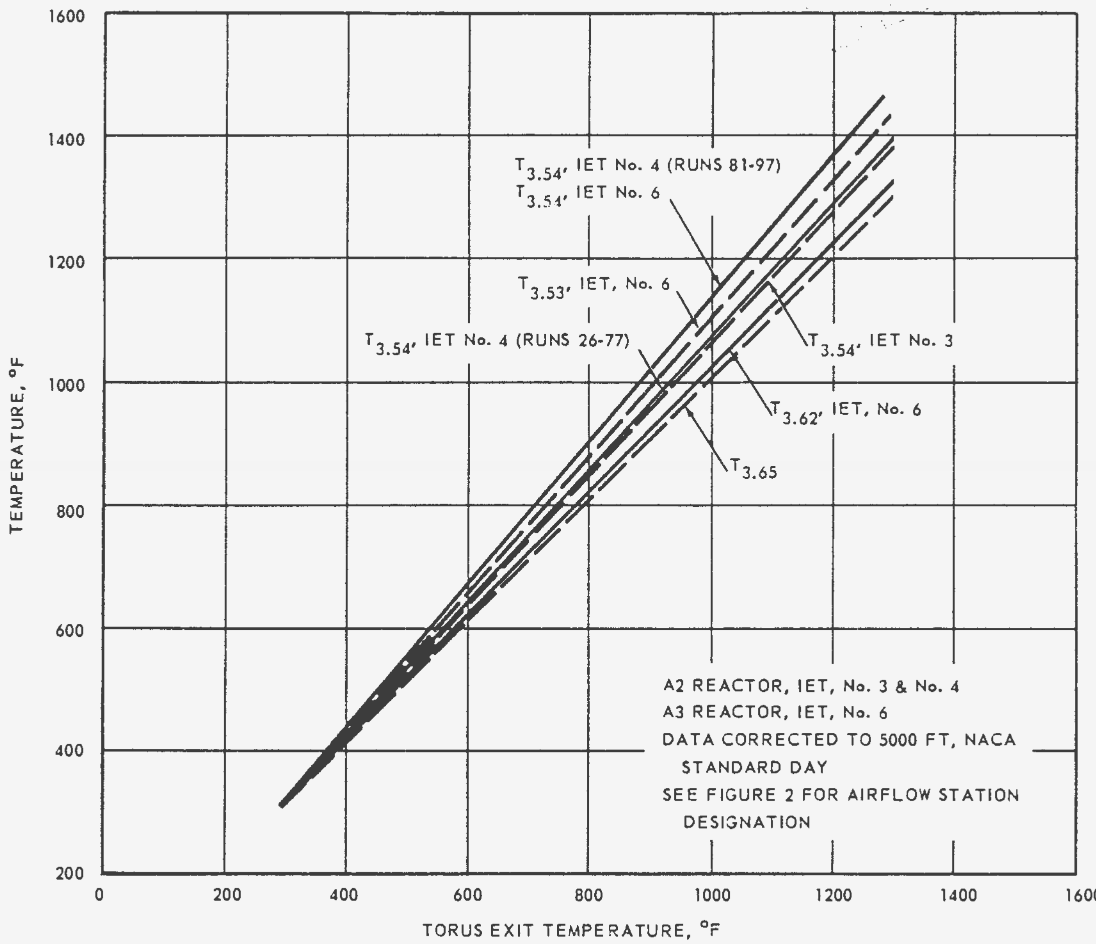

Fig. 4 – Core discharge air temperature versus torus exit air temperature

The comparison of the performance of IET No. 3, No. 4, and No. 6 is presented in Figure 5. The parameter ($T_{3.60}$-$T_{3.50}$) is the temperature rise across the reactor and is a measure of power delivered to the engine at a given speed.

The parameter T_{P18}-$T_{3.60}$ is the difference between the average of 18th-stage plate thermocouple readings and the core-discharge-air temperature. It is a possible index to reactor internal aerothermodynamic performance. Figure 5 indicates that the aerothermodynamic performance difference (assuming that $T_{3.60}$ is a valid temperature) between IET No. 4 and No. 6 was small, on the basis of plate-to-air temperature difference, even though the over-all performance of IET No. 6 operation was much better, on the basis of full-nuclear operation, number of hours of operation before fission product release, and the temperature rise across the reactor. The increased number of hours before fuel element failure is, of course, indicative of lower-peak plate temperatures in the reactor.

This points out the problem in the presentation of data which isolates the internal performance of the reactor from that of the rest of the system. One might conclude that the reactor thermodynamic performance was much improved during IET No. 6, yet the average performance was, in fact, about the same. The main system thermodynamic improvement was in the engine performance, mainly due to the addition of the bypass unit combustor, new compressor scroll, and the shortened tailpipe. Evaluation of the metallurgical performance of the reactor is also clouded by the use of corrected temperature since the correction largely removes the plate-temperature differences due to ambient inlet temperatures.

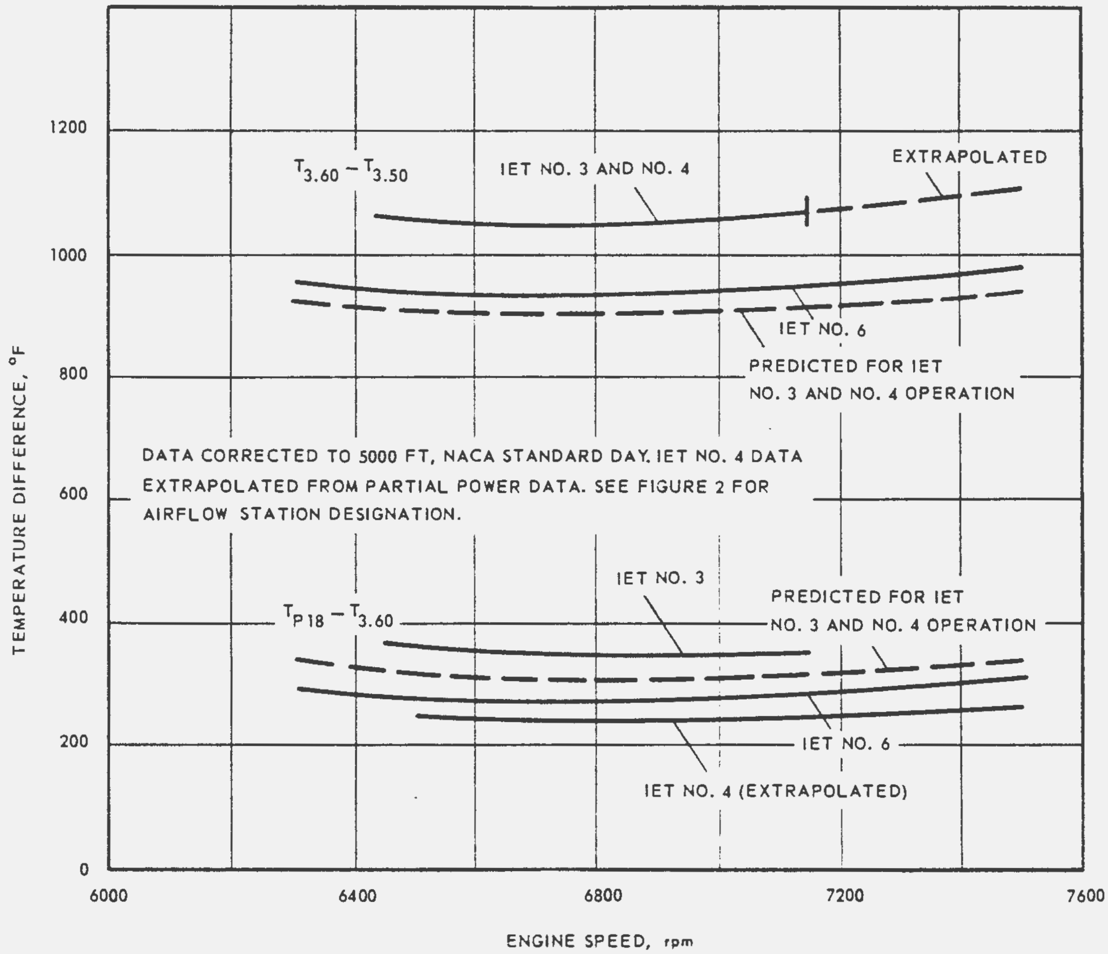

Fig. 5 – Average plate-to-air and reactor inlet-to-outlet temperature differences versus engine speed at full-nuclear power

Analysis of Fuel-Plate Temperature Variation - In an attempt to determine causes for variations in 18th-stage plate temperatures from an over-all average, a particular run of IET No. 6 was investigated in detail. This run had an over-all average plate temperature of 1604°F, with a maximum deviation of 190°F, and with 15 out of 30 existing readings deviating by more than ± 100°F.

These 30 thermocouple readings were separated into individual groups, each characterized by (1) being from tubes all the same distance from the center of the core, and (2) being from the same fuel element ring number. Averages were then obtained from each group. For this run the greatest deviation from the average was 87°F, with 20 of the 30 readings being within ±50°F of their respective averages.

Correlation of Heat Transfer Data - Heat transfer data for some 20 runs of IET No. 6 were correlated and compared with similar correlations for IET No. 3 and No. 4. Figure 6 depicts these correlations graphically together with a line representing ideal design values. The correlations are based on the averages of outer-ring temperatures, and the below-minimum slopes for IET No. 4 and No. 6 may be explained by the cooler-than-average outer rings as indicated by the fine radial temperature profile in Figure 7.

Effect of Control Rods on Air and Wall Temperatures - Full insertion of a control rod was found to depress adjacent tube power, as measured by bulk-air temperature rise,

[redacted]

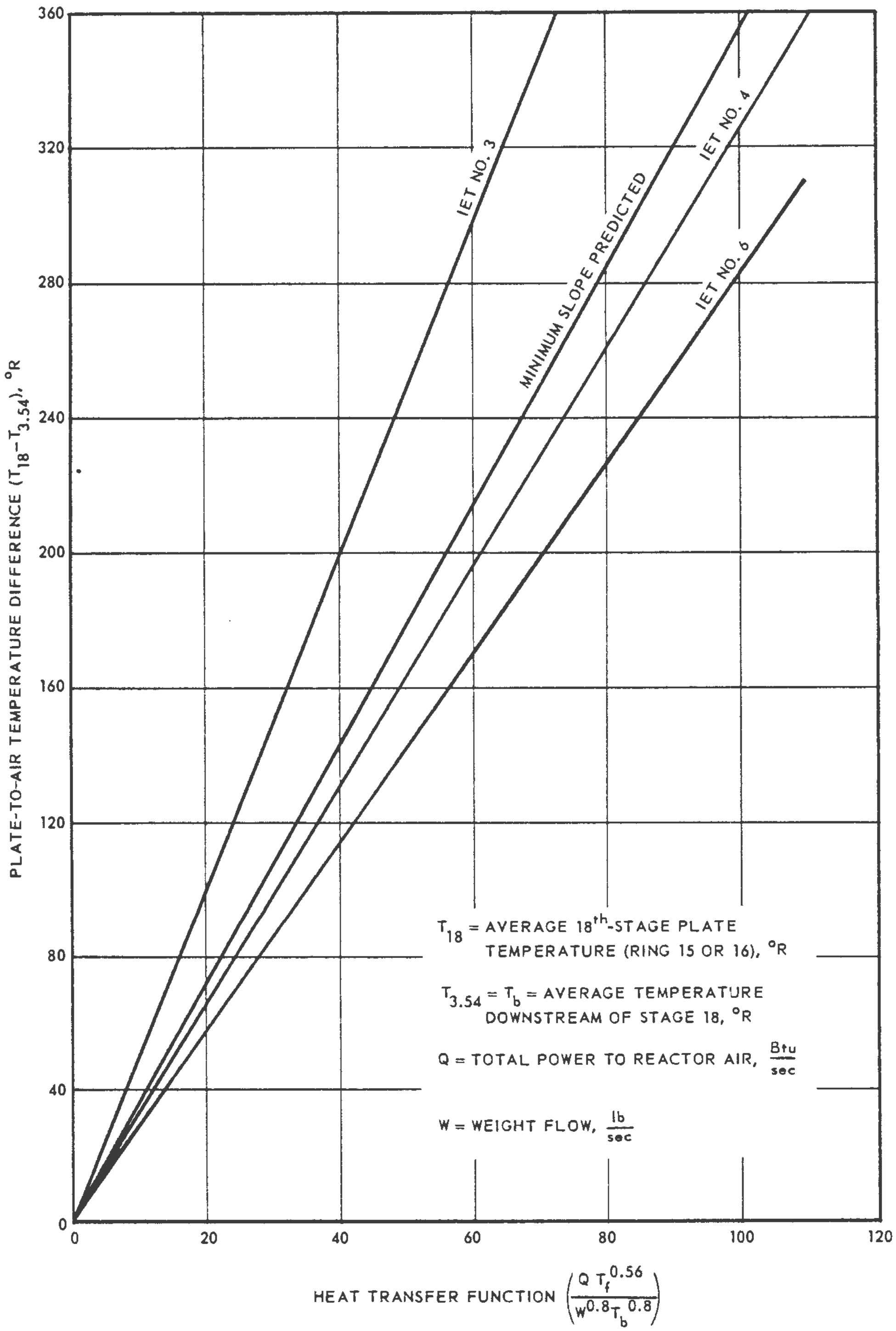

Fig. 6 – Gross thermodynamic performance comparison

[redacted]

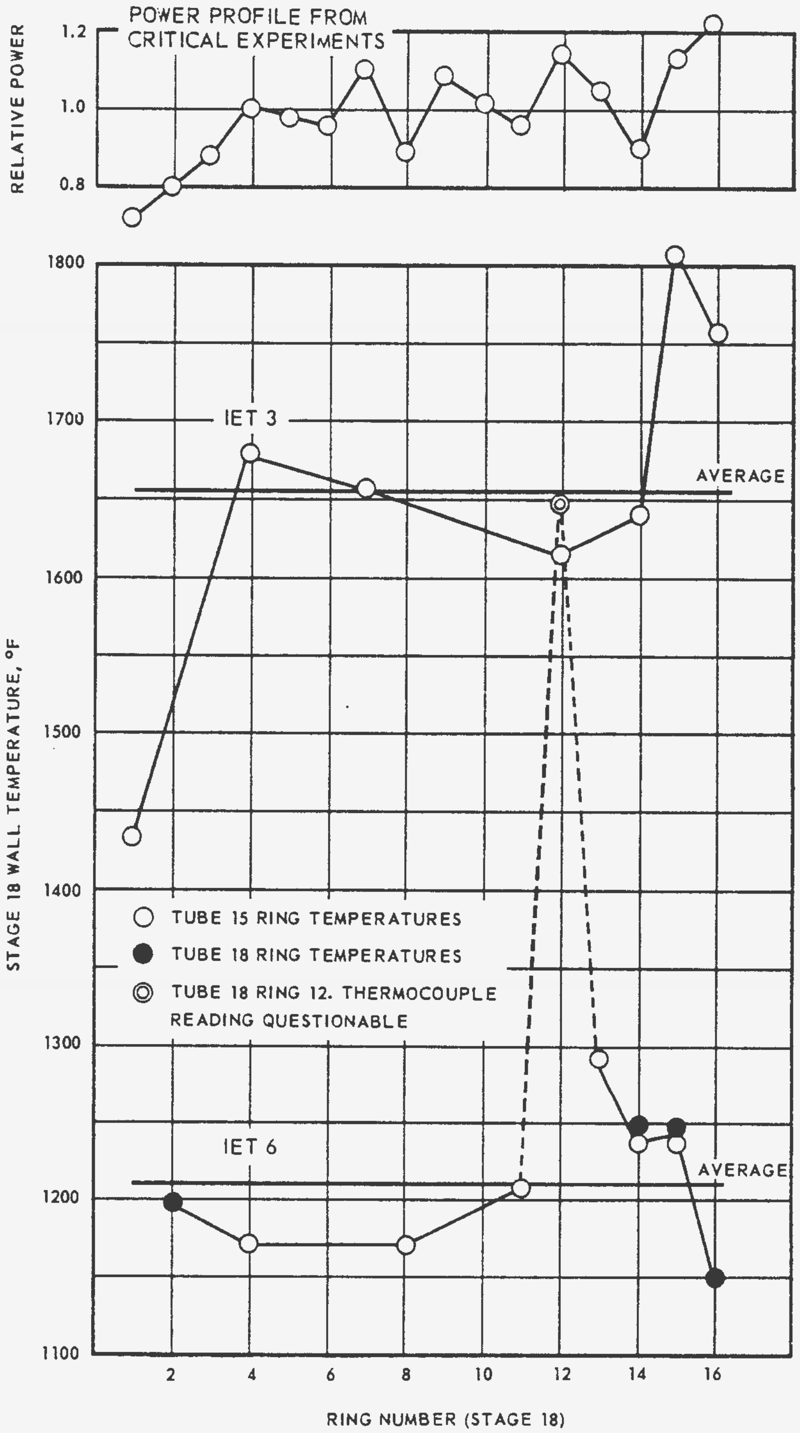

Fig. 7 – Fine radial temperature profiles

[redacted]

from 7 to 10 percent, for inner and outer tubes respectively. These values are in good agreement with values from critical experiments. A simple correlation for wall temperature variation was not found; however, maximum variations of the same magnitude as the average wall-to-bulk-air temperature difference were noted.

The effect of control rod insertion on tube power was determined by averaging temperature variations for tubes at a given distance from the control rod during two rod exchanges. These exchanges consisted of the simultaneous withdrawal and insertion of two rods with the remaining rods stationary, and the reactor power level and airflow constant. The positive and negative variations in temperature show a "tilting" about a line roughly midway between the exchanged rods.

The effect of rod pattern on exit air temperature is illustrated in Figure 8, on which the tubes are grouped according to distance from reactor center, and temperatures are averaged for each group. Although the two cases considered differed in total power, and consequently exit air temperature, they have been normalized to the lower exit air temperature. The rod pattern tabulated on Figure 8 represents the two extremes of the center rod pattern. The dotted line represents the case for frame 1 cocked 5 inches, whereas the solid line indicates the effect of having frame 1 fully withdrawn. These data indicate that 25 inches of frame 1 is worth approximately 125°F on group 2 and 75°F on group 6.

Gross Radial Power Profile

Figure 9 presents a comparison of power profiles obtained by three completely independent methods, power to air, transient temperature rise, and critical experiment data. All points were normalized to the same basis, a radial average excluding the central tube. Except for the region including the six outermost tubes, the power-to-air and transient methods show excellent agreement. There is fair agreement with critical experiment data except for a reversal at regions 3 and 4 (tubes 8 to 13, and 14 to 19, respectively).

The power-to-air profile was determined from the bulk-air temperature rise and weight flow, averaged for all tubes at a given radial distance from the core axis. Corrections for control perturbations were made from data obtained from the rod exchange run to arrive at a profile independent of control rod pattern. Excellent agreement was obtained between runs with different rod insertion patterns.

The transient-rise profile resulted from an analysis of the temperatures recorded during a transient rise in reactor power from essentially zero to 70 kilowatts, with zero airflow. This analysis predicted the gross radial power profile with the assumption of the knowledge of circumferential, fine radial, longitudinal, and fuel-element-plate trailing edge profiles.

Analysis Of Fission Fragment Release

Before the fuel elements of the HTRE No. 1 A3 core were removed for visual inspection at the conclusion of IET No. 6, inferences were made of the relative degree of fission fragment release from each of the 37 cartridges in a study designed to improve the damage-detection ability during operation and to assist the disassembly operation. These inferences were based on the results of the radiochemical analysis of the solids deposited on stainless steel and paper filters located in the air-sampling tubes at the exit of each fuel tube. In an attempt to correlate fuel element and air temperatures and control rod positions with the radiochemical analyses, a history during IET No. 6 of the air and fuel thermocouple readings was compiled along with a history of the control rod positions.

Radiochemical analyses of stainless steel filters removed from the reactor assembly late in the past quarter indicated that significant amounts of iodine were present in almost

[redacted]

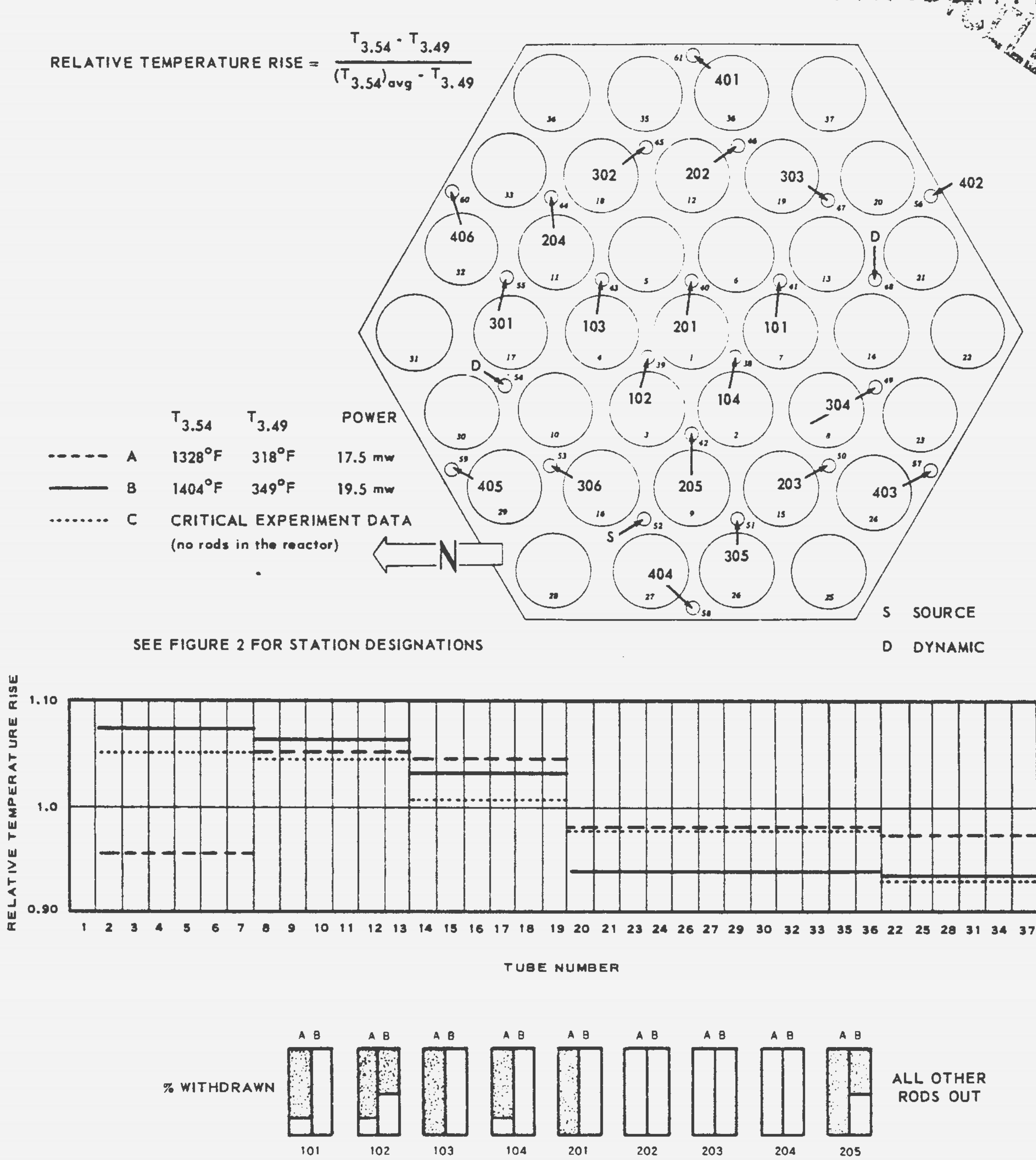

Fig. 8 – Variation of fuel tube exit air temperature as a function of control rod position

every case. The fission products Ba^{140}, La^{140}, Ru^{103}, Ce^{144}, as well as U and Cr^{51} were found on some of the filters.

Because of evidence that the stainless steel filters were possibly contaminated from previous use on the CTF during reactor failure, a low-power run at a fuel element temperature of about 800°F was made with the stainless steel filters replaced by No. 41 Whatman filter paper. The paper filters insure clean samples and result in better chemical analysis. Spectrometer analysis indicates that in quality the paper filter prototypes are equally as good as the existing stainless steel filter elements without having the inherent disadvantages of the latter. The paper samples may be collected in test tubes and

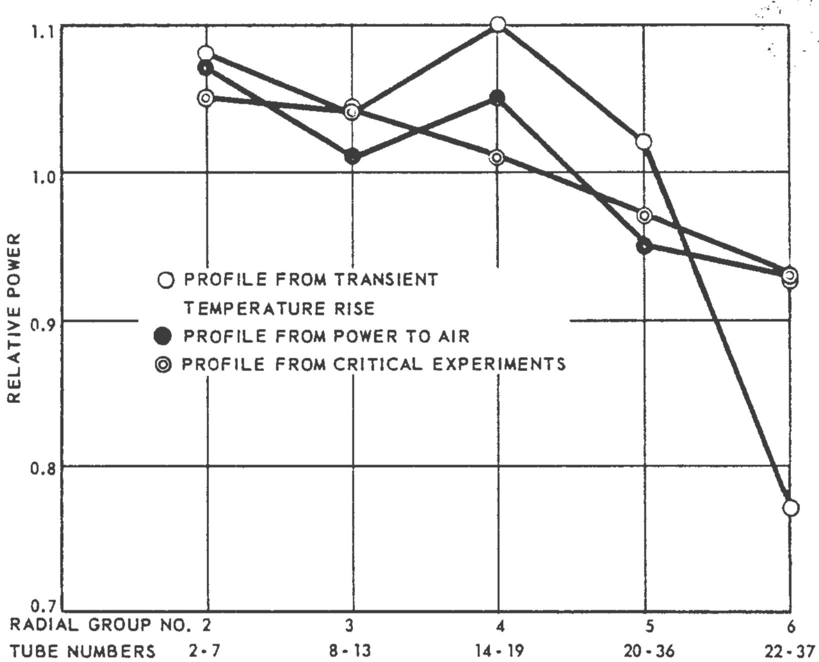

Fig. 9—Gross radial power profile

run through the spectrometer and the gross gamma counter without the 16-hour delay required for leaching the stainless steel filters. The time required to change the filters on the CTF has been reduced from a 4-hour to a 30-minute operation, and there is assurance of a more representative sample collected during the leaching, since the paper and sample are dissolved in the nitric acid.

Each of the 37 filter papers was placed in a scintillation crystal gamma-ray counter and the relative gamma activities determined. Gamma-ray spectral analysis proved the definite presence of fission products on some filter papers, a possibility of fission products on others, and the probable lack of fission products on the remaining. Since a 0.32-Mev line, proved to be due to Cr^{51} during the stainless steel work, appeared consistently in the paper spectra, it was tentatively assumed that Cr^{51} was present on the paper filters.

From the total body of information gained from both the stainless steel and the paper filters, predictions were made as to which fuel cartridges had released fission fragments. These predictions are presented in Figure 10 along with the following information:

1. The gross gamma-ray count rate in arbitrary units from each of the 37 filter papers from a low-power run.
2. The dose rate in milliroentgens per hour, measured by placing a survey meter in contact with each of the 37 stainless steel filters from a high-power run.
3. Intensity in arbitrary units of the I^{131} component of the filter-paper spectra.
4. Intensity in arbitrary units of the supposed Cr^{51} component of the filter-paper spectra.

During IET No. 6, temperature readings as a function of time were recorded for thermocouples on the fuel elements and at station 3.54 (core-exit-air temperature). Duration of thermocouple readings in chosen temperature brackets was compiled and is shown on Figure 10. Because of failures of the thermocouples on the fuel elements, some element data were extrapolated by assuming that a thermocouple which had operated in a given

LEFT SIDE OF CIRCLE:

1. Relative gross gamma count from filter papers exposed in low power run.
2. Relative dose rate from stainless steel filters exposed in high power run
3. Relative height of iodine peak in filter paper spectra.
4. Relative height of supposed chromium-51 peak in filter paper spectra.

Center strip of large circles indicates relative time that exit air thermocouples indicated over 1500°F and plate thermocouples indicated over 1800°F.

RIGHT SIDE OF CIRCLE:

1. Number of hours and minutes exit air thermocouple read over 1400°F.
2. Number of hours and minutes exit air thermocouple read over 1500°F.
3. Number of hours and minutes fuel thermocouple read over 1700°F (extrapolated)
4. Number of hours and minutes fuel thermocouple read over 1800°F (extrapolated)

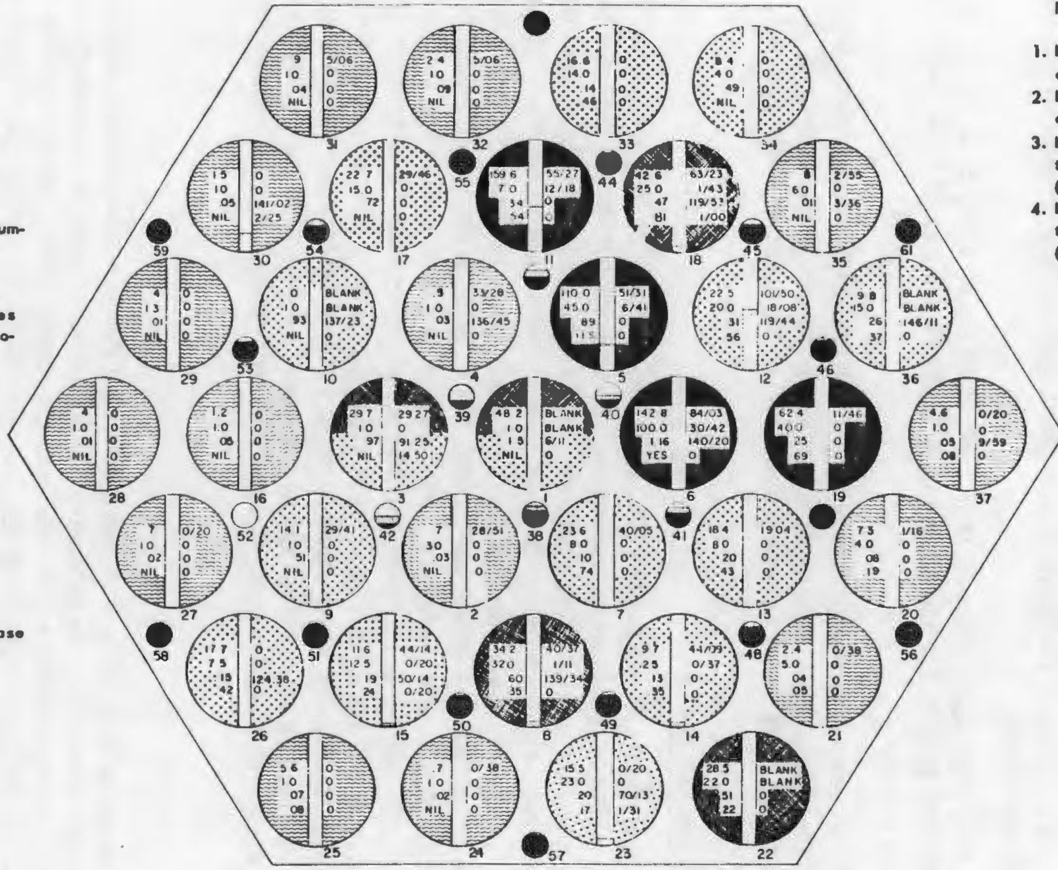

LARGE CIRCLES

Relative fission fragment release

- PROBABLE
- POSSIBLE
- UNCERTAIN
- IMPROBABLE

SMALL CIRCLES

- Percent of 150 hours that rod was out.
- Rod at mid-position.
- Rod in.

Fig. 10 — Predictions as to the probable degree of fission fragment release by individual fuel tubes

temperature bracket before failure would have continued to read in that bracket for the remainder of the test. This extrapolation was not necessary for the air temperatures since only four thermocouples failed at station 3.54 during the entire 150 hours of operation. Correlation between high temperatures and the radiochemical analysis for each fuel element was much better than would be expected by chance.

The control rod positions were determined from the operation log sheets as a function of time and were compiled in three groups: In (0 to 10 inches withdrawn), Mid (10 to 20 inches), and Out (20 to 30 inches). The percentage of the total running time which each rod remained in each position was computed and is shown graphically on Figure 10. No consistent correlation between the control rod positions and the results of the radiochemical analyses was found.

Examination of fuel cartridges showed that cartridges 2, 3, 4, 5, 6, 7, 8, 9, 10, 11, 15, 16, 18, 19, 21, 23, 25, 30, 32, and 36 had open blisters similar to those described in section 2.13 of this report.

In general, good agreement is shown between the filter analysis and cartridge examination, especially since the manifold discharging the sampling air from tubes 1, 2, 3, 4, 9, 10, 16, 17, 27, 28, 29, 30, 31, and 32 was later found to be plugged with boric acid precipitate.

Controls Analysis for IET No. 6

Limited data were obtained during IET No. 6 on the control system characteristics. Sinusoidal inputs and step inputs were impressed on the amplifier that compares the demand level and actual flux level. Instrumentation difficulties rendered the sinusoidal data of little value; however, the step-input data has been extensively analyzed. These data were obtained at relatively low reactor powers (5 megawatts) because of operating temperature limitations that were in effect late in IET No. 6. Analysis has yielded the relative response (ratio of a sinusoidal response amplitude to the step response amplitude at infinite time due to the same input amplitude), of flux ϕ, fuel plate temperature (T_{p18}), and exit air temperature ($T_{3.54}$) as a function of input frequency. Examples are presented in Figure 11. These responses were obtained by numerical integration of the step input response curves obtained by an oscillograph of adequate frequency response. Other parameter response data, such as dynamic-rod motion, have been obtained but are not presented here.

Xenon Analysis

Experiments on the HTRE No. 1 core have indicated that the xenon poison is considerably higher than was predicted. An extensive study has been made in an attempt to find a method which would predict from basic concepts the xenon poison effect experimentally determined in the HTRE No. 1. All methods used a two-energy-group multiregion model. The various methods are described below.

Diffusion Theory, Homogeneous Model - The reactor is divided into four radial regions. The fuel, moderator, and other materials in each region are homogenized by the use of cell corrections and volume fractions for each material. The xenon concentration is calculated by using average fluxes and the fission cross sections in each region. The reactivity of the reactor with and without xenon is then calculated with the IBM 704 computer.

Diffusion Theory, Homogeneous Model with Modified Cell Corrections - The same model as above is used with the exception that the cell corrections are modified for the additional depression of the flux resulting from xenon capture.

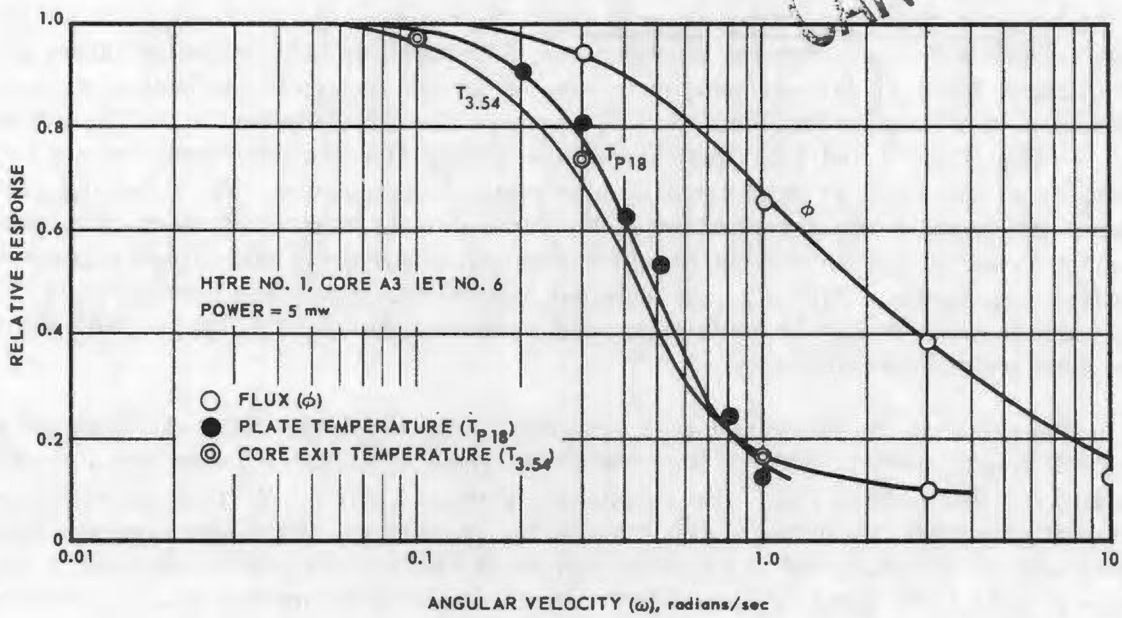

Fig. 11 – Frequency response of flux, plate temperature, and core exit temperature from numerical integration of the step input response

Perturbation Theory, Homogeneous Model - The reactor is divided into four radial and nine longitudinal homogeneous regions which divide the core into 36 volumes. The two-group constants for each region are obtained by the use of cell corrections and volume fractions for each material. The two-group fluxes and adjoint fluxes are determined with the IBM 704 computer, on this assumption that the radial and longitudinal fluxes are separable. The effect of xenon on reactivity is calculated using two-group perturbation theory.

TABLE 2

REACTIVITY LOSS DUE TO XENON POISONING FOR HTRE NO. 1 AT 17.9 MEGAWATTS

Method of Determination	4.75 Hours Operation, % Δ k/k	Equilibrium Xenon, % Δ k/k
Diffusion theory, homogeneous model	0.289	1.945
Diffusion theory, homogeneous model with modified cell corrections	0.368	2.392
Perturbation theory, homogeneous model	-	2.122
Perturbation theory, heterogeneous model	0.398	2.334
Perturbation theory, heterogeneous model ($\sigma_{a2\,Xe} = 2.84 \times 10^6$ barns)	0.460	2.557
Experimental	0.60	4.0 - 4.5[a]

[a] Equilibrium xenon was not obtained; this estimate is based on results of 23 hours of continuous operation.

Perturbation Theory, Heterogeneous Model - The reactor core is divided into four radial regions with 1 fuel element in region one, 6 in region two, 12 in region three, and 18 in region four. All fuel elements in any one region are treated in an identical manner; therefore, there are 4 representative fuel elements. Each fuel element in turn is divided into 9 radial regions and 9 longitudinal regions, giving 81 volume elements in each fuel tube, or a total of 324 representative volume elements in the core. The two-group constants and fluxes are determined for each volume element from which xenon concentrations are calculated. Then the effect of the xenon on reactivity is calculated by means of perturbation theory. This is a very detailed calculation, taking into consideration the variation in xenon within the fuel element both radially and longitudinally, and should give the most accurate prediction.

In order to compare methods and experimental data, the power level was assumed to be 17.9 megawatts for 4.75 hours of operation. Equilibrium xenon poison was also calculated for this power level. The results are given in Table 2. Various values for the thermal cross section of xenon are given in the literature. The Maxwellian averaged value used in this study was 2.4×10^6 barns. An estimate of the effect of increasing this value to 2.84×10^6 barns, a value which was calculated by Bernstein, is also presented in the table.

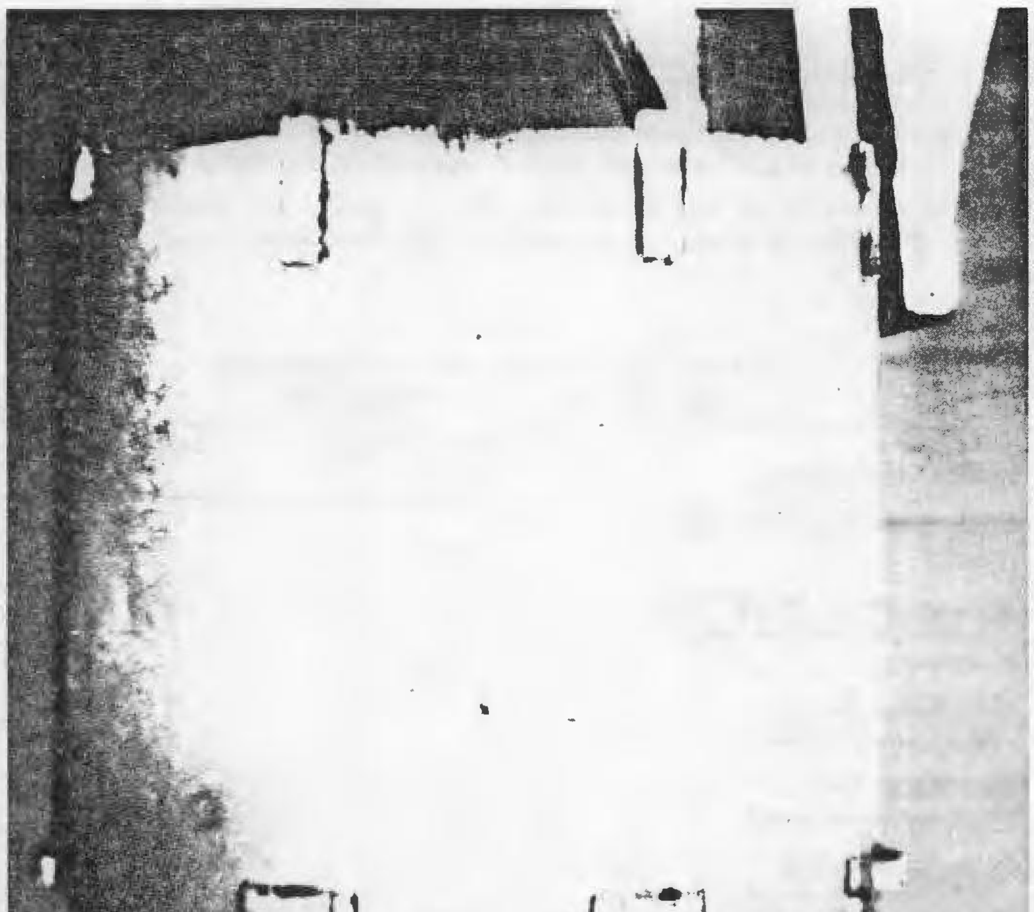

Fig. 12 – Ring 7, stage 16, of cartridge 325 (core tube 4) showing two adjacent blisters near trailing edge and one blister near leading edge.

The listed experimental value of xenon poison is from IET No. 6. This value may be adjusted later as more experimental data are made available. The highest calculated value of poison is about 23 percent lower than the experimental value.

2.13 FUEL ELEMENTS

Postoperation Evaluation of HTRE No. 1 Fuel Cartridges

Following operation of IET No. 6 all cartridges were removed and examined. During this examination a number of blisters were detected on certain of the cartridges. Subsequent examination of stages from core tubes 4, 6, and 19 have revealed blisters distributed as indicated in Table 3. The blisters varied in size from 1/8 inch to 1/2 inch in

TABLE 3

LOCATION OF BLISTERS ON FUEL RINGS REMOVED FROM THE CORE OF IET NO. 6, HTRE NO. 1

Cartridge From Tube No.	Stage No.	Ring Number															
		1	2	3	4	5	6	7	8	9	10	11	12	13	14	15	16
2[a]	18			1				1									
3	18								2								
	16								2					1			
	15			1		1		2			1	2					
	14							1			1	2					
	13								3		1	2					
	12							1			2						
	9			1													
4	18					2	1	6	3								
	17			1		5		1	5	6		1					
	16		2			1											
5[a]	18							1									
6	18							1	4		1						
	17					1						1					
	16				1	1		1									
	15							3		1	1	2	1				
	14						1		3	1		1					
	13			2	3			1	1		2		1				
	12							1									
	11			1	1			1									
	10					1	1	2									
	9						3										
	8							3									
7[a]	18				1	4	4	4			1						
8[a]	18								1				1				
9[a]	18					1			1		1	1					
10[a]	18						1										
11[a]	18					1											
15[a]	18											1					
16[a]	18					1		1									
18[a]	18						1	1	1								
19[a]	18			1		3	1				2	1					
21[a]	18					1											
23[a]	18					1											
25	18			1													
	17			2					5								
30[a]	18					1											
32[a]	18					2		1									
36[a]	18					2											
Total by rings		0	2	11	6	29	13	33	31	8	13	14	3	1	0	0	0

[a]Only the 18th stage examined

diameter. Their locations were not associated with hardware, with leading or trailing edge, or with any particular quadrant. All blisters examined to date have contained fissures on the outside surface of the rings (see Figure 12). No evidence of severe local overheating was observed on any blistered IET No. 6 cartridge. Metallographic examination shows the clad surface in the blistered area, as well as in areas removed from blisters, to be only slightly oxidized, with oxide penetration less than 0.002 inch. Cores within blistered areas were completely oxidized. Perusal of inspection data and in-process fabrication data has shown no correlation between blisters and fuel ribbon quality.

In most cases of a blister on the outside of a ring, a corresponding defect on the inside of the ring was observed. Such coexistence was not universal, but no defects were found on inside surfaces except in coexistence with outside blisters. It appeared, within the viewing limits of the periscope and lighting, that internal defects were predominantly still closed. Examination of internal blisters under greater magnification and stereoviewing conditions could well alter such conclusions.

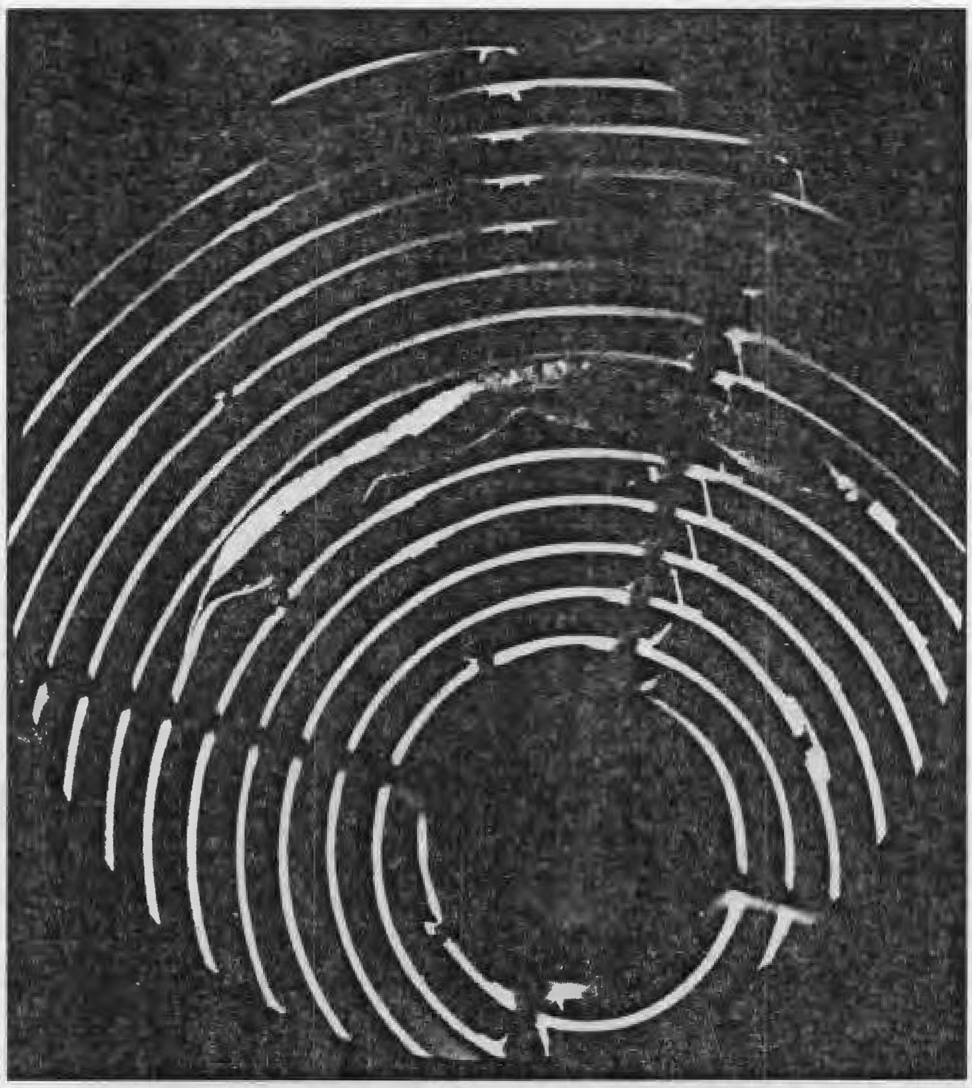

Fig. 13 – Photograph showing the trailing edge of ring 8, stage 18, of cartridge 323 (core tube 19), which had bellmouthed due to an apparent lack of dead edge

Some rails of the cartridges were buckled into the outermost rings of the section II stages, with one rail cracked in the buckled area. The inner liner of the insulation sleeve was oxidized in a pattern similar to that observed after IET No. 4 unloading.

Ring 8, stage 18, of core tube 19 was bellmouthed (see Figure 13). The X-ray of this segment showed the dead edge had been trimmed to a width of 0.001 inch in one area; this fact would account for exfoliation of the edge during operation.

2.2 HTRE No. 2 (Project 101)

2.21 GENERAL STATUS

The HTRE No. 2 reactor, as described in the previous quarterly report, is a power reactor designed as a test vehicle for experimentally providing design information on the geometries and properties of materials designated for use in future reactors. The HTRE No. 1 type reactor to be used in this experiment has a large test hole through the center of the active core into which the materials in the various geometries will be placed.

Two inserts are scheduled for the first series of tests. Insert No. 1 is composed of a bundle of seven, hexagonal, molybdenum- and stainless-steel-clad hydrided zirconium blocks as moderator. Insert No. 2 is composed of an array of six triangular bundles of UO_2-bearing beryllium oxide tubes held together by slabs of beryllium oxide, Inconel X rods, and silicon carbide plates. Nuclear mockups of both inserts were tested during the quarter.

Parent Reactor Assembly

The HTRE No. 2 A4 core, completed early in the quarter, was assembled for alignment and fitup checks. A trial insertion of a mockup insert core and shield plug was made, and the reactor was then disassembled and shipped to the Idaho Test Station. Figure 14 shows the complete A4 reactor in the assembly tower.

The initial criticality experiment dolly, carrying the A4 reactor, was received at the IET facility. Minor items of assembly were completed, and wiring connections were made and checked out. The moderator system was filled and pressure-tested satisfactorily, with no major leaks.

Operation of the initial criticality experiment was begun during the quarter, and the initial criticality of the A4 core was accomplished using nuclear mockups of the two insert assemblies. Power mapping and reactivity experiments were begun and were about 40 percent complete at the end of the quarter.

All controls and instrumentation components required for operation of the A4 parent-core have been delivered to Idaho. No evaluation of instrumentation component performance has yet been made.

The A5 reactor assembly is scheduled for completion by the end of July 1957. Component fabrication is proceeding satisfactorily. Assembly of the reactor core and the shield plug was begun in midquarter. All instrumentation components required for the A5 parent core will be delivered early in the next quarter.

Fifty parent-core fuel cartridges were completed during the quarter, bringing the total cartridges available for the A4 and A5 reactor cores to 66. Thirty cartridges are required for each core.

[redacted]

CONFIDENTIAL

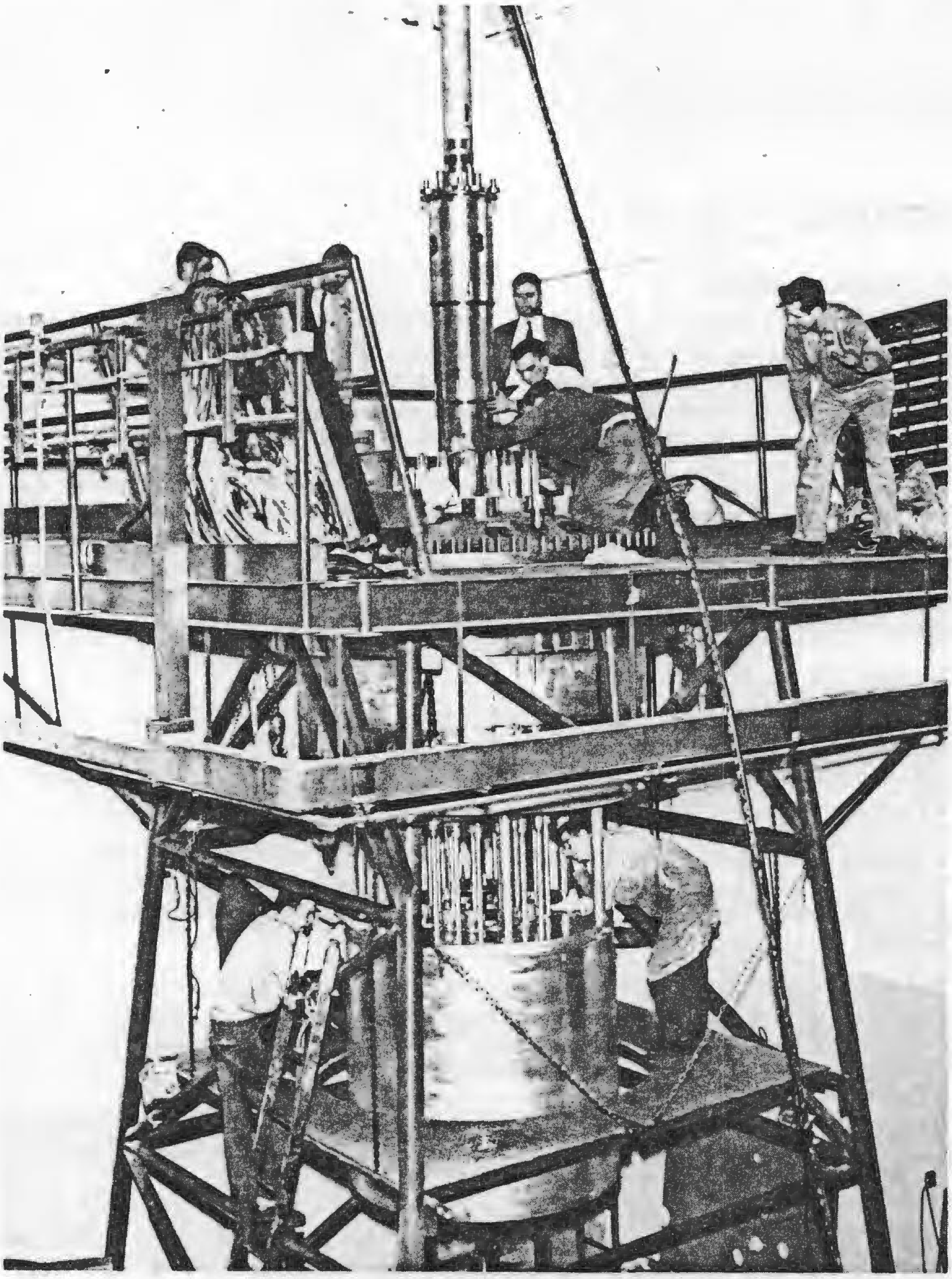

Fig. 14 — A4 reactor in assembly tower

[redacted]

CONFIDENTIAL

Although the specifications and fabrication methods for the A4 and A5 fuel cartridges assemblies are the same as those for the fuel cartridges of the A2 and A3 core, the assemblies will be operated at different temperatures. Whereas the HTRE No. 1 fuel elements operated to temperatures of 1750^{o} and 1850^{o}F, the HTRE No. 2 parent-core fuel elements are designed to operate at approximately 1500^{o}F. This fact should retard ruptured-blister-type failure considerably should it occur as it did in the A3 cartridges.

Insert No. 1

Eleven hydrided zirconium moderator tubes with an N_H of 3.95 were completed late in January for the Insert No. 1 nuclear mockup assembly. They are identical in design to the tubes for the operational insert, but were not fabricated to the proper tolerances and the cladding was not bonded to the outside surfaces of the hydrided tubes. Seven of the tubes were selected, assembled, and shipped to the Idaho Test Station. A photograph of this insert is shown in Figure 15.

A determined effort to develop cladding techniques and processes for application to the operating inserts is in progress. At midquarter a hot-swaging die (1650^{o}F) was placed in operation and has shown some promise in providing a bond between the 446 stainless steel and the molybdenum, and between the molybdenum and hydrided zirconium. Welding of the molybdenum continues to be a major problem. A new welding fixture has been devised and is being manufactured. When completed, it should be a valuable tool in alleviating this problem. Iron plating of the cladding stock appears to be another problem area in that traces of chlorine in the plating solution have proved to be a deterrent in the bonding process.

Testing has continued on moderator connectors and on 12-inch lengths of full-size moderator pieces to determine structural integrity of the end connectors and dimensional stability of the components. End-connector tests to date have indicated that the best joint efficiency of the crimped molybdenum ring and groove design is approximately 50 percent. Two new end-connector joints are under investigation. The first of these utilizes tube-rolling techniques in rolling the molybdenum tube into grooves in the end connectors. The second makes use of a welding ring backup for flare-rolled molybdenum end-connector joints.

Nine fuel cartridges containing 18 elements each, with 11 rings per element, and 10 fuel cartridges containing 18 elements each, with 10 rings per element, were completed during this quarter for Insert No. 1.

The 11-ring fuel elements were designed to maintain a moderator temperature of 1650^{o}F with a maximum fuel element temperature of 1750^{o}F based on the calculated power generation rate in the moderator. If the moderator power generation rate is actually lower than calculated, the fuel element temperature would have to exceed 1750^{o}F in order to operate the moderator at 1650^{o}F. The 10-ring fuel elements were designed to maintain the moderator at its design temperature without exceeding the fuel element maximum temperature.

Installation drawings for the core and plug instrumentation for Insert No. 1 were completed during the quarter, and the instrumentation will be ready for installation on the core and plug the first part of next quarter or as soon as the moderator tubes are finished for the insert.

The development work which has been carried on for the purpose of designing and improving attaching techniques for the thermocouples and pressure probes is essentially completed. With few exceptions all of the installation work will be performed at Evendale.

[redacted]

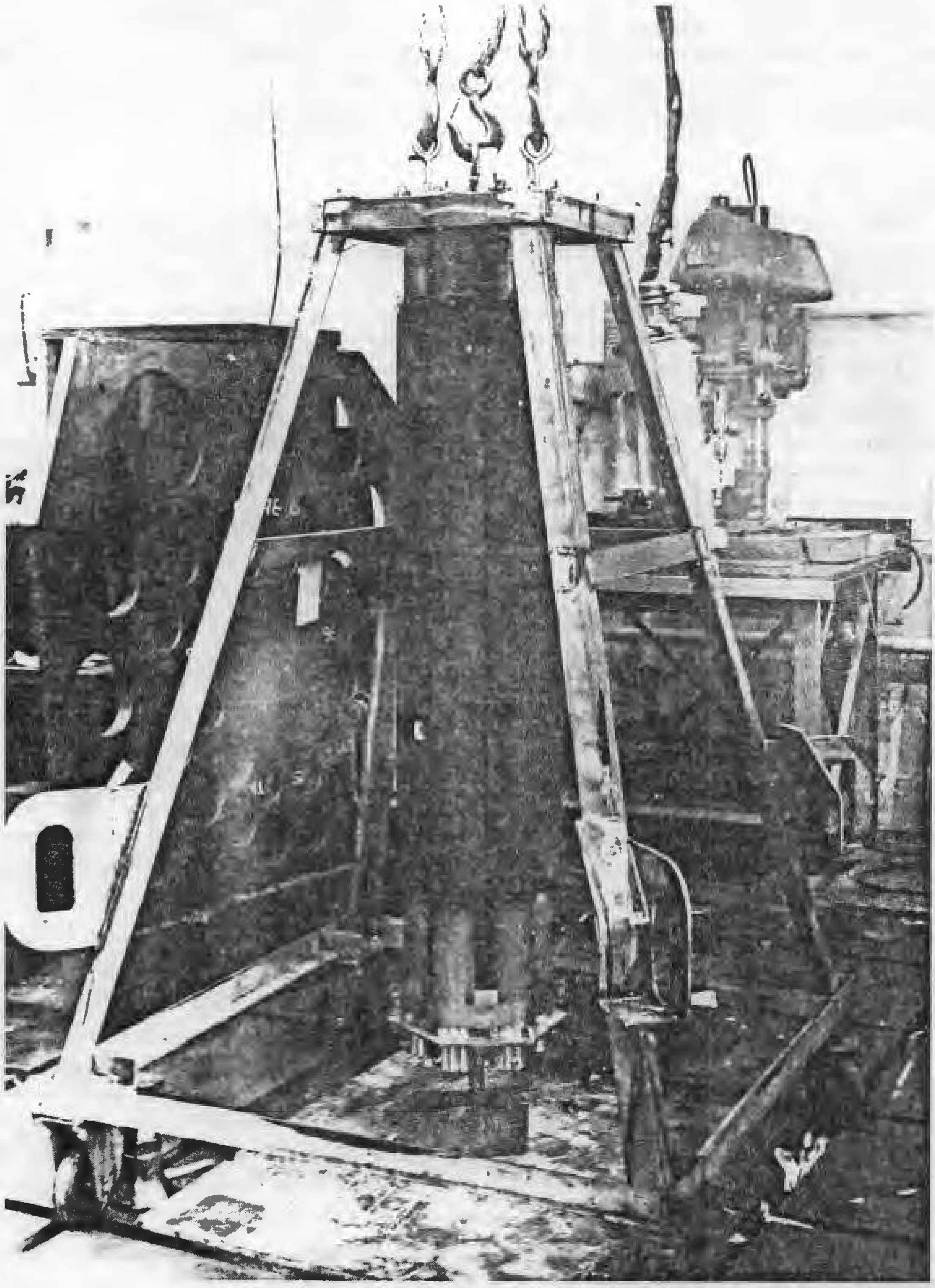

Fig. 15 – Nuclear mockup of Insert No. 1 for HTRE No. 2

[redacted]

The pressure probes located at the bottom of the core between the aft assembly of the fuel element and the aft assembly of the moderator tube have been completed, and the calibration of the probes will be finished at the start of the next quarter.

Insert No. 2

The nuclear mockup of the ceramic insert, which was completed and shipped to the Idaho Test Station, is composed of beryllium slabs and fuel sandwiched between beryllium foil. The mockup is being used in the critical experiments to determine the excess reactivity and power distribution. Delivery of silicon carbide and beryllium oxide components for the operating insert began late in the quarter.

Component testing is continuing. Two stainless steel support tubes were tested under expected insert operating temperatures. There was no evidence of damage to either of the tubes. Calibration of the top support plate is in progress. The calibration is necessary to establish the size of air passages required to provide the proper flow through the operating insert. Equipment has been accumulated for a dynamic test of the bottom retainer plate. This test will determine the strength of the retainer plate when subjected to various drag loads.

The instrumentation design has been completed for ceramic Insert No. 2, and essentially all of the instrumentation components have been accumulated. Assembly techniques are being practiced and improved. A study is being conducted to develop better thermocouple materials and systems.

A filter system, being designed to capture samples of eroded material and fission products, will be installed on the CTF for use with Insert No. 2 or any future insert, especially ceramic inserts. Iodine, in particular, will be captured and used as a quantitative measure of the total amount of fission products released.

2.22 EXPERIMENT RESULTS

HTRE No. 2 Critical Experiment

The HTRE No. 2 with the nuclear mockup of Insert No. 1 was made critical about the middle of the quarter. After the control rods were calibrated, the excess reactivity for the assembly was found to be 4.0 ± 0.5 percent at a water-moderator temperature of $95^{\circ}F$ and with 0.015-inch stainless steel insulation liners over the parent-core fuel cartridges. The assembly was calculated to have excess reactivity of 5.0 percent at a water-moderator temperature of $95^{\circ}F$ with 0.010-inch stainless steel insulation liners over the parent-core fuel cartridges. The excess reactivity value of the difference in stainless steel thickness is approximately a negative 1 percent. If this difference is taken into account, the calculation predicted very closely the excess reactivity of the system, an excess reactivity which is more than sufficient to operate the reactor and perform all of the desired experiments.

The HTRE No. 2 with a nuclear mockup of Insert No. 2 using beryllium in place of BeO was made critical shortly after Insert No. 1. After a rod calibration the excess reactivity of the assembly was determined to be 6.3 ± 0.5 percent at a water-moderator temperature of $95^{\circ}F$ and with 0.015-inch stainless steel insulation liners over the parent-core fuel cartridges. The BeO Insert No. 2 parent-core assembly was calculated to have an excess reactivity of 5.0 percent at a water-moderator temperature of $95^{\circ}F$, with 0.010-inch stainless steel insulation liners over the parent-core fuel cartridges. An experiment in which approximately 1/12 of the beryllium in the mockup of the insert was replaced with BeO indicated, through extrapolation, that a BeO insert in the HTRE No. 2 reactor would produce an excess reactivity of 5.0 ± 0.5 percent. When the design calculations

[redacted]

were corrected for these effects, the calculations under-predicted the excess reactivity of the assembly by approximately 1 percent. The extrapolated excess reactivity of the BeO assembly is, again, more than sufficient to conduct the test program.

Calibration of representative control rods for a symmetrical rod pattern gave the following results, which were approximately the same for both Inserts No. 1 and No. 2 (see control rod locations in Figure 16).

The water-moderator temperature coefficient for Insert No. 1 was measured to be 0.017 percent per $^{\circ}$F, and for Insert No. 2, 0.014 percent per $^{\circ}$F.

A fairly detailed power map of the HTRE No. 2 Insert No. 1 assembly has been completed. The resulting power distributions were essentially as expected. Figures 17 and 18 show plots of representative tube relative average power densities (total tube power divided by tube volume) as a function of reactor radius. Figure 17 shows relative power densities for the outer-ring rods In and Figure 18 shows relative power densities for the inner-ring rod In. The dotted lines on the graphs indicate calculated values. It is evident from these two graphs that, with the exception of insert tube 1, actual design values have been bracketed by adjusting the control rod pattern, indicating that actual tube powers can be adjusted to design values.

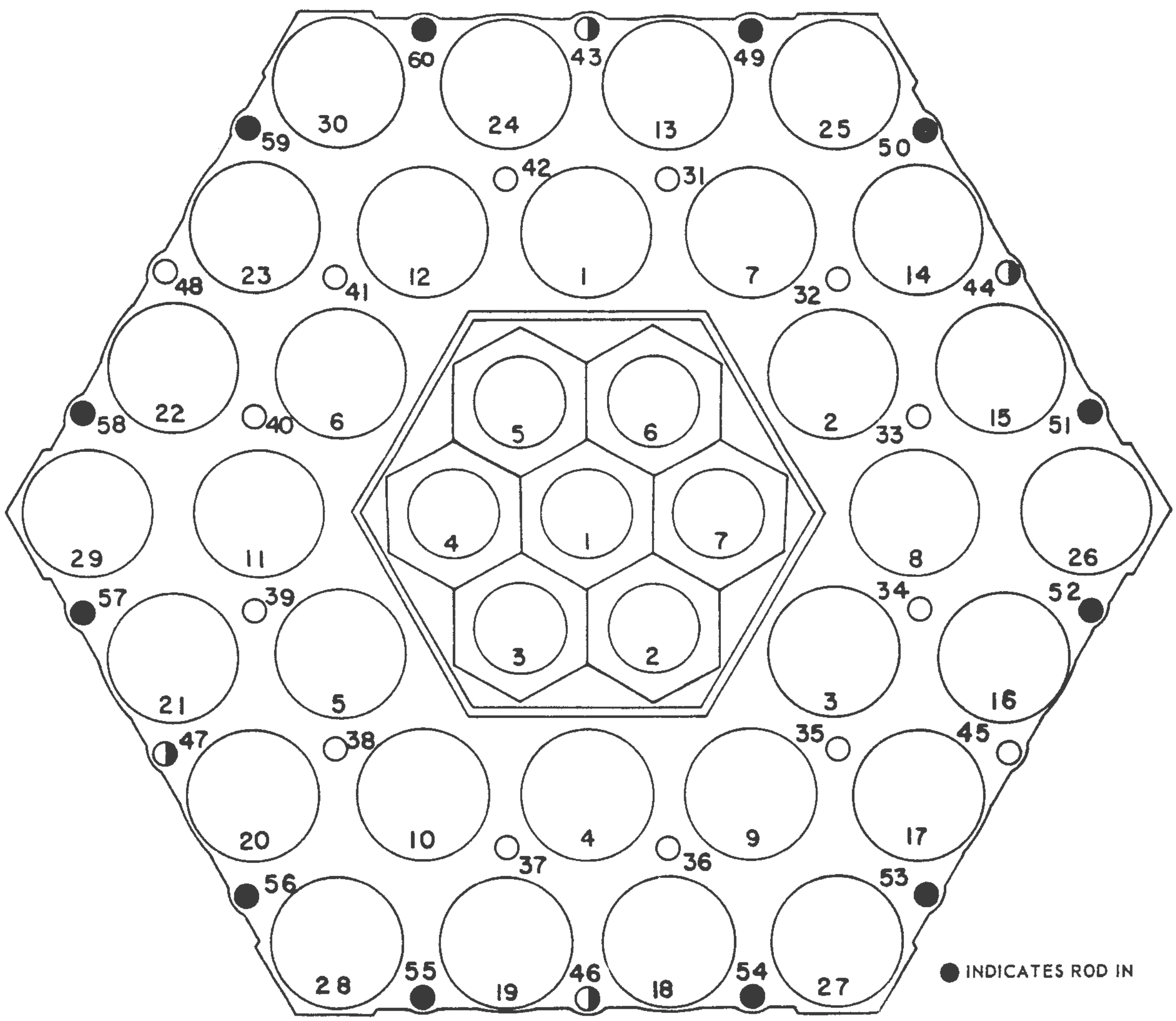

Fig. 16 – Approximate preliminary rod pattern for HTRE No. 2 critical experiment with Insert No. 1

[redacted]

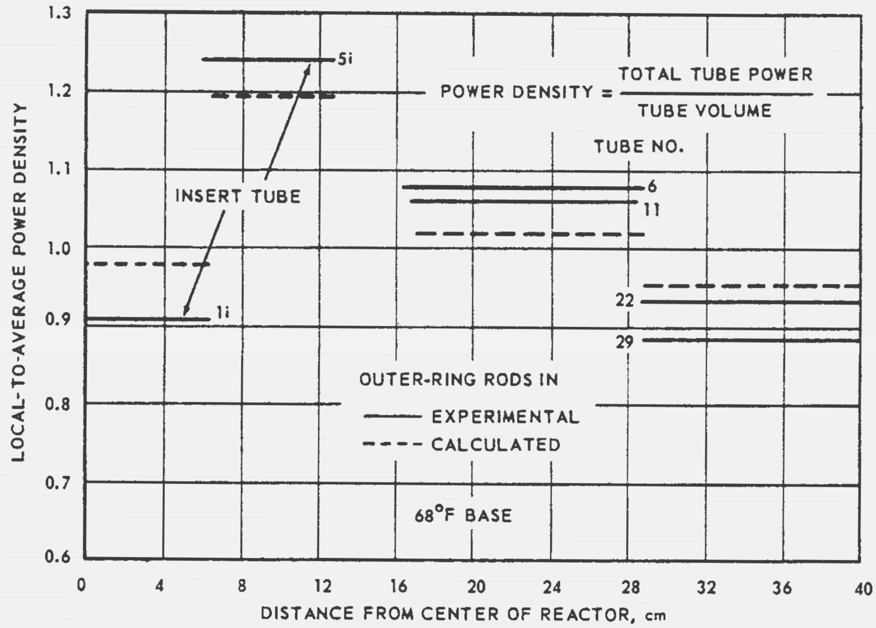

Fig. 17 – Relative power densities for the outer-ring rods "In" in HTRE No. 2 for Insert No. 1

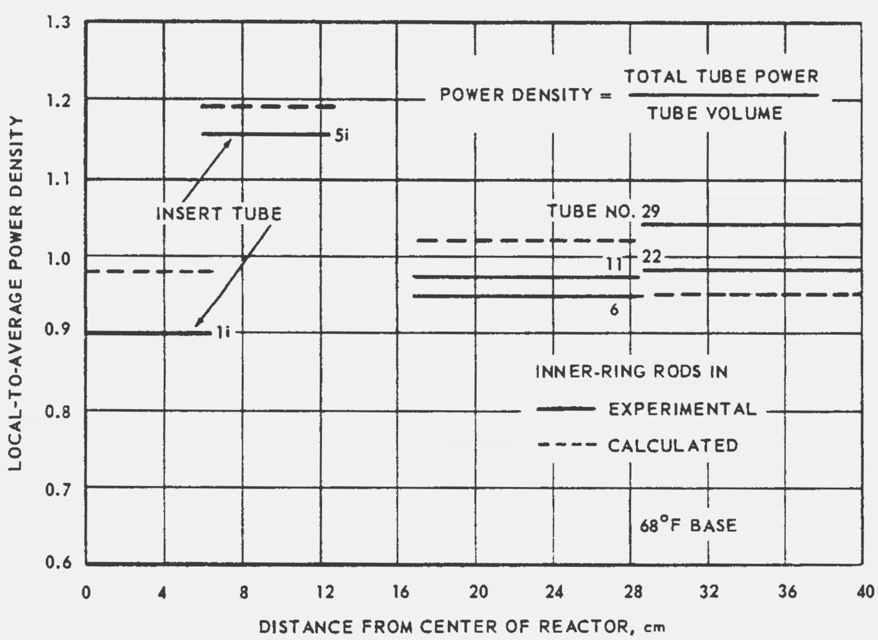

Fig. 18 – Relative power densities for the inner-ring rod "In" in HTRE No. 2 for Insert No. 1

 [redacted]

A series of health-physics gamma film badges was exposed in the HTRE No. 2 Insert No. 1 assembly to determine the absolute gamma fluxes in the reactor, which are used to compute secondary heat generation rates in the hydrided zirconium moderator. Preliminary results indicate that gamma fluxes, and consequently secondary heat generation rates, are from 30 to 40 percent below design values in the Insert No. 1 region of the reactor core. This would normally mean for this reactor that for the cooling supplied in the original design, the insert moderator would run cooler than is desired for the power experiments on Insert No. 1. However, in anticipation of the fact that gamma fluxes might be low, a second set of Insert No. 1 fuel cartridges was manufactured which will allow less cooling air to flow next to the moderator cell wall, thereby permitting a higher moderator temperature. The second set of cartridges was designed to a gamma flux 25 to 30 percent low.

With the exception of the gamma flux value, however, experimental values of power distribution and reactivity were well within the limits of the calculations Thus power operations of Insert No. 1 should proceed without complications.

2.23 CONTROLS AND INSTRUMENTATION

Insert No. 2 Instrumentation

The instrumentation of the ceramic insert will be considerably different from the instrumentation used on the A3 and A4 cores and Insert No. 1 because the fuel elements are beryllium oxide tubes instead of metal plates, and because the insert will be operated at an extremely high temperature. In thermocouples for this insert the physical limits of platinum and of vitreous-alumina insulating tubing are approached. Since high-temperature thermo-elements at the present state of the art are nonexistent, new techniques had to be devised for utilizing existing material. The shielding plug used on this insert, however, will be identical to that used on Insert No. 1. The termination of the thermocouple wires at the junction box on top of the plug will also be the same.

The ceramic insert will have a distribution of 80 thermocouples as follows:

59 thermocouples for fuel temperature measurements.
10 thermocouples for slab temperature measurement.
10 thermocouples for tie-rod temperature measurement.
1 open-junction thermocouple for insulation resistance measurement of vitrified alumina.

The fuel thermocouples will be placed in the interstices of the fuel tubes (10 per cell) using 10-mil platinum - platinum/10 rhodium lead wire for the thermo-elements. The wires are insulated in the fuel-tube region by 40-mil, double-bore, vitreous-alumina tubing. Preliminary testing has shown that platinum wire, at the expected operating temperature of the insert (2700° - 2900°F), does not have sufficient strength to support the alumina tubing; hence it is proposed to support each thermocouple by a 40-mil, single-bore, alumina support. This supporting column of alumina will run from the bottom support plate to the desired thermocouple junction depth.

Thermocouples to measure slab temperatures at various depths below the top plate will be placed in ground slots at the junctions of the slab in the center and in two corners of the insert.

Since the expected temperature in the tie-rod region (1700°F) is much lower than that in the main body of the insert, it will not be necessary to support the six tie-rod thermocouples. These couples will be installed using 25-mil, single-bore, alumina tubing, and will be fastened to the tie rods by small ribbon straps.

[redacted]

The plug and core will be completely assembled and instrumented separately. A splice in the wiring is planned in the region between the plug and core along the support rods. This method simplifies the wiring and makes it possible to ship the plug and core as separate units, if necessary.

In addition to the thermocouple wires, four 1/8-inch pressure tubes will be carried down the plug for static pressure measurements above and below the top support plate.

Work on the instrumentation drawings of the plug and the core is nearly complete. Almost all of the material necessary for the instrumentation of the core has been ordered or is on hand, so that assembly can be started in the early part of next quarter.

Actuators

The HTRE No. 2 actuators incorporate a number of new features not used in HTRE No. 1. These features include: (1) submerged-solenoid-type latch, (2) poison-tip quick disconnect, (3) servomotors with a minimum stall torque of 3.5 inch-ounces; (4) improved pinion gear in the second reduction in the gear train, (5) new type air-line caps designed for easy removal and replacement, (6) Carboloy Grade 608 chrome carbide retainers in the latch, (7) higher-load follow springs, (8) higher-strength mechanical stop mechanism, and (9) Garlock Klozure type pinion-gear seals.

Work is continuing on a pneumatic latch for the HTRE No. 2 actuator. The prototype has been successful, and manufacture of parts has started to permit tests of this latch in the HTRE No. 2 reactor at Idaho.

Work on other actuators has been discontinued pending results of operational tests in Idaho.

Kits are being assembled to alter rotary-type actuators presently in Idaho to the underwater solenoid type should this modification prove superior in its performance. Spare actuator components are being assembled to provide extra shim actuators for testing in Evendale.

2.24 AERODYNAMICS AND THERMODYNAMICS

During the quarter an analysis was made of the effect on fuel element temperatures of variations from the predicted (1) power distribution in the core, (2) pressure loss in the insert assembly, and (3) size of the outer annulus. The analysis was based on HTRE No. 2 operation at 10 megawatts and with 11-ring fuel elements in Insert No. 1.

Temperatures for predicted power distribution at a power level of 10 megawatts are shown in Figures 19 and 20. The variations in power distribution that might cause the insert fuel elements (design maximum temperature = 1750°F) or parent-core fuel elements (design maximum temperature = 1500°F) to exceed their design temperatures before the moderator reaches 1650°F are (1) less than predicted power in the insert, (2) less than predicted power in moderator, and (3) more than or less than predicted power in the outer ring.

Variations of this nature were considered, and resulting maximum insert temperatures at a power level of 10 megawatts were calculated. The results show that the insert fuel elements do not exceed their limit of 1750°F, except in one case in which the outer ring has 20 percent more than its predicted power (and then by only 3°F). Calculations also show that the maximum moderator temperature of 1650°F is exceeded except for cases of more than (1) 7 percent less than predicted power in insert, (2) 10 percent less than predicted power in moderator, and (3) 28 percent less than predicted power in outer ring. The maximum insert-fuel-ring temperature corresponding to the above situations when

[redacted]

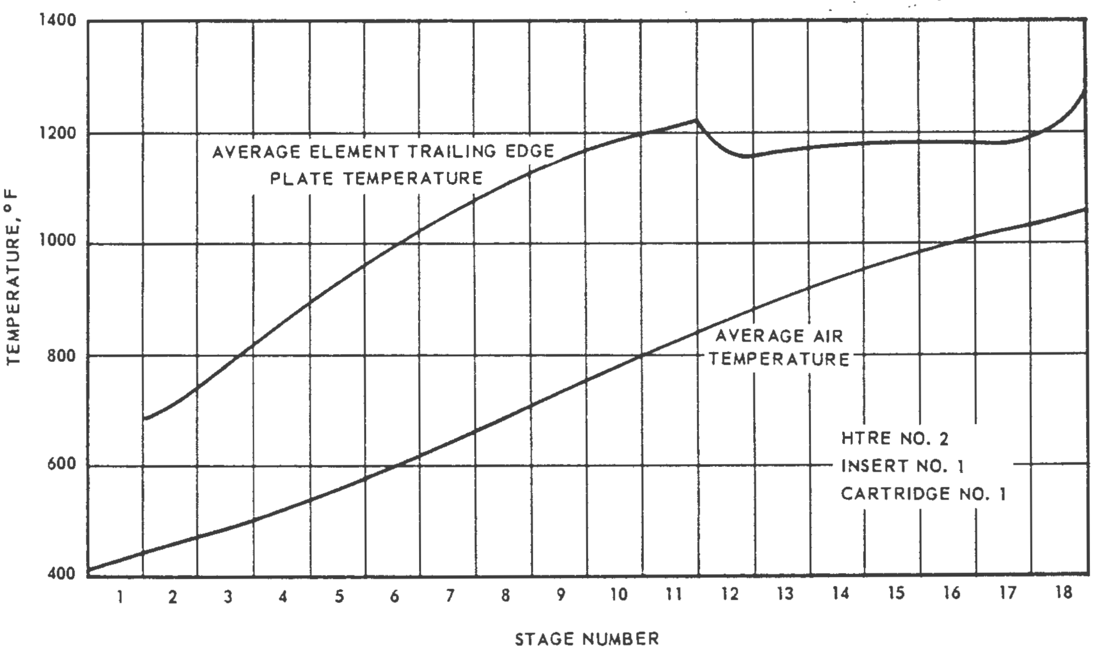

Fig. 19 – Longitudinal temperature profiles for parent-core fuel cartridge at 10 megawatts

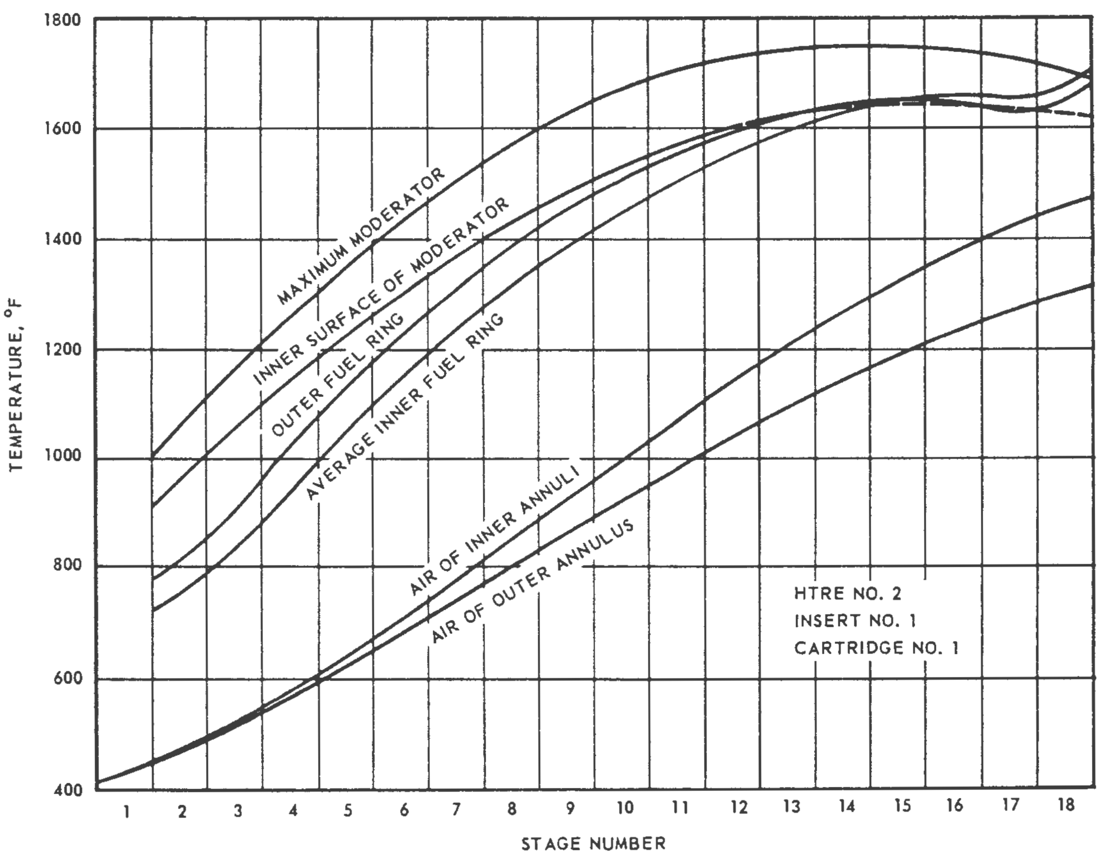

Fig. 20 – Longitudinal temperature profiles of insert outer tubes for predicted power distribution

[redacted]

the maximum moderator temperature is 1650°F are 1597°, 1703°, and 1659°F, respectively.

This indicates that at 10 megawatts the moderator will reach 1650°F without exceeding the design limits on fuel element temperatures unless the predicted power deviates greater than the 7, 10, or 28 percent as indicated, and that these limits can be extended to 30, 14, and 40 percent by increasing the power level (except if the outer ring should be in range of 20 percent more than predicted). It may be noticed that there appears to be an appreciable reduction in insert-fuel-element inner-ring temperature with decrease in power in the outer ring. This is probably not the actual situation but is the result of analysis assumptions. The temperature would remain nearly constant at approximately 1700°F for all variations of outer-ring power.

Maximum insert temperatures resulting from variations in predicted pressure loss through the insert cartridge inlet assembly were calculated. Results show that this variation did not alter the relative values of the moderator and fuel element temperatures, and the absolute values changed only 75°F from 50 percent to 150 percent of the predicted pressure loss.

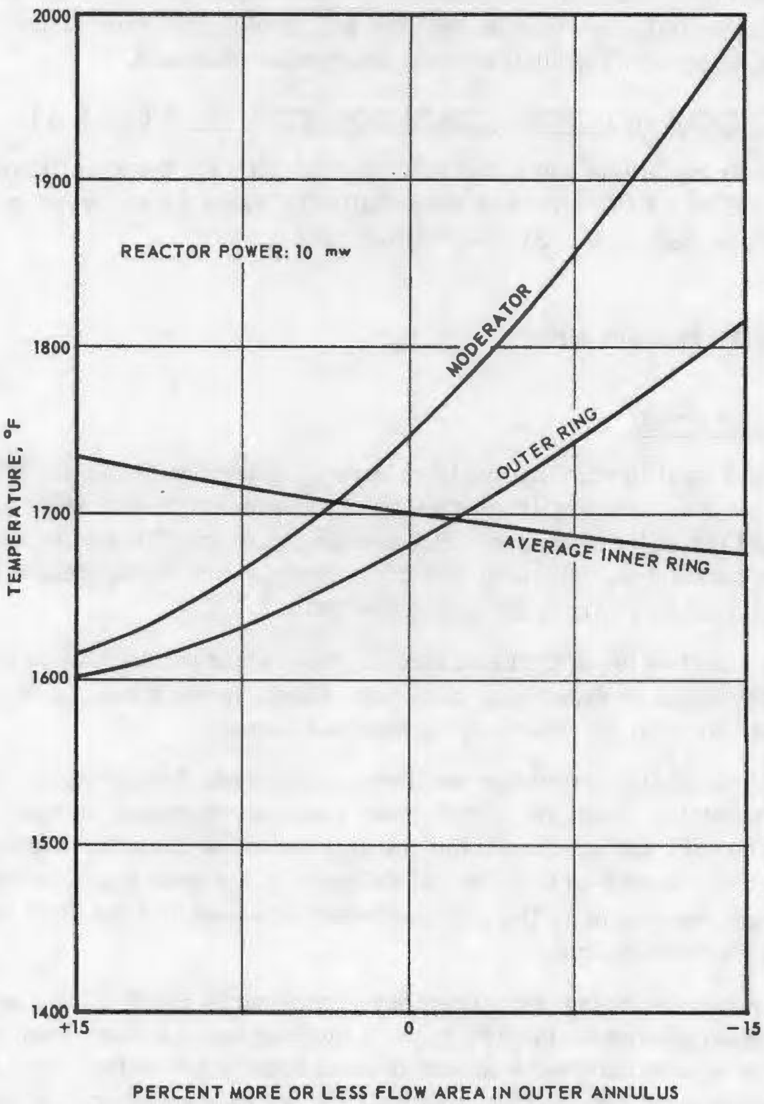

Fig. 21 – The variation of maximum insert temperatures with outer annulus flow area

Maximum insert temperatures resulting from variations in size of the outer annulus are shown in Figure 21. These curves indicate the sensitivity of the temperatures to variations in outer-annulus gap size. An increase of approximately 13 percent or more in flow area in the outer annulus can result in overtemperaturing the insert fuel elements before the moderator reaches 1650°F.

2.25 CTF AND IET MODIFICATIONS

CTF Interconnection Wiring

Among changes made in the CTF wiring was the complete rerouting of the flow-meter sensor-system circuits. These circuits have been completely segregated from all other systems. A number of obsolete circuits were removed from the dolly to increase maintenance efficiency. Modifications were made to the ICE and CTF dollies to meet the requirements of HTRE No. 2 and to give more satisfactory operation.

IET Facility Wiring

Modifications were made to the instrumentation and control systems at IET to meet the requirements of HTRE No. 2. These changes include expansion of the data reduction system, rewiring of the primary console, and the addition of new coincidence safety circuits and pulse preamplifiers in the nuclear instrumentation channels.

2.26 SPECIFICATIONS AND DESIGN DATA FOR HTRE No. 2 CORE A4

Since only minor revisions were made during the quarter, the specifications and design data for the HTRE No. 2 Core A4 are essentially the same as reported in APEX 21, Engineering Progress Report No. 21, September 1956.

2.3 HTRE No. 3 (Project 102)

2.31 GENERAL STATUS

All HTRE No. 3 final design layouts have been completed with the exception of moderator, reflector, aft plug, and auxiliary shields. Development testing of the dynamic actuator has continued through the quarter. Production drawings of the safety and shim actuators have been completed, and preproduction models are being readied for testing to affirm the results obtained from the prototype tests.

Considerable effort is being concentrated on the placing of fabrication orders for components, with emphasis on front plug and side shield fabrication. A dummy run of the HTRE No. 3 fuel element fabrication program has begun.

The X39-5 engine design program has been completed. This program consisted of the redesign and modification of the X39-4 gear case, compressor scroll, turbine scroll, turbine scroll cooling, and aft frame and the addition of a common combustor to be located just aft of the reactor-shield. Initial delivery of the gear case, compressor scroll, and aft frame has been made by the manufacturers. Delivery of the first turbine scroll is expected during the next quarter.

Preliminary power mapping measurements, rod-worth predictions, and core gamma heating rate measurements on the HTRE No. 3 nuclear mockup have been completed. Until now all work has been performed with nine manual rods in the center of the core. Measurements have been started with rods moved radially outward to determine the shift in gross radial power. Various rod patterns and a no-rod configuration will be investigated in the future.

Fuel inventory of the HTRE No. 3 reactor has been increased to 389.5 ± 6.0 pounds to provide sufficient excess reactivity for operation in excess of 100 hours under X39-5 operating conditions. This increase of 20 pounds of U^{235} was accomplished by the addition of a 19th stage to each fuel cartridge.

2.32 REACTOR

Nuclear Studies

A series of critical experiment measurements on the nuclear mockup of HTRE No. 3 was completed. This work included initial criticality, rod calibration experiments, and determination of detailed power distribution for the clean, startup condition. In addition, several measurements were completed on two special poison segments made up of euro-

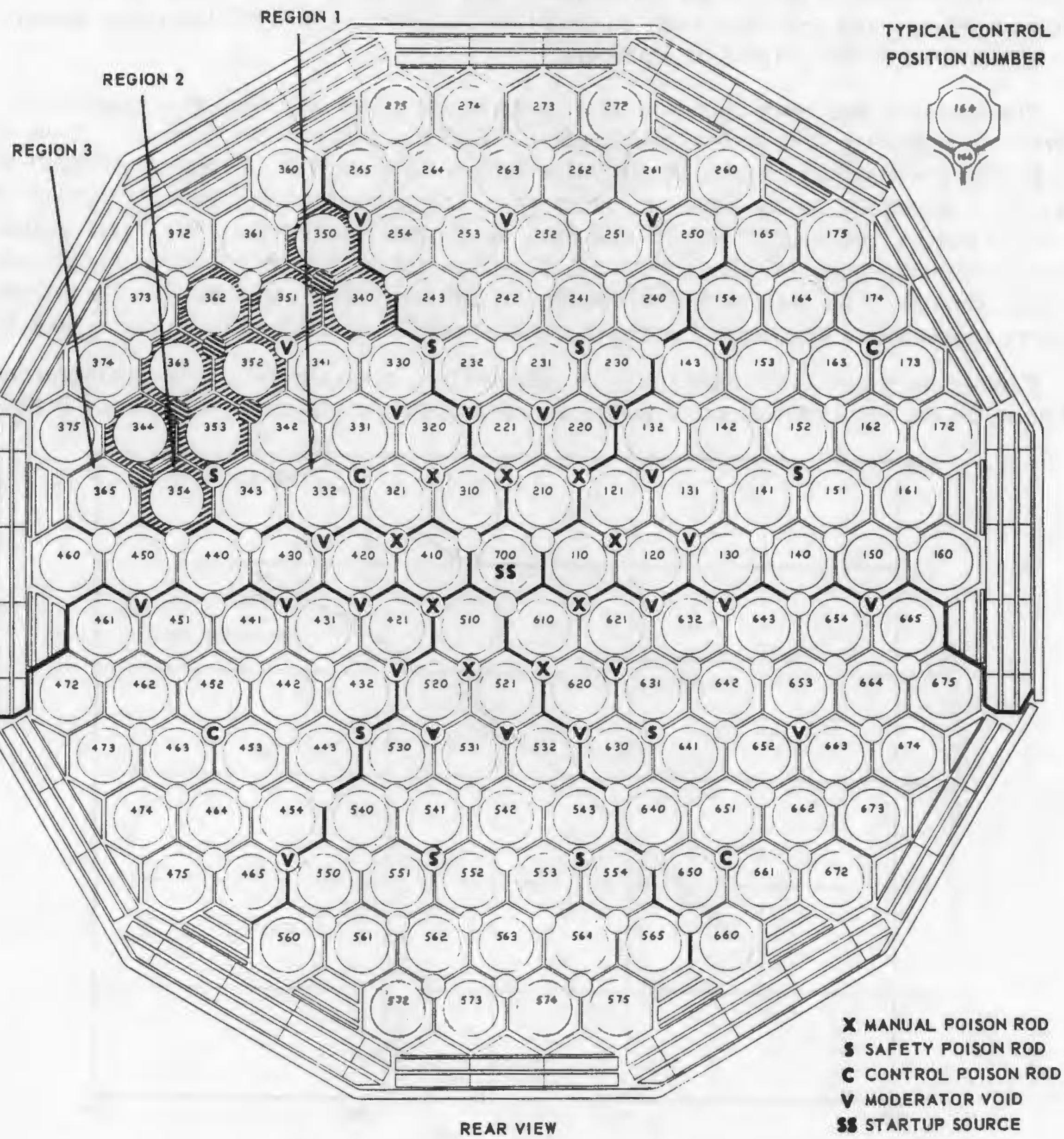

Fig. 22 – Cross sectional view of HTRE No. 3 nuclear mockup

pium oxide and metallic gadolinium to compare these materials with boron carbide to determine the possibility of using them in HTRE No. 3. A cross section of the HTRE No. 3 mockup is shown in Figure 22.

Criticality - The final preanalysis of the HTRE No. 3 nuclear mockup predicted an excess reactivity of 4.1 percent $\Delta k/k$. Early in the quarter the assembly was made critical with an excess reactivity, determined by rod calibrations, of 2.47 percent $\Delta k/k$. Since that time, a refined postanalysis showed an excess reactivity of 3.9 percent $\Delta k/k$. Thus, the overprediction in excess reactivity is now believed to be 1.43 percent $\Delta k/k$.

Using identical analysis methods for the design reactor (370-lb loading) as were used for the nuclear mockup, the excess reactivity was calculated to be 2.9 percent $\Delta k/k$, or 1.0 percent lower than that of the nuclear mockup. The difference in $\Delta k/k$ is the result of (1) minor differences in core composition, 0.2 percent; (2) differences in radial reflector volume and pressure shell composition, 0.2 percent; and (3) difference in core length and interaction effects, 0.6 percent.

The decision was made to add a 19th stage to each fuel cartridge as a means of increasing reactivity. The active core length of HTRE No. 3 is now 30.75 inches. This is 0.25 inch greater than the core length in the nuclear mockup. The calculated net result of adding this stage is an increase in reactivity of 1.0 percent $\Delta k/k$. Thus, HTRE No. 3 with 19 stages (390 lb U^{235}) should now have an excess reactivity exactly equal to that of the nuclear mockup (370 lb U^{235}), or 2.47 percent $\Delta k/k$. Figure 23 shows the calculated variation of k (clean) with U^{235} loading for the current 19-stage design. The broken curve represents a hypothetical power-flattened design in which the maximum N_H is 4.5.

Further increases in reactivity may be realized by increasing the hydrogen concentration in the core to an extent which the gross radial power distribution will allow. In gen-

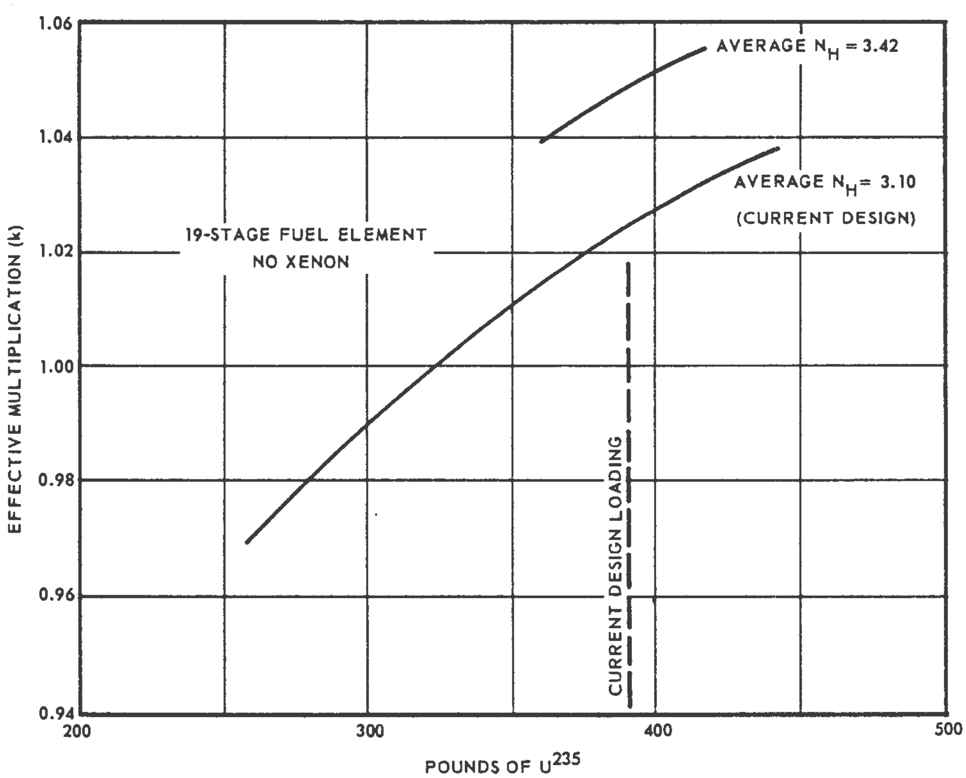

Fig. 23 — Reactivity versus loading, corrected by nuclear mockup criticality data, for HTRE No. 3; 19-stage fuel element, no xenon

eral, a 4.5 percent increase in total core hydrogen concentration will result in a 1.0 percent increase in effective multiplication.

Fuel element specifications have not changed from those established in the previous quarter. However, recent fine radial power measurements in the HTRE No. 3 nuclear mockup indicate a steeper fine power distribution than the one upon which the fuel element design was based. Some adjustment of fuel ribbon thicknesses will be required to compensate for the change in heat flux distribution. This work will be completed early next quarter.

During the quarter, xenon calculations were completed for the HTRE No. 3 reactor. These calculations were corrected by an empirical procedure which was based upon the observed gross discrepancy between HTRE No. 1 calculations and measurements. The final corrected predictions of reactivity loss caused by xenon as a function of operating time and power level are shown in Figure 24 for conditions between hot (1000°F neutron temperature), clean and hot, equilibrium concentration. Figure 25 shows the effect of xenon buildup and decay on reactivity loss following reactor shutdown from a hot, equilibrium xenon condition.

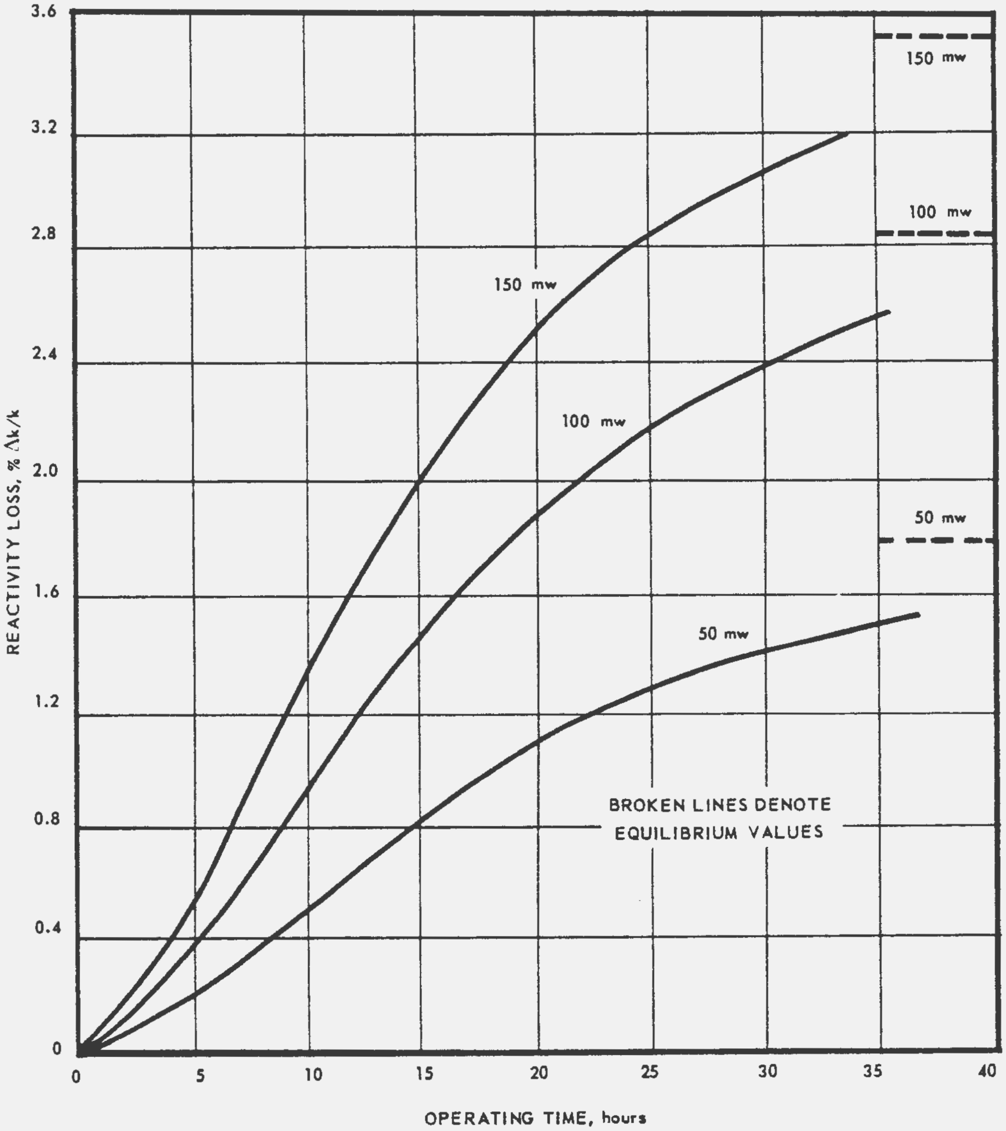

Fig. 24 – Predicted time variation of xenon reactivity loss, HTRE No. 3

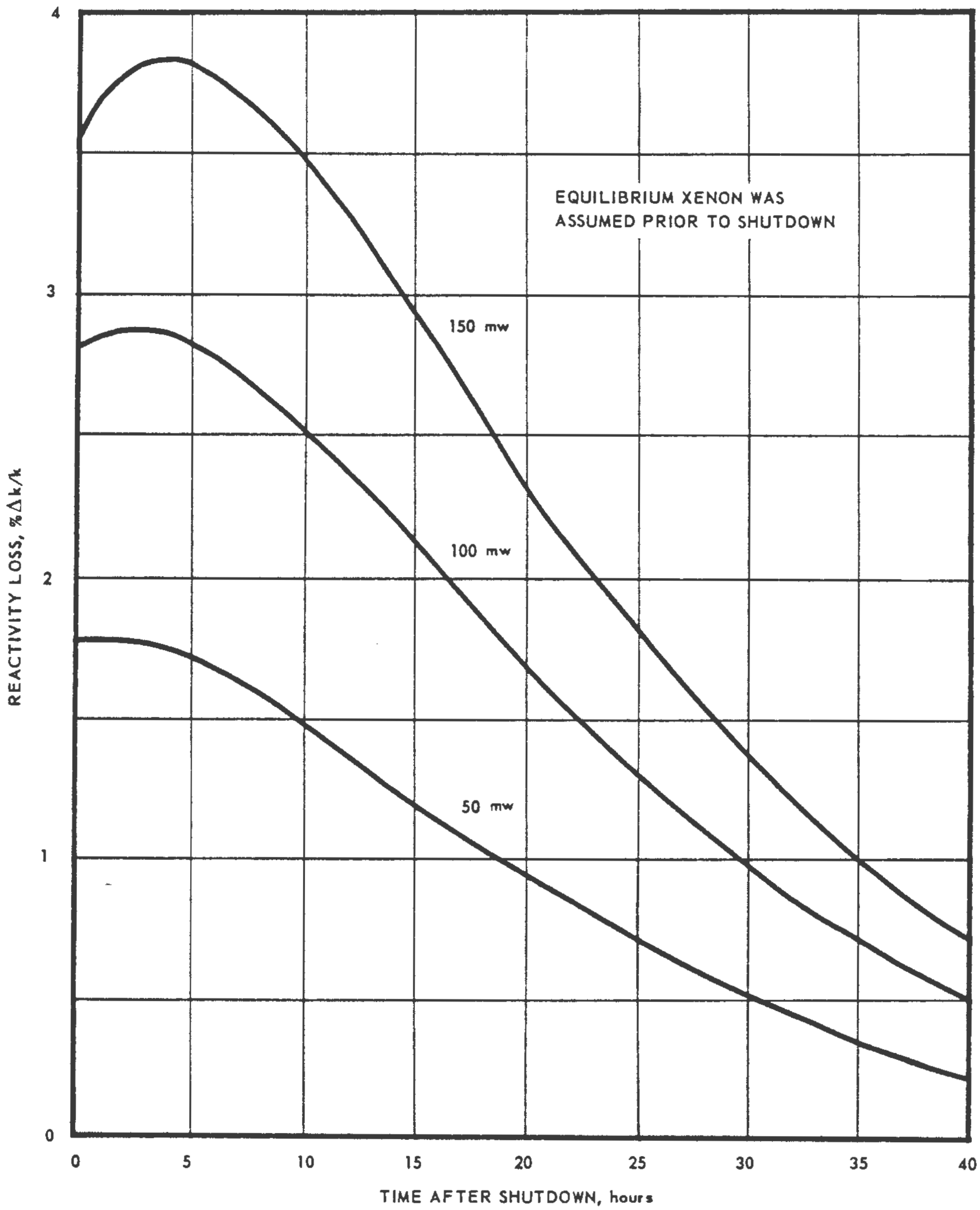

Fig. 25 – Predicted xenon buildup following reactor shutdown, HTRE No. 3

Using the standard inhour equation, the relation between a step change in reactivity and reactor period was derived. This relation is shown in Figure 26 for positive and negative periods.

Xenon override requirements for 1-hour startup following 100 hours of continuous operation at full power were compiled together with fuel depletion requirements, manufacturing tolerances, and calculational uncertainties. These data are shown in Table 4 for X39 and X211 engine operation.

If the final excess reactivity of the core were to be less than 4.5 percent $\Delta k/k$, the number of hours of full-power X211 operation would be limited by xenon poisoning. Figure 27 illustrates the relationship between hours of permissible full-power operation and the predicted cold, clean excess reactivity. The uncertainties shown in Table 4 have eral, a 4.5 percent increase in total core hydrogen concentration will result in a 1.0 percent increase in effective multiplication.

Fuel element specifications have not changed from those established in the previous quarter. However, recent fine radial power measurements in the HTRE No. 3 nuclear mockup indicate a steeper fine power distribution than the one upon which the fuel element design was based. Some adjustment of fuel ribbon thicknesses will be required to compensate for the change in heat flux distribution. This work will be completed early next quarter.

During the quarter, xenon calculations were completed for the HTRE No. 3 reactor. These calculations were corrected by an empirical procedure which was based upon the observed gross discrepancy between HTRE No. 1 calculations and measurements. The final corrected predictions of reactivity loss caused by xenon as a function of operating time and power level are shown in Figure 24 for conditions between hot (1000°F neutron temperature), clean and hot, equilibrium concentration. Figure 25 shows the effect of xenon buildup and decay on reactivity loss following reactor shutdown from a hot, equilibrium xenon condition.

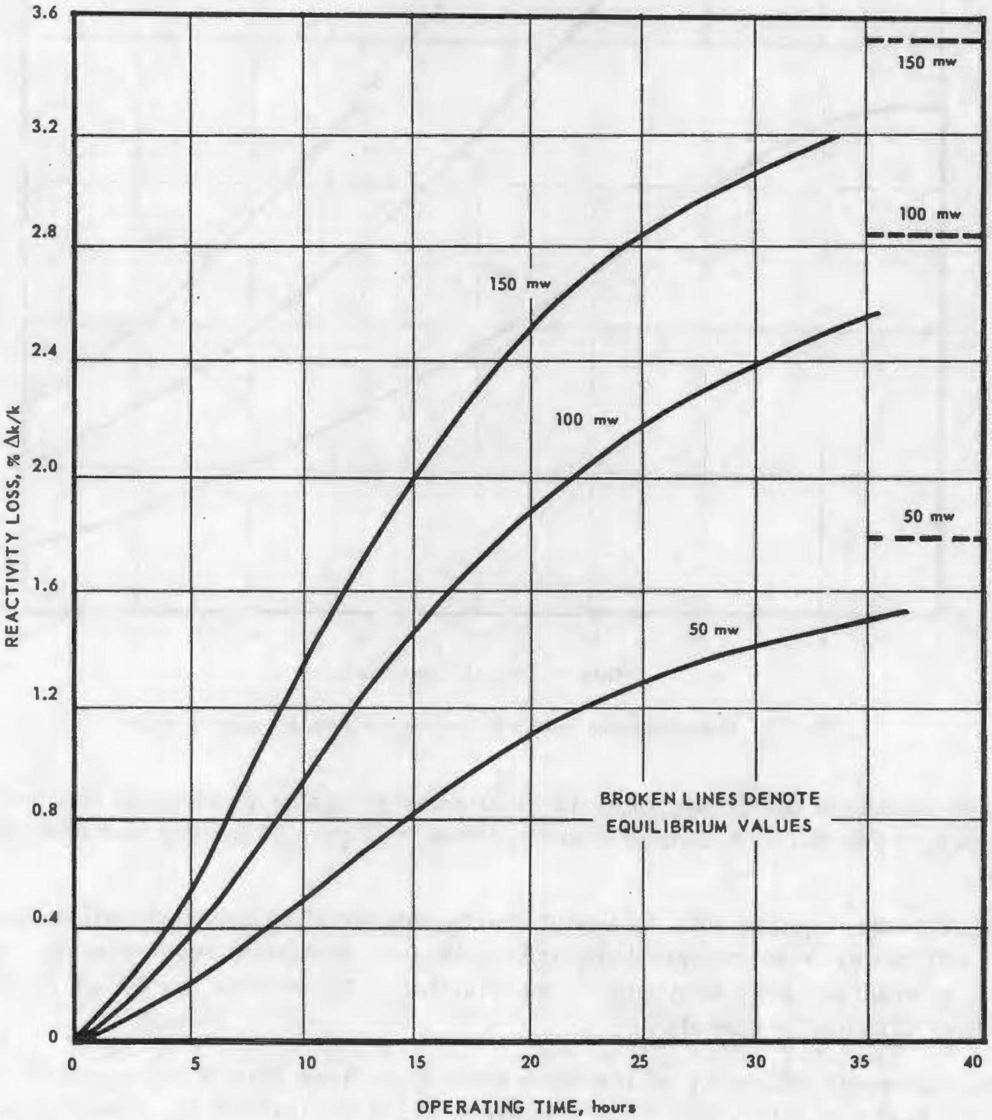

Fig. 24 – Predicted time variation of xenon reactivity loss, HTRE No. 3

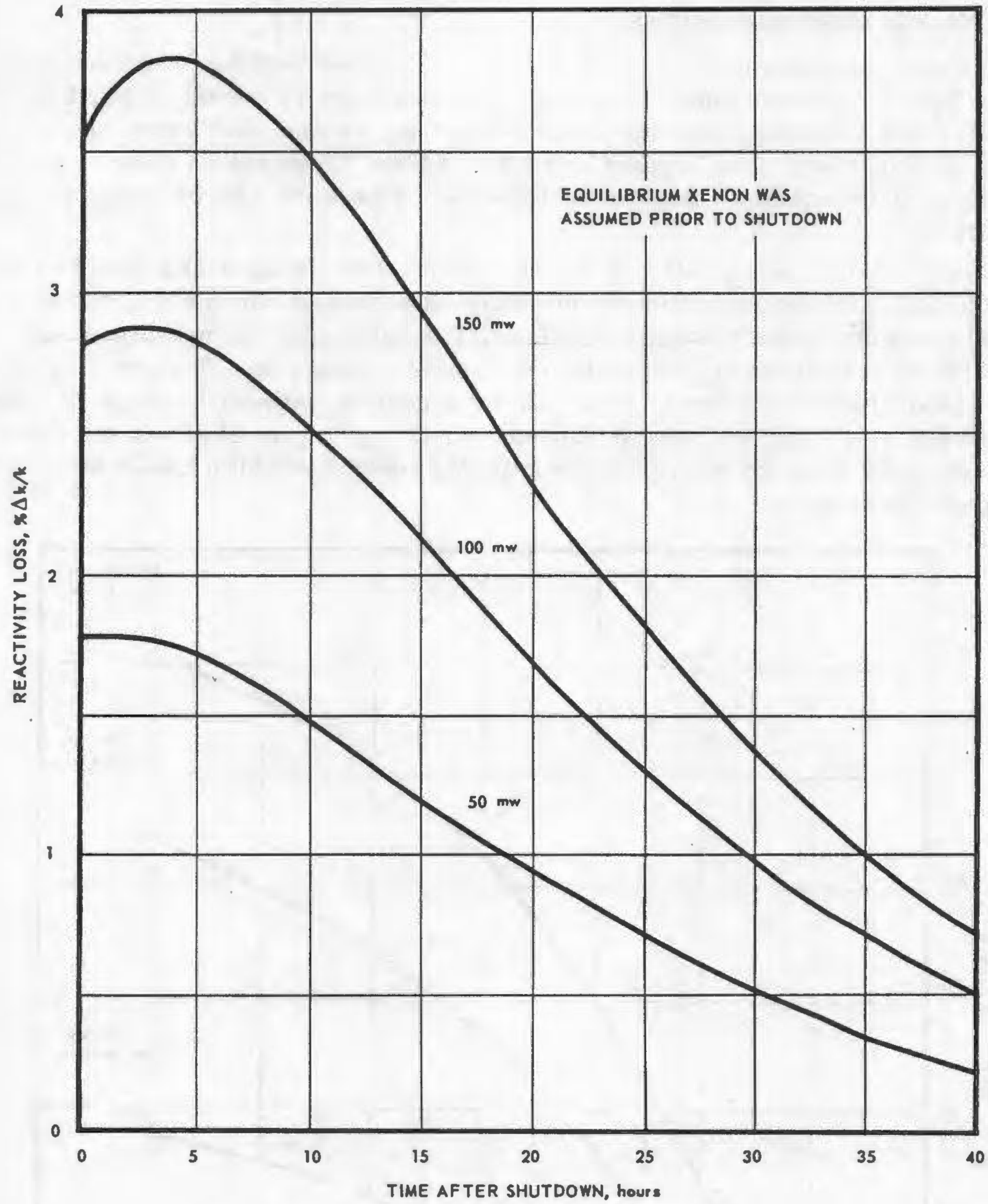

Fig. 25 – Predicted xenon buildup following reactor shutdown, HTRE No. 3

Using the standard inhour equation, the relation between a step change in reactivity and reactor period was derived. This relation is shown in Figure 26 for positive and negative periods.

Xenon override requirements for 1-hour startup following 100 hours of continuous operation at full power were compiled together with fuel depletion requirements, manufacturing tolerances, and calculational uncertainties. These data are shown in Table 4 for X39 and X211 engine operation.

If the final excess reactivity of the core were to be less than 4.5 percent $\Delta k/k$, the number of hours of full-power X211 operation would be limited by xenon poisoning. Figure 27 illustrates the relationship between hours of permissible full-power operation and the predicted cold, clean excess reactivity. The uncertainties shown in Table 4 have

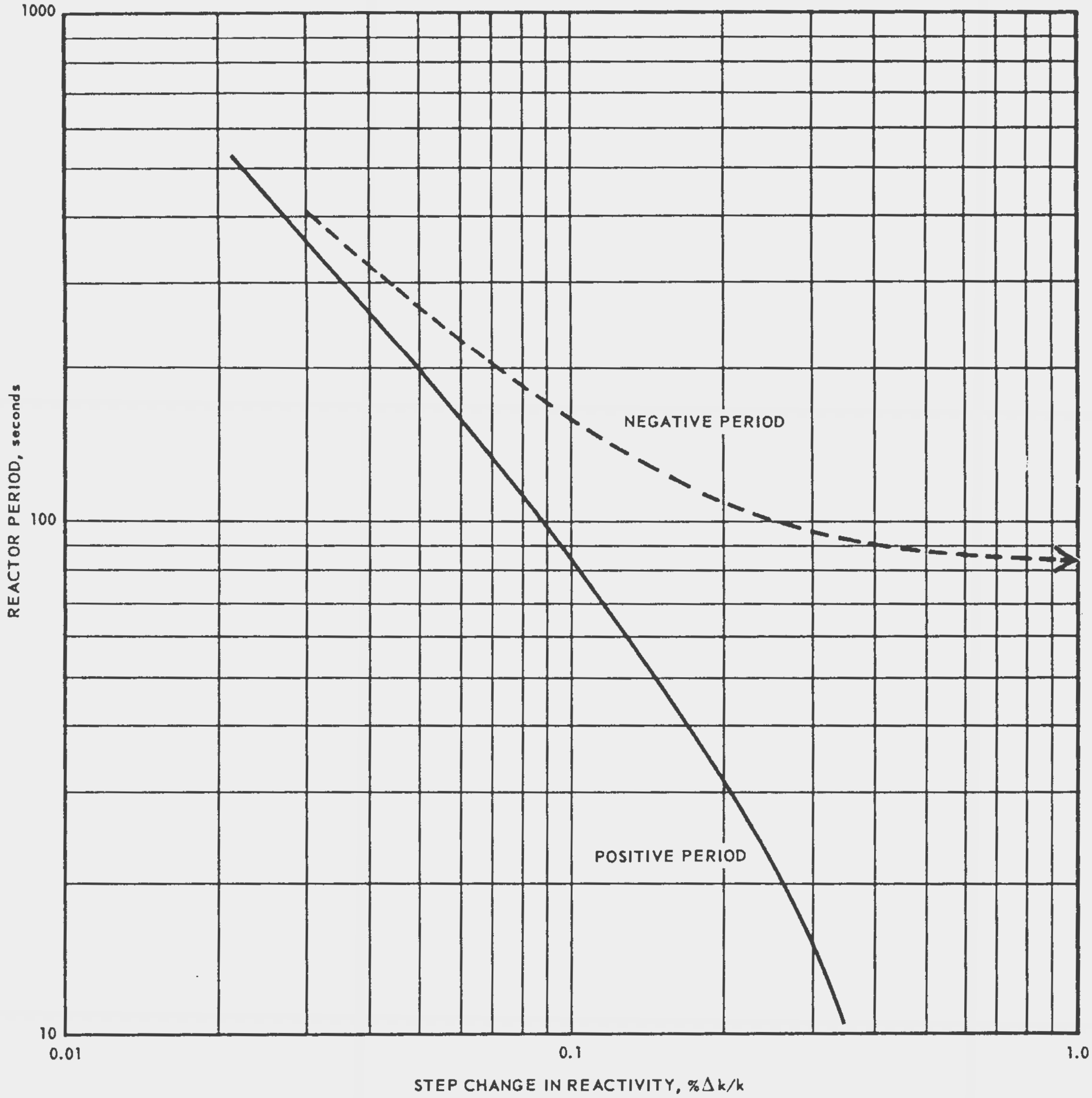

Fig. 26 – Predicted reactor period versus step change in reactivity, HTRE No. 3

been statistically factored into Figure 27 so that the curves represent the "probable" hours of operation.

Control Rod Evaluation - Recent reactivity measurements of a special europium oxide rod (0.60-inch diameter, 20-inch length, 1.52 g/cc Eu_2O_3) in the HTRE No. 3 nuclear mockup were compared with the B_4C rod measurements in the same positions. From these results the preliminary curves of total rod reactivity as a function of poison density were corrected. These corrected curves are shown in Figures 28 and 29. Figure 28 shows the total reactivity value of the inner 24 rods (21 shim and 3 dynamic) and the outer 12 shim rods as a function of europium oxide density. On the basis of these data, a europium oxide rod density of 3.0 g/cc was tentatively chosen for HTRE No. 3 requirements. This should provide a total control capacity of about 5 percent Δk/k, of which more than 3 percent Δk/k would be controllable with the inner shim rods alone. For comparison, Figure 29 shows the calculated reactivity of the inner 24 rods as a function of

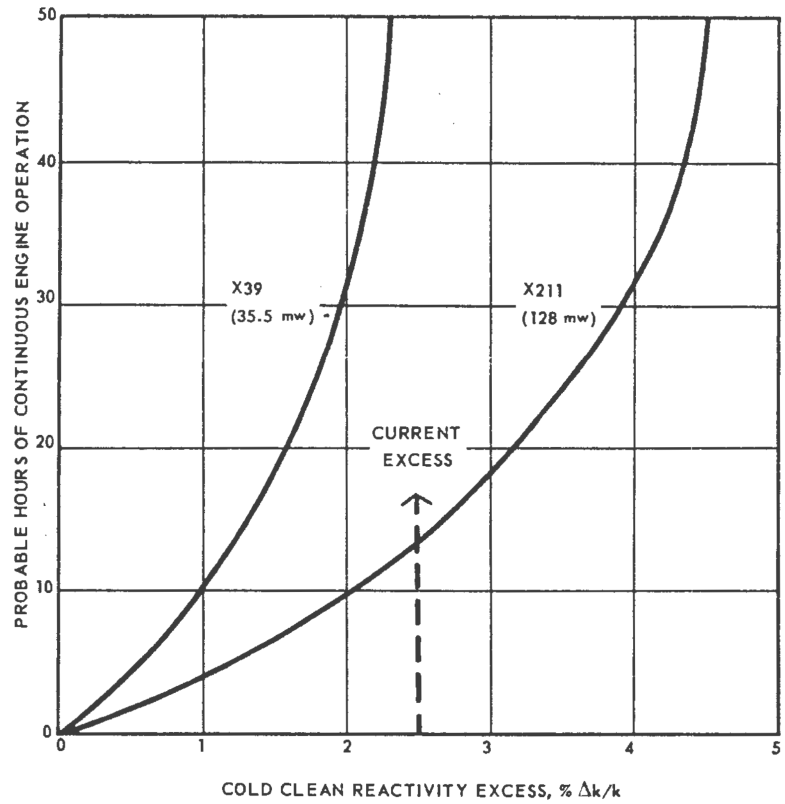

Fig. 27 – Probable hours of continuous operation versus excess reactivity, HTRE No. 3

poison density for both europium oxide and gadolinium metal. Reactivity experiments are now under way in the nuclear mockup with gadolinium rods to confirm these analyses. Further measurements are also planned for high-density europium oxide (HTRE No. 3 prototype) rods.

Power Distributions - The HTRE No. 3 nuclear mockup power distributions shown in Figures 30 to 32 have been normalized to the average power in the core. Circumferential power distributions were determined on the outer fuel layer in each of the four cylinders of the respective tubes. In tubes 210, 220, 230, 240, 250, 260, 261, 272, 273, 241, and 242, such circumferential distributions were determined in the middle of stage 5; in the

TABLE 4

EXCESS REACTIVITY REQUIRED FOR XENON OVERRIDE

	For X39 Operation, % Δ k/k	For X211 Operation, % Δ k/k
Xenon override for startup 1-hour after shutdown following 100 hours operation	1.4 ± 0.4	3.3 ± 1.0
Estimated temperature coefficient	0 ± 1.0	0 ± 1.0
Fuel depletion (30,000 mw-hr)	0.1	0.1
Manufacturing tolerance	0 ± 0.5	0 ± 0.5
Total	1.5 ± 1.2	3.4 ± 1.5
Estimated required excess reactivity	2.3	4.5

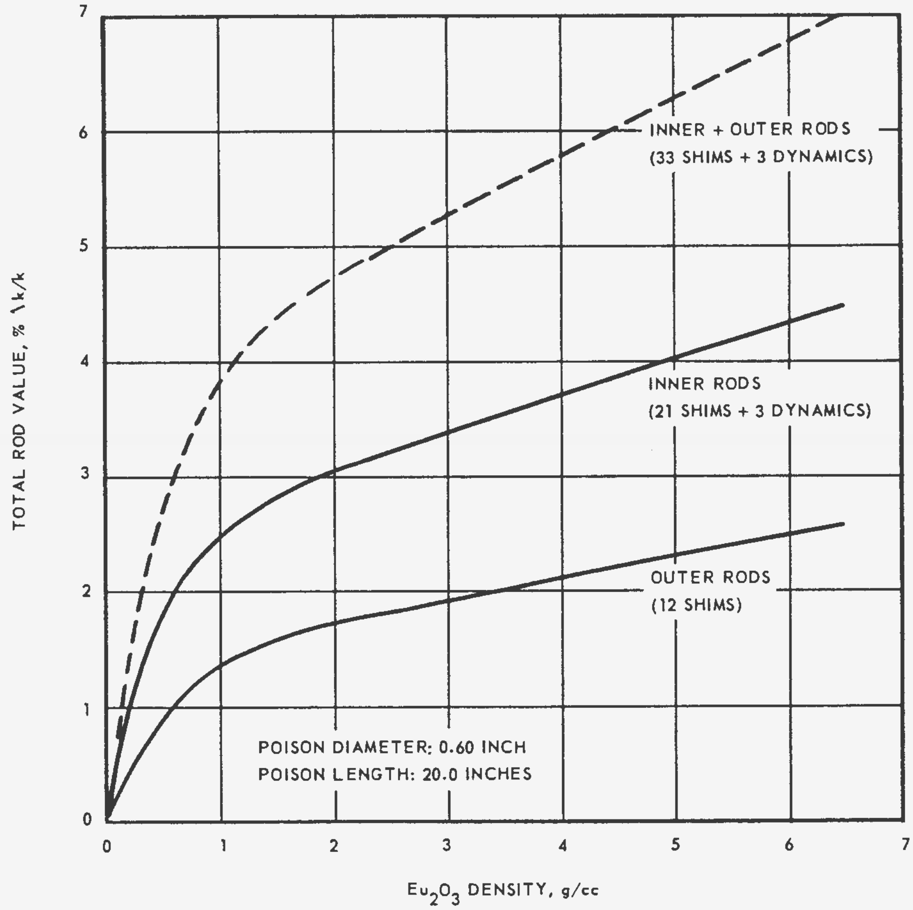

Fig. 28 – Calculated total rod value versus poison density, HTRE No. 3

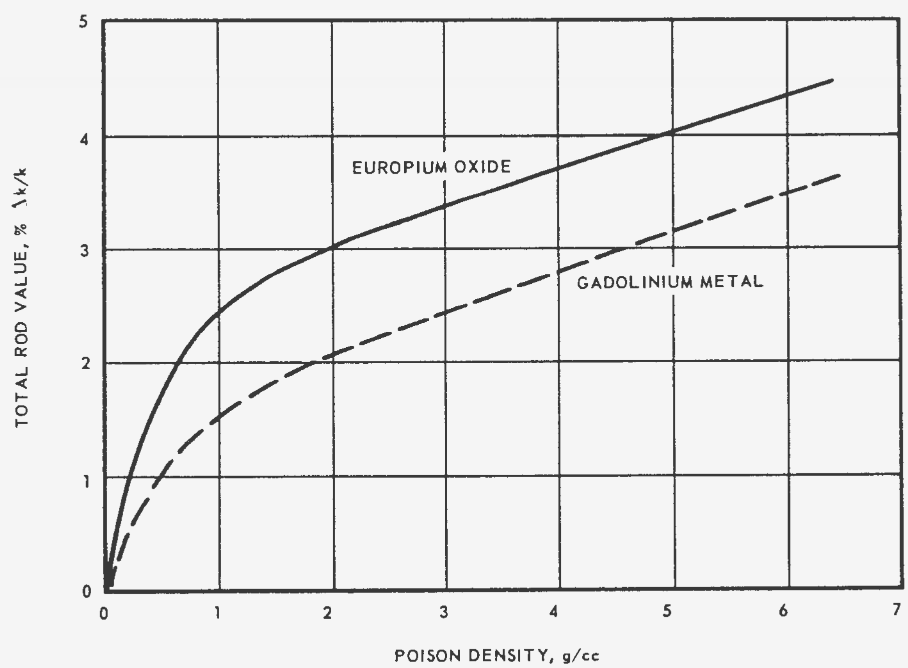

Fig. 29 – Calculated total value of inner 24 rods versus poison density, HTRE No. 3

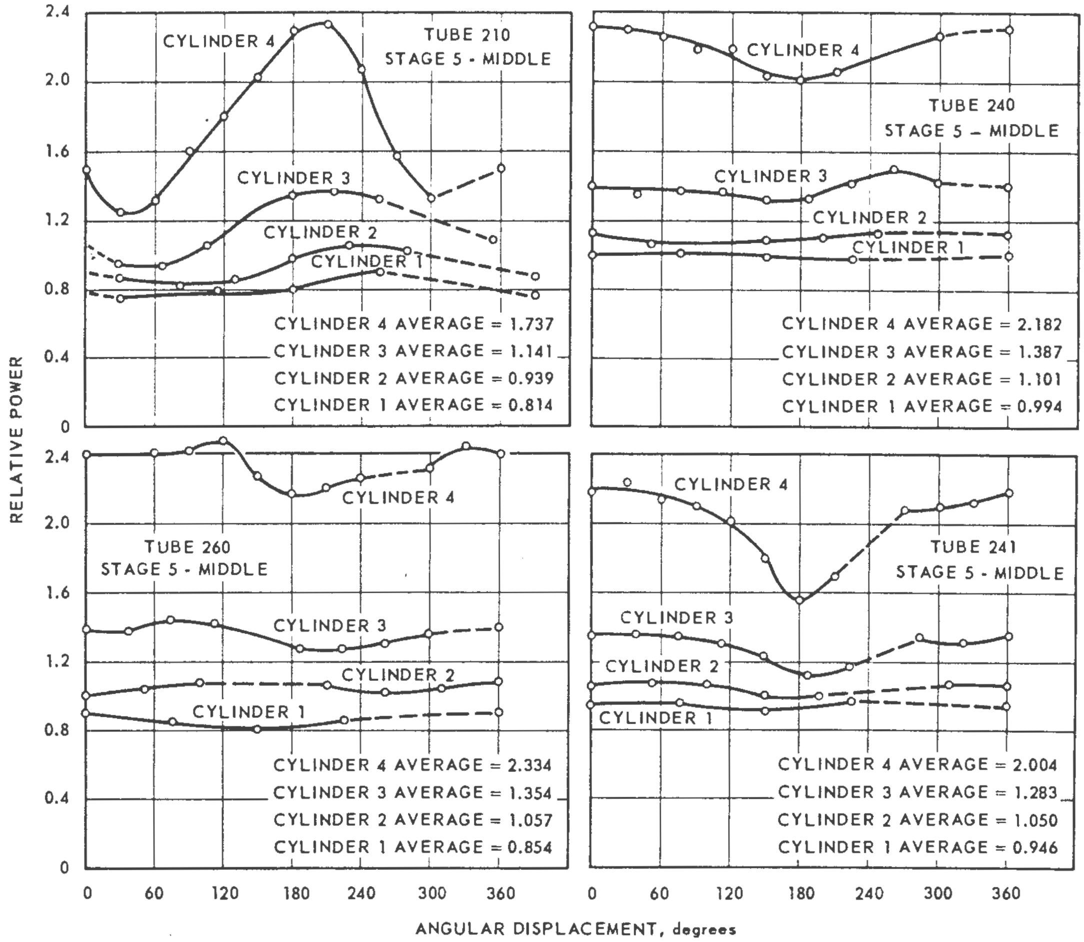

Fig. 30 – Circumferential power profiles, HTRE No. 3 nuclear mockup

middle of stage 2 in tubes 230 and 260; in the middle of stage 10 in tubes 210, 230, and 260; and at the front and middle of stage 1 in tube 210. The circumferential angular displacement was taken in a clockwise direction from the zenith when viewed from the rear of the core. Figure 30 shows representative circumferential distributions. Each plot lists the arithmetic average of the points on the curve. The fine radial power distribution determined in tube 230 is shown in Figure 31.

The longitudinal power distribution in tube 230 is shown in Figure 32. The solid line indicates a power distribution as determined by foils exposed at the middle of each stage only. The dotted lines connect other points measured in each stage, and thus present an approximation to a fine longitudinal power distribution in the respective stages.

Effort was applied to improving the theoretical calculation of the gross longitudinal power. In particular the effect of the forward end reflector was studied. It was found that the use of the Behren's leakage correction in the determination of end reflector constants improves both reactivity and power distribution correlation. The discrepancy between the calculated and the measured power distribution is reduced to less than 2 percent with this procedure.

A study was made to calculate the effect on longitudinal power distribution of hydrogen migration in the HTRE No. 3 moderator cells. Figure 33 shows the results of this study.

[redacted]

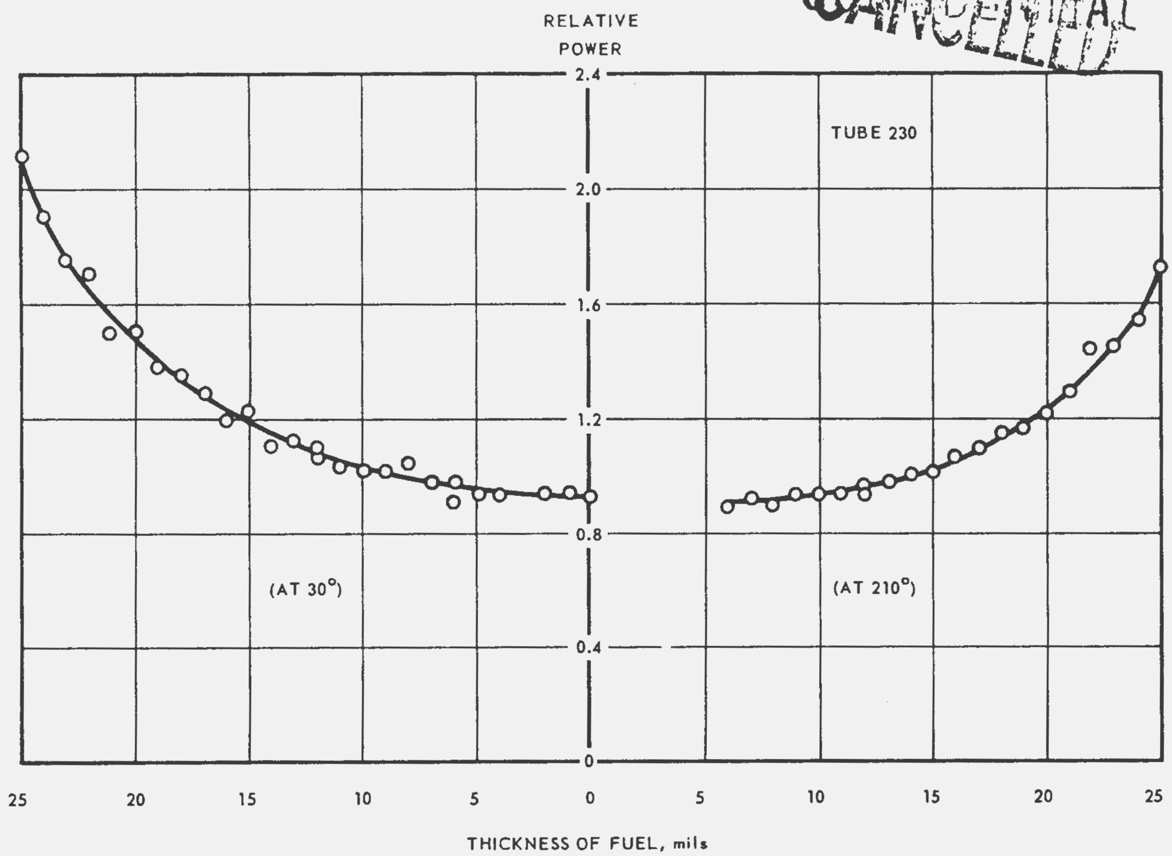

Fig. 31 – Fine radial power profile, HTRE No. 3 nuclear mockup

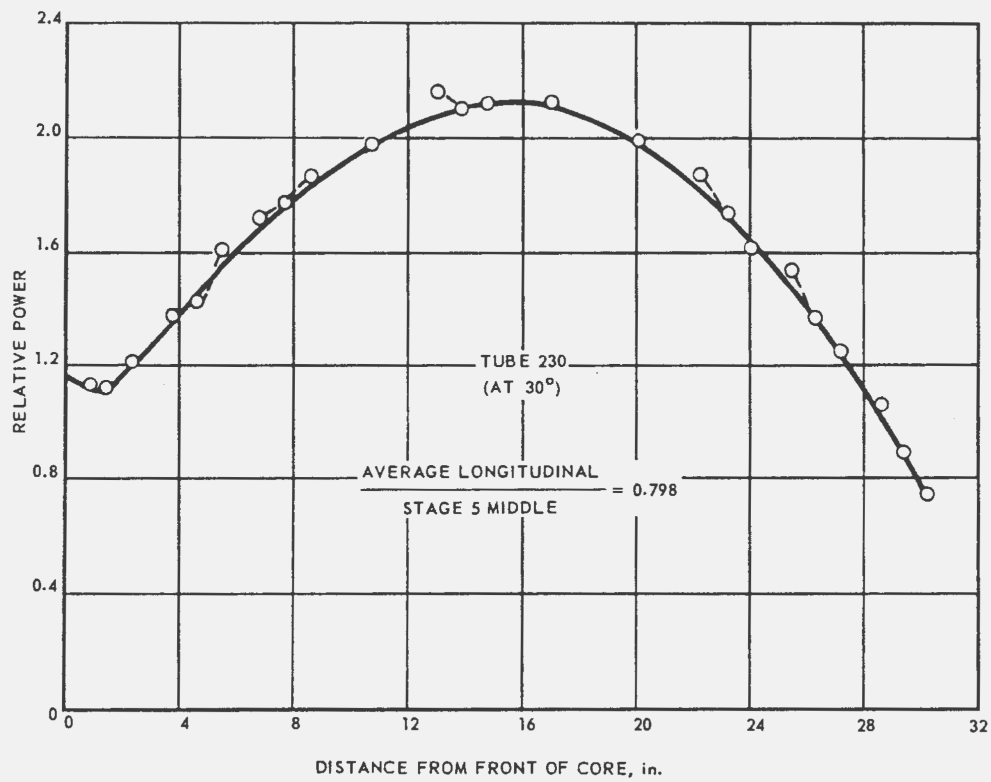

Fig. 32 – Longitudinal power profile, HTRE No. 3 nuclear mockup

[redacted]

[redacted]

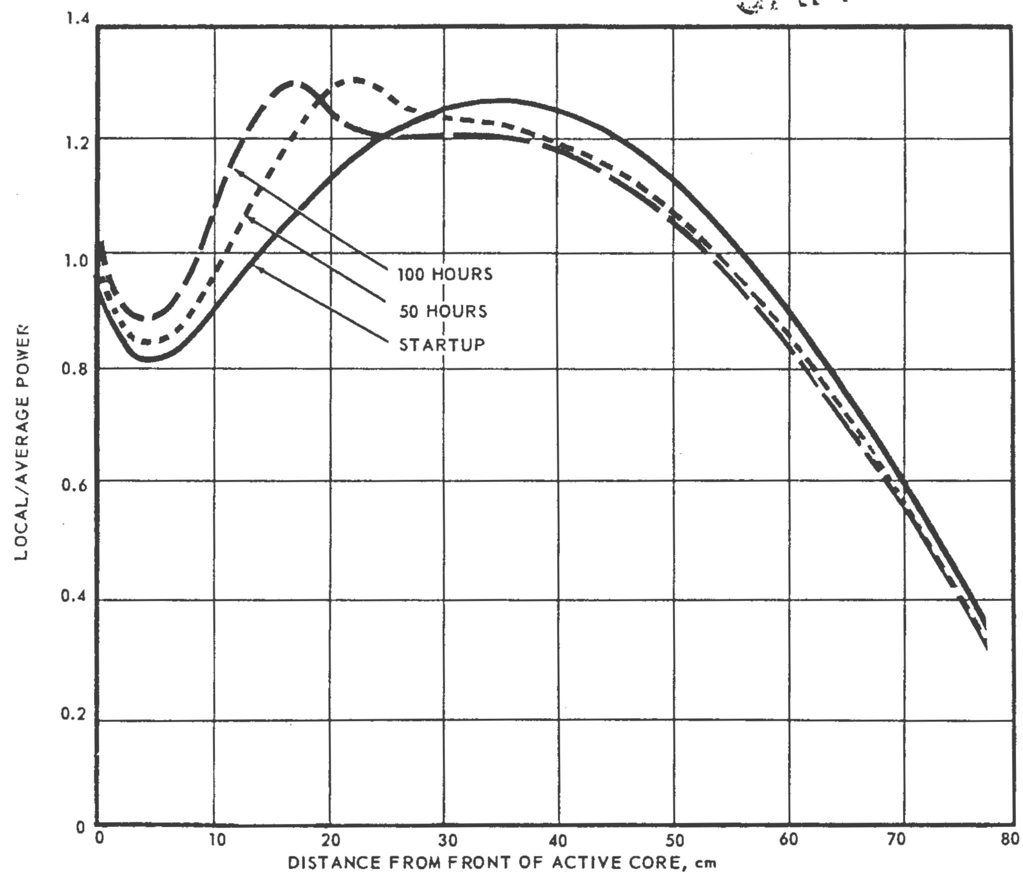

Fig. 33 – Predicted gross longitudinal power profile, HTRE No. 3

The hydrogen distributions used were those obtained from tests on bars subjected to a longitudinal temperature gradient. The effect of radial migration was not considered.

The gross radial relative power distribution of Figure 34 is a plot of the ratios of tube average power to core average power as a function of radial distance from the center of the core. The measurements for the traverse were made in tubes 210, 220, 230, 240, 250, and 260. The largest deviation from flat power may be observed in tube 220 in which the average tube power is approximately 16 percent below average core power. The highest average tube power, 6 percent above core average, may be seen in tube 240.

Gamma Ray Mapping - Determination of gamma ray dose rates inside the core, in the reflector, and outside the shield of the HTRE No. 3 mockup by using film dosimeters was initiated. Complete longitudinal power mappings through the center of the core from 18 inches in front of the reactor to 72 inches from the rear tube sheet have been completed. Also, a longitudinal traverse outside the Plexiglas has been completed. Radial traverses at the end planes and midplane in the core have been made. In addition, a radial traverse from the outer shield surface to 96 inches from the shield has been completed. The reduction of the data to roentgen/hour-watt has not been completed.

Mechanical Design

The core assembly shown in Figure 35 was prepared during the quarter to establish the final design concept, to review the functional operation, and to integrate the components into a complete assembly.

[redacted]

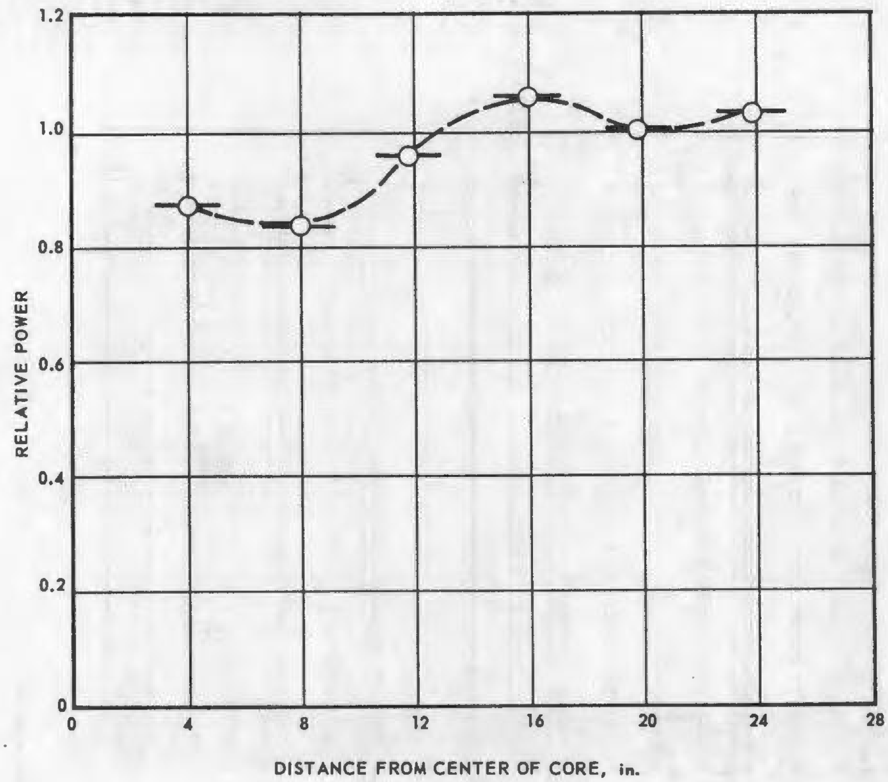

Fig. 34 – Gross radial power profile, HTRE No. 3 nuclear mockup

The stainless steel cooling tubes were eliminated from the present HTRE No. 3 reflector design because the predicted operating temperature of the beryllium is not to exceed 1100°F and the tube installation presented a difficult fabrication problem.

A one-half-scale steel model of an aft tube-sheet design was subjected to an experimental stress analysis. Test results on a simply supported edge condition and a fixed-edge condition established that the design is satisfactory insofar as bending loads are concerned. The results of the experimental analysis correlated very well with the theoretical stress analysis of the tube sheet. Tests on the model tube sheet loaded in-plane are inconclusive.

Moderator Development

Accomplishments in solid moderator development during the quarter included:

1. Hydriding of the HTRE No. 3 critical experiment moderator sections at N_H values of 2.50, 3.00, and 3.95.
2. Development of a hydriding process to produce hydrided zirconium sections with an N_H of 4.10.
3. Techniques for precision-forming and dimensioning of molybdenum and stainless steel hexagonal tubing.
4. Improved welding techniques of formed hexagonal tubing.
5. Improved assembly techniques incorporating the use of the "floating" end piece.
6. Design and procurement of new and improved tooling.

Experience gained in processing the clad moderator sections for HTRE No. 2 nuclear mockup inserts revealed that both design revision and additional process development would be necessary. Weld joints at assembly closures between cladding and end pieces

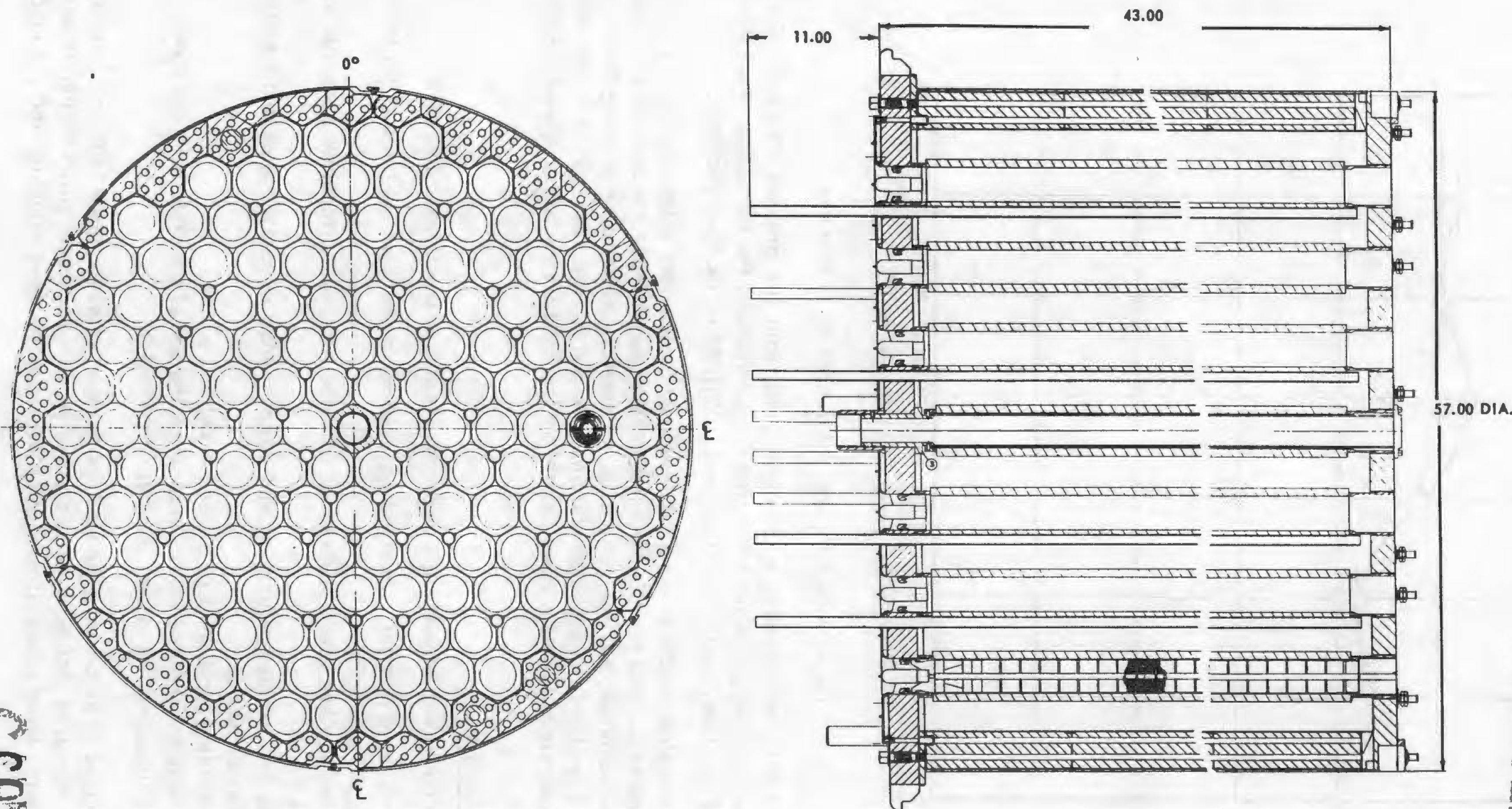

Fig. 35 – HTRE No. 3 core assembly

were too massive; final fitting operations after end tube attachment required higher temperatures; more precise dimensional control of cladding sections was mandatory; and tests on completed sections indicated that metallurgical bonding on all surfaces would be required for the HTRE No. 2 operational insert, instead of internal surface bonding only.

The welding of molybdenum and 446 stainless steel moderator cladding has been improved this quarter. Yields on molybdenum shapes now are in the order of 25 percent as compared to less than 5 percent at the beginning of the quarter. The welding jigs and tooling are being redesigned for additional improvement in weld properties and continuity.

During the past quarter some 300 zirconium pieces were hydrided to N_H values of 2.5, 3.0, and 3.95 for the HTRE No. 3 critical experiment. A fourth process was developed for an N_H of 4.10. The possibilities of developing hydrided zirconium at higher N_H values is being investigated both by GE-ANPD and by the TAM Division of the National Lead Co.

TAM has reported obtaining an N_H of 5.2 by using alternate heating and cooling cycles on a 1-inch-diameter by 3-inch-long piece of zirconium. The specimen was in a hydrogen atmosphere when at maximum temperature (1620° to 1650°F) and in an argon atmosphere when the piece was being heated or cooled. No surface cracks resulted from the temperature cycling. Successful application of this process to large, hollow, hexagonal sections that would have acceptable service properties has not yet been attempted.

Metallurgical bonding of all cladding materials is assumed to be required for reactor moderator sections. The internal swaging process has been changed to a heated die block operating at 1600° to 1650°F, which includes heating the work piece in the die block in an attempt to accomplish this bonding. This equipment is now installed and is in the process of being tested.

Laboratory tests have established that 750 psi and 1450°F under optimum conditions develop bonding between the various moderator section components. To further insure complete metallurgical bonding of the cladding, an autoclave, capable of applying up to 1125 psi gas pressure to full-size moderator sections heated to 1625°F, is being installed. Sections swaged in the new hot die will be treated for a minimum of 1 hour in the autoclave to promote bond diffusion.

As an alternative cladding method designed primarily to eliminate the need for forming and machining hexagonal sections of core or cladding, TAM has been developing a hot-die forming technique. Basically, the technique consists of assembling a moderator element made entirely of cylindrical parts.

A test was conducted to determine the possibility of controlling hydrogen migration by using a barrier in a moderator section subjected to a temperature gradient. A zirconium hydride specimen containing a molybdenum barrier was subjected to a temperature gradient for 100 hours. The molybdenum proved effective in controlling the migration of the hydrogen.

2.33 FUEL ELEMENTS

Fuel Sheet Production

Two experimental fuel-sheet production runs were made. In one run, enriched fuel sheet for critical experiment and MTR cartridges was produced to HTRE No. 3 specifications. In the other run depleted fuel sheet for HTRE No. 3 burner rig cartridges was produced. In the enriched-fuel run four minor variations in frame and core were evaluated with respect to their effect on core-width spread. The data obtained on these four variations showed that no advantage was gained with respect to spread in core width. It was observed that the spot-welding of clad stock was facilitated when the core and frame were more uniform in thickness.

Data accumulated in the depleted-fuel run showed:

1. The flattest ribbon and the most rectangular core were achieved with the 0.002-inch concave hot rolls in conjunction with the 0.001-inch crowned cold rolls, with or without oil used on the hot rolls.
2. Oil on the hot rolls tends to decrease core width, especially for thicker ribbon.
3. Oil has no effect on rectangularity of core or flatness of ribbon.
4. Using 0.001-inch crowned cold rolls results in a smaller core width and a more rectangular core than using 0.002-inch crowned cold rolls.

Mechanical Development

Fuel Cartridges - The number of fuel stages per cartridge has been increased from 18 to 19, and the cartridge nosepiece has been modified to accommodate the extra fuel.

Designs of the fuel element, bellmouth, nosepiece, tailpiece, and rail were finalized for critical experiment and dummy runs during the quarter. The method of attaching the fuel elements to the rails is still under development, and both metallurgical and mechanical joints are being considered. The feasibility of assembling fuel element cartridges by induction-brazing the comb to the rail has been demonstrated.

Burner Rig Testing - At the beginning of this quarter, 11 fuel elements for HTRE No. 3 had been tested in the burner rig. Of these, four were successful tests in that they completed 100 hours at a temperature of 1850°F and at a dynamic head in the last stage of 6 psi without having the pressure loss coefficient ($\Delta P/q$) increase by more than 10 percent. Of these four, the XR-25 had shown the best performance and was proposed for the HTRE No. 3 reactor. With the success of the XR-25, further burner rig testing has been directed primarily toward confirming the XR-25 performance data.

A 50-hour test has been conducted using the new induction-heating test section in the small burner rig. The primary purpose of the test was to gain operating experience and to determine the amount of core iron necessary to heat multiring fuel elements uniformly. The test indicates that the induction heater can run at maximum output for extended periods of time. Therefore, with more operating experience and minor adjustments in the test parameters, the induction heater should begin to yield meaningful test data.

Reactor Irradiation Tests

Two irradiation tests on HTRE No. 3 fuel elements were conducted in the MTR this quarter on six-stage cartridges, each stage containing 12 rings. Desired operating conditions in these tests were:

1. Maximum temperature - 1850°F.
2. Dynamic head, exit in last stage - 5.6 psi.
3. Time - 100 hours.

XR-22 - The XR-22 test ran for 16 hours at calculated dynamic heads varying from 5.07 to 6.5 psi and at a maximum indicated temperature of 1850°F before fission product release was detected by the system instrumentation. With the MTR operating at 40 megawatts, the maximum indicated thermal neutron flux was 5.5×10^{13} neutrons/cm^2-sec and the power generated by the sample was 248 Btu per second. Postirradiation examination of this cartridge will be conducted to determine the location and cause of fission fragment release.

XR-25 - The XR-25 was the most successful MTR fuel cartridge test on an HTRE No. 3 design to date. The sample ran for 125 hours and 7 minutes at 5.6-psi dynamic head and 1850^{o}F maximum indicated temperature. Thermocouple performance was excellent; of the 12 thermocouples 10 were operating at the end of the test. Of the two thermocouples not working, one was broken at the pressure cap during insertion, and the other, the thermocouple on ring 12 in the hottest quadrant, failed at about 65 hours when the platinum lead broke just behind the weld on the plate. The success of the XR-25 thermocouples is attributed to supporting and protecting the leads within the drawbar and along the sample from abrasion and differential thermal expansion.

Postirradiation inspection of the XR-25 showed severe damage at the trailing edges of the last stage, although no distortion was observed at the leading edge of the stage. This was the only stage of the six-stage cartridge damaged during the test, and the pressure loss coefficient increased by less than 2 percent.

2.34 CONTROLS AND INSTRUMENTATION

Core Instrumentation

Detailed design of all phases of HTRE No. 3 core instrumentation is presently in progress. It is anticipated that all drawings will be released during the next quarter.

The lead wire for fuel element thermocouples will be platinum - platinum/10 rhodium with an Inconel sheath. Plate temperatures will be measured using single-conductor "ceramo" construction; air temperature measurements will utilize two-conductor "ceramo" construction.

During the previous quarter difficulty was encountered in the air thermocouples because of low transient response in the probes. At five time constants the first probes gave values between 80 percent and 90 percent, as opposed to theoretical values of 99.3 percent. It was decided that the chief reason for these low values was the conduction of heat away from the thermocouple junction through the lead wires to the mass of the insulating supports. To reduce the amount of heat conducted away from the junction, greater immersion of the lead wire was indicated. Testing of a probe with 10-mil lead wires, with the junction supported between supports 1 inch apart, confirmed the judgement that immersion depth had caused the errors in the previous samples. Further experimentation produced a sample that was constructed with 20-mil wire, having 3/4 inch between supports. This probe attained 95 percent of final value at the end of five time constants. It was decided that this probe would be satisfactory, and since the strength is materially increased, three such probes will be constructed.

Shield Instrumentation

The shield-heating-rate sensor underwent extensive study from a heat transfer standpoint during the quarter. The results of this study indicate that three ranges of sensors are needed to determine the entire range of possible heating rates to be encountered in the primary shield.

Nuclear Sensors

Development on nuclear sensors for HTRE No. 3 continued with the construction of a fission chamber cluster model designed for test at ITS. The cathode follower circuit has been developed, and tests performed to determine the microphonic characteristics of the circuit. Manufacturing drawings for final models have been issued.

Models of the compensated and uncompensated ionization chambers for ITS testing have also been constructed. Manufacturing drawings for final models of both chambers have been issued.

A model of the new fission fragment detector has been built in accordance with the design completed last quarter.

Control Rods

HTRE No. 3 control rod development during this quarter has been confined to (1) determining the proper poison material, and (2) fabricating and testing prototype circular clad control rods.

Efforts have been made to determine the rare earth that will be most effective as a poison for HTRE No. 3. Boron cannot be used because it develops excessive chemical reactivity at HTRE No. 3 operating temperatures. Nuclear data suggest that europium is the most logical element since its epithermal neutron absorption is relatively high. These data have been confirmed in tests on the relative poison effectiveness of europium, gadolinium, and samarium for a system closely approximating the neutron spectrum of the HTRE No. 3 design.

Fabrication of initial pieces was performed with cold-packed Eu_2O_3 in 80 Ni - 20 Cr alloy packed in 310 stainless steel tubes, cold-worked by swaging to 50 percent reduction in cross section area. Because of the low poison density produced using "as received" Eu_2O_3, the oxide was sintered to 2730°F before processing. After processing, the density of the poison core was 85 percent of the theoretical density. Studies for producing higher-density poison cores are continuing.

A control rod poison tip was tested for 96 hours at 1950°F. Results from this test indicate that there is no reaction between the Eu_2O_3 and the 80 Ni - 20 Cr or the 310 stainless steel.

Actuators

A service test model of the pneumatically retracted, latched safety actuator was completed, and an operating panel was built to cycle the unit automatically. The test operation led to further simplification of design, to a redesign of the latch to insure fail-safe performance, and to reduction in over-all length of the actuator.

The design of the shim actuator has been finalized, and manufacturing drawings are being readied for release. The basic feature of the shim actuator is the conversion of the rotary motion of the drive head to a 20-inch linear motion of the guide tube which is directly coupled to the poison tip. Extensive tests have been conducted on various shim actuator prototypes; some units have accumulated more than 10,000 full-stroke cycles, operating continuously without failure.

Development testing of the HTRE No. 3 dynamic actuators has continued with special emphasis on the dynamic seals and the extensometer mounting details. Detailed technical requirements for components of the dynamic actuator hydraulic supply package were determined. Parts were ordered for three complete prototype systems, and final design of the package was started. Since recent tests revealed that very high oscillating pressure surges were occurring during the unloading valve cycle, an adjustable relief valve will be used to control the accumulator pressure. This change will result in a shorter pump life because the pump will be under continuous load, but it will eliminate the shock pressures that have accompanied the unloading valve cycle.

Circuitry

The final design drawings, displaying all information necessary to manufacture power range and intermediate range servo units, were completed and supplied to the vendor during the quarter. The design parameters were changed to require a linear increase in power, rather than a logarithmic increase as in the earlier equipment. This change necessitated the use of a new linear potentiometer assembly.

The magnetically regulated filament power supply for the intermediate range circuit was refined to yield a much better regulated filament current with line voltage changes. The value of the current-compensating resistor was altered so that, for a ± 10 percent line voltage change, the output current changed only 0.013 percent. This is a considerable improvement over the previous model, which showed a 0.2 percent variation with the same line voltage fluctuation.

Preliminary test of the simulated intermediate range (automatic startup) system disclosed that minor changes were necessary for proper system performance. To obtain the desired transient response, a new bias current source was built into the equipment to supply a rest current of 30 micro-microamperes for the log diode. A new filter network was designed for the period amplifier. This network furnishes a double break at 0.25 radians and provides an optimum, noise-free signal for period indication. The final manufacturing drawings for the log flux preamplifier were completed and issued during the quarter. Equipment designed especially for test of this unit has been constructed and found to be satisfactory.

Tests on the power range system model showed the need for minor circuit revisions. A phase correction needed in the reference voltage of the modulator was accomplished by providing a small transformer, rather than the R-C circuit initially used. The output stage of the cathode follower was found to be overheating. This situation was corrected by adding another tube of the same type, connected in parallel with the original stage. An increase in gain in the position loop amplifier was required to provide enough current to drive a new hydraulic valve. The increase was accomplished by changes in the component parts of the circuit.

Preliminary tests of the shim control service test model in the simulated system demonstrated erratic performance of the electronic control circuits. It was therefore necessary to redesign this system completely. The new system uses a micropositioner relay-controlled device that uses no tubes except for the demodulator. This new circuit has eliminated the need for a separate power supply and other electrical components. Tests in the simulated system resulted in accurate and repeatable performance. Manufacturing drawings were completed and issued to the vendor during this quarter.

Present plans do not call for any general change in the data recording system. It is anticipated that the present scanner arrangement will be utilized for the HTRE No. 3 tests with the X39-5 engines. This scanner system must be expanded to include ten scanners rather than the present seven. The present arrangement utilizing ten single-point Brown Recorders to record critical fuel element temperatures for use as a safety parameter in the control system will be continued.

2.35 SHIELD

Mechanical Design

HTRE No. 3 shielding effort during the quarter was focused on checking and releasing final drawings of the shield components for fabrication and on completing orders for all raw material needed for fabrication. Design changes made during the quarter were minor. A structural test program for the double-walled cylinder assembly was established. Review and approval of the pressure vessel and the outer tank assembly drawings were completed.

Nuclear Design

The HTRE No. 3 core gamma ray spectrum was corrected to include gamma rays produced from neutron capture by core materials. This correction was accomplished by summing the gamma radiation produced from the capture of neutrons with the prompt-fission and fission-product gamma radiation. Previously only the prompt-fission and fission-product gamma radiation sources were considered in obtaining the operating gamma spectrum. Results of the studies performed show that neutron gamma sources contribute a major portion of the radiation in the high-energy groups.

The HTRE No. 3 reactor shield contains a number of void or near-void passages which appear as irregularities in the shield. The most apparent irregularities are the forward and aft air ducts, which form the passages through the shield for the power plant air. Several different methods for calculating radiation leakage at these points were tested by applying them to experimental shields with duct geometries similar to those of the HTRE No. 3 shield and comparing the calculated and experimental results. Fast-neutron duct-leakage calculation methods assume isotropic neutron scattering at each bend in the duct. Thermal-neutron duct-scattering methods use the ratio of the thermal neutron flux to fast neutron dose rate for equilibrium conditions in the material surrounding the duct. Gamma-ray duct-scattering methods, although not strictly comparable to the other two methods, involve the use of a scattering function that depends upon the angle of bend of the duct.

These methods were used to determine the duct-scattered dose rates in the vicinity of the air passages. Table 5 lists the dose rates at the points indicated in Figure 36. At points 3 through 6 and 12 through 17 the radiation levels are due primarily to duct scattering.

In addition to the forward and aft air ducts, the other shield irregularities studied were the control rod holes in the front plug and the instrumentation wells in the side shield.

TABLE 5

CALCULATED DOSE RATES AT SURFACE OF HTRE NO. 3 SHIELD
(Direct plus Duct Scattered)

Pos.[a] No.	Fast Neutrons, rep/hr	Thermal Neutrons, n/cm^2-sec	Operating Gammas, r/hr	Shutdown Gammas,[b] r/hr
1	1.57×10^3	1.07×10^9	5.10×10^3	2.35
2	1.57×10^3	1.07×10^9	5.10×10^3	2.35
3	4.13×10^3	9.52×10^7	5.71×10^1	1.93×10^{-2}
4	8.54×10^2	1.53×10^7	2.79×10^2	2.01×10^{-2}
5	8.22×10^2	1.45×10^7	3.80×10^1	2.00×10^{-2}
6	9.34×10^2	1.77×10^7	2.47×10^1	1.98×10^{-2}
7	2.41×10^2	2.14×10^6	1.24×10^2	1.63×10^{-4}
8	2.46×10^3	2.63×10^7	1.84×10^3	6.79×10^{-3}
9	2.47×10^4	4.0×10^{10}	1.28×10^7	7.36
10	2.27×10^3	2.59×10^7	1.68×10^3	6.03×10^{-3}
11	1.76×10^2	4.22×10^6	8.18×10^1	1.58×10^{-4}
12	1.16×10^4	9.15×10^7	8.04×10^4	4.41×10^{-1}
13	1.06×10^4	8.44×10^7	8.91×10^4	3.05×10^{-1}
14	1.02×10^4	2.45×10^{10}	7.09×10^2	3.29×10^{-1}
15	7.97×10^4	3.29×10^{11}	1.22×10^4	12.0
16	1.20×10^4	9.00×10^9	1.86×10^3	1.83
17	3.95×10^4	1.40×10^{11}	2.66×10^2	5.33×10^{-1}

[a] See Figure 36.
[b] 18 hours shutdown after 100 hours operation at 175 mw.

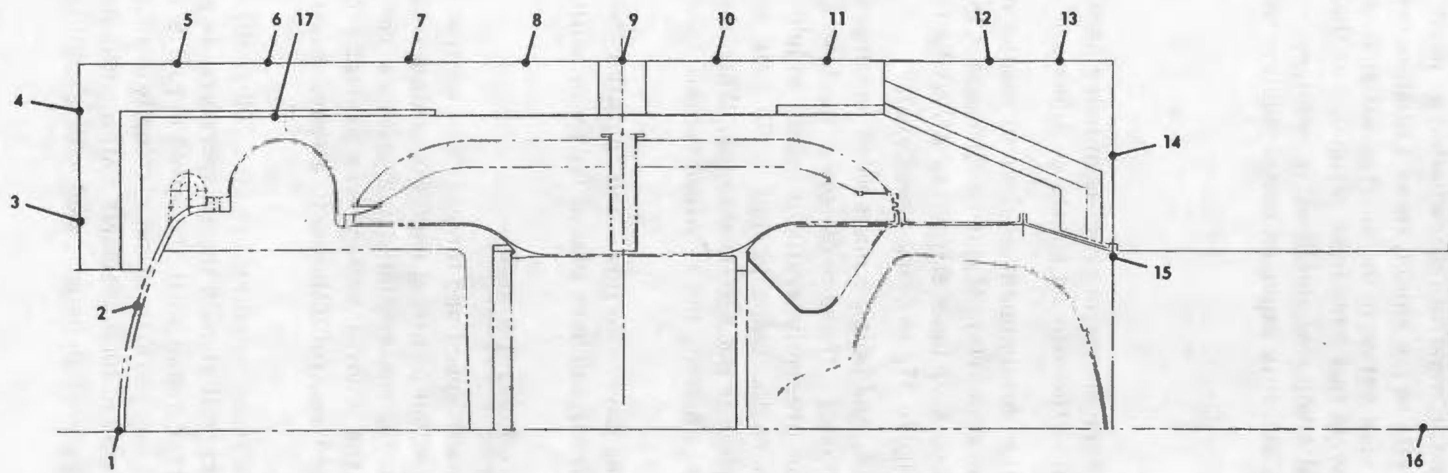

Fig. 36 — Points at which shield dose rates were calculated (Table 5)

[redacted]

Because of the overshielding effect of the material in the front plug, the control rod leakage constitutes the major portion of the radiation indicated for points 1 and 2 in Figure 36. The values shown for these points were computed for one rod at the shield surface. It is expected that the radiation levels between rods would be considerably lower. Instrumentation-well leakage accounts for most of the radiation at point 9 in Table 5. Since there are nine instrumentation wells in the shield, these radiation levels represent peaks only. The radial surface dose rates between the instrumentation wells should be considerably lower. The radiation levels that have been estimated at the ducts, control rods, and instrument wells indicate that additional shielding is required in these areas. These problems are being investigated, and it is expected that a solution will be obtained in the next quarter.

2.36 ENGINES

Engine Development

The three X39-5 development engines are in process of being assembled. Compressor sections, exhaust cones, and two of the exhaust nozzle sections are assembled.

Parts are being procured for the development engines in preparation for development testing which should start in the next quarter. Major components of the turbine-scroll test loop and the single-engine test loop have been shipped to ANPD by the vendors. The single-engine test loop, shown in Figure 37, is being assembled.

Basic X39 compressor, turbine, and tailpipe maps were developed from data obtained during test of a Sawyer-Bailey starter. These maps cover the low-speed operating range of the engine and supplement the presently available maps which cover only the high-speed region. These low-speed region maps permit cycle calculations in the starting region of operation where the engine is not self-sustaining. When the performance characteristics of any given starter are known, the required turbine inlet temperature can be calculated.

Five modified fuel control valves have been flow- and operation-tested, and their performance was satisfactory. An order has been placed for the modification of the remaining 11 fuel control valves.

Automatic Speed and Temperature Control System

A prototype of the X39-5 automatic speed and temperature control system for chemical operation was made up and checked out on actual engine operation at the single-engine test pad at Idaho. Results showed that the contemplated temperature control system was unstable. In the ensuing redesign, the control system was basically changed from a temperature control system with speed-control followup to a speed-control system with temperature trim.

A speed override circuit that signals speed errors of $\pm$ 200 rpm has been incorporated into the speed amplifiers. This circuit signals the temperature amplifier and will override any existing temperature error signal until the speed error is corrected. This circuit has been built and tested and has performed satisfactorily over a speed range of 4000 to 7950 rpm and a temperature range of 800° to 1600°F. All modifications of the automatic speed and temperature control system can be operated with a modified form of the X39-4 magnetic amplifier system.

Combustors

Design of the HTRE No. 3 combustors has been completed and manufacturing drawings released for bids. The capacitor-discharge surface-gap-plug ignition system was given a preliminary tryout on a test loop in the SET cell. Lightoff was obtained, but was delayed and rough.

[redacted]

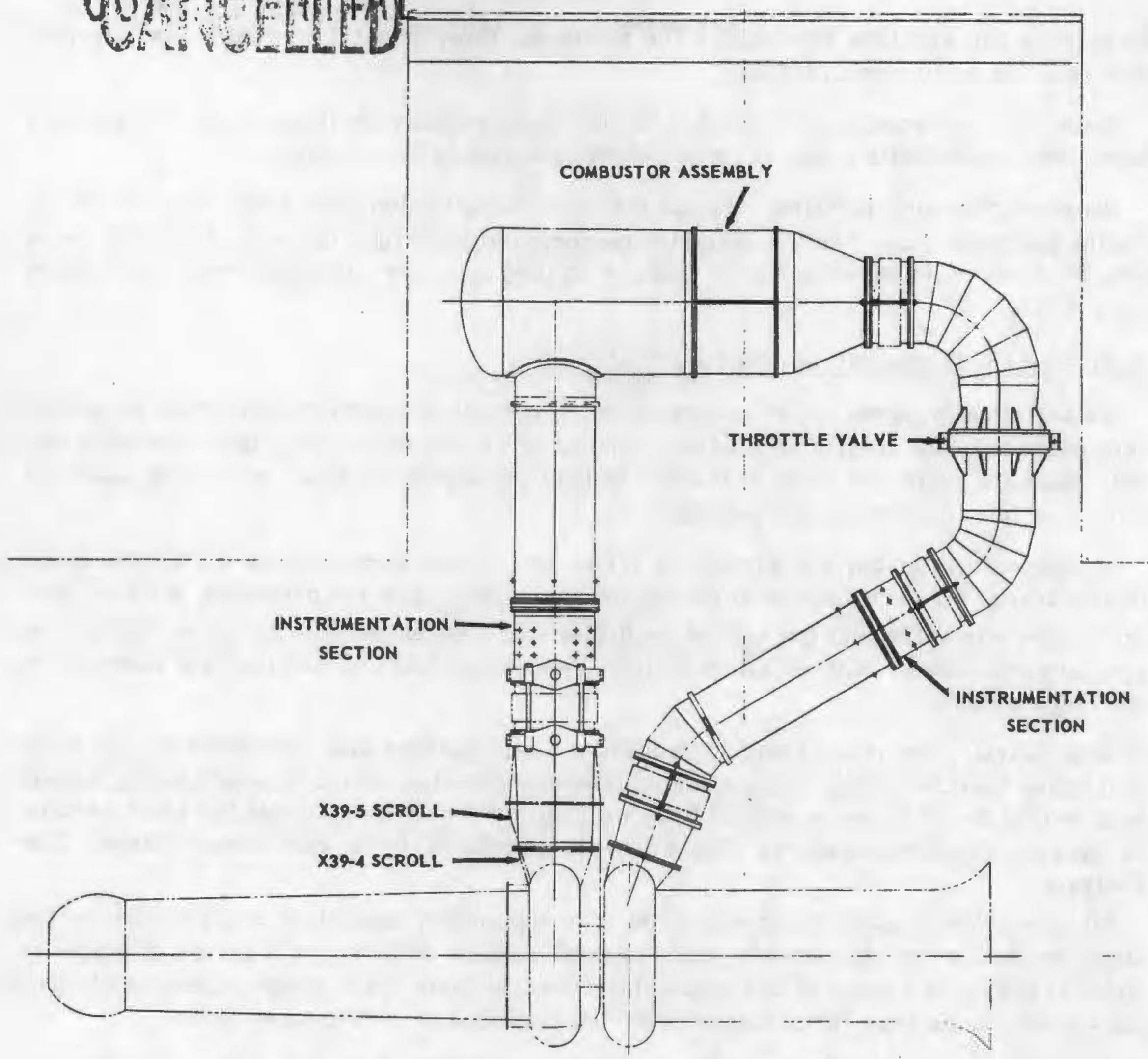

Fig. 37—Single-Engine-Test ducting loop

Aftercooling Study

Power plant aftercooling studies, begun in the last quarter, continued with an attempt to compare HTRE No. 1 aftercooling operating points with those of HTRE No. 3. Data obtained from HTRE No. 1, although inadequate, indicated that deadheaded X39 compressor operation at speeds up to 1600 rpm is not harmful.

With the use of the low-speed performance maps and an aftercooling blower flow of 10 pounds per second, 5 psig, and 500°F at the turbine inlet of one X39 engine, a balance point of approximately 1500 rpm was determined. Therefore it appears that deadheaded operation during aftercooling is feasible.

2.37 AERODYNAMICS AND THERMODYNAMICS

Reactor-Shield Flow Model

During the quarter tests were conducted with the 1/4-scale HTRE No. 3 flow model using an inlet scroll and transition ducting. The results indicated that the presence of the scroll had no measurable effect on core tube-to-tube weight flow distribution with either one- or two-engine flow conditions. The flow distribution is essentially constant circumferentially for any flow condition. The minimum flow, about 3 percent below average, occurs in the outer row of tubes.

Because of the small size of the 1/4-scale tubes, velocity profiles within the tubes are being investigated with a full-scale two-dimensional duct-tube system.

Dynamic pressure profiles obtained for this configuration are reasonably flat except for the upstream tube. The low-weight-flow region for this tube is about 12 percent below tube average. Various exploratory changes in tube entrance are being made to improve the profile.

Fuel Element Temperatures and Flow Distribution

An analytical process has been formulated to predict flow distribution trends in parallel flow passages. The computing process consists of finding those mass-flow velocities that will cause the static pressure at the exit of each passage to be equal to its neighbor for any given inlet total-pressure profile.

A computer program for predicting HTRE No. 3 fuel element flow distribution, air temperatures for each annulus at the exit of each stage, and temperatures for each ring and moderator surface at the exit of each stage was developed for the above analysis to predict performance with an assumed inlet velocity profile and varying heat fluxes from the fuel elements.

Qualitatively, the results tend to confirm the expectations that underloaded inner rings will cause the outer rings to attain higher temperatures than would be predicted by merely considering the differences in heat flux, and that low-velocity input into the outer annulus produces higher temperatures than would be predicted by a continuous-channel flow analysis.

To check the validity of this method of computation, analytical calculations by the above method were compared to experimental results obtained on a series of stages of parallel plates in a channel of rectangular cross section. Each stage consisted of three plates, and there were three stages in series preceded by a 90-degree elbow.

The calculated mass-flow velocities at the exit of the third stage together with the corresponding experimental mass-flow velocities are plotted versus passage numbers in Figure 38. Also shown are the experimental mass-flow velocities at the entrance to the first stage.

The assumption of constant static pressure at the exit of each stage seems to be a reasonable one in that it results in flow distribution trends comparable to those obtained by experiment. Static-pressure measurements in the experiment at the end of the first and third stages also confirmed this assumption.

As a consequence, the above method of computation is being used in the analytical prediction of the thermodynamic performance of concentric-ribbon-type fuel elements.

Shield Structure Temperatures

For certain regions of the pressure vessel, temperature distributions have been calculated using relaxation methods. Because of the uncertainties involved in predicting nuclear heat generation rates in the regions considered, a dimensionless temperature coefficient was introduced which incorporates both temperature and heat generation rate. The results are plotted as lines of constant temperature coefficient which correspond to isotherms in the region. By means of an equation for each distribution, the magnitude of each isotherm can be calculated when nuclear heat generation rates and reference temperatures are known.

[redacted]

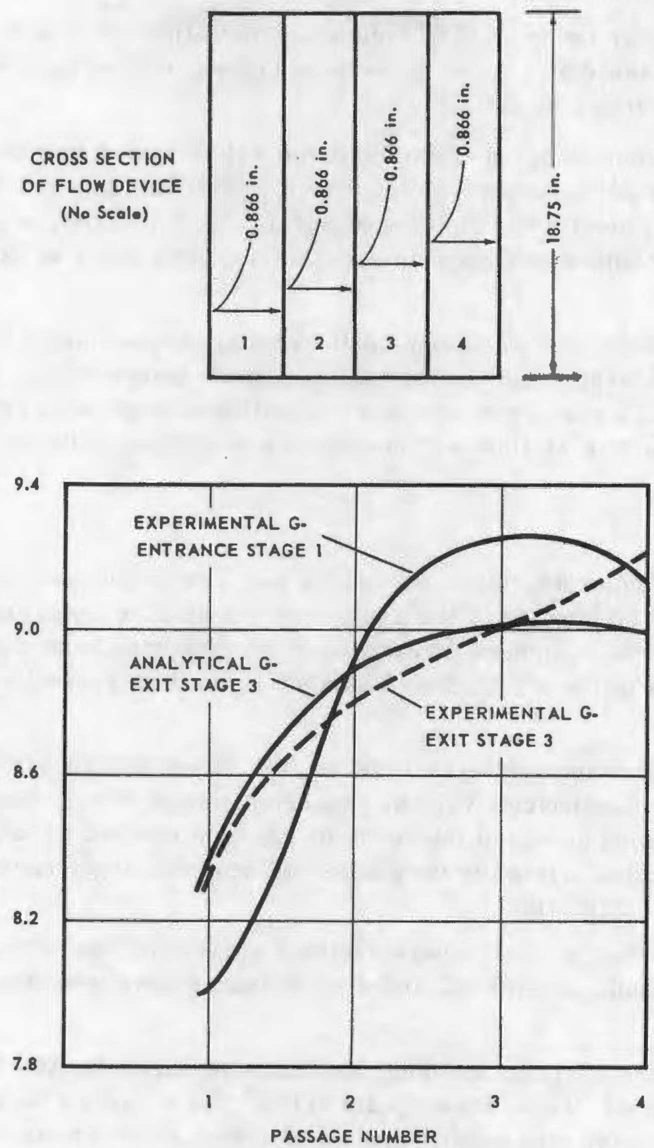

Fig. 38 – Plot of experimental and analytical third-stage exit mass flows compared to experimental entrance values

Control Rod Cooling Requirements

An analysis of coolant requirements for europium oxide control rods was performed during the past quarter. It was found for X211 operation at 100 percent rpm, a compressor temperature discharge of 698°F, and a reactor power of 162 megawatts, that an airflow of 0.035 pound per second to each rod coolant passage would keep maximum rod temperatures below 1459°F and maximum guide-sleeve temperatures below 1517°F, provided the control rod is symmetrically centered. Heating rates were calculated assuming only gamma ray heat generation. The pressure drop associated with the calculated airflow is 4 psi from front to rear tube sheet, and air exit temperature is 1248°F. A condition in which the rod has become distorted due to wear is presently being investigated, and the results are expected to raise the actual airflow required.

It was determined that during full-scram operation the control rod temperature would not exceed 1554°F if the orificing to give 0.035 pound per second during regular operation is maintained.

[redacted]

Control rod cooling in the front plug region was investigated, and it was found that the rods, together with associated guide sleeves and tubes, can be kept sufficiently cool by radiation without resorting to cooling air.

In an analysis conducted for a europium oxide safety rod it was determined that if a constant orifice is used to supply cooling air, it would have to overcool during regular operation in order to meet requirements at scram. With this device a 0.27-pound-per-second cooling air, which discharges through the rear tube sheet at 725°F, would be required.

An analysis was performed to determine the cooling requirements for the annular region between the moderator and the control rod guide sleeve in the central moderator core. An airflow of 0.5 pound per second which will discharge at 1116°F was found to be necessary. This quantity of flow will necessitate additional orificing in the front tube sheet.

2.38 AUXILIARIES

The design of the superstructures for HTRE No. 3 is 85 percent complete. Work remaining includes the integration of the equipment installation requirements as these become known. Platform equipment arrangement studies have been completed. A weight and balance diagram of the HTRE No. 3 assembly, as it is presently defined, has been finished.

Detailed engineering requirements covering the latest design criteria for the shield liquid system quick-disconnects, valves, expansion joints, etc., were issued during the quarter. All major components of this system are now covered by applicable specifications. Vendors' certified prints for the pumps and heat exchanger have been received and were approved for construction.

Design of the aftercooling system was finalized to the point where procurement of some of the components could be started. Detailed drawings have been issued on most of the system components.

During the quarter all of the hot-duct insulation required for the HTRE No. 3 power plant has been designed. Valve drawings for HTRE No. 3 ducting have been received for review. Ducting actuator components are all on order or under construction. Complete detailed drawings of the outlet header have been issued and vendor bids received.

Specifications for expansion joints were completed, and bids are currently being received.

Evaluation tests were run on a "counterpoise" constant-support hanger of the type proposed for suspension of HTRE No. 3 ducting. The hanger displays good flat response through a full-range travel of approximately 3.25 inches.

Design of the initial criticality experiment (ICE) equipment has reached a stage of 80 percent completion. Effort has been concentrated primarily on mechanical design; work on controls and other electrical equipment has been delayed for final actuator control data. The plans for the Low Power Test facility were examined and found satisfactory for this test; it will be necessary, however, to extend electrical power supply to the ICE cell. A simple 40-inch x 50-inch standpipe was installed at the top center of the test tank for use in shield studies.

2.39 SPECIFICATIONS AND DESIGN DATA FOR HTRE NO. 3

The following is a list of current physical, nuclear, and thermodynamic characteristics of the HTRE No. 3. Changes and additions from the previous quarterly report are indicated by an asterisk.

Primary Shield

Type	Flight prototype
Structural material	Inconel X
	Stainless steel
Shielding material	Lead (gamma)
	Boral
	Water (neutron)
Required heat removal	2% reactor power
Cooling water flow	612 gpm
Maximum cooling capacity	2.5% (175 mw operation)
Augmentation	Mercury
Outside diameter	97.5 in.
Inside diameter	58.0 in.

Shield Weights

	Structure	Water	Weight, lb Lead	Lead Cladding	Mercury	Total
Side shield	5,200	7,700	46,100	6,200	-	65,200
Side shield[a]	5,200	3,800	46,100	6,200	53,200	114,500
Front plug	6,300	4,000	12,100	1,600	-	24,000
Rear plug	4,300	3,300	13,300	2,500	-	23,400
Auxiliary shield	16,300	22,300	31,800	2,400	-	72,800
Transition ducts	930	-	-	-	-	930
Elbows	2,000	-	-	-	-	2,000
Scroll	4,400	-	-	-	-	4,400
Total	39,430	37,300	103,300	12,700		192,730
Total[a]	39,430	33,400	103,300	12,700	53,200	242,030

[a] With mercury augmentation.

Engines

Type	X39-5	X211
Quantity	2	2
Compression ratio	4.95	14.2
SLS airflow	75 lb/sec	425 lb/sec
Maximum turbine inlet temperature	1600°F	1700°F
Combustor	Common	Parallel*

Moderator

Material	Hydrided zirconium
Clad	
Molybdenum	0.015 in.
446 stainless steel	0.015 in.
Volume fraction	0.3979
Distance across flats	3.923 in.
Corner radius	0.92 in.
Element spacing	0.030 in. nominal
Length of hydrided zirconium	35.50 in.
N_H (central - 55 cells)	2.50 ± 0.05
(middle - 54 cells)	3.00 ± 0.05
(outer - 42 cells)	3.95 ± 0.05

Moderator - Fuel annulus hydraulic diameter	0.238 to 0.256 (hot) 0.268 (cold)

<u>Reflector</u>

Material	Beryllium
Outside diameter	57.0 in.
Configuration	Hexagonal shapes
Cooling configuration	7 holes per hexagon

<u>Fuel Elements</u>

Material	80 Ni - 20 Cr
Number of identical fuel cartridges per core	150
Number of identical stages per cartridge *	19
Nominal spacing between successive stages	0.125 in.
Number of rings per stage	12
Ring spacing tolerance	$\pm$ 0.003 in.
Active cartridge length (reference) *	30.750 in.
Meat width of rings	1.450 $\pm$ 0.030 in.
Dead-edge width	0.025 + 0.015 in. - 0.019 in.
Over-all width of rings	1.500 + 0.060 in. - 0.068 in.
Ring thickness tolerance	$\pm$ 0.001 in. maximum per ring $\pm$ 0.0005 in. weighted average
Cut length tolerance	$\pm$ 0.010 in.
Cladding thickness	0.004 $\pm$ 0.0006 in.
Linear density tolerance	$\pm$ 3.5%
Area density tolerance (reference) *	$\pm$ 6.0%
Weight percentage uranium in UO_2	87.5 $\pm$ 0.5%
Weight percentage U^{235} in uranium (enrichment)	93.2 $\pm$ 0.5%
Total UO_2 weight per stage	0.1674 $\pm$ 0.0050 lb
Total UO_2 weight per cartridge *	3.180 $\pm$ 0.030 lb
Total weight of assembled stage *	0.6734 $\pm$ 0.0150 lb
U^{235} weight per core (reference) *	389.5 $\pm$ 6.0 lb

Breakdown of nominal 80 Ni - 20 Cr weights	Grams per stage
Cladding $\pm$ dead edge	99.07
80 Ni - 20 Cr mixture in core	105.05
Inner structure (combs, spacers, etc.)	23.4
Rails	11.1
Wire seals	1.99
Total	240.61

Total 80 Ni - 20 Cr weight per cartridge (in active region)	9.548 lb
Total 80 Ni - 20 Cr weight in active core	1432 lb
Inside diameter of moderator section	2.914 in.
Center-to-center distance of cells	3.953 in.
Fuel and air frontal area	1000 in.^{2}
Heat transfer area	3200 ft.^{2}
Hydraulic diameter	0.160 in. (cold) 0.162 in. (hot)

Control Rods

Material		Europium oxide
Type and quantity - dynamic		3
- shim		33
- safety		13
Location of rods - center		24
- outer		25
Clad	310 stainless steel	0.040 in.
Diameter		0.70 in.
Active length		20.0 in.

Core, General

Structural material	Inconel X	
Over-all length	43.5 in.	
Active length	30.0 in.	
Nominal diameter	51.0 in.	
Materials of active core (excluding tube sheets, reflector, and control rods)	Volume Fraction	Weight, lb
UO_2	0.017	390
80 Ni - 20 Cr	0.076	1432
446 stainless steel	0.025	420
Molybdenum	0.025	560
Hydrided zirconium	0.401	5330
Inconel X	0.004	80
Void	0.452	
Approximate total reactor weight	14,000 lb	

Performance

	X39-5	X211
Compressor discharge temperature	379°F	626°F
Compressor discharge pressure	51.6 psia	153 psia
Reactor airflow	122.2 lb/sec	616.4 lb/sec
Compressor airflow (both engines)*	126 lb/sec	655.7 lb/sec
Reactor power design point	36.1 mw (See note)	133 mw
Turbine inlet temperature*	1433°F (See note)	1384°F
Turbine inlet pressure*	41.5 psia	98.3 psia
Core inlet air temperature	379°F	626°F
Core inlet air pressure*	47.9 psia	137.6 psia
Core airflow	118.6 lb/sec	597.9 lb/sec
Fuel element exit air temperature* (Excluding outer annulus)	1620°F (See note)	1512°F
Outer annulus exit air temperature*	1169°F (See note)	1233°F
Moderator cooling-slot exit air temperature	628°F (See note)	879°F
Fuel element airflow*	82.6 lb/sec	424.0 lb/sec
Outer annulus airflow*	27.7 lb/sec	132.0 lb/sec
Moderator cooling-slot airflow	8.3 lb/sec	41.9 lb/sec
Pressure ratios:		
Compressor-to-core	0.95	0.90
Across-core	0.91	0.79
Core-to-turbine	0.98	0.90

Fuel element temperature*	1800°F (See note)	1820°F
Moderator flat temperature*	1370°F (See note)	1610°F
Moderator inner-surface temperature*	1325°F (See note)	1400°F
Moderator corner-surface temperature*	1300°F (See note)	1365°F
Pressure drop across fuel stage	2-3 psi	
Maximum dynamic head within fuel elements	6.0 psi	

NOTE: The performance values presented above are based on an idealized mechanical design and ideal nuclear and fluid flow characteristics. These values were produced for component design and are not indicative of actual reactor performance. It is expected that an accumulation of perturbations produced by airflow distributions, power distributions, and manufacturing tolerance will be experienced and result in lower total reactor power and turbine inlet temperatures than those values indicated above. In actual operation the fuel elements will be limited to a maximum temperature of 1850°F in any location in the reactor and the moderator will be limited to a maximum temperature of 1650°F in the 3.95 hydride region. With these limitations coupled with the expected perturbations, it is estimated that the actual maximum reactor air temperatures will be on the order of 1330°F.

* Indicates additions or changes since last quarterly report.

2.4 XMA-1 POWER PLANT DEVELOPMENT (Project 103)

2.41 GENERAL STATUS

Activities on the XMA-1 power plant development during this quarter consisted chiefly of: (1) final resolution of the configuration of the fuel tube through the reactor that will be used in the first prototype of the XMA-1; (2) rescheduling of the design and development program; (3) continuing analysis of the reactor and shield design; (4) continuing development of moderator, fuel element and shield materials; and (5) release of manufacturing drawings and completion of procurement details on all components for the first block of four X211 turbomachinery assemblies.

The possibility of using a fuel tube that was tapered to provide a ratio of exit-to-inlet flow area of approximately 1.7 was more completely evaluated from the standpoint of both nuclear design and aero-thermo design considerations. Although the performance gain from an aerodynamic basis appeared attractive, it was more than offset by problems of power distribution. Therefore the tapered-fuel-tube concept for the first development model was abandoned in favor of the more conventional constant-diameter design.

The date of the first nuclear run was delayed because of funding limitations established by the Government for the Fiscal 1958 and 1959 time period. The budget support that can be made available for development of X211 turbomachinery will delay the Mechanical Reliability Test qualification approximately 1 year beyond the previous schedule.

Nuclear analysis of the reactor has continued in order to establish the uranium inventory necessary to handle fuel burnup and xenon override. Power distribution and control rod patterns are being studied; however, this work has not been completed. Nuclear analysis of the shield has continued, including effects of structure, turbomachinery, and nonhomogeneity of the reactor. Structural analysis of the shield structure and connection to the transition section have also continued.

Considerable progress has been made in the development of an edge seal for fuel element ribbon, both by brazing and seam welding. Yttrium metal has been delivered at an average rate of 10 pounds per week in the form of 4-inch ingots. Unfortunately this metal has contained more impurities than are acceptable. Experimental work on hydriding of yttrium has continued.

The design of all components for the first series of development X211 engines has been finalized and detailed for manufacture and procurement. During the quarter, a full-scale mockup was completed of the turbomachinery components. The mockup was fabricated chiefly of plastics and is so arranged that the nuclear components between compressors and turbines are also simulated, with the total structure being self-supporting. A photograph of the mockup appears as Figure 39.

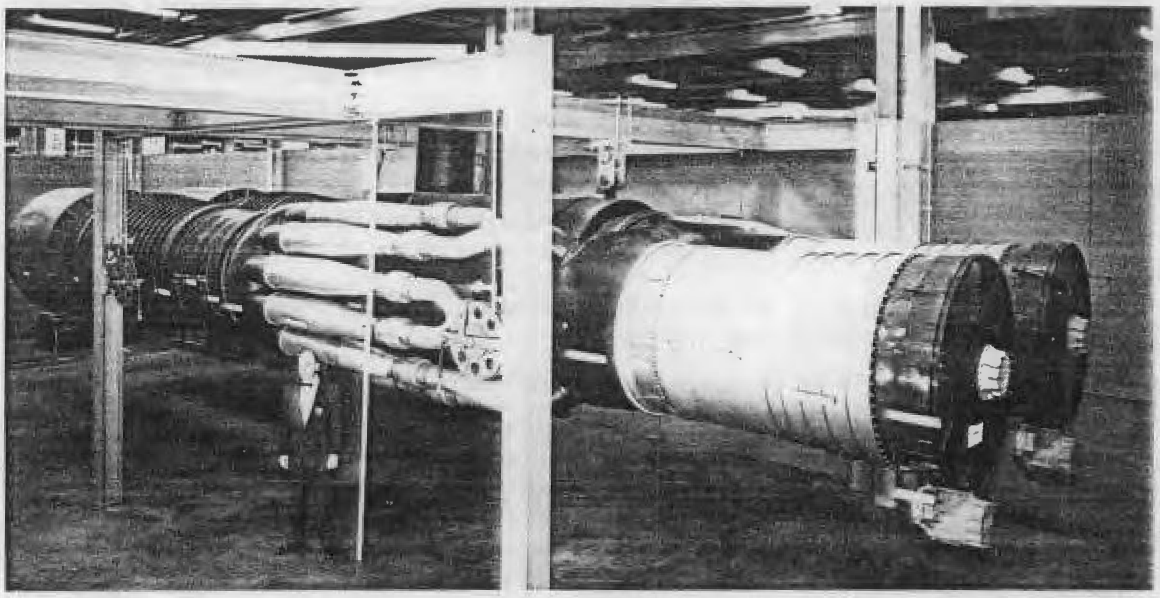

Fig. 39 – Full-scale mockup of XMA-1

2.42 REACTOR

Nuclear Studies

During the quarter, additional nuclear studies were conducted on the tapered-fuel-tube reactor concept. An attempt was made to achieve a reasonably flat gross radial power profile at all longitudinal sections of the reactor by varying not only the size and taper of the center moderator rod but also the size and taper of the fuel tube. This resulted in only a slight improvement over the geometry previously studied in which all the hexagonal moderator elements, although containing tapered holes, were identical. The new, more complex geometry still produced an inverted gross radial power distribution at the front of the reactor as compared to the rear; neither front nor rear power profile was acceptable from the standpoint of flatness. Although the new geometry was not fully optimized, the gain achieved was so slight that this approach was abandoned as a means for achieving a practical tapered-tube design. Another conclusion was that power flattening could not be achieved by radial moderator displacement and adjustment of thermal disadvantage factor alone for a reactor having moderator rods and fuel tubes tapered to the extent that an airflow area ratio of 1.7 is realized. Power flattening in a tapered-tube design could probably be achieved by variation of either uranium concentrations or moderator hydrogen content in conjunction with radial moderator displacement, but this would complicate the design considerably and would undoubtedly result in a considerably longer reactor-development time. For these reasons, it was decided that a nontapered-tube re-

 [redacted]

actor design would be employed in the first XMA-1 test power plant, and further nuclear analysis of tapered-tube reactors was discontinued.

Straight Tube Design - A rather flat gross radial power distribution (1.15 peak to average) was achieved analytically for a straight-tube XMA-1 reactor by means of radial moderator displacement and variation in thermal disadvantage factor which is effected by the use of center moderator rods of different diameters. Four moderator rod diameters are used (0.866, 1.024, 1.192, and 1.415 inches), the smallest rods being located in the centermost region of the reactor. A much flatter power profile is expected to be obtained by this means, particularly for a clean reactor, by further adjustment of the moderator sizes. A reasonably flat power profile must be eventually worked out, however, for various operating states of the reactor, including poisoning effects and various control rod positions.

The effect of xenon-135 poisoning and fuel burnup on reactivity of the XMA-1 reactor has been computed. Since a fairly large empirical correction has been applied to the xenon poisoning, the uncertainties in quoted xenon effects are considered large enough to cover the effects of stable fission products. The empirical correction was derived from data on the HTRE No. 1.

The effect on the reactivity of the reactor produced by the xenon-135 as it approaches equilibrium is shown in Figure 40, and the effect of the xenon-135 decay on the reactivity after shutdown from equilibrium is shown in Figure 41.

A uranium investment of 230 pounds in a hot, clean XMA-1 reactor provides a computed multiplication of 1.06. The combined effects of 1-hour-after-shutdown xenon, U^{235} burnup, and temperature were computed to be -0.07 in Δk; therefore, a slight increase in required uranium inventory is indicated.

A preliminary control rod pattern was established for mechanical design purposes only, without benefit of nuclear analysis. The pattern contained a total of 49 rods - 3 dynamic, 1 source, 10 safety, and 35 shim rods.

The average amounts of secondary heating produced by gamma and neutron heating in various elements of the reactor core were calculated. It was calculated that 5.78 percent of the reactor operating power would be generated in the moderator as secondary heat and

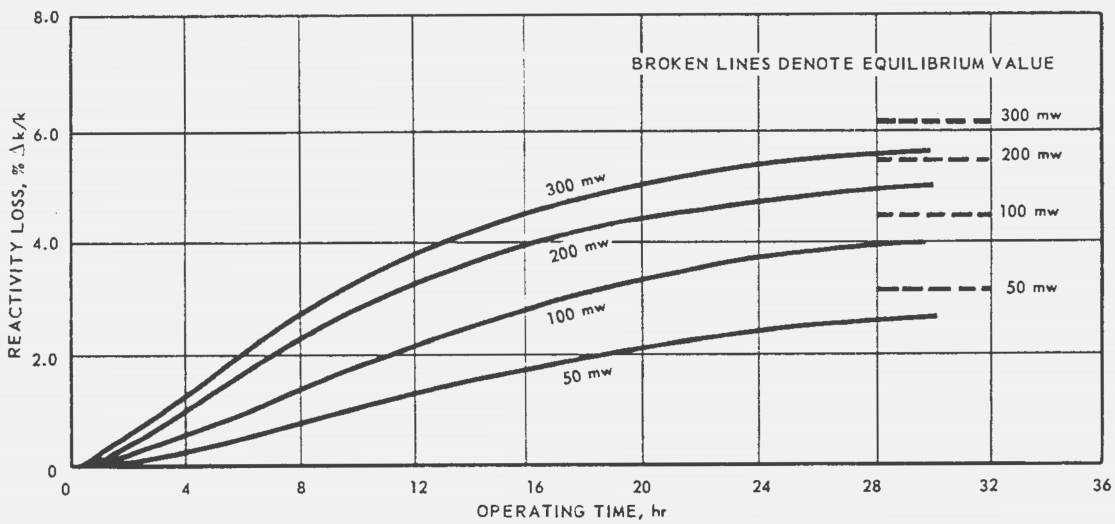

Fig. 40 – Predicted time variation of xenon^{135} reactivity loss, XMA-1

[redacted]

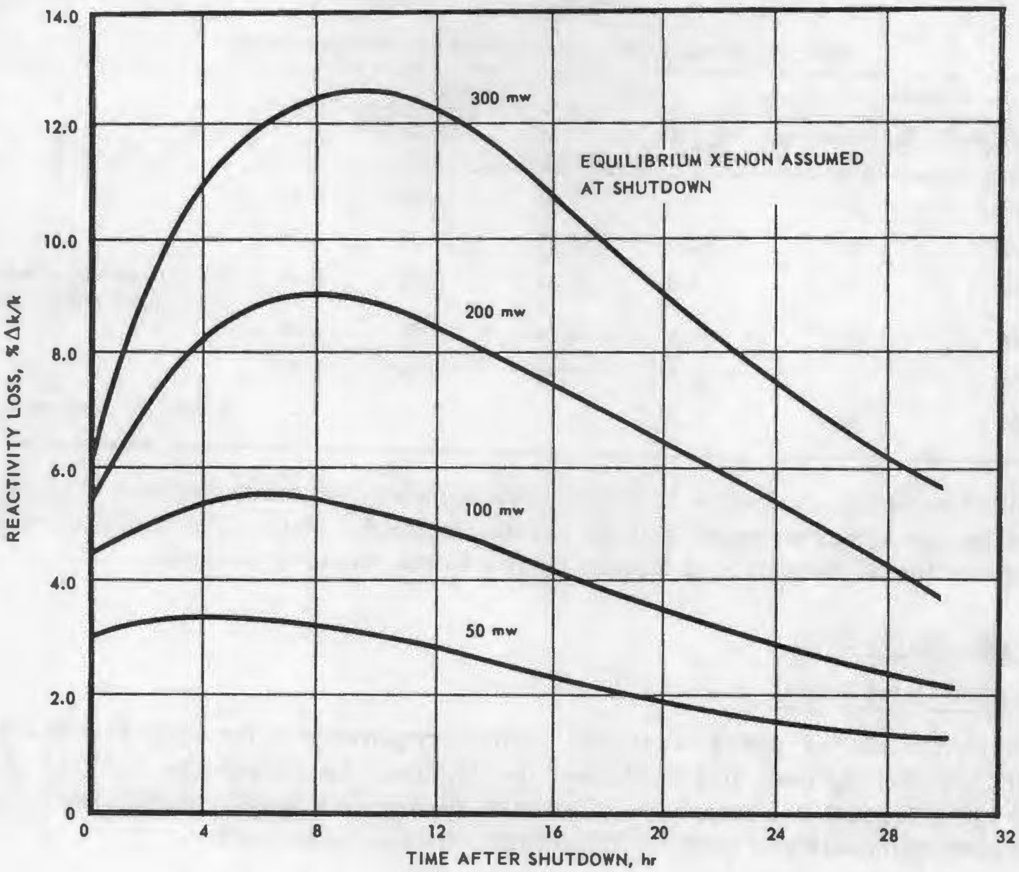

Fig. 41 – Xenon^{135} buildup following reactor shutdown, XMA-1

1.77 percent in the fuel elements. These gross results are considered fairly reliable, although a number of assumptions and simplifications were made.

Moderator Material

Yttrium Metal Development - The Ames Laboratory has been delivering yttrium metal at an average rate of about 10 pounds per week in the form of 4-inch double-arc-melted ingots. The metal produced to date has generally been of poor quality, with the major impurities being oxygen, calcium, and magnesium. Metallographic examination of the as-received metal shows the known metallic impurities to be generally distributed throughout the grains. These inclusions appear to migrate to and collect on the grain boundaries after hydriding. This effect is possibly enhanced by the recrystallization which takes place.

Since the yttrium metal cannot be readily cold-worked, the metal has been extruded hot and clad to protect it from oxidation. Because of the economic advantages of coldor warm extrusions, this process is being explored for application to yttrium. One such test has been carried out with negative results, and a number of additional tests will be conducted as adequate metal becomes available. The first of these tests will be run in the next quarter.

One-inch-diameter by 2-inch-long specimens of yttrium metal were prepared from hot-extruded metal for a series of hydriding tests. The initial tests on hydriding are designed to determine possible hydriding schedules, preferably at pressures no greater than 2 atmospheres and at a temperature no greater than 2000°F. In addition, based on experi-

[redacted]

TABLE 6

RESULTS OF PRELIMINARY YTTRIUM HYDRIDING STUDIES

Hydriding Conditions			Results			
Temperature, ^oF	H_2 Pressure, psia	H_2 Flow, ft^3/hr	Weight, % H_2	Density, g/cc	N_H	Remarks
1900	16	1	1.95	4.25	4.97	
1900	8	0.5	1.87	4.25	4.74	
1900	4	0.5	0.32	4.41	0.85	Run not completed because of furnace control failure.
1900	29	0.5	2.09	4.28	5.34	
2000	7	0.5	1.94	4.29	4.97	
2000	3.8	0.5	-	-	-	Results not complete.

ence with zirconium, the rate of hydrogen absorption was limited during hydriding. Table 6 shows the conditions employed and the results obtained to date. The preliminary data indicate that the N_H developed is closely related to the hydriding pressure.

2.43 FUEL ELEMENTS

Fuel Ribbon Development

To meet the XMA-1 power plant fuel element requirements for temperature and life capability, effort has been directed toward development of a ribbon-type sandwich structure in which the fuel is a dispersion of uranium dioxide in a powder-metallurgy niobium matrix clad with oxidation-resistant iron chromium-aluminum alloy.

Cladding - In the development of fuel ribbon cladding during the quarter, tests on a series of Fe-Cr-Al alloys of reduced chromium content (15 - 19 Cr) have indicated that their oxidation resistance is comparable to that of the 25 Cr alloys at a common aluminum level of 6 percent. Post-test bend ductility was noticeably greater for the lower-chromium alloys. To evaluate further the effect of chromium level on cladding properties, a larger development heat is being processed.

Core Development - To study the effect of UO_2 particle size distribution, 80 niobium cores incorporating four fuel-particle size ranges were evaluated at various stages of processing. It was found that fuel in the range of 5 to 10 microns was unsatisfactory in that the cold-pressed cores were extremely friable and could not withstand ordinary handling. The green strength of cores using fuel particles ranging from 15 to 20 microns was marginal. Cores containing 40- to 50-micron and 60- to 75-micron UO_2 particles had satisfactory green strength. Fuel loss during sintering was independent of particle size, as was sintered density. X-ray inspection of finished ribbon showed that high-density areas were associated with the use of fine particle sizes. At the 40- to 50-micron range and larger, high-density areas were not a problem.

In an effort to increase the strength of the niobium fuel ribbon, a series of 75 cores containing 1 to 3 percent molybdenum and/or titanium was pressed and sintered. Processing through sintering indicated that no major problems result from the alloying.

Fuel Ribbon - Wrought Fe-Cr-Al frames have been successfully utilized in fabrication of niobium fuel billets. Stress-oxidation tests have shown that substitution of the wrought alloy for the standard Fe-Cr frames has resulted in greater resistance to nitriding at elevated temperatures. A series of 80 billets was fabricated using metal foils between the core and the cladding. Four 20-billet groups were made using molybdenum, iron,

[redacted]

tantalum, and tungsten as interface foils. Billets with the tantalum interface could not be successfully processed because of poor bonding between the interface and the cladding. Most of the billets in the other three groups were successfully rolled, but bonds in the molybdenum and tungsten interface units were of no better than average quality. There is evidence that the iron interface may improve the fuel ribbon by reducing core spread below that of standard ribbon, retarding grain growth in the cladding material adjacent to the core, and improving post-test bend ductility of ribbon exposed to elevated temperatures.

To test the effect of surface flaws in niobium fuel ribbon, pinholes approximately 0.010 inch in diameter were drilled in the cladding of fuel ribbon segments which were then subjected to oxidation tests. After 4 hours at 2000^{o}F the core beneath the pinholes had oxidized over a zone approximately 1/8 inch in diameter. In 8 hours the oxidized zone had increased to approximately 1/4 inch in diameter.

No failures occurred in a recent series of 26 stress-oxidation specimens subjected for 100 hours to a core stress of 1500 psi at 2000^{o} and 2200^{o}F. Under these conditions the elongation for the 2200^{o}F tests averaged about 1-1/2 percent; 2000^{o}F tests produced negligible elongation. Fuel ribbon has now been subjected to a temperature of 2200^{o}F for 500 hours without failure under 1000-psi stress. During the next quarter, tests will be conducted at higher temperatures and stresses, and under cyclic temperature conditions.

Major progress was made in edge sealing by brazing during the quarter. A series of ferrous-base alloys was used for edge-sealing samples for oxidation testing. One alloy with the composition 5 Al, 20 Cr, 10 Si, 1 P, and the balance Fe was tested successfully for 100 hours at 2300^{o}F. Until the testing of these alloys the best edge-seal life obtained was 4 hours at 2300^{o}F. Initial tests on specimens sealed by cover-caps seam-welded over cut edges show that the method has merit. Specimens sealed by seam welding have withstood exposure at 2300^{o}F for 100 hours.

Two reactor irradiation tests were conducted on niobium fuel ribbon specimens at the LITR. The first was operated at a maximum indicated temperature of 1800^{o}F, and the second at 1900^{o}F. Flux levels in both tests were of the order of 2×10^{13} neutrons/cm^2-sec. Both test specimens failed prematurely at the junction between the platinum thermocouples and the fuel ribbon. The 1800^{o}F specimen was exposed for 22 hours and the 1900^{o}F specimen for 8 hours. Metallographic examination is not yet complete; however, it is apparent from hot-lab examination that in both cases failure occurred at the thermocouple nearest the air inlet end of the specimens. Further tests are planned during the next quarter.

Mechanical Development

Fuel element testing in the small burner rig was begun with a series of three identical tests of the 2-1/2-inch-diameter 80 Ni - 20 Cr elements designated XRH-1, XRH-2, and XRH-3. The XRH-2 element was operated at a temperature of 1900^{o}F, a dynamic head of 7.3 psi, and a Mach number of 0.350 within the last element for a total time of 173 hours. Distortion was visible but was very slight, and there was little change in the pressure loss coefficient ($\Delta P_t/q$) value (1.60 throughout test). The other two XRH designs will be tested at these same conditions for comparison purposes.

A cold-flow test was conducted on the XRH-1 (staggered ring), three-stage assembly and the XRH-3 (tiered ring) three-stage assembly. There was no difference in pressure drop in the two cartridges. The curve relating $\Delta P_t/q$ and Mach number was essentially identical for both cartridges.

Testing at WADC has been temporarily discontinued. The program will be resumed after design and manufacture of a new liquid fuel nozzle system that is needed because recent tests indicated nonuniform test temperatures resulting from combustion difficulties.

The following descriptive numbering system is being used for XMA-1 fuel elements:

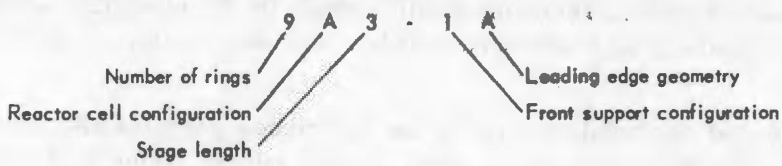

Three designs of leading-edge geometry are presently being tested in the 2-1/2-inch size: "A"-leading edges aligned; "S"-leading edges alternately staggered: and "T"-leading edges tiered.

Agreement has been reached on the design of two "A" cell, 3.156-inch-diameter fuel elements designated the 9A3-1A and 13A3-2A (See Figure 42). This design embraces all of the successful features of the XR-25 fuel element design for HTRE No. 3. This design includes: (1) a reinforcing inner ring which provides a continuity of beam support for the support ribs; (2) comb spacers so spaced between ribs that the lengths of unsupported arc of the "fueled" rings are equal for a given ring, and decrease in approximate proportion to the decrease in arc strength as the radius increases; (3) elimination of all supporting trailing-edge spacers in the initial design to minimize pressure drop across each stage.

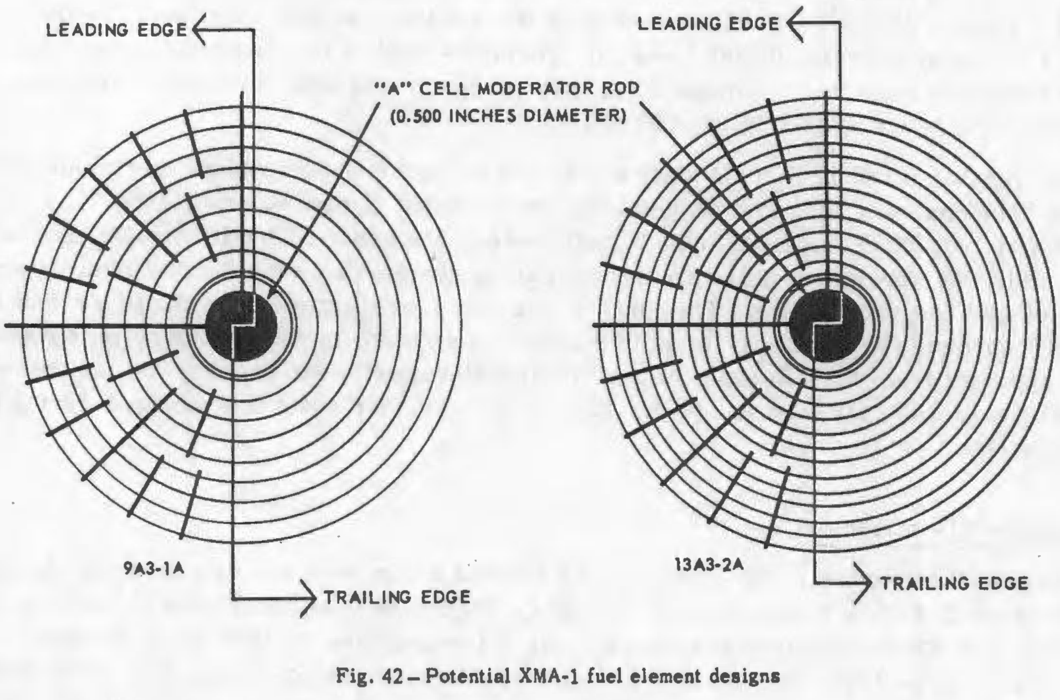

Fig. 42 – Potential XMA-1 fuel element designs

The high dynamic heads (up to 9.4 psi) required in testing XMA-1 fuel elements in the present burner rig facilities would necessitate operating at higher Mach numbers than those corresponding to the design values because the pressure is limited to approximately 90 psig. Since the $\Delta P_t/q$ ratio increases with Mach number above about M = 0.35, a test at the design dynamic head but at a higher Mach number would subject the element to a greater pressure drop than it would otherwise encounter. A simulated testing technique has been proposed in which the test dynamic head and the Mach number are adjusted to impose the same ΔP_t that the sample would encounter at the design Mach numbers. It is felt that this method of testing will provide the justification required for the MTR test in which the pressures are high enough to match design conditions almost exactly.

2.44 CONTROLS AND INSTRUMENTATION

Work during the quarter on power plant controls included the following: reactor startup and power range systems, an actuator for the reactor shutoff valve, a control system for reactor and combustor shutoff valves, and auxiliary power supplies. Progress in this area was significant in further defining the systems for startup and power range control and in advancing component designs for these systems.

Provisions for safety action in the power plant have been modified to a degree. Neutron flux, fuel element temperature, reactor exit temperature, and engine speed have been chosen as parameters to initiate action to first prevent power increase and second to decrease power demand. This will be accomplished by a proportional integrating action rather than the interlock and override switching used on the heat transfer reactor experiments. Current plans call for providing for an ultimate scram action on each of the parameters, but more thorough consideration will be given to minimizing the number of parameters causing scram on a flight power plant.

Startup Range

Work on the startup control system design progressed from a general formulation of the system through perturbation studies of closed-loop stability and computer studies confirming the original hand analysis. Results of the stability studies indicated a low margin, and modifications are being made to improve this condition. The mathematical determination of period computing was found to be too conservative, and adjustments will be made for a more accurate determination.

A computer study was conducted to confirm design analysis. The response of the period computing circuitry for the reactor on stable periods and for the reactor experiencing ramp inputs of Δk was determined. The transient response of the period computing circuitry to short-period inputs was also investigated.

The basic block diagram of the nuclear instrumentation circuitry which will be used to provide automatic reactor startup on a constant period has been designed. Three channels will be used to cover the range from source level to 1 percent of full power with overlap between channels. There will be interlocks between the three channels and the power range, which will automatically transfer control of the shim rods from channel to channel, and from the last channel to the power range control. Effort so far has been directed toward perfecting the circuitry required to mechanize this block diagram and to lay out the equipment packaging method which will be followed.

Power Range

The basic design of the XMA-1 reactor power range control is similar to that for the HTRE No. 3 power plant. Reactivity of the reactor would be controlled by three dynamic rod position loops operating in parallel with an On-Off shim rod circuit. The position loop demand would be proportional to the flux error generated by a flux loop. The flux loop demand would be either a computed power demand signal supplied by the engine during accelerations or the integral of the temperature loop error for steady-state operation.

The flux loop would be a Type 1 servomechanism. A variable gain amplifier would be employed in the forward elements in order to maintain a constant open-loop gain. A lag network with a gain and time constant varied as a function of airflow would be employed in the feedback for stabilization purposes.

The temperature loop would be a Type 1 servomechanism to insure good steady-state accuracy. It has been possible to eliminate the need for opening the temperature loop when the control shifts from steady-state to acceleration demands. Speed or temperature error forces the temperature error-integrator against a limit established by the acceleration power demand.

Work on the power range control system design during the quarter resulted in two significant decisions:

1. To permit the system design to proceed pending additional information, airflow will not be a required function in the flux loop for the ground test power plant.
2. Duplication of channels will be avoided in favor of developing reliability, although duplicate channels available upon operator choice will be provided for the ground test power plant.

Work on all of the electrical system components for the power range have received breadboard development attention. However, lack of finalization of system specifications is delaying the placement of a supporting subcontract deemed advisable to achieve a thoroughly developed system.

Turbomachinery Control

Within the turbomachinery controls development program orders were placed with vendors for design and procurement of an aft lube scavenge pump, a main lube pump, a forward transfer lube pump, a variable-stator actuation pump, a main ignition system, and the electromechanical part of the main control system. The detailed engineering requirements for the overspeed governor were issued, and orders for design and procurement are expected to be placed early in the next quarter.

IBM programming for determining engine transient conditions for parallel engine operation was completed. The initial engine-acceleration time study was also completed. Final cam schedules for use in design of the development model for the pneumatic parts of the main control system were released to a vendor. A J47-D17 engine was operated successfully using the variable-area jet nozzle to control speed and the fuel flow to control turbine discharge temperature.

Actuators

A study is presently being conducted to determine the feasibility of utilizing a pneumatic piston-type actuator for positioning the dynamic rods in a nuclear reactor. A computer study was initiated to predict actuator performance and to make possible a more systematic approach to valve selection and control circuitry design. Testing, including high-speed motion pictures, has permitted calculated data to be replaced by test information. Tests to date are encouraging, and the computer setup predicts that such an actuator can be controlled with a high degree of reliability. The actuator has been able to follow valve reversals up to 16 times per second (8 cycles per second) with an amplitude of rod travel of approximately 3 inches. This represents the limit of the present test setup and not that of the actuator. The actuator is presently being prepared for closed-loop operation.

The most acute of the component problems in the high-temperature hydraulic actuation program is the seal problem where the hot piston rod re-enters the cylinder. Since results indicate that there is little hope of solving the problem through finding a suitable seal material, new concepts appear to be required.

Successful testing has been obtained on a 500°F bellows accumulator, and a life test is in progress.

Test results on a ball pump for use at $500^{\circ}F$ have indicated short life before leakage becomes excessive.

Temperature Sensors

The most significant fuel element thermocouple test performed during the quarter was one in which six platinum versus platinum - 10 rhodium thermocouples were spot-welded to a fuel sheet and heated to $2250^{\circ}F$ for 250 hours in static air.

Microscopic examination of fuel sheet cross sections at the location of the thermocouple junctions revealed that the platinum had migrated into the Fe-Cr-Al cladding and that elements in the cladding had migrated into the thermocouple wires. The thermocouple leads immediately adjacent to the junctions, noticeably enlarged in diameter, were very weak and brittle and were found to be ferromagnetic, indicating the presence of either chromium or iron in the wires. There was evidently some embrittlement of the Fe-Cr-Al in the area of the junction, since in the process of mounting the samples, a fracture occurred in the cladding on each side of some of the welded thermocouple wires. It had been expected that the noble-metal thermocouple materials would migrate into the niobium core and that the resulting low-melting eutectics would destroy the fuel sheet. There was no evidence of this in the test described, but it was concluded that the reactions between platinum and the Fe-Cr-Al cladding would preclude the feasibility of spot-welding noble-metal thermocouples directly to the XMA-1 fuel sheets.

An unsuccessful attempt was made to find another thermoelement material that would be suitable for welding to the fuel sheets.

Some method of placing thermocouples as close as possible to the fuel sheet without actual contact will be sought. Preliminary tests using a ceramic cement show promise.

Various iron-aluminum alloys are being procured in a search for some other thermo-element materials suitable for welding to Fe-Cr-Al.

Nuclear Sensors

The nuclear sensor development program has been firmed up. Experimental designs of both fission and ionization chambers have been completed, and a fission chamber has been operated at $1000^{\circ}F$. Pertinent specifications which would allow preliminary investigations have been received.

Vendors were contacted to determine types and availability of specific materials and services, and a set of preliminary specifications for the nuclear sensors has been worked out.

2.45 SHIELD

Mechanical Design

The XMA-1 reactor shield assembly, which consists of the side shield assembly, front plug, reactor shutoff valve, and the rear plug, is the same as described in the previous quarterly report except for the relocation and redesign of the front and rear trunnion support rings and the redesign of the shaft alley shield plug as a subassembly. Design studies have again been concentrated on porous shield plugs of the wavy-wall configuration, and these will continue until nuclear, aerodynamic, or thermodynamic data indicate greater over-all efficiency of another design.

Pressure Shell and Side Shield

The straight, Inconel X pressure shell is flanged on both ends for assembly of the turbo-machinery, and the power plant mounting trunnions are attached to the front and rear trunnion rings. The front trunnion ring was removed from the front flange and redesigned as a box section welded to the pressure shell. This box section serves as a ram-air, side-shield plenum chamber. The aft trunnion ring was changed from a deep full ring, bridged at the engine shafts, to a yoke design that eliminated the bridge structure. This ring also serves as the ram-air exit plenum chamber.

Figure 43 illustrates a proposed method of side shield assembly. The Hevimet side gamma shielding is attached to the pressure shell by splines, thus providing for differential expansion.

A method was devised for making the shaft alley plug as a subassembly in which the shaft, shaft bearings, and shielding can be assembled and attached to the side shield as one unit. This method improves remote handling and provides the rigid bearing foundation required by recent specifications.

Several methods of attaching transition duct support braces to the shield structure were investigated. The transition ducts as now designed require these braces in order to support the compressor and turbine sections under vertical loads without exceeding the allowable compressor-turbine shaft deflections. Preliminary studies indicate that supports of adequate rigidity can be provided for about 350 pounds added weight.

Because drawings must be released at an early date for manufacture of the four power plants to be used in the first tests, the present transition ducts with external braces will be used. However, since tests conducted early in the transition duct development program showed that large mechanical loads as well as the pressure loads could be carried by ducts made from thin shells. Also, since design studies on completely self-supporting ducts are not completed, a decision on the design of the transition ducts to be used on subsequent power plants has been deferred until the design studies for self-supporting ducts are completed.

Three methods of mounting the struts to the pressure shell were studied. Each configuration was sized to limit the deflections of the strut in the axial direction to between 1/16 inch and 1/8 inch under an 80,000 pound-per-strut axial load. The first two designs were based on a strut geometry in which the loads were reacted axially and radially by rings attached to the pressure shell. The third design was based on a new strut geometry in which the struts intersect the pressure shell approximately tangentially and are supported by the combination of the trunnion ring and an additional flange plate. Further study may reveal that the addition of the flanged plate is not necessary. This design adds approximately 350 pounds to the shell as compared to 550 and 660 pounds for the other two designs. JED was instructed to use the strut geometry of the third design for the first engine tests.

Front Shield Plug

The front shield plug presents an airflow problem due to the blockage of air passages by the control rods. The aerodynamic and nuclear aspects of this problem are being investigated.

A more detailed stress analysis is being conducted to establish the required sizes of the plug supporting structure and the gages of the wavy-wall skins. Various methods of supporting the wavy walls in the plug structure are being investigated. Portions of the wavy wall and attaching structure will be fabricated and tested during the next quarter.

Rear Shield Plug

Various design configurations for the rear shield plug have been considered and investigated, but no definite solution has evolved.

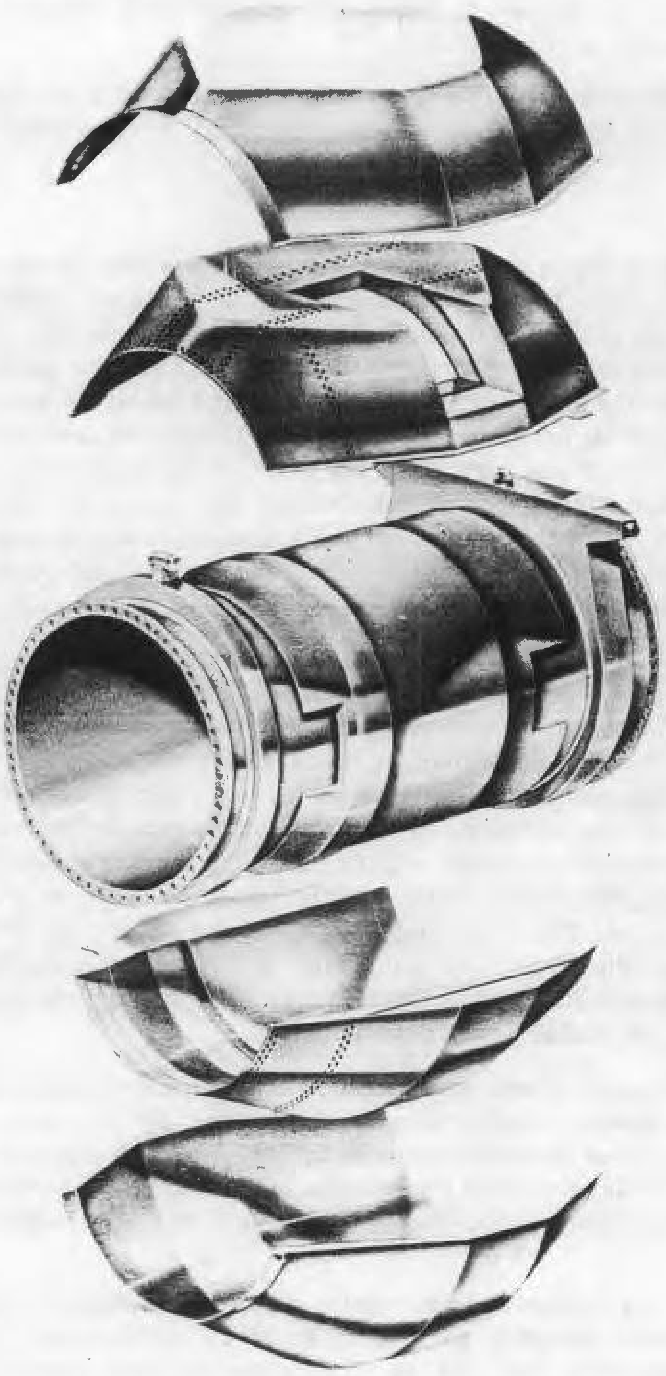

Fig. 43 – Side shield assembly, XMA-1

It was decided that the bolting flange of the rear plug will be made of the same material as the bolting flange of the pressure shell. This will eliminate stresses on the bolting flange caused by difference in coefficients of expansion of dissimilar metals, especially between molybdenum and Inconel X, where the molybdenum coefficient is approximately one-third that of Inconel X.

Methods of attaching molybdenum plug structure to an Inconel X plug bolting flange have been studied, and some of the designs appear promising. This problem requires further investigation.

Nuclear Analysis

Previous shield analyses on the XMA-1 power plant have been based on the assumption of a homogeneous reactor. The reactor composition is far from homogeneous, however, because of the air passages that run longitudinally through the reactor, reducing the effect of self-shielding in the forward and rearward directions. Studies were conducted to determine the extent of the error entailed in calculations based on homogeneous reactor composition and to provide numerical factors for correcting the dose rates. Two receiver points were considered: 50 feet directly to the front and 50 feet directly to the rear of the reactor midpoint. A typical front reactor shield was assumed. Radiation streaming through the front and rear plug of the shield was not considered. Consideration of the non-homogeneity of the reactor increases the calculated neutron and gamma dose rates by factors of 10 and 5 respectively at the front of the reactor. At the rear the corresponding factors are calculated to be 8 and 4.

A study was conducted to determine the effects of components of the XMA-1 power plant on radiation levels 50 feet from the core midpoint. Previous dose rate calculations considered only the reactor core and shield. In this analysis, the additional shielding afforded by the following components were considered for each engine: compressor, gear box, burner cans, shaft, turbine, tailpipe, and jet nozzle. The reactor control mechanism outside the front plugs was also considered. The shielding effects of one power plant on the other was not investigated. Dose rate calculations were based on a reactor operating power of 194 megawatts. The core composition, gamma source spectrum, nuclear data, and longitudinal power distribution were the same as those used in former shield studies. However, a radial power distribution function $p(r) = \cos 0.01\, r$, was used in place of the previously assumed flat radial power distribution.

The engine components caused reductions in the radiation beam (as applied to crew compartment calculations) by factors as high as 40 and 250 for neutrons and gammas, respectively, at the angles of radiation emission that were most affected. Although a complete shield analysis was performed wherein the major engine components were taken into account, the integrated effect of the engine components on shield weight has not yet been determined.

An investigation was conducted to determine the effect of induced radioactivity of core materials on the XMA-1 shutdown gamma ray spectrum and intensity. Calculations were based on a reactor shutdown time of three hours following forty hours of reactor operation. For these conditions it was concluded that the shutdown decay gamma rays from neutron-activated core materials are insignificant as compared to the shutdown gamma rays resulting from the decay of fission products.

Nuclear Testing

During the past quarter, the test schedule in the Convair shield testing facility was renegotiated to provide for the nuclear testing of XMA-1 shield components in the first

[redacted]

quarter of the next fiscal year. In that period it is planned that the following shield mockups will be tested:

1. Strut-type porous plug made of plastic and lead-impregnated plastic.
2. Wavy-slab-type porous plug, made of plastic and lead.
3. Slab-type control experiment for tests 1 and 2, made of plastic and lead.
4. Slab-type material mockup of side shield or portion thereof (Hevimet or steel, LiH).
5. Slab-type material mockup of front plug or portions thereof (Hevimet or steel, Be, CaH, or LiH).
6. Slab-type material mockup of rear plug or portion thereof (BeO, ZrH_x).

Material procurement or fabrication of all of these mockups has begun.

The mockups are to be tested in an above-ground pool in order to allow measurement of radiation levels in air at distances of 50 feet or more around the shield mockups. A large water tank, 14 feet in diameter and 14 feet high, will be constructed for these and future tests. As a matter of operating convenience, it is planned to build the above-ground tank so that the Convair GTR, in a moderator tank, can be lowered directly into the test tank to serve as a radiation source. The test shields will be supported between the reactor face and the external wall of the tank. The design of this test tank has been initiated and sources of commercial steel storage tanks are being investigated.

Work has continued on the three porous-plug-type shield mockups intended for testing at Convair. These include a wavy-slab-type shield, a strut-type shield, and a flat-slab construction that will serve as a control in testing. Material for these mockups was specified during the quarter after consideration of several alternative mixtures. The gamma shield material selected is a borated, lead-loaded plastic with a density of 4.7 to 5.0 grams per cubic centimeter. The final product will be uniform in density within approximately one percent. The plastic will be an epoxy resin with nuclear properties similar to those of polyethylene. The neutron shielding in these mockups will be the same type material without lead loading. Its density will be about 1.6 grams per cubic centimeter.

Work is nearly complete on a new wavy-slab-type porous shield configuration that incorporates large air-gap width and is compatible with current designs of control rod patterns. When the configuration is established a nuclear shield test model will be constructed for future testing.

Test data obtained with the wooden wavy-slab-type porous plug mockup described in the last quarterly report were received from Convair during the quarter. The primary object of the tests was to determine the extent to which a wavy-slab shield plug could be treated as a homogeneous mixture of void and shielding material. This was done by comparing it to a flat-slab array which, because the slabs were aligned perpendicularly to the reactor axis, could be considered equivalent to a homogeneous mixture. Both arrays were built of white pine and contained approximately the same average weight of wood per unit volume. Direct neutron dose rates penetrating through the wavy-slab-type plug were measured at a factor of 2.9 and 1.8 higher than those measured through the flat-slab control plug, at distances of 32 feet and 62 feet respectively. Since the density of the wood strips from which the wavy slabs were made varied by as much as 10 percent, it is felt that no qualitative conclusions can be drawn from the test results. The plugs were constructed of wood as an emergency measure to meet test schedules. It is felt that the tests did meet the minimum requirements for which they were intended, since they lend some evidence that the duct-leakage dose rate through a wavy-slab-type shield of the design tested can reasonably be expected to be no greater than the direct-beam dose rate through the same shield.

[redacted]

2.46 AERODYNAMICS AND THERMODYNAMICS

Primary Airflow Circuit

Design of the 1/4-scale model of the primary-flow circuit of the XMA-1 power plant was completed during this quarter, and construction of the front half is essentially complete. Aerodynamic tests using the model will begin early next quarter. Present plans are to test each component before the tests of the entire flow circuit are made. First tests of the entire flow circuit will be made using a tube bundle which is now in use for tests of the primary-flow circuit of the HTRE No. 3 power plant. Design of a new 1/4-scale tube bundle which will simulate that of the XMA-1 power plant will be started as soon as the full-scale design is finalized.

Investigations of fuel element stage length and taper of the fuel tubes have been completed. Results indicate that, depending on the longitudinal power distribution, up to 10 percent reduction in reactor core pressure drop (2 percent increase in thrust at cruise) can be obtained by tapering the fuel tubes while holding core size and moderator volume constant. Slightly larger gains than these can be obtained through the use of fuel-element stage lengths three to five times the 1-1/2-inch length of the original design. Calculations were based on an isothermal fuel element temperature of 2100°F. The values of pressure ratio calculated for a single fuel tube at the cruise condition are given in Table 7.

TABLE 7

FUEL TUBE PRESSURE-RATIO VALUES AT CRUISE

Number of Stages	Tube Taper	Forward Profile		Cosine Profile	
		Fractional	Integral	Fractional	Integral
1	0.000°	---	0.864	---	0.787
	0.561°	---	0.860	---	0.699
	0.858°	---	0.847	---	0.653
5	0.000°	0.877	0.870	0.860	0.846
	0.651°	0.875	0.870	0.870	0.860
	0.585°	0.869	0.857	0.869	0.863
18	0.000°	0.852	0.838	0.839	0.830
	0.561°	0.849	0.839	0.856	0.845
	0.858°	0.841	0.829	0.856	0.845

The calculations have been based on two assumptions. The first is that the fuel element temperature is exactly 2100°F. This results in the use of a geometry that is equivalent to a fractional number of rings. The second set of calculations is based on a geometry where an integral number of rings are assumed. Since the values of heat-transfer area are discrete, the minimum heat-transfer area necessary to limit the fuel element temperature to 2100°F is approximated by the next higher discrete value of heat-transfer area. This results in the use of heat-transfer areas that are conservative by approximately 5 percent.

Power Plant External Cooling

A preliminary report has been completed on the engine external cooling requirements analyses carried out on a subcontract basis by the Flight Propulsion Laboratory Department. The work in this area is expected to continue for several months, with the end goal of establishing the complete airflow and pressure-drop requirements for the cooling of the turbomachinery.

Turbomachinery

Afterburner inlet diffuser contours, strut shape, and strut orientation were established, and afterburner combustion and aerodynamic objectives were reviewed.

Jet-nozzle cooling studies have been carried out and have revealed problem areas on which further cooling design effort is being carried out. Development of nozzle-performance analysis methods and investigation of performance with high secondary nozzle flow were also carried out.

Long-range turbomachinery performance improvement has received intensive general study, and programs for detailed investigation of specific concepts and configurations will be established within the next few weeks.

Completion of studies of improvements for hot-day cruise performance revealed no practicable method whereby thrust deterioration with temperature increase could be significantly reduced. However, certain ideas developed in connection with the hot-day studies show some promise in over-all power plant performance improvement.

Progress was made in identifying long-range performance improvement objectives and capabilities. It appears that, in addition to cruise thrust, the thrust available for acceleration to sprint conditions is extremely critical at hot-day conditions. Future major effort is planned in the area of long-range performance improvement.

2.47 REMOTE HANDLING

Studies on remote handling have evolved some basic objectives that will be applied to the design of turbomachinery components. Additional studies are in process to determine the most desirable power plant axis position for optimum remote assembly and disassembly, tooling requirements for remote handling of flange bolts, and minimum clearances required for remote handling equipment that is presently available.

The following remote handling design objectives were established for the turbomachinery components:

1. It shall be possible to remotely assembly the major assemblies and also remove them from the reactor-shield assembly. The major assemblies are:
   a. Engine compressor assembly. This assembly consists of all turbomachinery parts forward of the compressor transition duct.
   b. Transition ducts.
   c. Bypass burners.
   d. Turbine-tailpipe assembly. This assembly consists of all turbomachinery parts aft of the turbine transition duct.
   e. Coupling shafts.

2. All piping and wiring which extends from one assembly to another must be capable of being connected and disconnected remotely in order to permit the remote assembly and disassembly of the major turbojet assemblies on the reactor-shield assembly.

[redacted]

CONFIDENTIAL

CONFIDENTIAL

[redacted]

3. POWER PLANT TECHNICAL DESIGN AND APPLICATION STUDIES

3.1 ALTERNATIVE POWER PLANT STUDIES

Separable-Engine Power Plants

The primary effort on the separable-engine power plant during the quarter has been expended in attempting to adapt ceramic fuel elements to the basic configuration. A two-phase study has been initiated:

1. Ceramic fuel elements in conjunction with a hydrided zirconium moderator.
2. An all-ceramic (BeO) core design.

Cooling the hydrided zirconium moderator appears to be difficult. Preliminary studies on both single-pass and counterflow cooling-air systems are in progress.

The all-ceramic core study has been concerned with core sizing (on the basis of thermodynamic considerations only) for a BeO core. Fuel element designs which will permit more efficient use of the ceramic heat-transfer area than the present tube design are being investigated.

Single-Engine Power Plants

Work has continued on the single-engine power plant design with emphasis concentrated on design and development of mechanical components.

Engine studies show that a shaft length of 140 inches with a diameter of 10 inches is possible. At present a length of 120 inches is considered practical and feasible. Cooling requirements for this shaft at Mach 0.9 and sea level indicate that 2 pounds per second of seventh-stage bleed air is adequate. Interburner designs are progressing, and two types will be considered for final analysis. One is a parallel system utilizing cold valves and a reverse-flow combustor. The other will be a series bypass system with a hot valve and reverse-flow combustor.

Cellular metallic cores and shielding similar to that of the XMA-1 are assumed. Reactor control may be achieved by using either electrical or pneumatic control of reflector-absorber drums. At the present time a pulsed or digital drum position control is being investigated.

Criticality calculations for the single-engine power plant reported in the previous quarter have been extended to include studies of longitudinal power shaping. The power density at a space point is the product of flux and macroscopic fission cross section. It is possible to skew the flux in the desired direction by preferential end reflection, to alter both flux and fission cross section by nonuniform fuel distribution, or to combine the effects.

Uniform fuel distribution and variable end reflection for the single-engine power plant results in power shifts as shown in Figure 44. Reflector thicknesses on the forward and aft end of the core are varied in three steps as indicated in the figure.

[redacted]

[redacted]

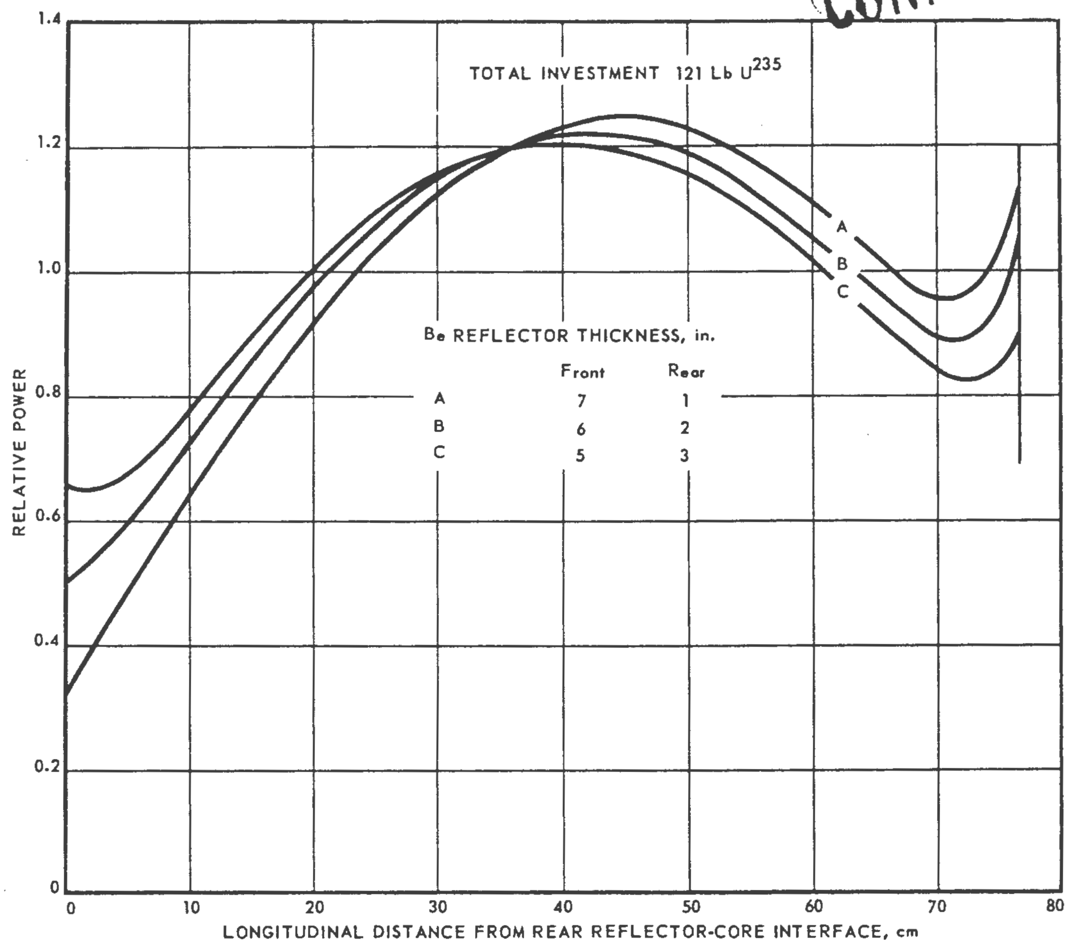

Fig. 44 – Calculated longitudinal power distribution – single-engine power plant with uniform fuel distribution

The modification of power thus obtained is in the desired direction, but the detailed distribution can be further improved by varying fuel density. A series of trials guided by the general rule of increased fuel in regions of depressed flux will make it possible to approach the desired monotonic longitudinal distribution. Figure 45 shows typical results for a fuel density variation of three steps wherein the forward and aft concentrations differ from the midsection by 20 percent and end reflection is varied.

In principle this can be extended to a finer spacing approaching a continuous function, and the power can be shaped within wide limits.

3.2 ADVANCED MISSILE PROPULSION SYSTEM

Performance Studies

A design-optimization study has been undertaken for application of the AC-210 ceramic reactor to a ramjet power plant at the design conditions of 70,000 feet and Mach 4.25. Payload capabilities are expected to be increased over those of the AC-210-3 power plant, which was optimized at 90,000 feet and Mach 4.25; the increased payload is at the expense of altitude reduction to the 70,000-foot condition.

[redacted]

[redacted]

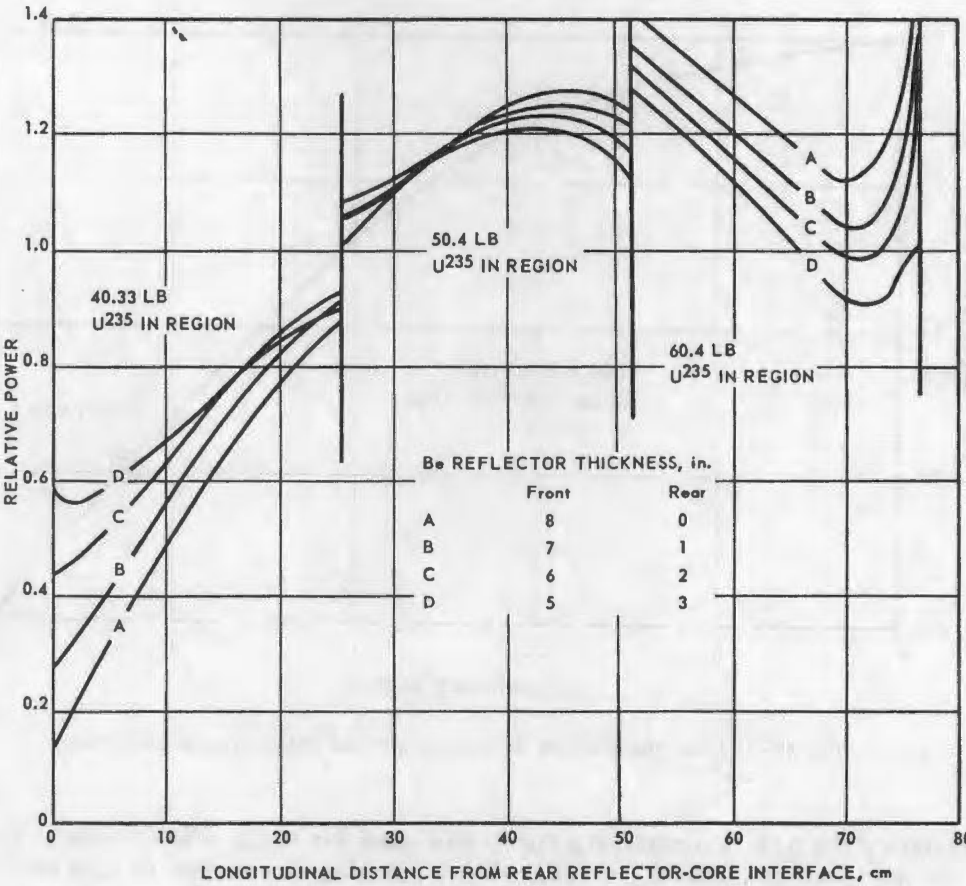

Fig. 45 – Calculated longitudinal power distribution – single-engine power plant with three regions having different fuel densities

Evaluation of the AC-210-3 missile power plant off-design performance has been divided into three general categories: evaluation of the ramjet inlet, diffuser, and nozzle-performance characteristics; evaluation of the reactor thermodynamic performance characteristics; and, finally, evaluation of the over-all missile off-design performance characteristics (net thrust, power density, etc.) at all altitudes and corresponding flight speeds concomitant with matched and compatible flow, pressure, and heat transfer conditions in the inlet, diffuser, reactor, and nozzle.

The supersonic spike inlet design of the AC-210-3 has been altered to improve pressure recovery. The subsonic diffuser design was also more completely evaluated than heretofore; specifically, the conical center body with a 15-degree half-cone angle and a length of 176.51 inches yielded a throat area of 1061 square inches with a 12.5-degree divergent half angle and a diffuser exit area of 7088 square inches. Also, the nozzle design was altered to effect improvement; the throat diameter was made 57.16 inches and the divergence angle of 10 degrees was retained to eliminate an overly long nozzle and yet to keep divergence losses at a minimum. With the limitation imposed on the nozzle-exit diameter by the maximum diameter of the body, 105 inches, the nozzle will operate under-expanded at the design point, and an exit-to-throat area ratio of 3.37 will prevail (the ideal ratio is 6.2); the required length from throat to exit becomes 135.6 inches.

Performance characteristics of the improved inlet and diffuser designs have been evaluated to enable off-design missile performance calculations. The characteristics of the fixed geometry inlet are given in Figure 46. For the inlet and diffuser pressure recovery

[redacted]

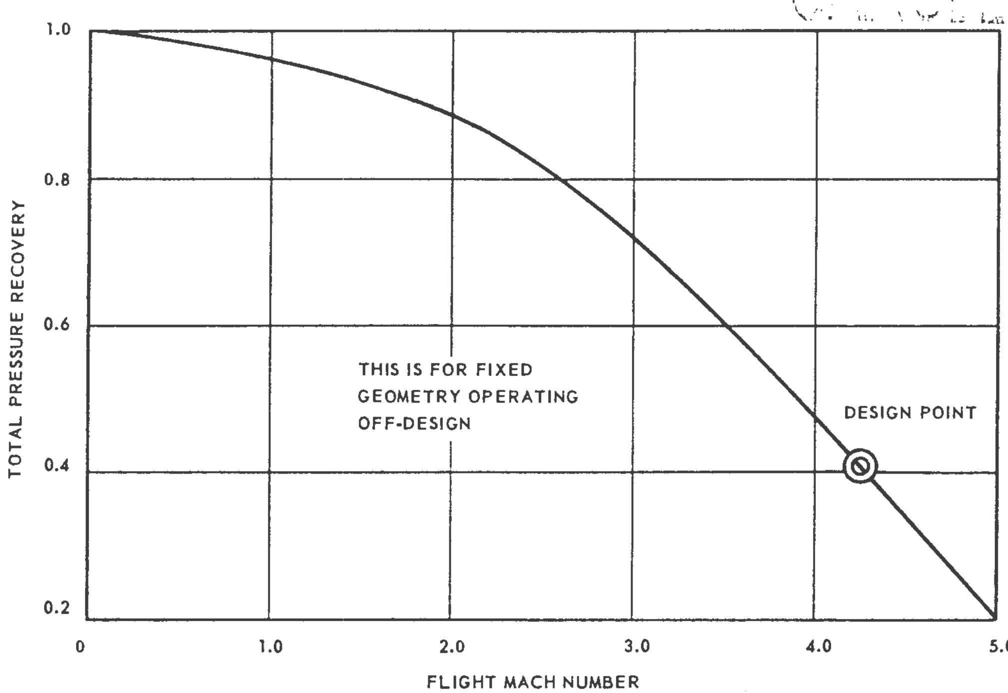

Fig. 46 – Over-all total-pressure recovery of inlet and diffuser versus flight Mach number

characteristics the AIA ram recovery curve was used for flight Mach numbers from 2.5 to 5.0; for the lower range of Mach numbers the curve is an average of data made available in numerous NACA reports.

The nozzle characteristics, reactor thermodynamic characteristics, and missile off-design characteristics will be presented in a forthcoming report; reactor pressure losses, taken from the computer output, are currently being plotted as a function of inlet-flow temperature and pressure parameters. Complementary values of reactor discharge air temperatures for these same parameters have been plotted from computer results; these curves appear in Figure 47. For any point on these curves the reactor is operating with a maximum fuel element wall temperature of $3000^{\circ}F$. The fractional longitudinal distance within the reactor at which the maximum fuel element temperature is $3000^{\circ}F$ is not the same for any two points on these curves. At the design point the reactor is isothermal; i.e., the fuel element wall temperature is $3000^{\circ}F$ throughout the reactor.

Controls

The reactor characteristics were studied to evaluate effectiveness of control means and to determine more fully the axial flux and fuel distribution in the core. The control calculations investigated the effectiveness of black rods and gray rods, and the flux calculations determined flux and fuel distribution using one-group, one-region; two-group, one-region; and two-group, two-region models.

The amount of reactivity controlled by variation in fuel loading was evaluated and is depicted in Figure 48. The reactivity change as a function of void fraction in the jacket reflector is given in Figure 49.

In order to adequately delineate control requirements and to be flexible on initial calculations, the effects of nonuniform fuel loading were considered. As indicated above, several nuclear models and assumptions were used in progressive evaluations. The most sophisti-

[redacted]

CONFIDENTIAL

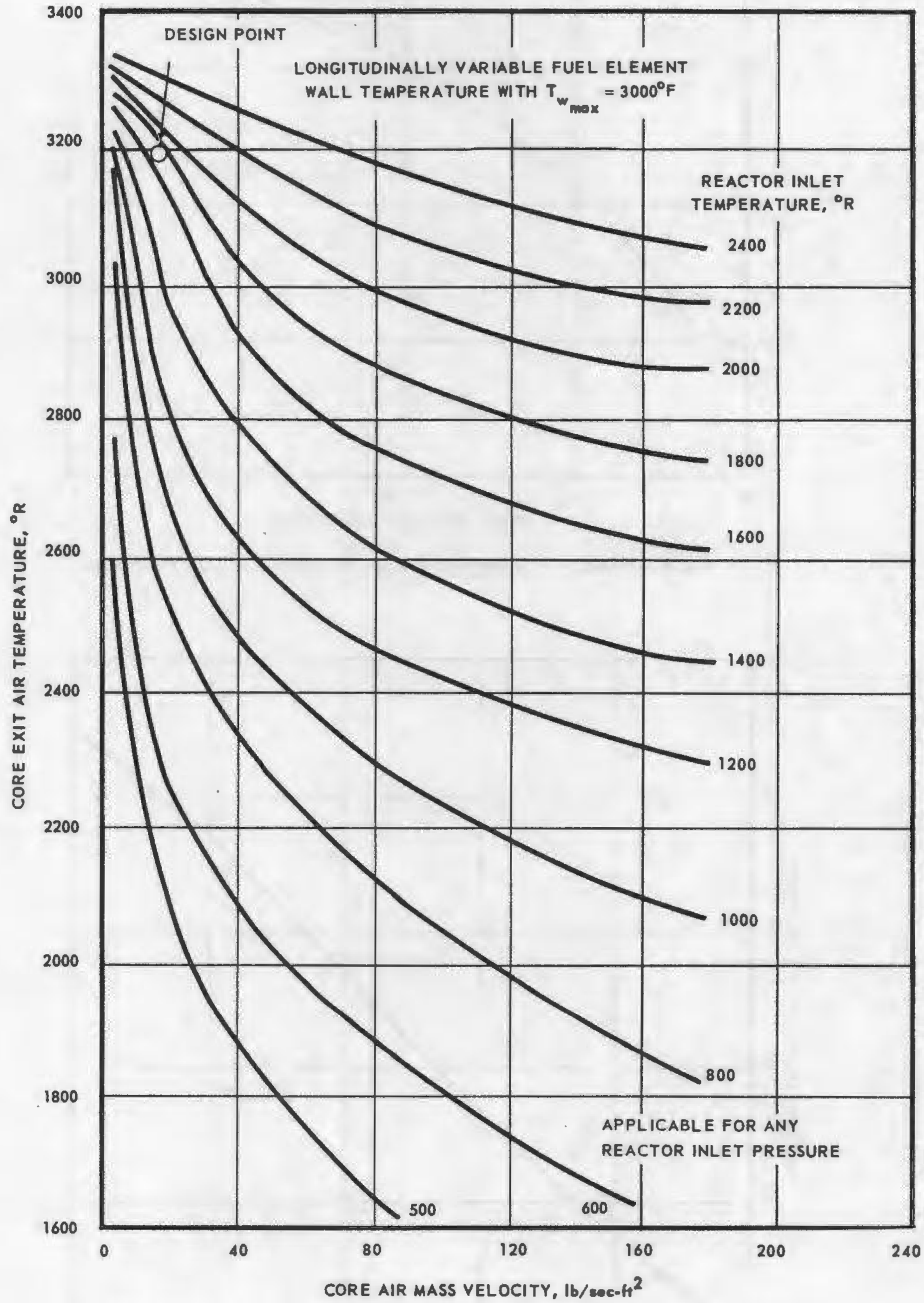

Fig. 47 – Off-design reactor thermodynamic characteristics

CONFIDENTIAL
CANCELLED

[redacted]

[redacted]

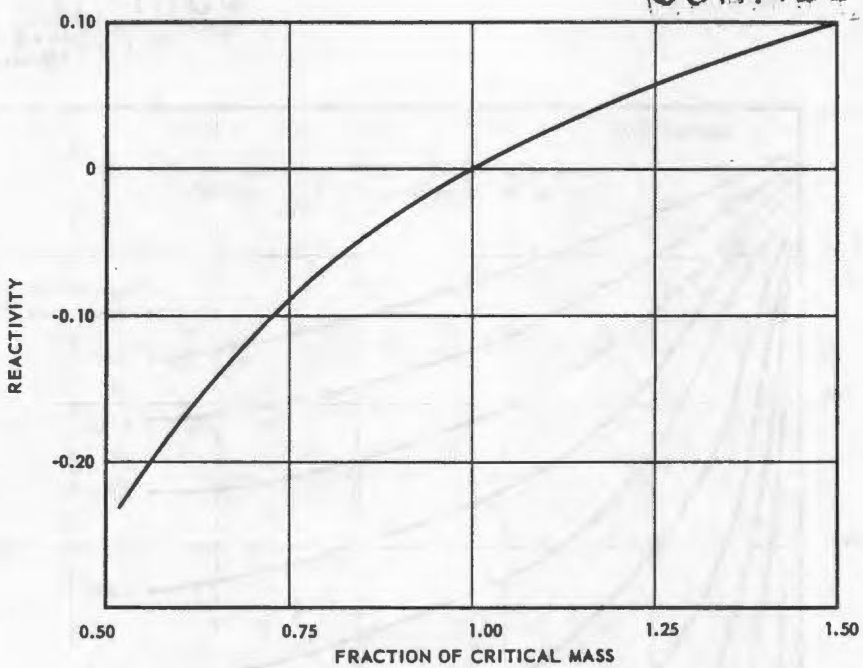

Fig. 48—Reactivity change with change in fuel loading, missile reactor

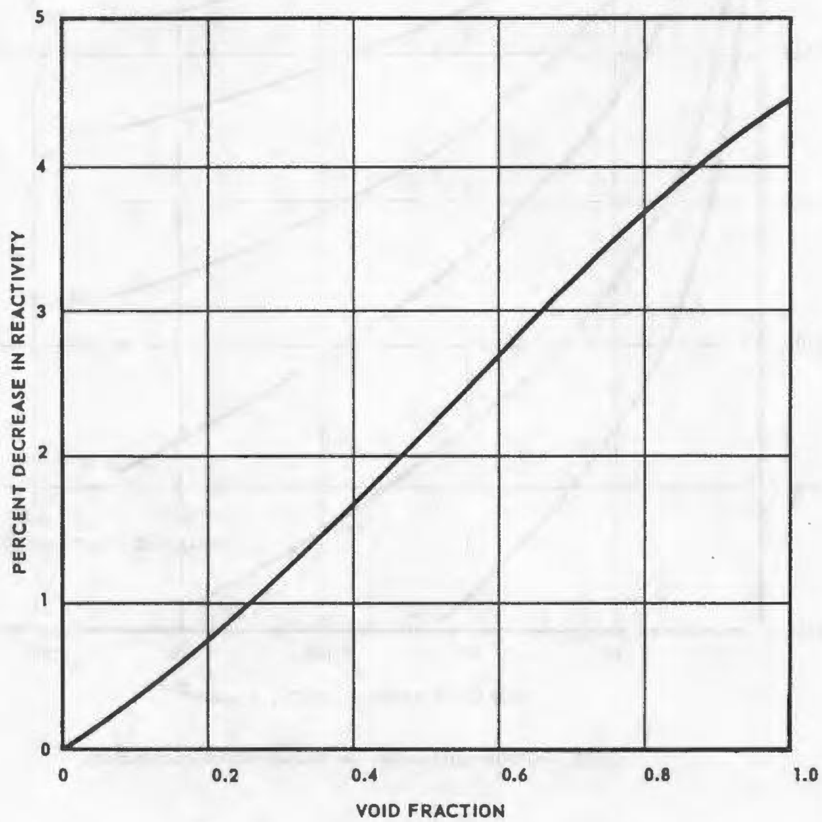

Fig. 49—Decrease in reactivity resulting from void fraction in jacket reflector, missile reactor

[redacted]

cated (and last) study involved a design modification of the AC-210-3 reactor; an 8-inch hydrided zirconium reflector was assumed at the front end of the core. It appeared advantageous to increase the reflectivity at the core front end in order to bias the power toward that end (to obtain an isothermal reactor) and to reduce the relatively high fuel loading near the front of the core. Since the temperatures at the front face are not excessive, hydrided zirconium was chosen as the front reflector material because of its excellent nuclear properties. In this calculation, the reflector savings for the rear axial BeO reflector were assumed the same as used in the original calculations. The radial buckling was also assumed to remain constant, as in the previous calculations.

The resulting two-group, two-region calculation was performed, and relative axial flux profiles and fuel distributions were obtained. Figure 50 shows the relative axial fast and thermal neutron flux distributions, the fuel distribution normalized to unity at the minimum value, and the normalized axial power distribution. The normalized axial power distribution was assumed to have the form $P = 1.3 + \cos 100 (X/L + 0.6)$ where the argument of the cosine function is in degrees, L is the core length, and X is the distance from the front of the core. This agrees very closely with the values plotted for the core longitudinal power distribution.

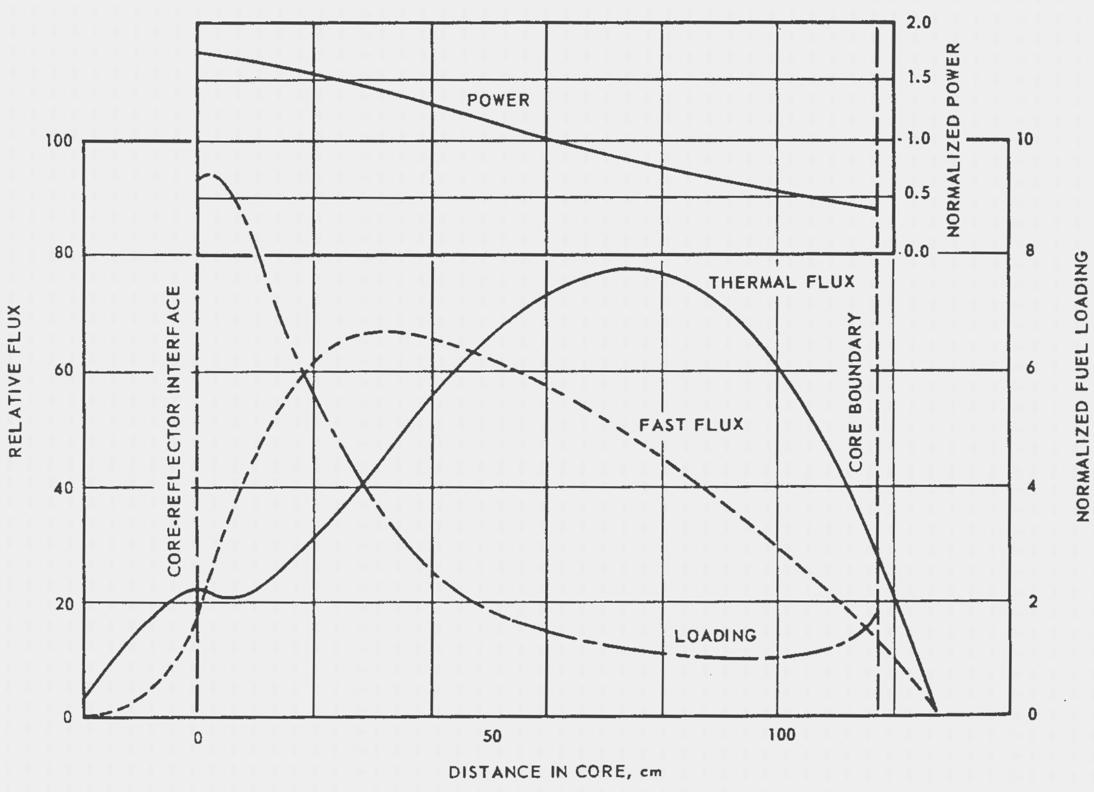

Fig. 50 – Missile power plant – two-group, two-region calculation – ZrH reflector

Control Components - An experimental "screw-nut" for use in the 1/4-scale controls mockup was designed and fabricated and is undergoing tests. This nut employs rolling motion instead of the more conventional sliding friction. Therefore, this design should offer good possibilities at elevated temperatures where lubrication is not feasible.

Design layouts were made of control actuator systems which could be used in a missile power plant. The most promising design was selected and the required parts have been ordered.

Ceramic Assembly Burner Rig Tests

During the final quarter of 1956, burner rig tests on a silicon carbide assembly were conducted at temperatures up to 2000°F. In order to gain additional information about the high-temperature capabilities of this assembly, a design was completed for an experiment on a similar configuration at temperatures up to 2500°F. This assembly will be tested in a burner rig test section which is presently being installed at Wright Air Development Center for experiments in connection with the development of components for the gas dynamics facility. This apparatus has a slow initial temperature rise and temperature capabilities up to 2500°F.

It is anticipated that the component parts of the test assembly will be delivered late next quarter. The actual date for the testing phase is contingent upon this delivery date and also upon the availability of the experimental facilities. It is expected, however, that the tests will be completed during the third quarter of 1957.

Systems Analysis

A study was conducted with the aid of the Aircraft Gas Turbine Division to gather data on chemical ramjet systems for comparison with existing data on nuclear ramjet systems. Additional performance data on advanced chemical rockets have been obtained from the General Electric Rocket Engine Section for comparison with nuclear rocket data. Re-evaluation of hydrogen tankage weights and critical mass values for nuclear rockets is being performed.

3.3 ADVANCED NUCLEAR TURBOPROP STUDIES

A report that presents flight performance data on a nuclear turboprop power plant for both chemical and nuclear operation from sea level to 36,000 feet altitude was issued during the quarter. This power plant is based on the bleed-turbine principle and is designated the AC-300-3. In the study the turbomachinery was sized for the condition of operation at Mach 0.6 at 20,000 feet. Because of off-optimum matching of the split between the basic gas generator and the bleed turbine, the ESHP available at sea-level-static conditions on all-nuclear operation does not equal the performance of a single-shaft or non-bleed turboprop machine.

Controls

A control system study was performed in order to identify some of the problems associated with the bleed-turbine arrangement of the turboprop power plant. Reactor controls for a turboprop power plant do not present any serious problems because of the low temperature and radiation environment. Hydraulic equipment developed for HTRE No. 3 would be applicable for dynamic rod control, and much of the electronic computing elements used in that system can probably be replaced with magnetic amplifiers. A proportional plus integral flux or temperature controller can be constructed of magnetic amplifiers with presently available components, and when it is connected with the hydraulic actuators, a complete system would be available. Synchronous-motor-driven shim rods such as those developed for the HTRE's would be satisfactory for this application. A final mechanization study will be performed in order to have an adequate comparison between electrical, mechanical, hydraulic, and pneumatic components.

No attempt was made to segregate reactor control from engine control in the study. A bleed-turbine arrangement such as is presently being investigated requires integrated control of two gas generators, two bleed turbines and two propellers, and a reactor or heat exchanger.

Three major problem areas which may require special consideration exist in a mixed chemical-nuclear bleed-turbine arrangement. One of the problem areas is concerned with the transfer from chemical power to nuclear power and vice versa. Two burners must be controlled during the transition, and each burner must be operated on a different temperature schedule since a higher temperature is desired at the gas generator turbine than at the bleed or power turbine. Such requirements dictate the use of at least partial temperature control of the burners and tend toward a speed-controlled reactor. Several methods for mechanizing the transfer control are under investigation.

A second problem area that may exist in a bleed-turbine arrangement is that of overspeed protection. The bleed turbine is independent of the compressor; thus, in the event of a mechanical failure of the transmission or propeller actuator systems, the turbine load becomes very small, and the bleed turbine may accelerate rapidly beyond the maximum speed limit.

The third problem area of major significance exists in starting the engines on chemical fuel. Two condition levers may be required to properly sequence the control operations associated with the ignition of the gas generator and bleed-turbine combustors. Starting up a bleed turbine power plant can undoubtedly be performed successfully; however, it is desirable to maintain a simple starting procedure by using only one condition lever for each power turbine.

Reactor Shield Design

The first phase of the reactor-shield-assembly preliminary design study has been completed. The AC-300-3 reactor-shield assembly was specifically designed to operate with the bleed-turbine type of engines. This reactor-shield assembly differs from the AC-300-2 RSA in that the fuel elements are set in a horizontal position and the design incorporates a porous-plug-type rear shield. Figure 51 shows the general configuration layout for the power plant.

The solid-moderated solid-shield reactor shield assembly with its associated cooling ducts is shown in Figure 52. This work represents an initial study on the bleed-turbine-type turboprop power plant. Studies are in progress to refine and extend the work accomplished to date.

Parametric Shielding Data

Parametric reactor-shield assembly data previously issued for one altitude have been adjusted for altitudes of from sea level to 35,000 feet. Figures 53, 54, and 55 are typical curves showing reactor shield assembly weights and dimensions for an altitude of 20,000 feet. These data are based on the AC-300-2 turboprop power plant.

Isodose data are reported here for the first time and are shown in Figures 56, 57, 58, and 59. Although obtaining isodose curves for the complete parametric family of power plants studied previously would have been desirable, the isodose calculations were necessarily limited to a single power plant representing one combination of parameters. Extrapolation of these results to those for other combinations of parameters may then be accomplished, provided care is taken when large differences in shield thicknesses exist.

Direct dose rates were obtained through the use of Program 04-0 on the IBM 704 computer. Since the AC-300-2 reactor is mounted vertically on the wing, direct dose rates were computed for points every 15 degrees in the vertical plane which is perpendicular to the fuselage centerline and at distances from the reactor of 10, 20, 50, and 100 feet. Air-scattered radiation levels were computed assuming the RSA to be a point isotropic source. Values were obtained by using air-scattering calculations for one distance from the re-

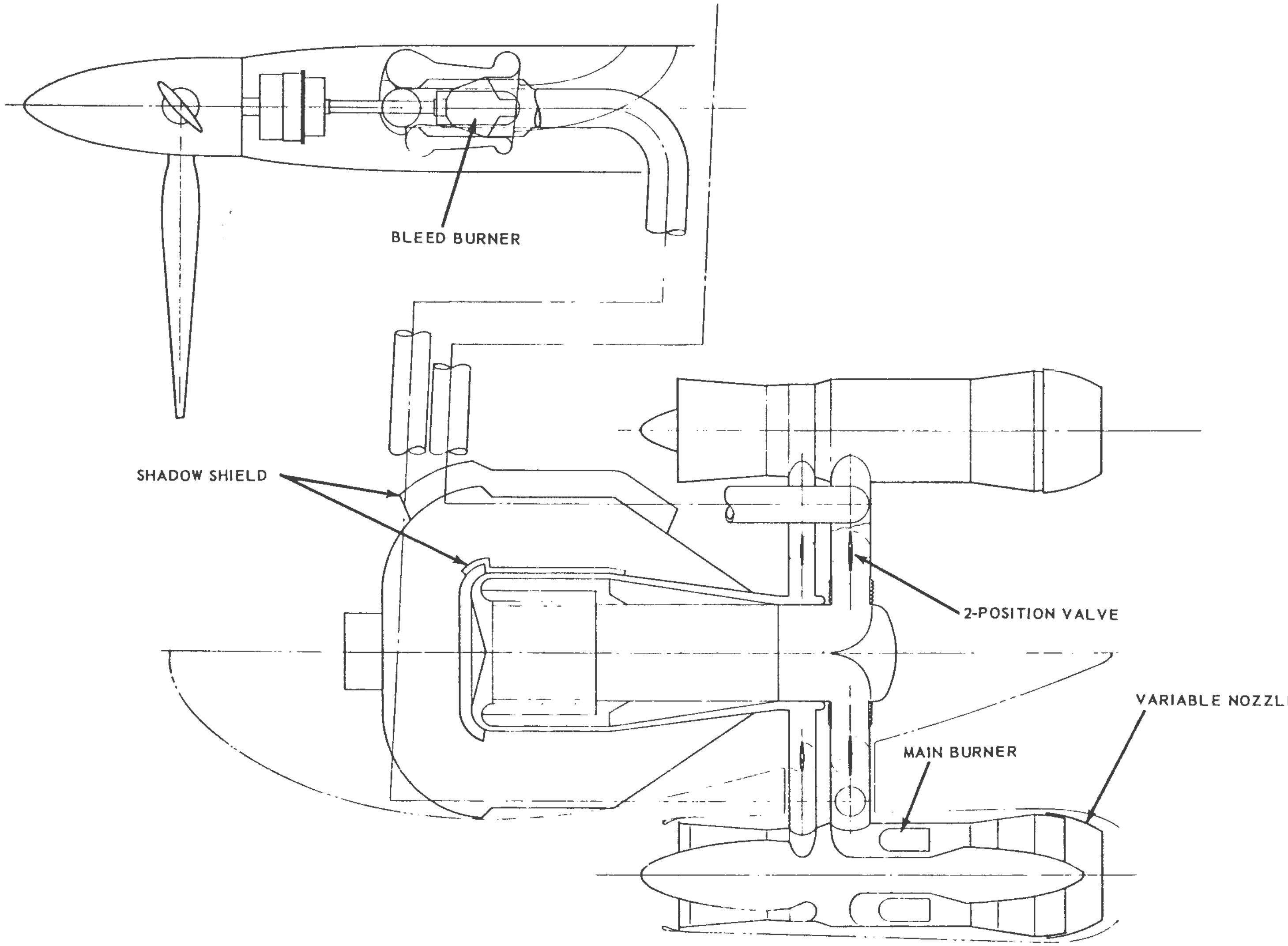

Fig. 51 – AC-300-3 power plant

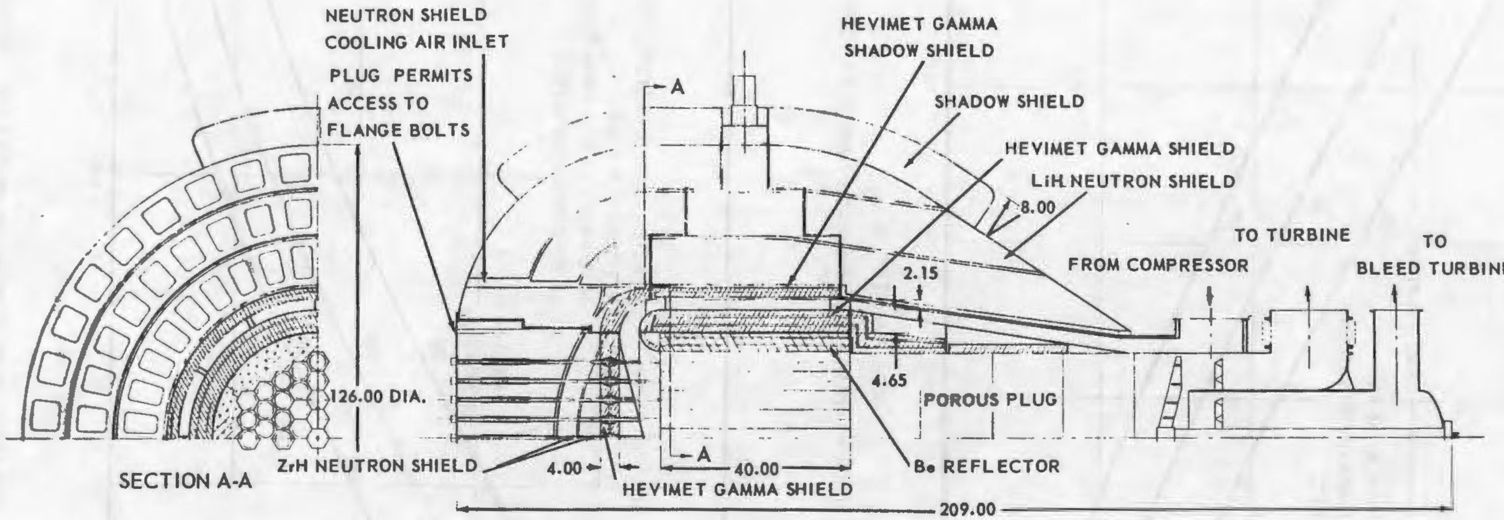

Fig. 52 – Reactor shield assembly for AC-300-3 power plant

[redacted]

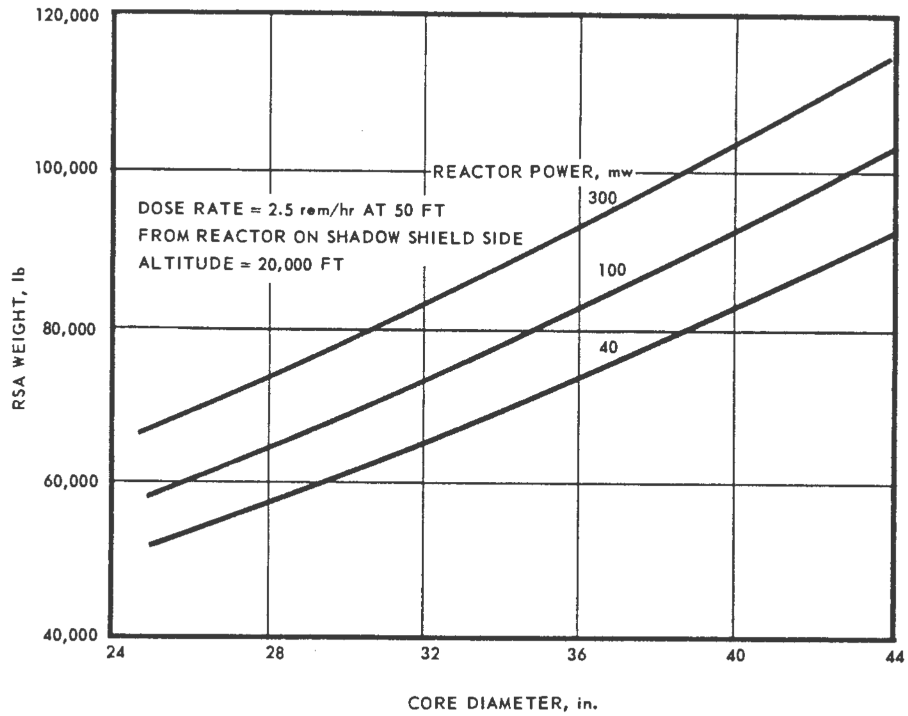

Fig. 53 – Reactor shield assembly weight versus core diameter - AC-300-2

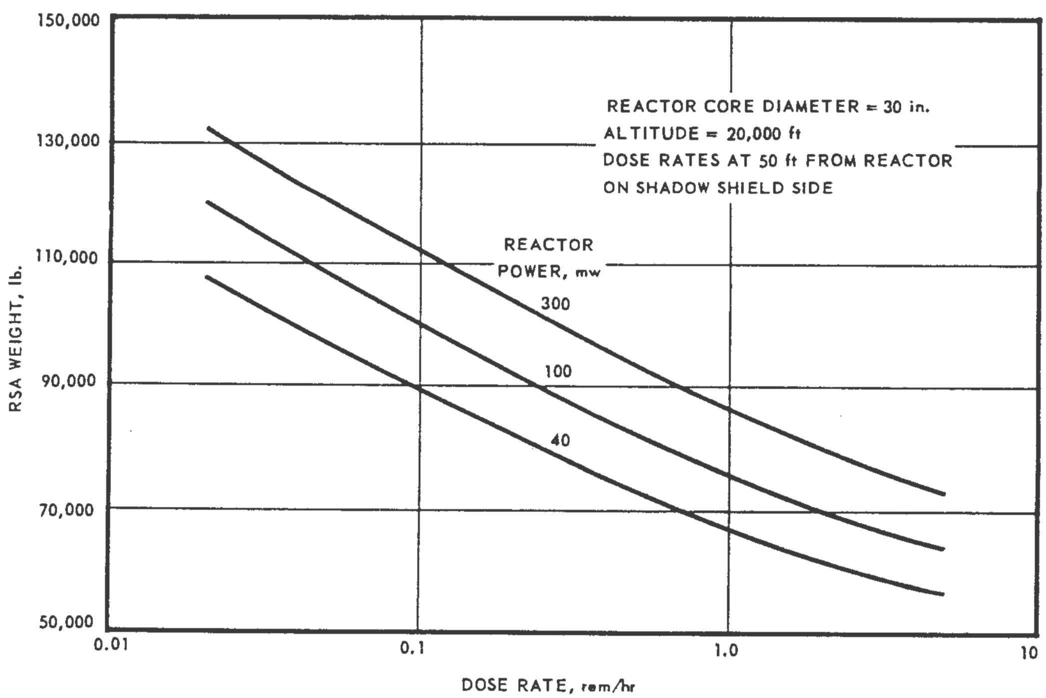

Fig. 54 – Reactor shield assembly weight versus dose rate - AC-300-2

[redacted]

[redacted]

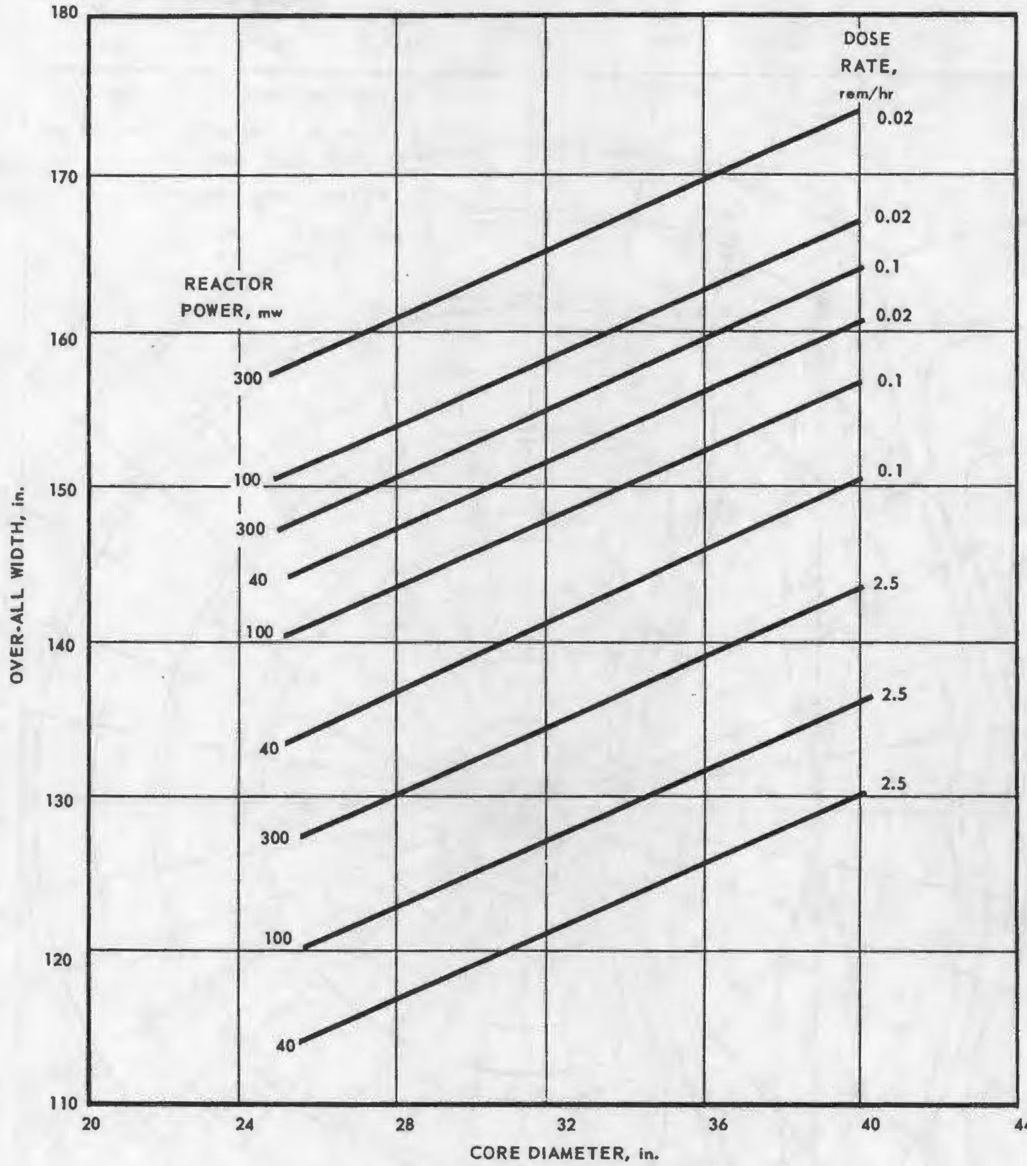

Fig. 55—Reactor over-all width versus core diameter - AC-300-2

actor only and varying the results with the inverse of the distance. The total dose rates in the vertical plane were then computed by taking the sum of the direct and air-scattered dose rates at each point.

Dose rates in the vertical plane were used to determine the isodose curves in the horizontal plane of the wing. Except in the shadow-shield region, the shield thicknesses are constant in the horizontal plane because the RSA is symmetric about its axis. Thus the horizontal isodose curves are circular for about 240 degrees around the reactor. In the 120-degree region of the shadow shield, the isodose curves were obtained from the inboard levels of the vertical isodose curves.

The specific reactor shield which was used corresponds to the parametric values of 66 megawatts power, 15,000 feet altitude, and a dose rate of 0.05 rem/hr-reactor at 50 feet from the reactor. Figures 56 and 57 show the operating isodoses in the horizontal and vertical planes respectively. These isodoses are for an aircraft with one power plant

[redacted]

[redacted]

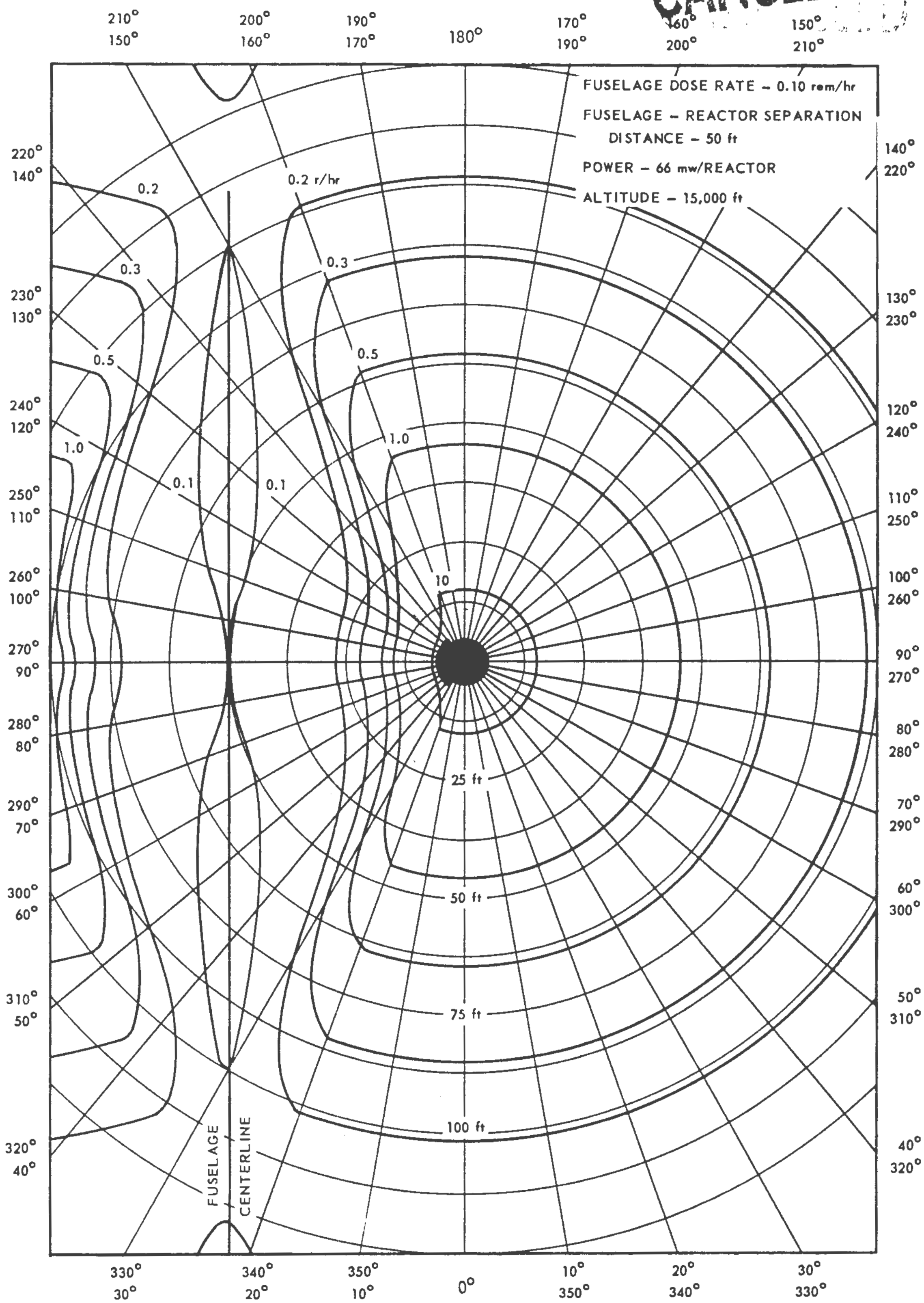

Fig. 56 – Operating fast neutron and gamma ray isodose contours for two AC-300-2 power plants – horizontal plane

[redacted]

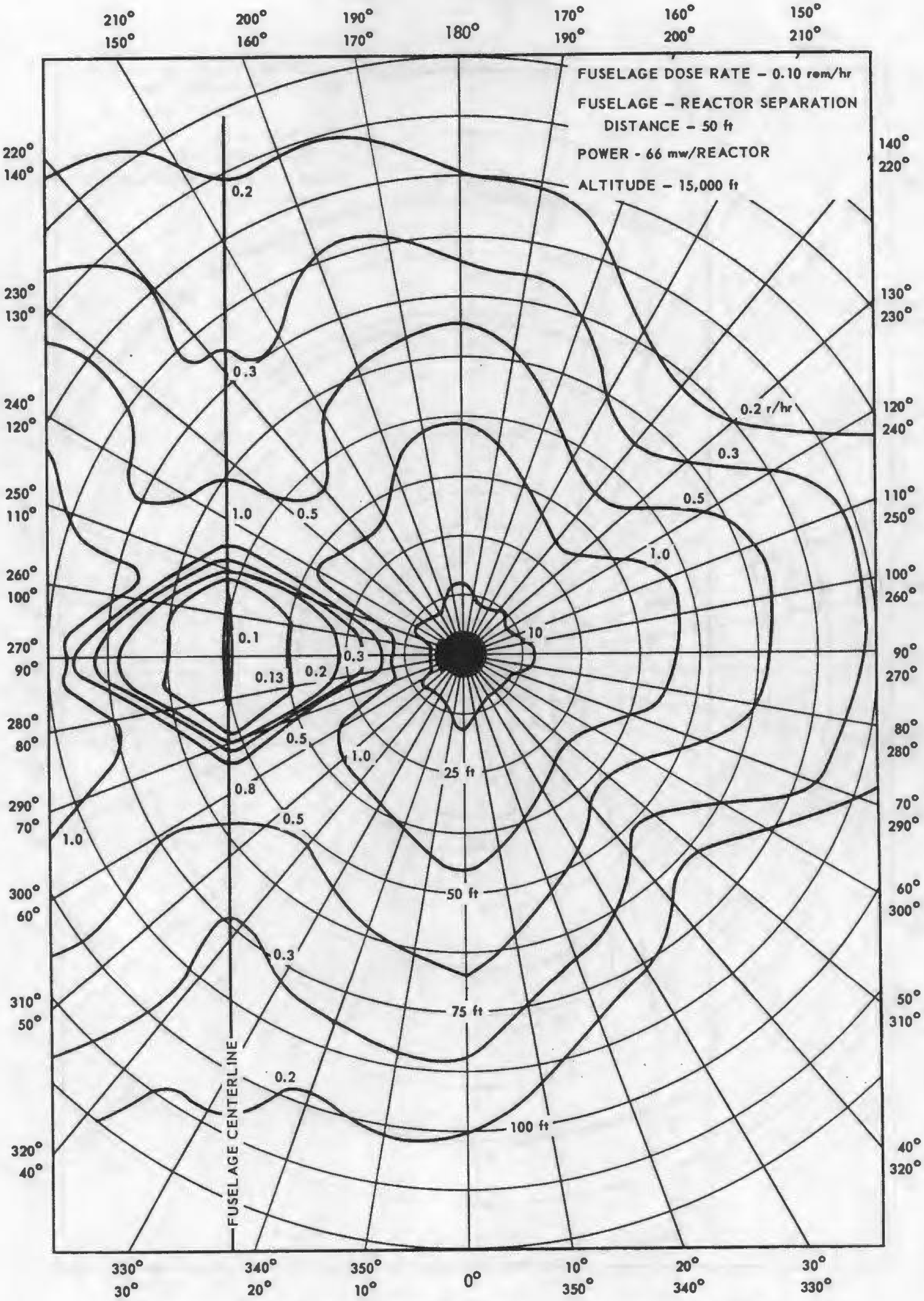

Fig. 57 – Operating fast neutron and gamma ray isodose contours for two AC-300-2 power plants – vertical plane

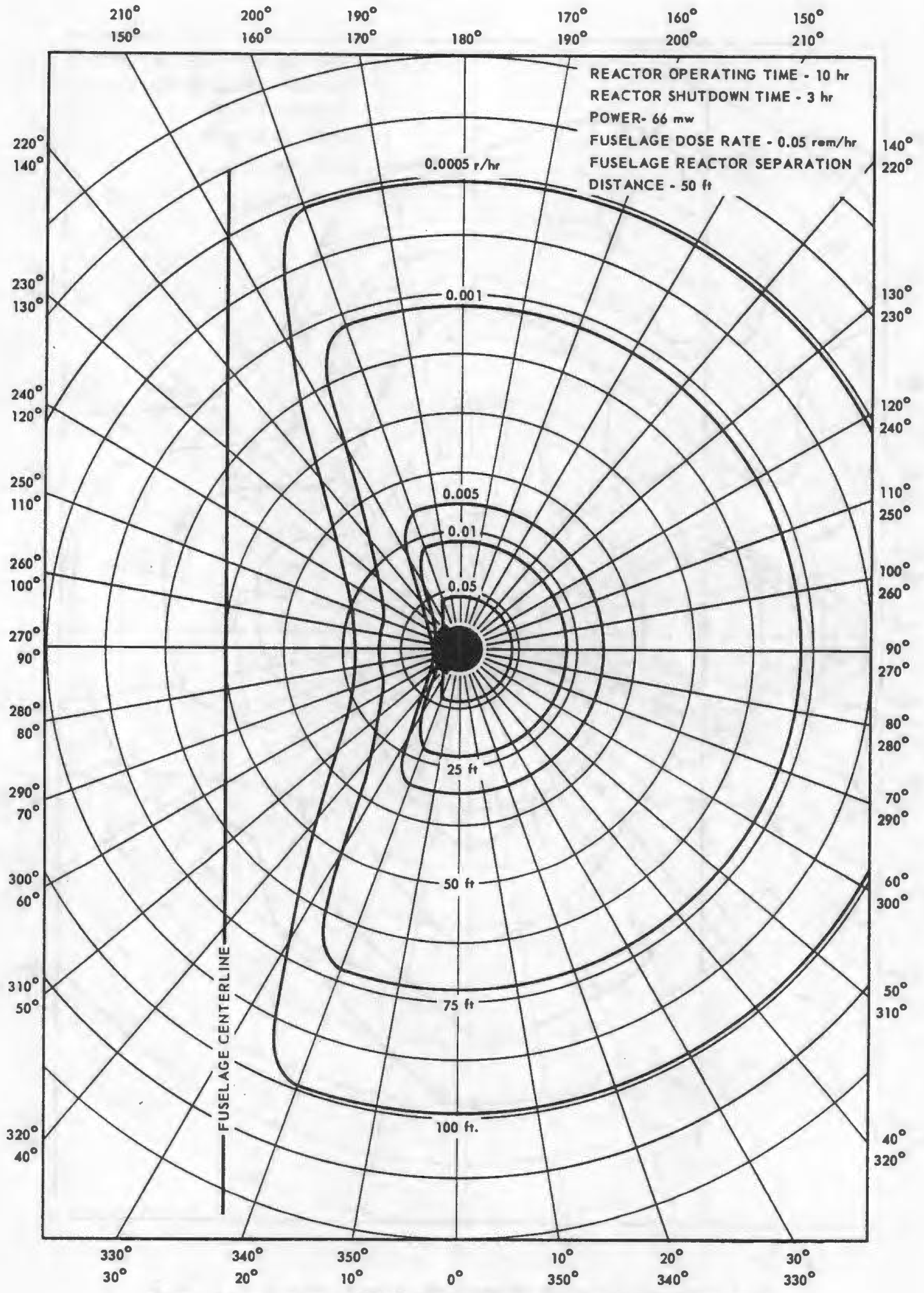

Fig. 58 – After-shutdown gamma ray isodose contours for one AC-300-2 power plant – horizontal plane

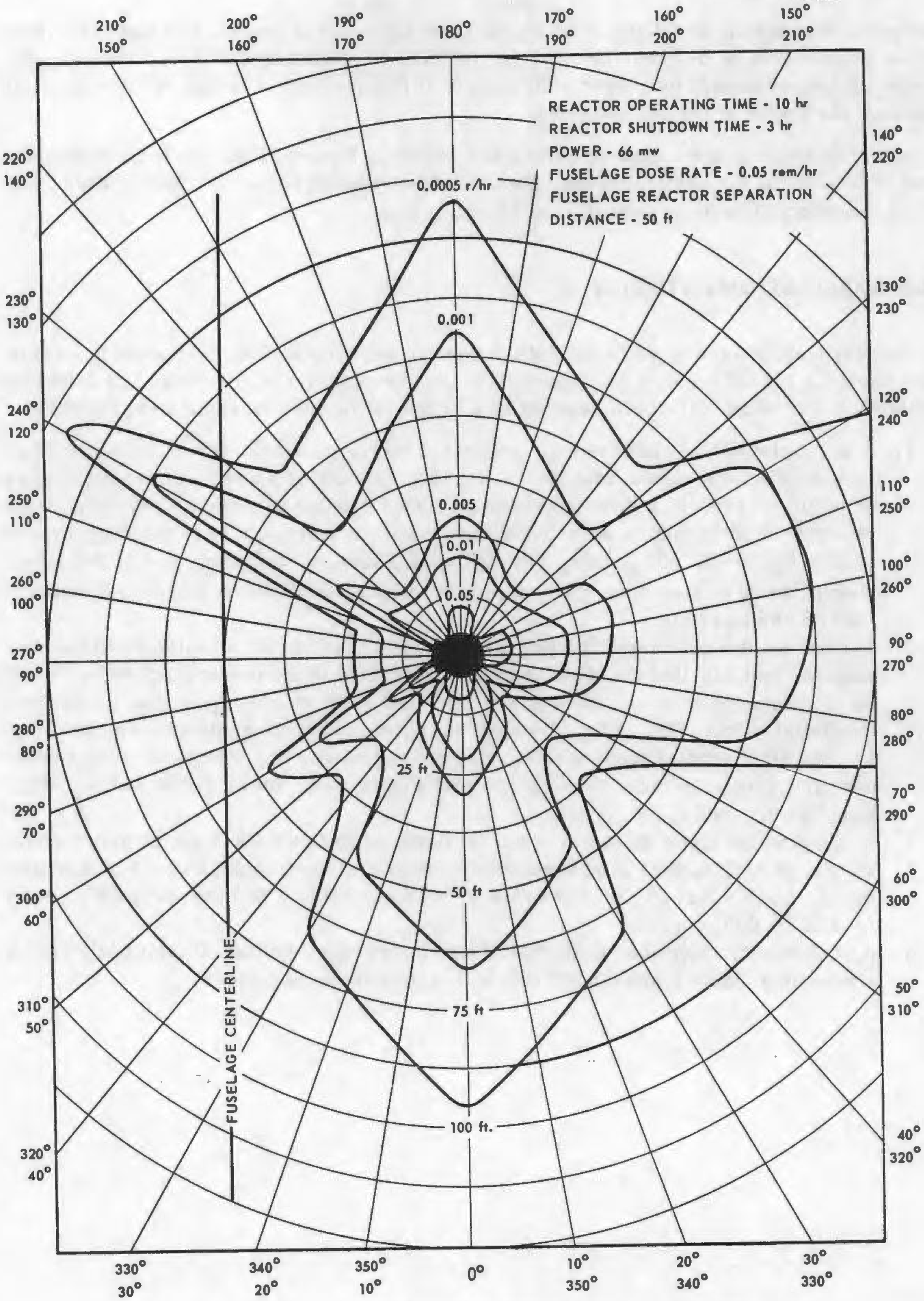

Fig. 59 — After-shutdown gamma ray isodose contours for one AC-300-2 power plant — vertical plane

mounted in each wing at a distance of 50 feet from the fuselage center. The isodose curves show the position of one reactor only, but include the effects of the second reactor. The center of the fuselage is located at a distance of 50 feet from the reactor on the radial line through the center of the shadow shield.

After-shutdown gamma isodose curves are shown in Figure 58 for the horizontal plane and Figure 59 for the vertical plane. The conditions considered were 3 hours after shutdown following 10 hours of operation at 66 megawatts.

3.4 APPLICATIONS STUDIES

General studies were made of the XMA-1 power plant for possible application to aircraft and missiles for subsonic, cruise-sprint-cruise, or supersonic missions. The following tentative conclusions have been reached as a result of the various application studies:

1. It is concluded that either one or two XMA-1 power plants can power subsonic strategic bombers capable of Mach 0.9 at sea level, assuming a turbine inlet temperature of 1600° to 1800°F and design radiation levels similar to those for the 125A. With two XMA-1 power plants the gross weight of the aircraft would be in the neighborhood of 350,000 to 400,000 pounds. With only one XMA-1 power plant, the flyable gross weight would be less than 250,000 pounds, which leaves little margin for military load or chemical fuel.
2. Studies on the application of two XMA-1 power plants for a cruise-sprint-cruise mission indicate that the most useful improvement in the power plant design would be to reduce the total weight of power plant and crew shield rather than to increase the thrust output. This is true because an increased thrust would only permit flying an aircraft of greater gross weight, whereas reductions in power plant weight would permit a greater combat zone radius with the same or lower gross weight, which would be desirable.
3. It is estimated that a supersonic bomber powered by two XMA-1 power plants operating at 1800°F turbine inlet temperature could cruise on nuclear power at approximately Mach 1.4 at 30,000 feet with a gross weight of 320,000 pounds and a military load of 10,000 pounds.
4. A preliminary study of an unshielded XMA-1 power plant indicated that it could propel a missile at Mach 2 and 40,000 feet with a 10,000-pound payload.

[redacted]

4. TECHNOLOGY AND COMPONENT DEVELOPMENT STUDIES

4.1 FUEL ELEMENT DEVELOPMENT

4.11 MATERIALS DEVELOPMENT

Chromium-Base Core Materials

The major emphasis on metallic fuel element core material (other than the Fe-Cr-Al-clad niobium fuel element) is being applied to chromium and chromium-base alloys with a continuing effort on the development of niobium-base alloys for high-temperature service.

The objective of the work on chromium is the development of sound fuel sheet with sufficient ductility to be cold-formed and sufficient strength and metallurgical stability for $2300^{\circ}F$ service. This work includes the study of chromium-base alloys with usable high-temperature strength and an investigation of oxidation-resistant chromium-base alloys.

During the quarter, a number of chromium-base alloys containing various strengthening elements were prepared by powder metallurgy. Tensile tests which were in progress as the quarter closed indicate that strengths approaching that of molybdenum have been attained. Figure 60 shows the tensile curves for three chromium-base alloys compared with unalloyed chromium and molybdenum. The composition Cr - 1 Y - 2 Mo is the strongest of this series of alloys, having a strength only 2000 psi less than that of molybdenum at $2200^{\circ}F$, and 4000 psi better than niobium. Closely approaching this alloy in strength is the composition Cr - 1 Nb with a strength of 16,100 psi at $2200^{\circ}F$ and 28 percent elongation. Additions of 1 percent cobalt, vanadium, manganese, or tungsten are not significantly effective.

A program concerned with the development of chromium-base alloys is also active at Nuclear Metals, Inc., where both high-temperature strength properties and oxidation resistance are under investigation. Stress-rupture data had been obtained at the close of this quarter on unalloyed chromium and on one alloy, the 0.17 weight-percent niobium composition. These data indicate that the rupture life of the 0.17 weight-percent niobium alloy is five times that of unalloyed chromium at $1800^{\circ}F$.

Fuel Ribbon Development

Chromium Work - The efforts to produce clad chromium-UO_2 fuel sheets with a variety of alloys as core matrix materials in the previous quarter revealed some problem areas in fabrication of this type fuel element. These problems were resolved this quarter, and a total of 59 well-bonded clad sheets have been produced by refinement of sintering and rolling techniques.

Oxidation tests at $2300^{\circ}F$ were conducted on strips of ten chromium alloy cores clad with Fe-Cr-Al alloy, as cold-rolled to 0.015-inch thickness. The strip specimens had

[redacted]

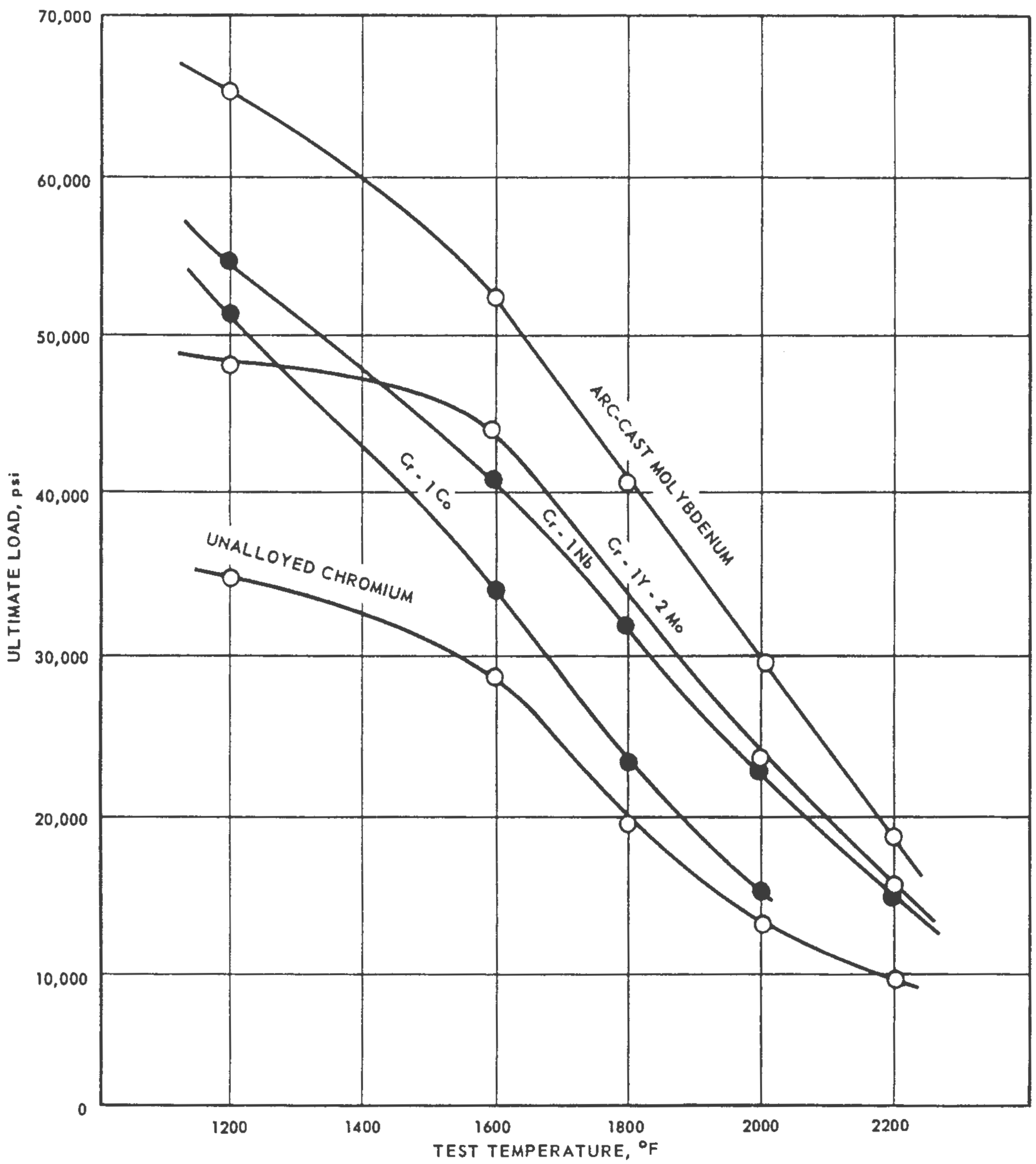

Fig. 60 – Tensile strength of chromium-base alloys compared to that of molybdenum

exposed cores at each end. Most of the strips showed some oxidation of the dead edge, but in only one strip, which had a core of unalloyed chromium, did oxidation of the core occur. Cores containing additions of yttrium, iron, molybdenum, and tungsten, with and without UO_2, were not penetrated by oxidation.

Niobium Cores - A project which has been under way for the past year at the General Electric General Engineering Laboratory on the development of an oxidation-resistant niobium alloy has been completed. From this study it has been concluded that it is improbable that workable niobium-base alloys exist which in the unclad state have sufficient oxidation resistance for service at temperatures above 1800°F.

Ceramic Fuel Materials

Development of Stable Fuel Additives - Minimizing the volatility and loss of fuel from fuel additives and fueled matrices has been a continuing study with the work concentrated on the binary systems UO_2 - Y_2O_3 and UO_2 - Yb_2O_3. When additions based on these systems are incorporated into BeO to give a fuel loading of 5.8 weight-percent UO_2 and tested for 10 hours at 3000°F in -90°F-dew-point air flowing at Mach 0.003, these compositions had fuel losses of 1.76 percent and 2.0 percent respectively.

The program for studying matrix materials has been continued with emphasis on the oxides of magnesium, zirconium, and yttrium. Fueled MgO has been evaluated at 3000°F and appears to be essentially as stable as fueled BeO. It does not have the thermal shock resistance of BeO, but may conceivably be useful at higher temperatures than BeO.

Fueled Beryllia Tubes - The fabrication of tubular BeO fuel elements was continued by Battelle Memorial Institute, their major effort being devoted to overcoming density difficulties encountered in producing fueled BeO tubes, 0.380-inch OD by 0.300-inch ID by 4 inches long, for MTR evaluation. The problem of low density which hampered their work was overcome during the quarter, possibly as the result of obtaining a readily sinterable grade of BeO from Brush Beryllium Company. It now appears that this grade of oxide can be made on a reproducible basis, and several hundred pounds are being processed at this time.

Evaluation of Silicon Carbide - The studies at Carborundum Company for determining the usefulness of dense silicon carbide as a structural material and as a fuel element body have been continued. Strength testing of dense SiC was used as an indirect method for determining thermal shock resistance. Specimens 1/4 inch by 1/2 inch by 3 inches were automatically cycled into a furnace operating at 2730°F, held there for 2 minutes (reaching a temperature of 2620°F), and cooled in an air blast (dropping to a temperature of less than 930°F in 20 seconds). The cycle was repeated 30 times, and transverse strength tests were then made on the specimens. Uncycled specimens showed an average strength of 16,000 psi compared with an average of 10,000 psi for specimens cycled as described. This amounts to a loss in strength of about 38 percent, indicating that the cycling treatment degrades the strength of the dense SiC appreciably.

Efforts to improve the oxidation resistance of dense SiC during the quarter were centered around a study of refractory silicides. The $CrSi_2$ - SiC mixture, the most oxidation-resistant composition tested thus far, had a rate of weight loss of 3.0 milligrams per square centimeter per hour at 3180°F, compared with 11.1 for plain SiC under the same conditions. The weight change for the $CrSi_2$ - SiC body was negligible for almost 3 hours, and then the indicated weight loss occurred during the remainder of the 7-hour test period.

One of the major problems encountered in the work on SiC fuel elements has been the tendency of the fuel additives in the fueled bodies to oxidize and disrupt the SiC bodies. This condition is especially severe in the 600° to 2000°F temperature range. Last quarter it was reported that a stable fueled body could be produced by the addition of a mixture of $Ba_3(PO_4)_2$ and Y_2O_3 to the silicon used in siliconizing the porous SiC - UO_2 - C compact. Results of oxidation tests at 2750°F have shown such bodies to be excessively oxidized and unsatisfactory for operation at this temperature for periods as short as 7 hours. Silicon carbide fuel additive studies are continuing with the objective of eliminating the low-temperature cracking problem and retaining the refractoriness and oxidation resistance of the base material.

4.12 DESIGN AND NON-NUCLEAR TESTING

Structural Testing

Twisted-Ribbon Fuel Elements - A feasibility study of a twisted-ribbon fuel element was completed during the past quarter. Both cold-flow pressure loss studies and a high-temperature structural test in the burner rig were made on a 6-inch-long element. The specimen consisted of 91 elliptical 80 Ni - 20 Cr ribbons 0.160 inch in width and 6 inches long; each ribbon was 0.020-inch thick at the center and 0.008-inch thick at the edge. The element was tested in a hexagonal duct having a cross-sectional area of 2.08 square inches.

The cold-flow test showed that the friction factor of the twisted-ribbon fuel element is considerably less than that of a concentric-ring fuel element with a 1-1/2-inch stage length. Figure 61 shows the pressure loss comparison between the 6-inch twisted-ribbon fuel element with an A_H/A_F (heat transfer area per unit frontal area) of 88.2 and the three, 1-1/2-inch-long, XR-25 concentric-ring elements with an A_H/A_F of 76.4. If a proportional correction in the pressure loss coefficient ($\Delta P_T/q$) value is made for the heat transfer area per unit frontal area, the concentric ring fuel element shows a ($\Delta P_T/q$) value of approximately 1.5 times that of the twisted ribbon.

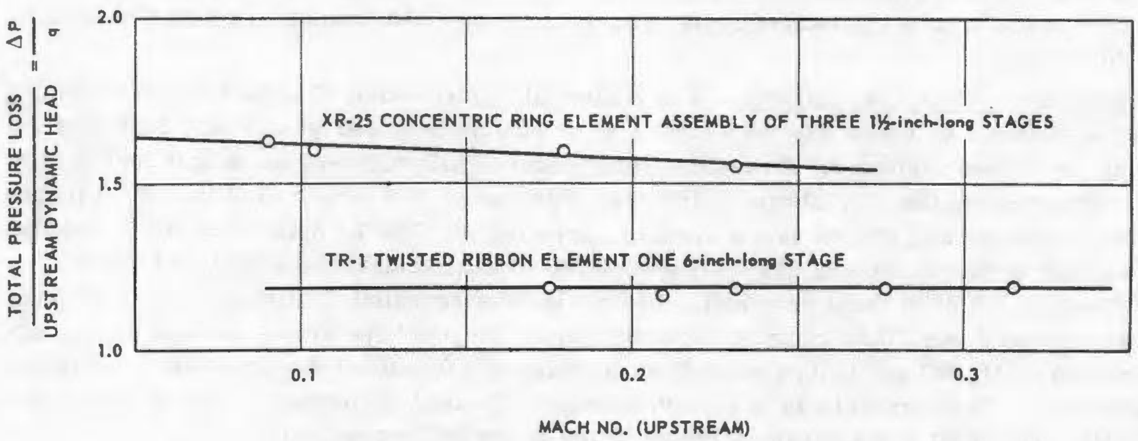

Fig. 61 – Pressure drop comparison - concentric ring element and twisted ribbon element

The structural integrity of the twisted-ribbon element was tested in the burner rig at a gas temperature of 1850°F and an estimated dynamic head of 7.2 psi. The fuel element after 49 hours of testing at the above conditions is shown in Figure 62. The structural damage consisted of broken brazed joints between adjacent ribbons and warping of the ribbons. At one point, two ribbons had overlapped until they were nearly in contact. The increase in pressure loss during the test was about 10 percent.

In addition to the structural problems it appears that uneven power generation and uneven heat transfer might be significant obstacles in the development of this fuel element. In view of the existing problems and a performance expectancy only comparable to a long-stage concentric-ring fuel element, no further development of the twisted-ribbon fuel element is planned.

Simulated Fuel Elements - The structural tests of concentric-ring fuel elements usually show a much greater distortion in the outer fuel ribbon than in the inner ribbons. It was hoped that the effect of the radial pressure forces which were presumed to be acting on the outer ribbon could be observed by replacing the outer ribbon of a fuel element with a paper ribbon and flow testing the element in a glass tube. Subsequent flow tests showed that the outer ribbon collapsed in all quadrants starting at the leading edge and progressing toward the trailing edge. The flow test was repeated with the fuel element positioned eccentrically within the glass tube with a zero gap between the bottom of the element and the glass tube and a gap at the top of the element approximately twice the gap spacing

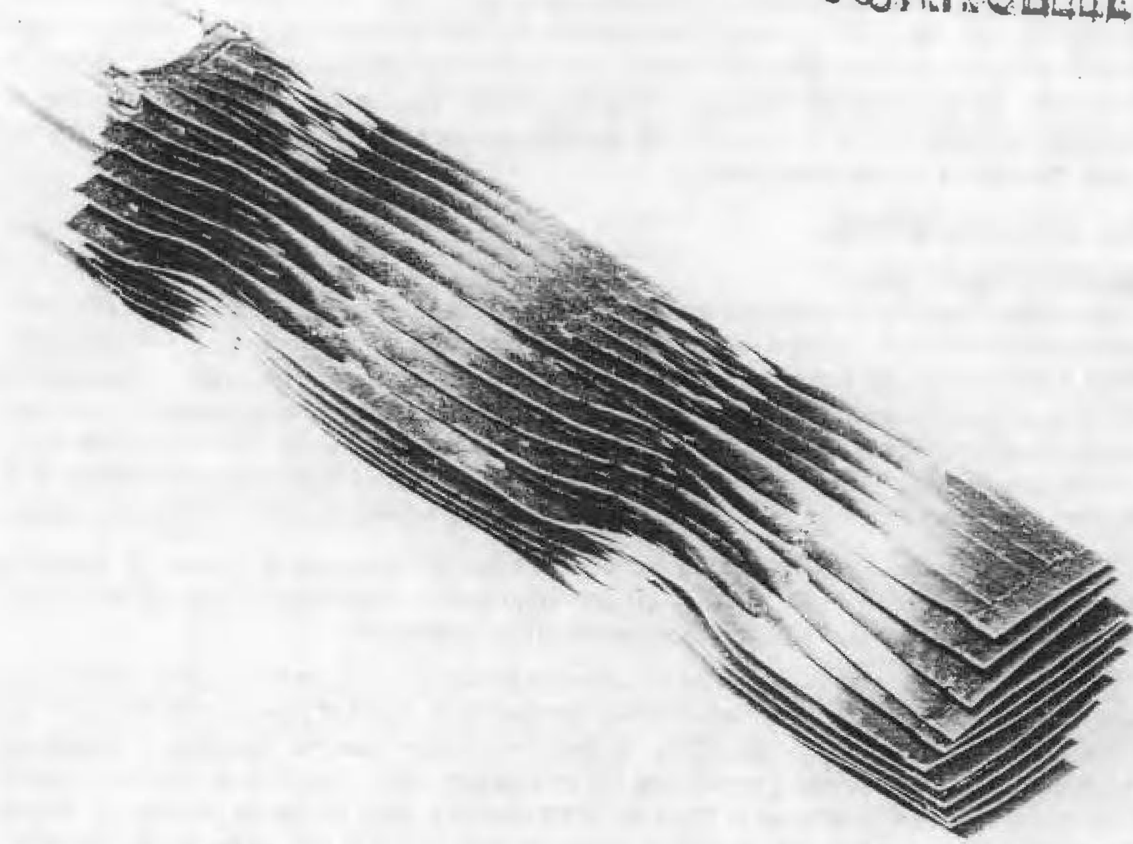

Fig. 62 – Twisted-ribbon element, exposed to 1850°F air for 49 hours at 7.2 psi dynamic head

of the ribbons. The outer ribbon during the flow test again collapsed toward the center of the fuel element as it did in the concentric test.

A new paper model using the structural steel hardware of an XR-27 type fuel element was assembled with all paper ribbons. The fuel element was center-supported and positioned concentrically within the glass tube. This specimen was tested at a dynamic head of 1.2 psi and a Mach number of 0.35, but no structural damage to the ribbons was observed. The model was then wetted with water which reduced the tensile strength of the 0.004-inch-thick paper from 4000 psi to 700 psi. The wet element was then tested, and no structural deformation was observed until a small section of the trailing edge of the outer ribbon was torn loose. The outer ring became very unstable and fluttered violently in the torn area. This caused more small sections to be torn loose from the outer ribbon. The damage became progressively worse and moved upstream as well as to the inner ribbons.

Fuel-Element-Temperature Perturbation Study

A study is being made to identify the factors that cause fuel-element-temperature perturbations in GE-ANPD reactors and to establish their numerical relationship by analytical and experimental means. Recommendations will be made for appropriate extremes to be permitted and of means to achieve such control. The study will encompass all perturbations of 15°F, or smaller if cumulative.

As a result of instrumentation studies, techniques are being selected for thermal sensing of element surfaces in test rigs.

A visit to the Aeronautical Research Laboratory at Wright Field resulted in recommendations as to the best way to apply instrumentation to geometries similar to fuel cartridges for the purpose of determining pressure and flow distributions. Studies of the effects of overpowering fuel element rings of HTRE No. 1 are being made. An effort was begun to establish quality control tolerances for manufacturing fuel elements in order to prevent overtemperature during operation.

4.13 NUCLEAR TESTING

Ceramic Fuel Assemblies

One small ceramic fuel sample was tested in the MTR as part of the materials research and radiation studies program to determine the physical integrity of ceramic fuel elements while operating at high temperatures with self-power generation. The sample consisted of a bundle of seven identical tubes arranged with one central tube surrounded by six other tubes in contact. They were 4 inches long, had an outside diameter of 0.38 inch and a wall thickness of 0.040 inch, and were made of an extruded homogeneous mixture of 85 percent beryllium oxide, 9 percent yttrium oxide, and 6 percent enriched uranium oxide.

The fueled-ceramic test operated for a scheduled 25 hours at a maximum indicated sample temperature of $2750^{\circ}F$. The self-power generation was approximately 8 Btu/in^3-sec. The physical integrity of the sample appeared unaffected.

Postirradiation Analyses - Postirradiation examinations were performed on the ceramic specimens from the four irradiation tests conducted in the LITR and from the fifth irradiation test conducted in the MTR. Inspection showed that no changes in weight or physical dimensions had occurred during the irradiation tests. The fission-product leakage from the specimens irradiated in the fifth MTR test was determined by passing an aliquot of the exit coolant air through cooled activated-charcoal traps to collect the fission products present in the air. The charcoal was then counted on a gamma spectrometer to analyze for the I^{131} and Ba^{140} content. The result of these determinations indicated that the leakage rate may be as high as 0.2 percent of the fission-product formation rate.

Metallic Fuel Elements

Two single-plate tests were conducted on small 0.75- x 1.5-inch samples of fueled sheet in a life-versus-temperature test. There was no preheating of the inlet air, and dynamic heat was not controlled. Sample temperature was used to control airflow. The tests were made on 25-mil-thick 80 Ni - 20 Cr fuel stock. Sample GE-ANP-3V1 was operated at $1850^{\circ}F$ for 200 hours with no failure. Sample GE-ANP-3W1 is presently operating on a 500-hour test.

Thermocouple performance has been a major concern in the MTR testing, particularly since tests have progressed to higher dynamic heads. Failure of the asbestos insulation within the drawbar had been found to be the main source of difficulty. Several variations in methods of insulating the thermocouple leads were tried on the fuel cartridge samples being tested.

4.2 POWER PLANT MATERIALS

4.21 MODERATOR

The primary research effort on moderator materials is to provide basic information relative to the development of high-temperature moderator components based on the utilization of hydrided yttrium for airborne reactors. A secondary effort is continuing on general fundamental hydriding studies.

Hydriding Studies

It was discovered last quarter that if zirconium is hydrided at 30 psia, the N_H is almost double at 2000°F. Further hydriding pressure studies made this quarter by using pressures as high as 240 psia have shown that major gains in N_H are obtained in the 15- to 60-psia range, but that pressures in excess of 60 psia do not produce significant N_H increases.

Progress has been made in the high N_H hydriding of large bodies of zirconium. By using a hydrogen pressure of 35 psia at 1650°F, it was demonstrated that sections of extruded moderator components can be hydrided to N_H values as high as 5.6 without loss of integrity. However, the high N_H material is more brittle than the lower N_H bodies. Analytical determinations of the hydrogen content of samples selected at random from these hydrided bodies have shown them to be homogeneous.

Yttrium Technology

During the quarter studies leading to the preparation of high-purity yttrium metal became a major effort in materials development.

The reduction process employed by present yttrium producers carries over into the final product calcium, magnesium, and yttrium oxide impurities. These impurities lead to both hot- and cold-short metal materials and to some restriction on the amount of hydrogen which the yttrium metal can absorb. Lithium reduction methods are being intensively investigated as a means of producing a metal free of these contaminants.

Properties of Yttrium and Hydrided Yttrium

The hot-hardness studies of yttrium and hydrided yttrium were completed by Battelle Memorial Institute this quarter. The measurements were made on extruded arc-cast metal which was annealed before hydriding. The results obtained for both the extruded metal and two of the hydrides of different hydrogen contents are shown in Figure 63. It is apparent from these data that hydrogen significantly increases the strength of yttrium to the extent that it may have some load-bearing capabilities at moderately high temperatures (1600°F). Yttrium metal, zirconium metal, and hydrided zirconium are much weaker.

Moderator Fabrication

During the quarter cladding techniques have been developed using pressurized gas for applying the pressure required to bond molybdenum to zirconium or hydrided zirconium and to 446 stainless steel. Metallographic examinations of polished sections taken from the bonded specimens showed that excellent metallurgical bonding had been formed at the 446 stainless steel - molybdenum interface and at the molybdenum - hydrided zirconium interface.

Previous tests have shown that a relatively large amount of hydrogen migrates from the hot to cold areas in moderator components subjected to a large temperature gradient. Tests conducted this quarter indicate that tungsten or molybdenum barriers 0.002 to 0.005 inch thick can prevent such hydrogen migration.

Two hydrided yttrium moderator billets, 2.85 inches in diameter by 4.5 inches in length and clad with 446 stainless steel and niobium, were successfully extruded at 1650°F to a 1/2-inch-diameter rod. This is a very important accomplishment in that it establishes the ductile, metallic nature of hydrided yttrium at elevated temperatures.

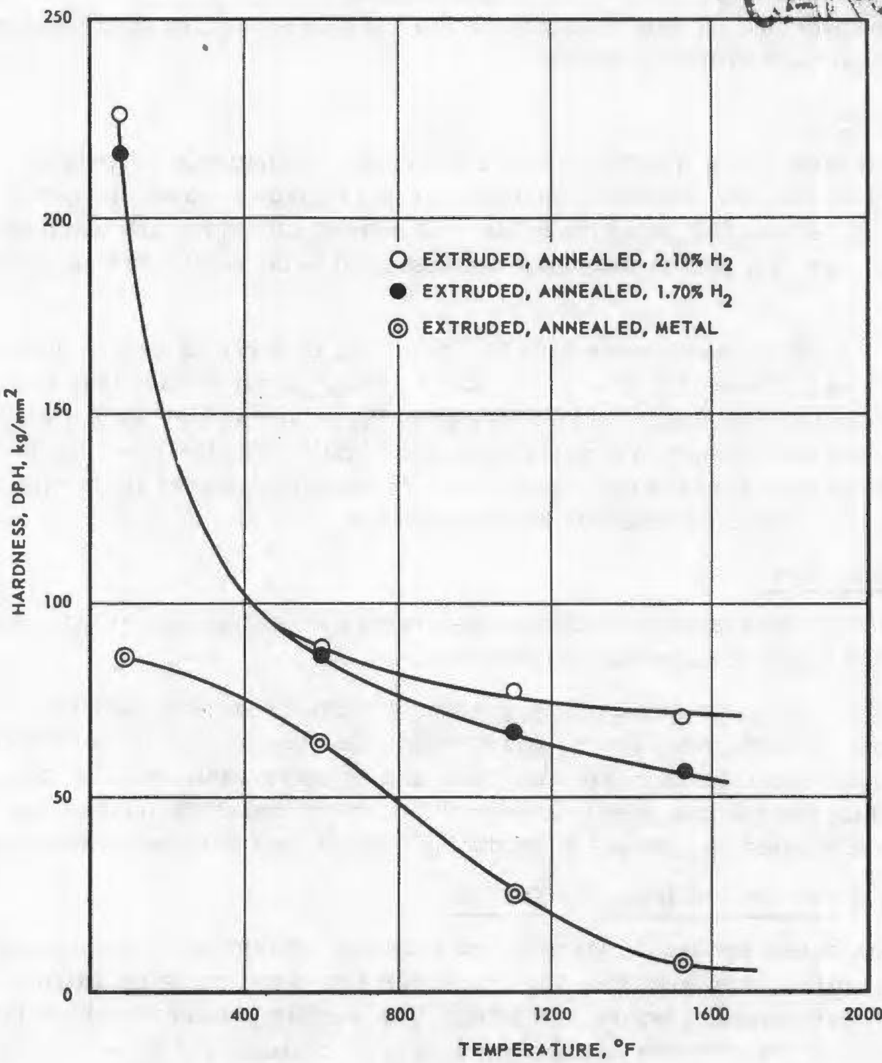

Fig. 63 – Hot hardness of yttrium and hydrided yttrium at various temperatures

4.22 GENERAL RADIATION EFFECTS STUDIES

Hydraulic Fluids

A test program to obtain thermal and radiation stability data on promising fluids for use in high-temperature hydraulic systems was completed during the quarter. Six fluids, selected in previous work from an initial list of 14 high-temperature materials, were tested at 500° and 600°F for periods up to 100 hours and dosages from 10^7 to 10^8 rads. All tests were made in an inert atmosphere to simulate hydraulic system conditions. The fluids included OS-45, Hercules J-7, MLO-8200, Esstic-45, and two specially formulated jet engine lubricants ANP-33* and ANP-55.*

Results of the tests indicate that all of the materials are potentially useful to dosages of about 3×10^7 rads if the high-temperature exposure is restricted to short periods such as might occur in cruise-sprint-cruise missions. For extended periods of high-temperature exposure, however, the best materials are MLO-8200 and Esstic-45; both of these materials withstood 600°F for 50 hours and a dosage of 3×10^7 rads with comparatively small changes in properties.

*ANP is a designation used by WADC for lubricants potentially applicable in nuclear powered aircraft. ANP-33 consists of di-2-ethylhexyl sebacate base fluid with 0.5 percent phenothiazine oxidation inhibitor. ANP-55 is the same material with the addition of an acryloid viscosity improver.

Elastomers

Elastomer studies in progress during the quarter were a continuation of studies concerned with the effect of the temperature of irradiation on radiation damage.

The most generally applicable result of the experimental work is the establishment of Buna-N as unique among the elastomers studied with respect to the additivity of damage due to temperature and damage due to radiation. The synergistic effect of temperature and radiation in damaging Neoprene, reported last quarter, was also observed with the three silicone elastomers SE-551, SE-371, and SE-750.*

Electric Motors

Results of tests on electric motors in the Systems Panel Test No. 2 at the Convair Nuclear Aircraft Research Facility (NARF) demonstrated excellent radiation stability for Alkanex insulated electric motors at temperatures in the range from 350^{o} to 400^{o}F. The motors, which were of the fractional-horsepower type (approximately 1/40 horsepower), were operated in groups of ten each at temperatures of 356^{o}, 392^{o}, and 428^{o}F. Twenty-five of the twenty-nine motors which began the test, including all of those in the two lower-temperature groups and five in the high-temperature group, were operating satisfactorily at its completion. Although radiation damage possibly contributed to the failures, it is believed that three of the failures were due to excessive temperatures and that the fourth was due to a lack of lubrication. The motors which completed the test had a total of 700 hours of operation, of which 500 hours were in a radiation field which totalled about 5×10^{7} rep.

Structural Materials

Eight physical-property-test specimens are being irradiated under a fast neutron flux in the L-49 hole in the lattice of the MTR. The tests on these specimens are to aid in evaluating the usefulness of Inconel X and Inco 702 proposed as materials for use in the in-pile tubes of the GE-ANPD experiments in the Engineering Test Reactor. The samples will remain in the reactor about nine weeks.

4.3 REACTOR PHYSICS

4.31 CRITICAL EXPERIMENTS

During the quarter all fuel, moderator, and reflector materials were removed from the flexible critical experiment matrix, and the fuel was transferred to the HTRE No. 3 mockup. During the process of removing the fuel-moderator assemblies, measurements were made to determine the minimum critical mass for the core length (30 inches) and volume fractions unique to the series of cores under investigation. A core with an effective diameter of 19.2 inches and an effective beryllium reflector thickness of 9.1 inches was made critical as shown in Figure 64. Although the location of the control and safety rods prevented further reductions in core size, it is estimated that a core with minimum critical mass under the given conditions would be one with an effective diameter of 18 inches and an effective reflector thickness of 13 inches, which, for practical purposes, is an infinite reflector.

4.32 GENERAL EXPERIMENTAL PHYSICS

An investigation of the techniques used in measurement of nuclear heating was initiated during the quarter. It became evident that two types of measurements are desirable.

*Products of the General Electric Company Silicone Products Department.

 [redacted]

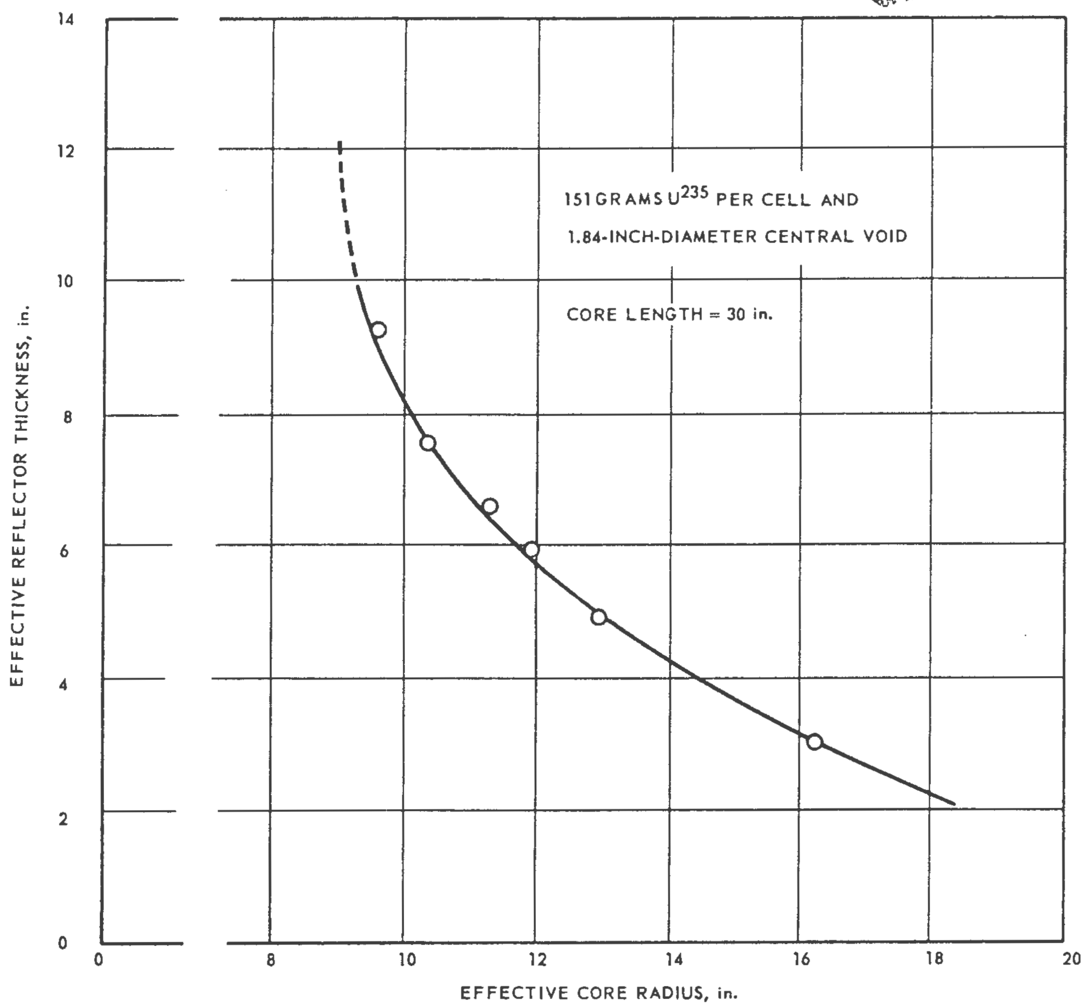

Fig. 64 – Reflector thickness versus core radius for critical assemblies in flexible critical experiment matrix

Gamma and neutron dose rates are needed for correlation with predicted dose rates, and accurate determinations of gamma and neutron distributions in energy and space are needed for calculation of the heating effects.

Among the instruments considered for dose measurements are photographic film, silver phosphate glass needles, and chemical dosimeters. Photographic film is easily obtainable; readout is simple but time-consuming. Darkening of the film has a significant gamma energy dependence and an absolute accuracy better than 20 percent is difficult to attain. Although silver phosphate glass needle dosimeters offer better reproducibility than film, they also exhibit an energy dependence. This could probably be reduced by further development work. Chemical dosimeters appear at present to offer distinct advantages over the other systems. Preparation is relatively simple and inexpensive. Readout is time-consuming, but improvements in the readout technique can be expected. The stabilized aqueous-hydrocarbon dosimeters have negligible energy dependence between 40 kev and 10 Mev, no detectable rate dependence, and little temperature dependence from 5° to 50°C. Certain types of chemical dosimeters may be made gamma-sensitive only; other types are both neutron- and gamma-sensitive. Therefore two chemical dosimeters may be used simultaneously for both neutron and gamma dose measurements. Gamma dose measurements about the HTRE No. 3 nuclear mockup and the flexible critical experiment assembly are planned using chemical dosimeters and film for comparison.

[redacted]

A single-crystal scintillation spectrometer is being assembled for gamma energy measurements about the HTRE No. 3 nuclear mockup. The spectrometer will have a continuous scan and count rate print-out. The possibility of using microcalorimetric techniques for direct measurements of heating effects is also being investigated.

4.33 REACTOR ANALYSIS

Machine Computation

Machine computation development continued, with emphasis on consolidation of the existing array of machine programs dealing with various aspects of reactor theory into a completely mechanized general reactor program designated "George." This program will be sufficiently flexible to span the range of interest in nuclear analysis work, with engineering specifications of geometry and composition as input, and with a complete portrayal of nuclear performance as output. Work continued also on completion of the following programs: the bare reactor program for calculation of energy-averaged cross sections; the monoenergetic cell program for calculation of cell-averaged cross sections; the parameter study program for reactor design optimization.

Reactor physics development effort was concentrated upon control rod effects, temperature dependence of reactor performance, xenon poisoning, and homogenization theory.

A control rod interaction study progressed through rough draft formulation of a machine-codable two-energy representation of a ring of control rods concentric with the axis of a cylindrical core. An attempt to extend McLennan's successive collision method to anisotropic entrance flux progressed through construction of a machine-codable anisotropic albedo representation for a cell consisting of a control rod centered in a void annulus.

The attack on temperature effects is a balanced effort, including both an interim method, involving the machine coding of an empirical synthesis of thermal neutron energy distribution measurements, and a theoretical study, directed toward constructing a machine-codable transport theory slowing-down model including the effects of thermal agitation of the nuclei. Both approaches to the problem have progressed through initial feasibility studies.

The work on xenon poisoning and on homogenization theory proceeded halfway through initial exploratory study. Formulation of machine programming specifications for the calculation of photon-activation cross sections progressed through preparation of a rough draft.

Recent improvements in experimental data on U^{235} fission neutron distribution in energy and in delay time were prepared for digital computer use. The composite prompt-plus-delayed spectrum recommended for engineering use has been stored in the digital computer peripheral memory.

4.4 SHIELD PHYSICS

4.41 SHIELD MOCKUP EXPERIMENTS

Tower Shielding Facility Experiments

The series of tests at the ORNL Tower Shielding Facility using 2π shielding covers was completed early in the quarter. In addition to the scheduled altitude traverses, a number of other tests were made with these shields. A complete mapping of direct-beam dose rates around shield No. 1 (low gamma-to-neutron ratio) was made. Excessively high shutdown-gamma fields prevented making extensive direct-beam mapping around shield No. 2 (high gamma-to-neutron ratio). Some gamma spectrum measurements inside the crew shield were made using reactor shield No. 1.

Both shield configurations were used to measure independently the primary and secondary gamma radiations reaching the crew position; the data indicate that this separation was actually achieved. The current analytical methods appear to be adequate to account for the observed effects of adding a 2π cover to either the reactor or crew shield, although it is not yet indicated that these methods will account in detail for the observed effects of using both 2π covers simultaneously.

In this discussion primary gamma radiation includes all gamma rays emitted from the reactor shield; secondary gamma rays are those originating from neutron interactions with any materials outside the reactor shield. All dose rate measurements not otherwise identified are to be understood as measurements taken in the crew compartment with the side and front water tanks drained (i.e., with the sides and front shielded only by the light aluminum structure of the crew shield).

Figures 65 through 68 show the variation of dose rate (or flux) with altitude. The solid-line curves are presented in sets of four corresponding to the four possible 2π cover conditions, other conditions remaining the same. Within each solid-curve set all values shown are in correct relationship to each other; but each set has been normalized independently of the other sets for ease and compactness of presentation. Consequently, no magnitude relationships can be inferred between curves taken from two different sets; nor can absolute magnitudes be inferred.

The broken-line curves of Figure 65, 66, and 68 are data taken under the same conditions that applied for the solid-line curves immediately adjacent, except that the intermediate shielding wall, described later, was present during the "broken-line" measurements. The broken-line curves have been arbitrarily normalized to the corresponding solid curves to facilitate an easy comparison between the curve shapes with and without the shielding wall.

The broken-line curves in Figure 67 are for plain water in the reactor shield, whereas the solid-line curves are for borated water in the reactor shield, the crew-shield water being borated in both cases. Again, the broken curves have been normalized to the solid curves.

When no 2π covers were used, all measurements showed a marked variation with altitude, the maximum values observed being generally greater than twice the minimum values. As altitude above ground was increased, the measurements increased fairly sharply from ground level up to the region of 40 to 60 feet, where a maximum was usually reached. The measured values then decreased monotonically with altitude, apparently tending toward some asymptotic value. However, at the maximum altitude available (195 feet above ground) the quantity being measured was still decreasing with altitude in nearly every instance, the apparent rate of decrease varying somewhat from one set of conditions to another; this apparent downward slope in the curve of dose rate versus altitude was most extreme for the secondary gamma ray measurements taken while both the reactor and crew shields were borated. In all, seventeen altitude traverses were made without 2π covers; and in the great majority of such cases it is clear that some ground effect is still present at an altitude of 195 feet.

The curves of dose rate as a function of altitude are quite similar in shape for both fast neutrons and primary gamma rays, as may be seen by comparing corresponding curves

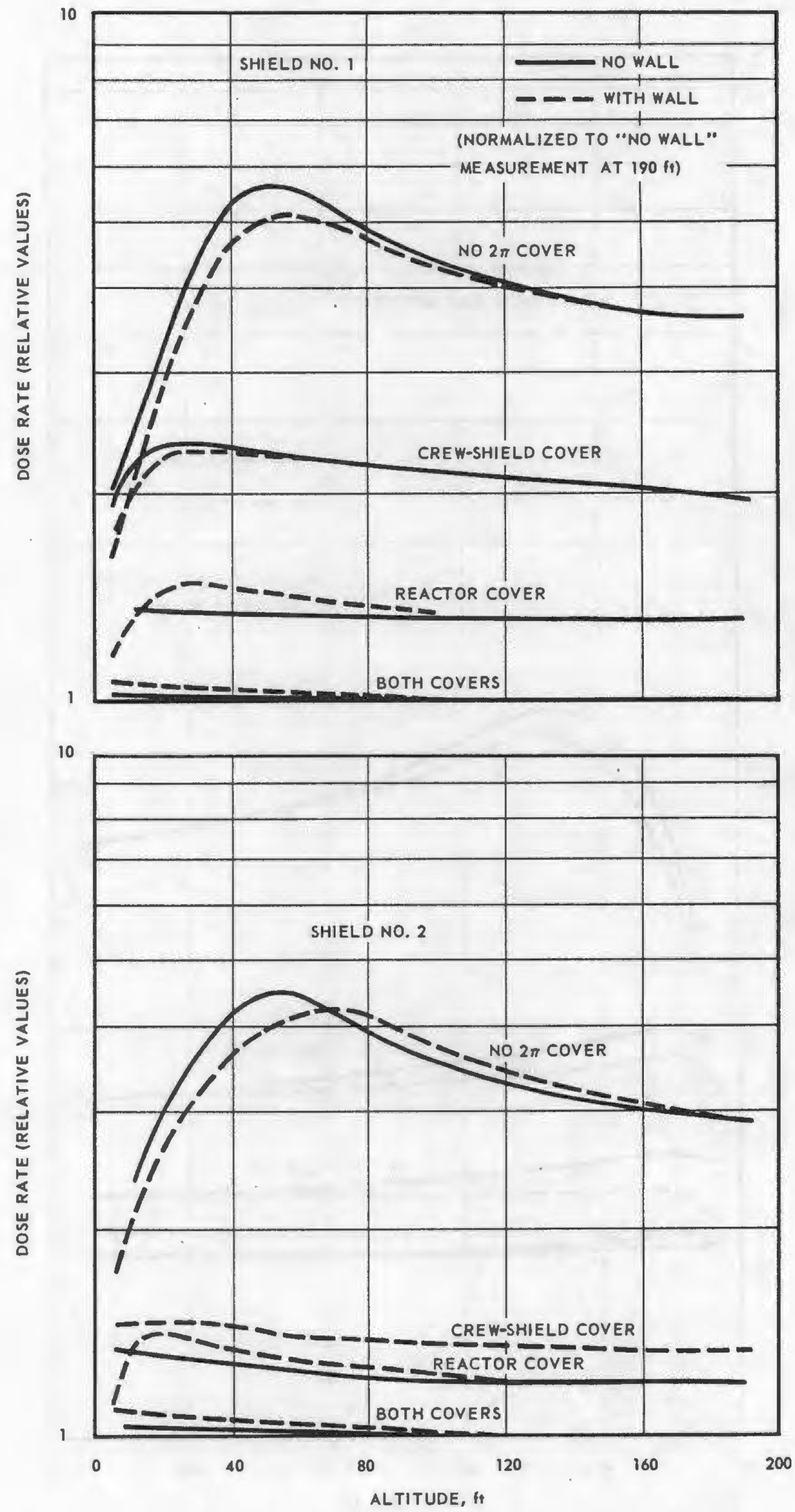

Fig. 65 – Effect of wall and 2π covers on fast neutron dose rate

 [redacted] CONFIDENTIAL

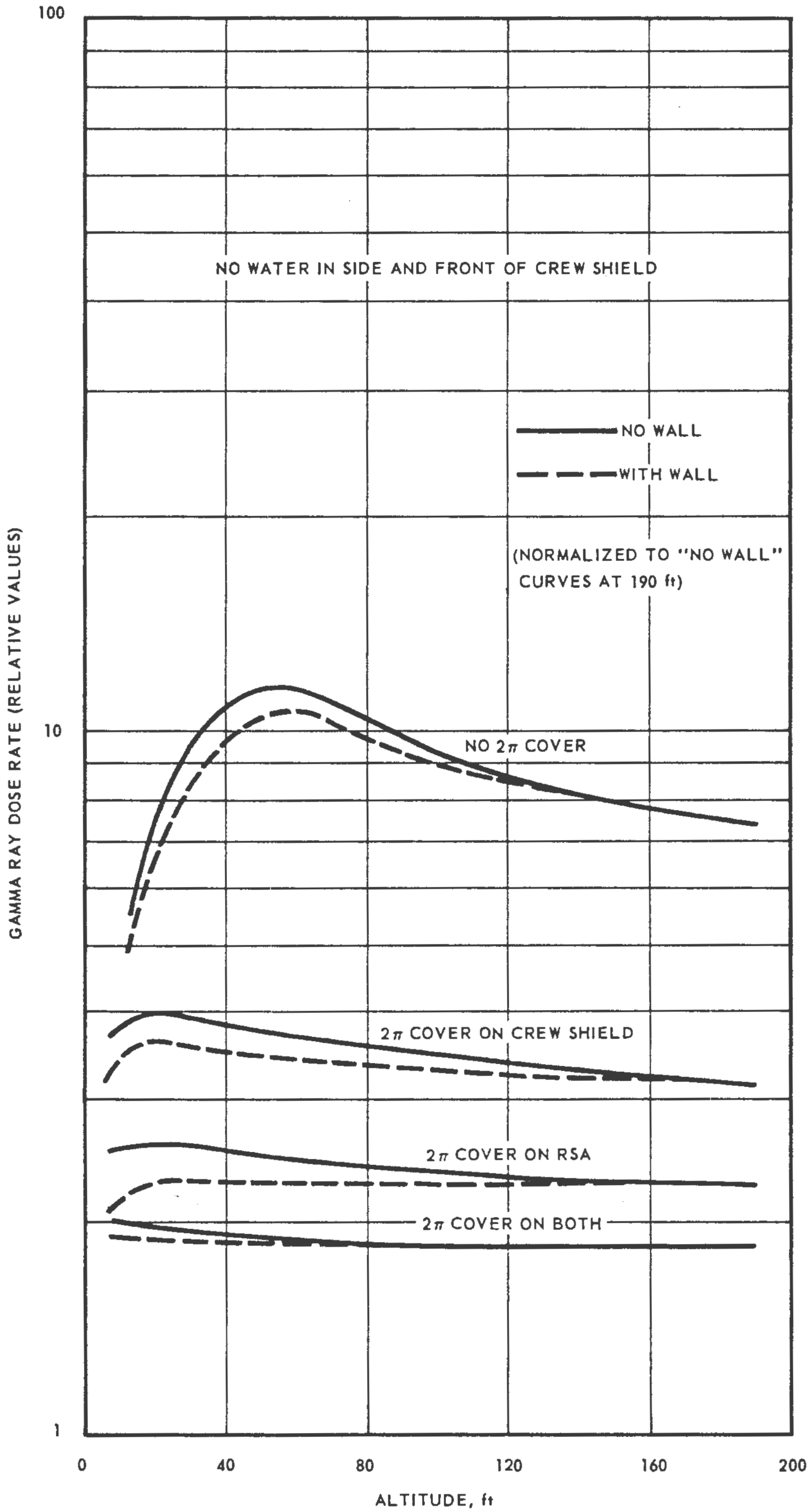

Fig. 66 – Shield No. 2 gamma dose rates as a function of altitude for different cover conditions

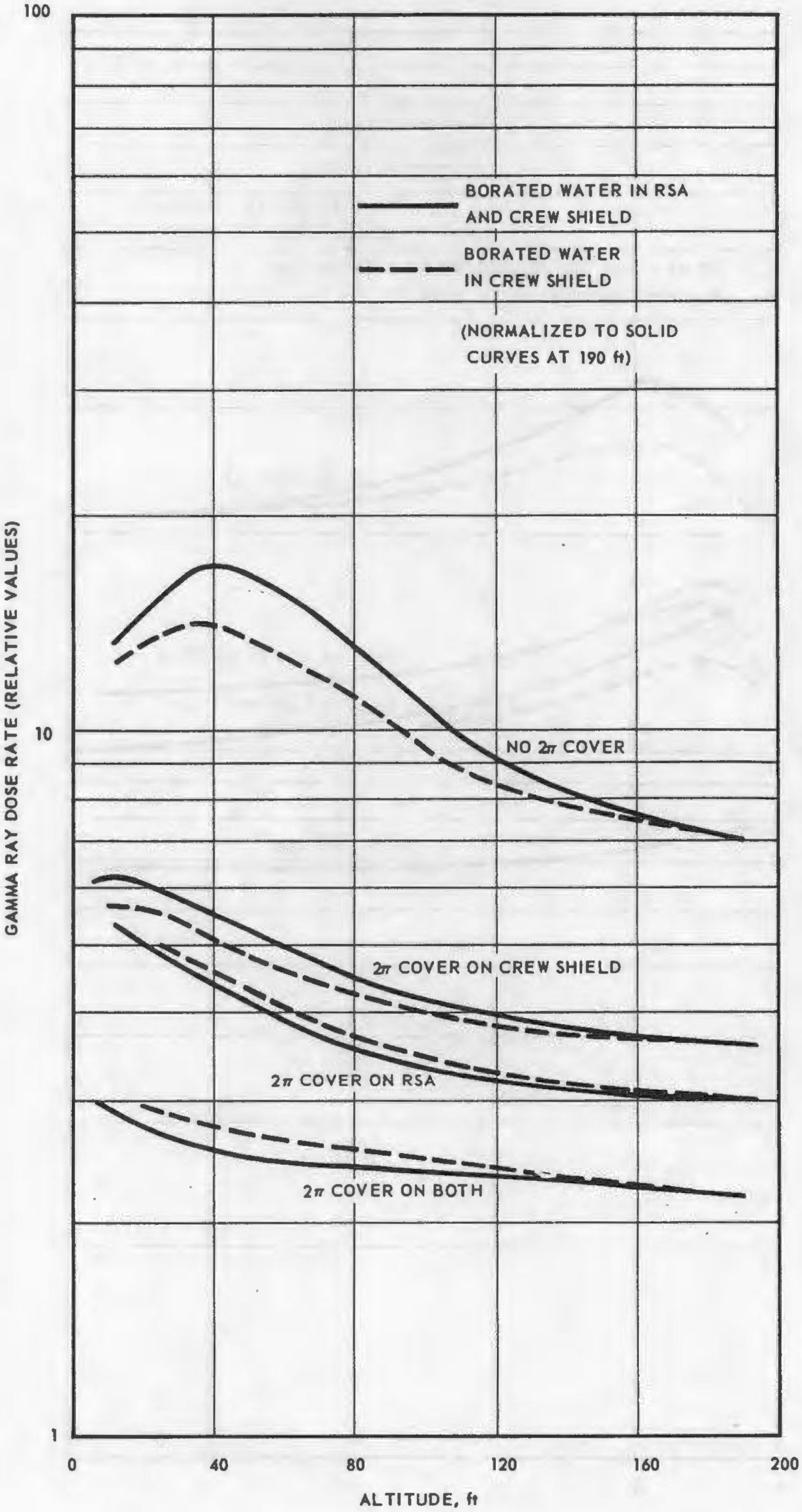

Fig. 67 – Shield No. 1 secondary gamma dose rate as a function of altitude for different cover conditions

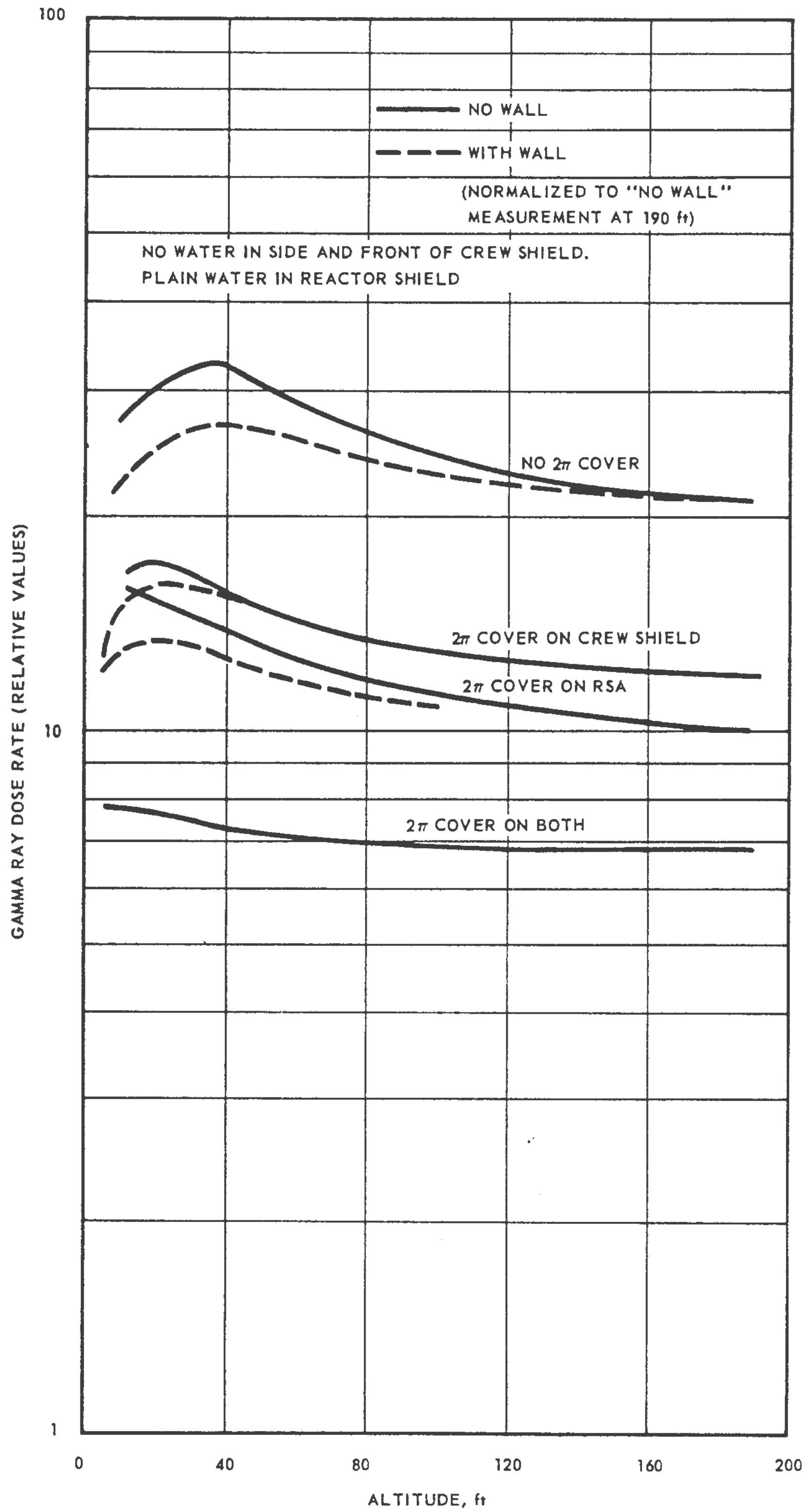

Fig. 68 – Shield No. 1 gamma dose rate as a function of altitude for varying cover conditions

in Figures 65 and 66. For both these types of radiation, the use of a 2π cover on the reactor shield yields a dose-rate curve which decreases monotonically with altitude, but with the ground-level value not more than 15 percent greater than the full-altitude value, which in turn is the same as the value at 100 feet, to within about 4 percent.

Measurements were made of secondary gamma rays under a wider variety of conditions than for any other variables. Fluxes of thermal neutrons were measured with a BF_3 counter under some of these conditions. In those cases where both types of measurements were made under identical conditions, the curves of secondary gamma dose rate as a function of altitude are very similar in shape to the curves of BF_3 response versus altitude. Figure 67 presents a number of the secondary gamma ray curves obtained with the crew shield side and front tanks filled with borated water, whereas Figure 68 presents similar data for the case where the crew shield side and front water tanks were empty.

When no 2π covers are used, the curves in question show a behavior somewhat similar to that obtained for primary gammas and fast neutrons, with the exception that the full-altitude measurements of secondaries or thermals is always considerably lower than the value observed at an altitude of 12 feet, whereas the opposite is true for the fast-neutron and primary-gamma-ray measurements.

The gross effects of 2π covers may be summarized by stating that the use of either cover results in a noticeable "flattening" of the curve in question, and that the effect is more pronounced when both covers are used; however, the use of both covers still does not reduce the apparent ground effect as much as does the reactor shield cover alone in the case of fast neutrons and primary gammas.

A number of secondary gamma measurements were made with the reactor shield 2π cover in place. The dose rate observed at an altitude of 12 feet is from 1.4 to 1.75 times that observed at full altitude, the lower figure applying to the condition of plain water in the crew shield and the higher to the borated-crew-shield condition. The corresponding dose rates at 100 feet were 1.06 to 1.13 times those observed at 195 feet, the maximum deviation from full-altitude values again occurring for the case of the borated crew shield.

As has been stated, the available thermal-neutron data exhibit much the same behavior with altitude and with the changing of 2π covers as do the corresponding data on secondary gamma rays.

Many of the altitude traverses were repeated with a shielding wall interposed midway between the reactor and crew shields. The wall was constructed of solid blocks of ordinary concrete; it was built 2 feet thick, 6 feet high (the height of the reactor-crew centerline when the reactor shield was resting on the ground), and 100 feet long.

The shapes of the curves obtained with the wall in place may be seen by inspection of the broken-line curves in Figures 65, 66, and 68. The normalization applied to these curves has already been described. The presence of the wall made no drastic change in the shapes of the curves of dose rate versus altitude except when 2π covers were entirely absent, and then only in the case of the secondary-gamma dose rates.

The shield systems used in these experiments contained very heavy shadow shielding. The direct-beam penetration to the crew compartment was thus negligibly small for all types of radiation in all of the scheduled configurations tested. The great majority of the measurements, therefore, exhibit the characteristics of a system which, from the optimum-weight standpoint, is certainly over-shielded in the shadow region.

A few additional measurements were made in which the configuration 1 reactor shield was reversed in direction, leaving no shadow shielding between it and the crew shield, so that the total shadow shield thicknesses were merely those of the crew shield alone. It is probable that the over-all system thus composed is one at the lower limit of shadow-shielding thicknesses likely to be encountered in practice. Certainly, the radiation pattern from the reactor shield is nearly isotropic in the forward half-plane, and hence is at the opposite extreme from the heavily shadow-shielded case studied throughout most of the experiments.

The measurements made under this reversed-shield condition were of secondary gammas and fast and thermal neutrons, both with crew shield 2π cover and with no 2π covers. The curves so obtained in general exhibit less variation with altitude than do the corresponding curves for the "standard" condition (see Figure 69). It would appear that magnitudes of variation thus far quoted represent in general a set of extreme cases and that they would therefore apply conservatively to the scattered radiation reaching the crew shield from any reactor shield which has thus far been considered in the AC-110 family of designs. To establish such a generality with certainty would require a repetition of the main body of the experimental program under the reversed-shield condition. Nevertheless, in view of the results from the few measurements which were made, it is considered highly unlikely that such a repetition would uncover any strong dependence of the curve shapes upon reactor shield radiation pattern.

The analysis of the 2π experiments has progressed to the point at which the fast neutron dose rates measured inside the crew-shield mockup due to reactor shield No. 1 can be broken down into the following components:

1. Single air scattering from the air above the reactor (A).
2. Single air scattering from the air below the reactor (A').
3. Single scattering from the ground (G).
4. Double scattering due to any combination of 2 of the interactions listed above (AA', A'A, GA, and AG).
5. Direct-beam dose rate (Do).

In addition, it has been possible to calculate, within a reasonable limit, the shapes of typical curves of fast neutron dose rates as a function of altitude.

4.42 GENERAL SHIELD EXPERIMENTS

Lid Tank Experiments

The scheduled slab experiments on LiH-backed arrays of advanced shield materials have been brought essentially to completion at the ORNL Lid Tank Shielding Facility. Over 15 basic configurations were tested.

The main effort in the analysis of these experiments was placed upon understanding the gamma ray data (dose rates along the centerline) which have been received. This effort has resulted in a new gamma ray source spectrum which is more accurately based upon the nuclear reactions occurring in the source plate (fissions, fission product decays, U^{235}, U^{238}, and Al^{27} neutron captures) than is the previous one. In addition, the contributions to the measured gamma ray dose rates from (n, γ) reactions occurring outside the source plate are being taken into account. The resulting calculated gamma ray dose rates agree with the measured ones as well as those calculated previously for configurations A, B, and C (one or more slabs of nonhydrogenous material backed by 1, 2, or 3 feet of lithium hydride, respectively); all measurements were taken in oil behind the lithium hydride. The calculated gamma ray dose rates, obtained using the new spectrum,

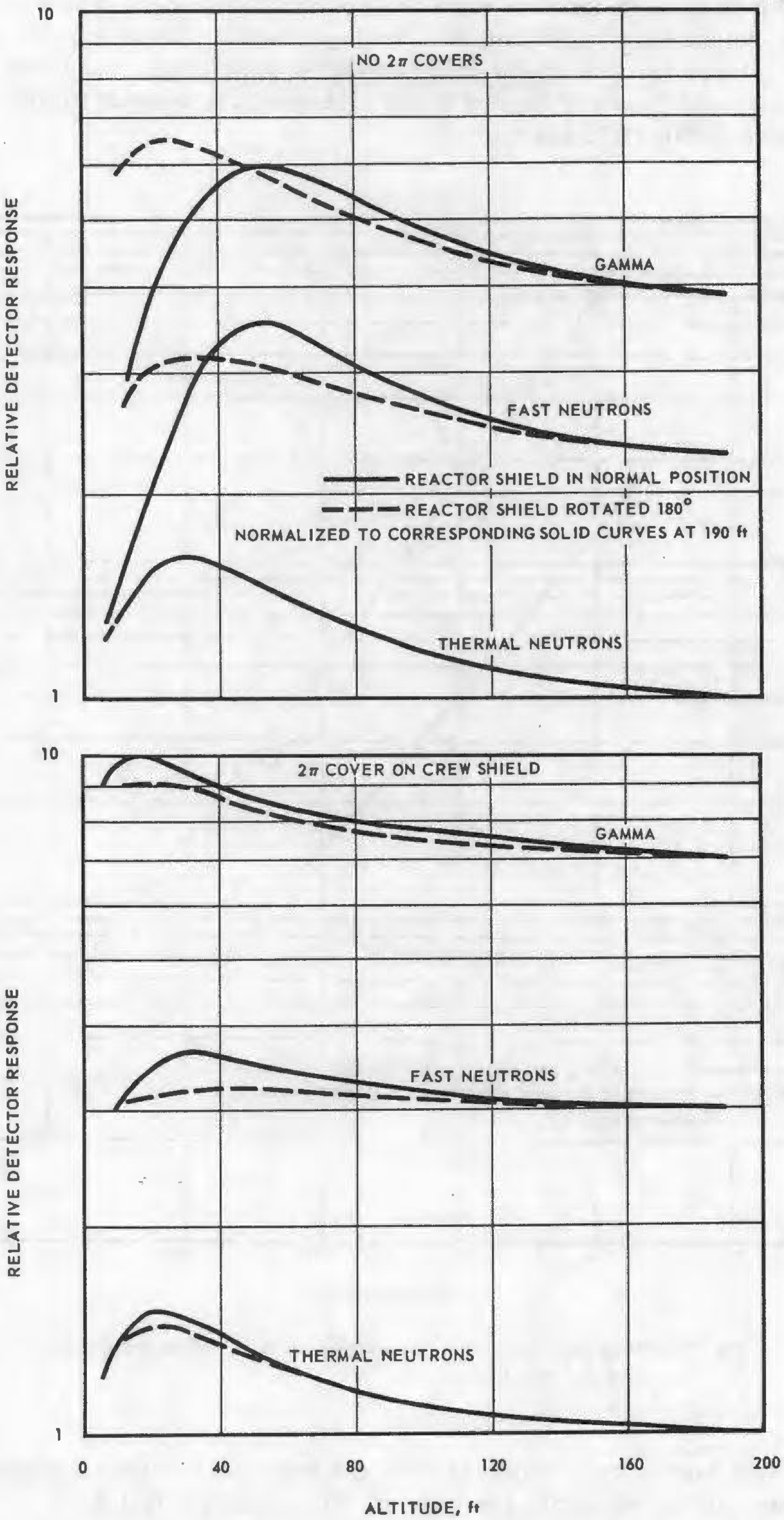

Fig. 69 — Effect of reactor shield assembly No. 1 shadow shield on dose rate as a function of altitude for three types of radiation

agree with the measured dose rates much better than the previously calculated ones for configuration D (one or more slabs of nonhydrogenous material backed by oil). For configuration D the gamma rays originating from hydrogen capture of neutrons are responsible for a reasonably large fraction of the total measured dose rates, and these are being considered as a second "source" located in the oil beyond the nonhydrogenous material. The results shown in Figure 70 are typical.

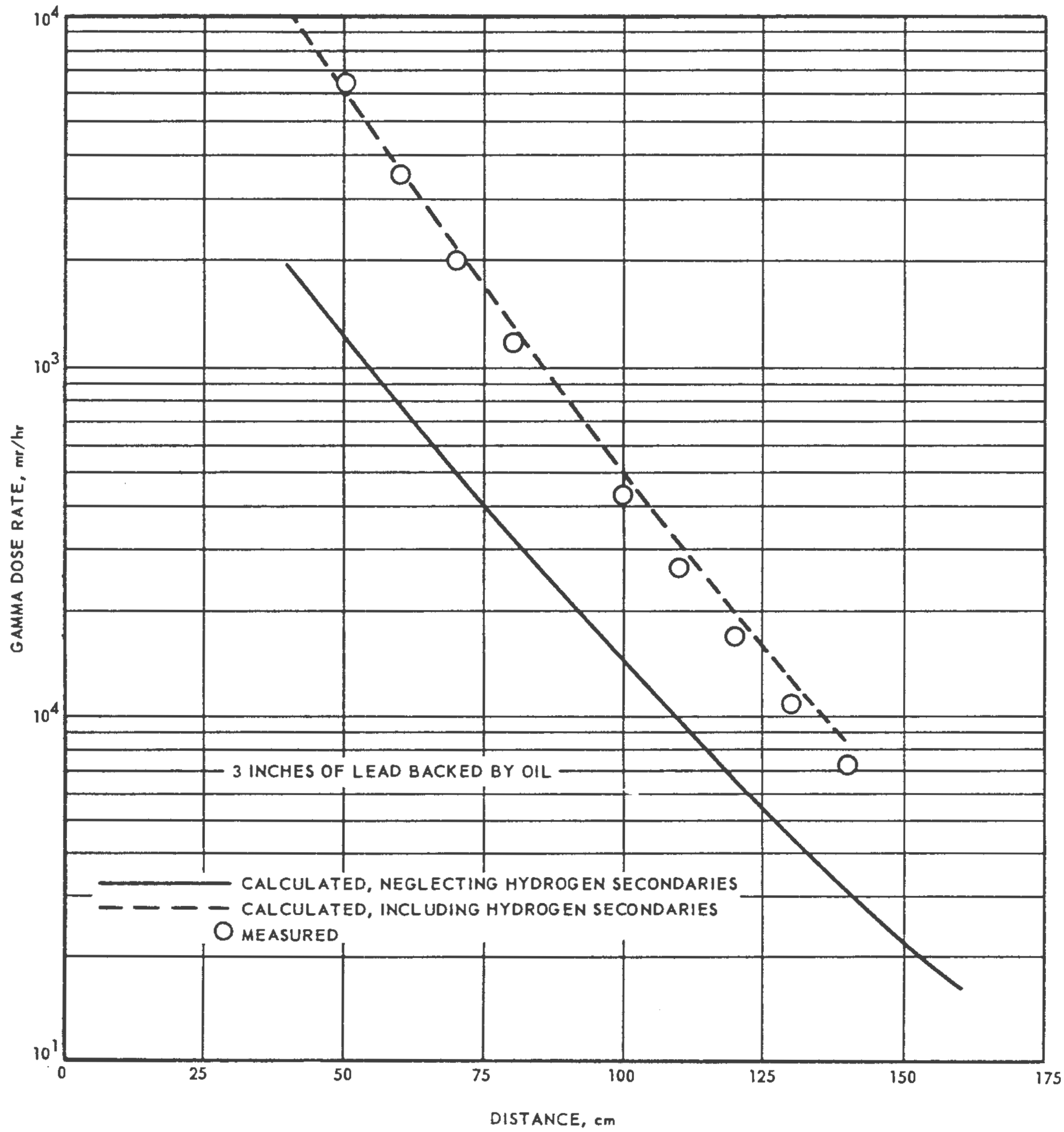

Fig. 70 – Comparison of measured gamma dose rates in lid tank experiment with calculated dose rates

The experiments with slabs of stainless steel and Hevimet (an alloy of tungsten, nickel, and copper) were carried out during the quarter. The measured fast neutron dose rates agree well (within a factor of 1.8 for all points measured) with the calculated ones. The gamma ray measurements indicate that secondary processes are present to an important degree. The calculated gamma ray dose rates available for comparison with the measurements were those which were calculated using the previous spectrum and which neglected secondary gamma rays. The results of such a comparison were:

4 in. stainless steel + LiH	factor of ~ 2
4 in. Hevimet + LiH	factor of ~ 100
1 ft LiH + 4 in. Hevimet + LiH	factor of ~ 1.5

The above summary indicates that secondary gamma rays are very important for those cases in which the n/γ ratio in the Hevimet is high. It has not as yet been determined whether the secondary gamma rays are produced in the tungsten of the Hevimet or in the LiH can, immediately following the Hevimet. Further analysis is planned.

A3 Shielding Measurements

The analysis of the water centerline measurements on the A3 core has been refined to take into account more of the detailed structure of the core. This has resulted in an improved agreement between the calculated and measured dose rates.

4.5 CONTROLS AND INSTRUMENTATION

4.51 COMPONENT DEVELOPMENT

Efforts are being continued to provide electrical, electronic, and mechanical components capable of operation at 500°C and above at radiation levels equivalent to those encountered in the shield structure.

Electronic Subassemblies

An evaluation of base materials on which to mount components, circuit connections, and subassembly designs was made. The two most promising units investigated are:

1. A sheet-aluminum chassis, using terminal strips made of ceramic with nickel tie points, and using spot welding for connections.
2. A ceramic baseplate with either print wiring or overhead wiring, with connections made by wire wrap or spot welding.

A mockup of the modular subassembly design was constructed. The subassembly was designed for practical fabrication from ceramic materials.

Electron Tubes

Three electron tubes are being developed to operate at 600°C and to withstand up to 2×10^6 rep of neutrons or gammas.

Performance characteristics of two log diodes, received during the quarter, show that at 200°, 300°, and 600°C leakage resistance causes the plate-current versus plate-voltage characteristic curve to drop away leaving 5 decades of linearity at 200°C, and less at 300°C and 600°C. At 600°C the heater voltage is 3.5 volts, and at 300°C the heater voltage is 3.9 volts to correspond with the 4-volt value at room temperature.

The log diode terminals consist of 0.005-inch 305 stainless steel sheet wrapped around the titanium tap that projects from the tube, welded, and then brazed to the titanium. The stiffness as yet has not been adjusted to completely withstand vibration. Oxidation of this stainless steel is much lower than the oxidation of titanium at 600°C for 1000 hours. The Power Tube Department laboratory tests at 600°C for 1000 hours show 305 stainless steel to be excellent as compared with other stainless steels and with titanium. After this exposure the stainless steel is still apparently dulled very little by oxidation.

[redacted]

Capacitors

Electrolytic capacitors in the range of 1 - 20 microfarads are being developed for continuous operation at 500°C under nuclear radiation at voltage levels from 200 - 400 volts direct current. These units must also have the capacitance-to-volume ratios of conventional electrolytic capacitors.

The development program for such an electrolytic capacitor may be divided into the development of (1) a dielectric film-forming metal, (2) an electrolyte, and (3) an inert separator. These materials must be mutually compatible. Initial efforts have been aimed at obtaining up-to-date information regarding high-temperature electrolytes and dielectric film-forming metals.

Circuits

A high-temperature radiation-resistant version of the pulse preamplifier circuit is being developed. Electrical and mechanical design specifications and environmental test specifications have been made.

A single-stage pulse amplifier circuit was constructed using an aluminum chassis and ceramic terminal strips to provide a more rugged mounting of the components. The new circuit incorporates a single-crystal capacitor from the Electronic Laboratory. The circuit was tested successfully at room temperature.

Feasibility studies of transistorized reactor control equipment have proved encouraging enough to warrant placing contracts for transistorized circuitry. This equipment will be used for test and evaluation for future applications.

It is contemplated that transistors will be useful in such locations as the crew compartment or in other areas not subject to temperatures in excess of 125°C or integrated fluxes in excess of 10^{10} nvt.

A transistor version of a complete startup channel has been ordered for evaluation. This unit consists of a pulse amplifier, discriminator, log count rate computer circuit, differentiator, and period amplifier. It will also contain its own transistor power supply and transistor trip circuits, such as are ordinarily used in safety circuits.

Specifications were written for a nuclear battery reference and a variable gain modulator for an advanced magnetic amplifier system. Various vendors have been contacted for quotations on these components.

Motors and Alternators

Small motors and alternators capable of operating 500 hours in an ambient temperature of 500°C while exposed to nuclear radiation are being developed for control system application.

Ceramic Encapsulation - An initial investigation of vacuum firing conducted by the General Electric Research Laboratory has shown promise in reducing porosity and improving the penetration of ceramic-encapsulated stators wound with glass-served wire. The Fort Wayne Laboratory has now conducted similar trials on vacuum treatment and are arranging necessary equipment to perform vacuum firing.

Ceramic Core Bonding - A fixture has been built for ceramic core bonding, and about 12 inches of servomotor stator punchings have been made from B9E14B steel for further development.

Ceramic-Integral Ground System - Several modified turn-to-turn testers have been ceramic-integral insulated successfully demonstrating the feasibility of this type of insulation. A film-drawing die has been built for the servomotor stator.

[redacted]

800°F Insulation System Evaluation - All 75 modified turn-to-turn testers have been built and are ready for insulating, winding, and encapsulating. Eighteen glass-Micamat-glass insulated testers have been wound.

Motor Life Tests - The slipped-slot liner that caused a ground fault in motor No. 13 during the first room-temperature test was repaired, and this motor, wound with 0.0126-inch ceramic-coated Inconel clad copper wire was returned to life test. After operating approximately 20 minutes at 57-1/2 volts per phase, with no load, this motor failed. The failure was caused by shorted conductors in both phases. The degree of success with this type wire has been very low, and it is unlikely that it can be used in random-wound servomotors.

Pneumatic Actuators

Work is continuing on the development of pneumatic devices capable of being incorporated into high-speed and shim-type actuators and the power and position translation mechanisms required to produce adequate control.

Air Motors - Laboratory evaluation of the performance of four-, six-, and eight-vane air motors has been accomplished during this quarter.

A preliminary thermodynamic analysis of an ideal air motor has been completed, and upon completion of the mechanical analysis of an actual air motor, the thermodynamic and mechanical equations will be combined and programmed on the 704 digital computer. Air-motor designs can thus be obtained automatically from the computer for given design parameters.

Because of the high operating force associated with the four-way valve, a pneumatic amplifier is being developed to translate the rotary motion of the torque motor into linear motion and to amplify this motion. A mathematical analysis of the amplifier is being performed to supply information for designing an amplifier for any specific set of operating conditions.

An investigation was initiated to determine the feasibility of theoretically predicting damping coefficients in a pneumatic amplifier. It was shown that considerable simplifying assumptions were required to complete this analysis on schedule; an experimental technique for determining this coefficient is therefore being employed.

Air Cylinders - A feasibility study of a pneumatic cylinder as a position control was made. Positioning, regardless of load, was proved to be possible. The study showed that the cylinder could be positioned within 11/16 inch of any desired position over a 20-inch stroke.

Systems Panel Test

Three assemblies - a television camera, magnetic amplifiers, and electronic amplifiers - for the Systems Panel Test No. 2 at Convair were subjected to approximately 500 hours of reactor flux generated at reactor powers of 100 kilowatts and above. The total dose of all neutrons was approximately 1.2×10^{15} neutrons per square centimeter with approximately 9×10^{14} epicadmium neutrons per square centimeter. The gamma dose was about 4×10^{7} roentgens.

The most severely affected unit was the television camera. Postexposure examination showed that the lens, f:1.9 originally, was almost opaque. This alone would cause failure of the television system. There was further evidence of radiation effects in the physical appearance of a few components and some liquid leakage. The circuit stability was somewhat impaired and probably could be made tolerant to doses of 10^{15} nvt by component choice and good design.

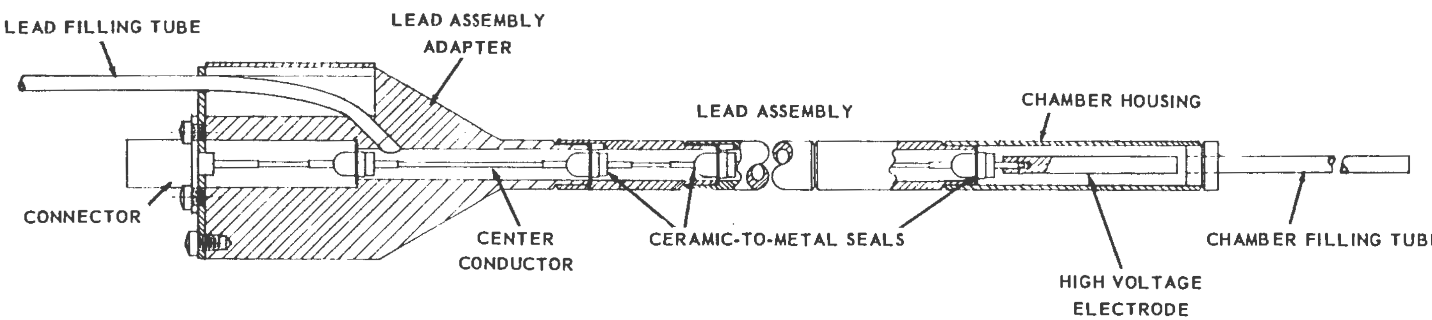

Fig. 71 – High-temperature fission chamber assembly

The GE-ANPD magnetic amplifier withstood the radiation dose it was supposed to tolerate and began to deteriorate. Calculations from a previous test showed the total dose was about 1.265×10^{13} nvt epicadmium when a 25 percent decrease in output was noted. These data correlate well with other information predicting failure after exposure to 10^{12} nvt fast for silicon diodes. The GE-ANPD magnetic amplifier contained six 1N338 silicon diodes, all of which exhibited drastically changed resistances.

The other two magnetic amplifiers, which used selenium diodes, showed very little change throughout the experiment. One unit was a commercial Vickers, and the second was fabricated by GEL for high radiation-damage resistance.

The electronic amplifiers exhibited no effect until shortly before the end of the test, when one of the tubes failed. Examination revealed the presence of gas in the tube that failed and in most of the other tubes.

4.52 SENSOR DEVELOPMENT

A developmental fission chamber, shown in Figure 71, was successfully operated at elevated temperatures. Counting rates were initially recorded as functions of chamber ambient temperature and pulse-height-discriminator settings. Figure 72 shows the counting rates as a function of pulse-height-selector setting for noise pulses, noise pulses plus alpha-induced pulses, and noise pulses plus alpha pulses plus fission-fragment-induced pulses, while operating at approximately 20°C. All data were automatically taken and recorded in digital form. Figure 73 shows typical graphs of chamber counting rate as a function of temperature during the first experiment having chamber temperature as a variable. It should be noted that the neutron flux may be considered constant for any single experiment, but may be different in different experiments. Therefore, absolute counting rates obtained during different experiments should not be compared. In general the data obtained were reasonably consistent and promising.

The second experiment in which the chamber counting rate was recorded as a function of temperature extended the range of operation to 580°C, as shown in Figure 74. Again it was noted that at a few points the data deviated from that expected because of statistical variations and equipment drift. However, the data as a whole appear promising. The results of an experiment to determine the counting rate as a function of time with the chamber operating at 550°C are shown in Figure 75. The results are satisfactory except for an apparent downward drift in counting rate during initial operation, most of which is probably due to a decrease in the gain of the cathode-follower output tube in the preamplifier. This experiment continued for approximately 200 hours, at which time the fission chamber and the furnace heating the chamber assembly apparently failed simultaneously. The chamber failure was probably caused when a brazed joint corroded and the hermetic seal was lost.

A considerable amount of work has been put into fabrication methods for the high-temperature chambers. The basic problem is that of obtaining hermetically sealed assemblies that are adequate for 700°C operation and that can be obtained without deleterious effects on the lead and the chamber-leakage resistances. Nickel and stainless steel parts were successfully brazed in an induction heater in a hydrogen atmosphere. In attempts to braze stainless steel lead segments to ceramic-to-metal seals with nickel flanges best results were obtained using a furnace rather than an induction heater. Hermetic welds were achieved by heliarc welding of stainless steel and nickel pieces, but insulator contamination also resulted. In the efforts to overcome the insulator contamination by maintaining argon gas pressures inside the assembly it was not possible to obtain hermetic

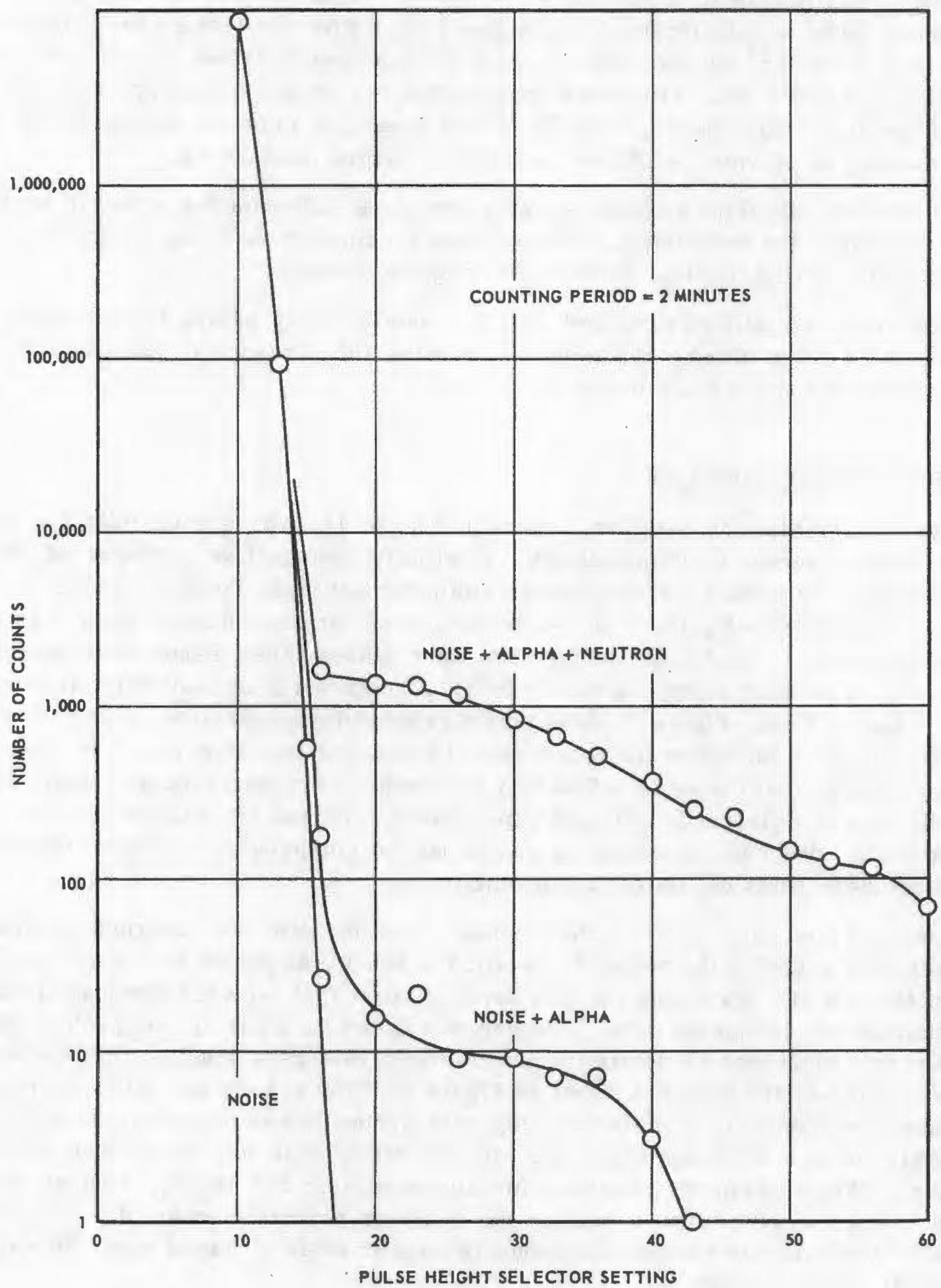

Fig. 72 – Counting rate versus pulse-height-selector setting

welds. After further development to determine optimum argon gas pressures, hermetic welds should be achieved without insulator contamination.

In development of a high-temperature ionization chamber the immediate need is for a power level sensor to operate from 1 percent to 200 percent of full power in a minimum ambient temperature of 350°C. Present designs will be limited to uncompensated ionization chambers. If compensation is necessary it can be achieved by subtracting the signals obtained from alternate neutron-sensitive and neutron-insensitive chambers. Fission chamber data indicate that ambient temperatures up to 580°C do not noticeably change the

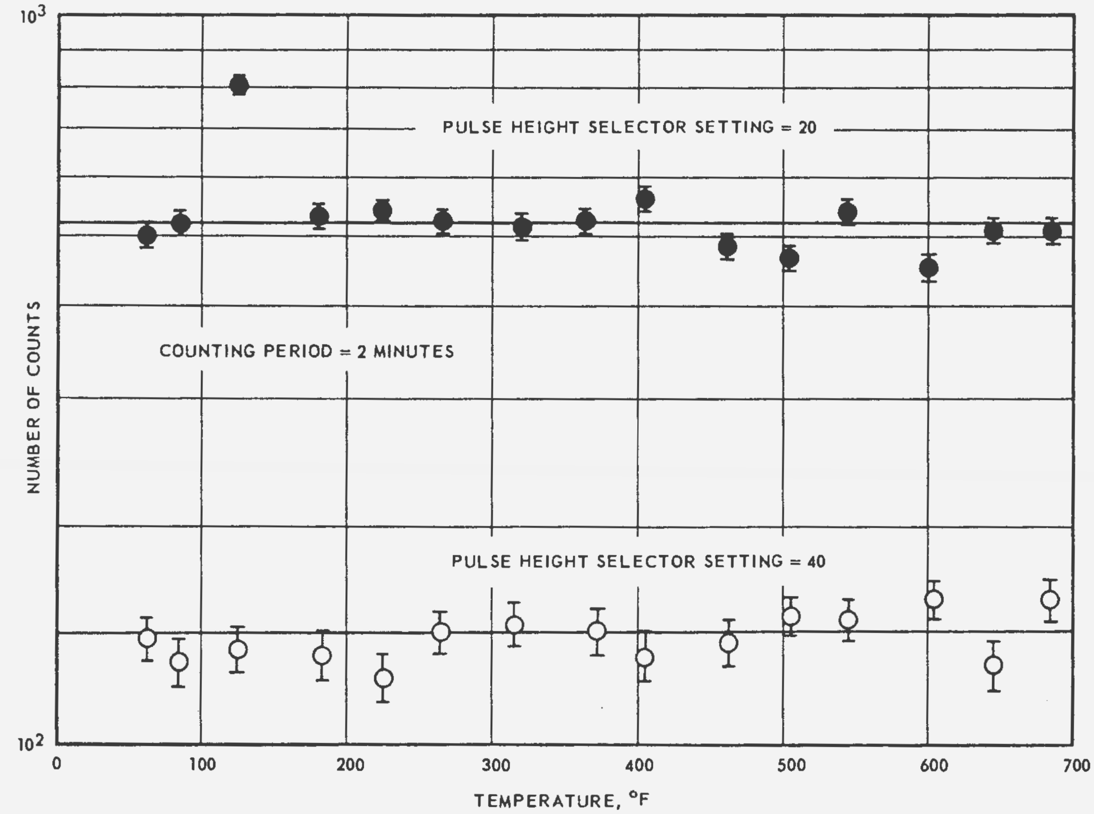

Fig. 73 – Counting rate versus temperature for high-temperature fission chamber.

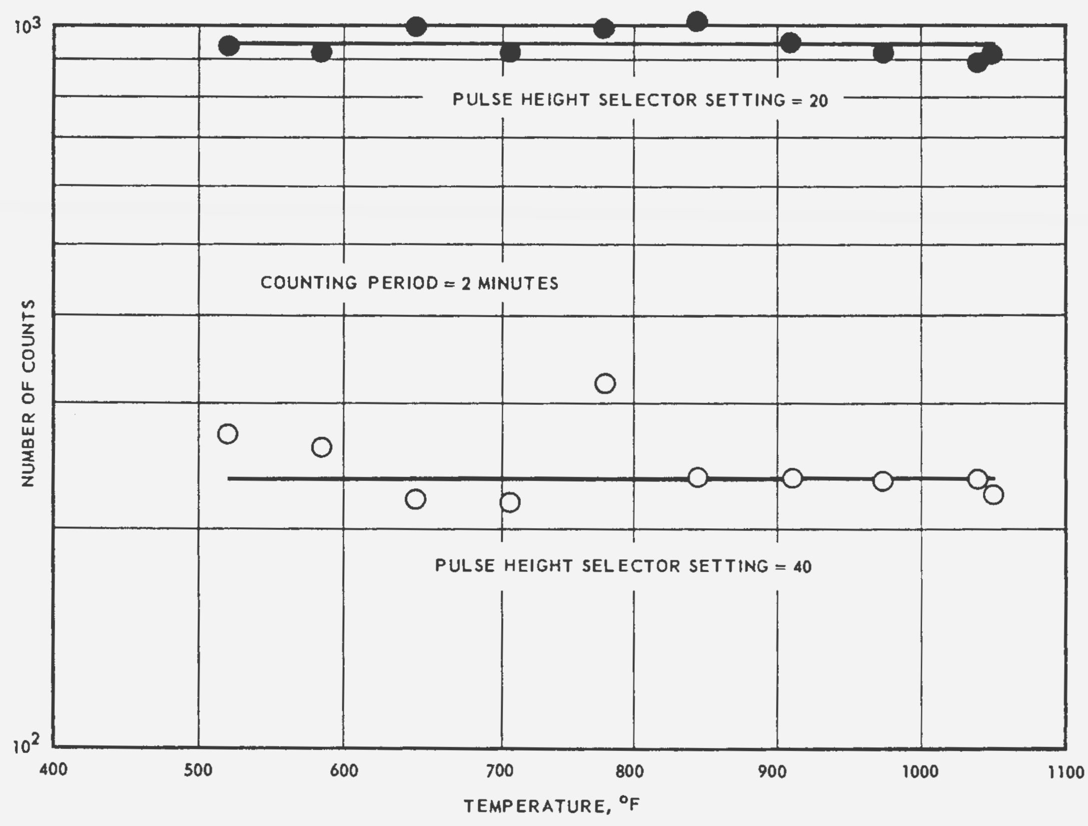

Fig. 74 – Counting rate versus temperature for high-temperature fission chamber

energy spent to form an ion pair. The only major effect of temperature observed in initial experiments was the expected increased leakage current. Two conceptual designs involving the chamber guard system and ceramic-to-metal seal assemblies have been submitted to component manufacturers for evaluation of fabrication problems.

Studies have begun on the development of alternating current ionization chambers. The current produced by the usual type of ionization chamber is normally very low for the neutron fluxes to be measured, and the amplification of these low currents with the desired accuracy and stability involves equipment whose size, weight, and complexity are undesirable for use in aircraft. Because of the comparative ease of amplifying a low-level

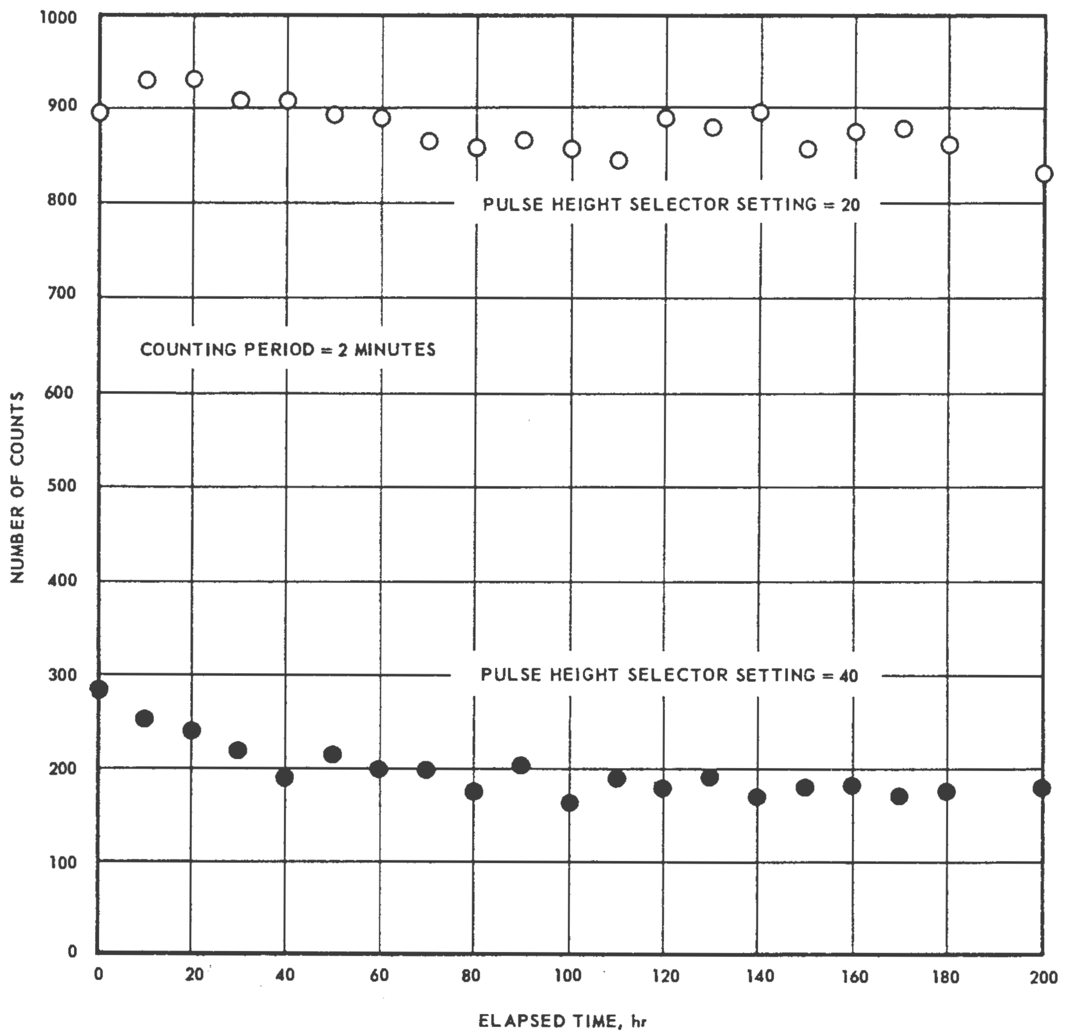

Fig. 75 – Counting rate versus time at 1000°F for high-temperature fission chamber

a-c signal with precision and accuracy, it would be desirable to build an ionization chamber whose output current is an a-c signal with amplitude proportional to the incident radiation flux level. Several possible designs for such a chamber have been studied. Modulating the electrons produced by the alpha ionization seems to be the only promising non-mechanical means of producing the a-c signal, and several devices have been proposed to accomplish this. Three have passed the conceptual design state, and one device is under construction.

4.6 POWER PLANT COMPONENT MECHANICAL DEVELOPMENT STUDIES

4.61 EXPERIMENTAL STRESS ANALYSIS

General planning concerning the experimental measurement of the thermal stresses in a tube-sheet design subjected to a given radial temperature gradient has been completed. The idea of using a mild-steel model to perform this program has been discarded in favor of a one-half-scale Inconel X model. Drawings and preparations for fabricating the model tube sheet have been completed, and work should start in the immediate future. It is estimated that approximately 200 channels of thermocouple and strain-gage information will be recorded in the tests. The temperatures to which the tube sheet will be subjected will be about 900°F, the upper temperature limit of static strain-gage measurements. This temperature limit is a function of gage stability and zero drift at elevated temperatures.

A vibration program with two primary aims, to test components environmentally and to test structures for vibratory stresses, is in progress. Familiarization training and checkout of equipment is currently under way. Although the Calidyne shaker has not always performed satisfactorily, it should be available for test work in the early part of the next quarter. Currently scheduled are life tests on a shim rod actuator and a multiposition selector valve.

The General Engineering Laboratory has been contacted on the over-all program and will be invited to participate at a later date. Other groups have been contacted to supply test specimens.

4.62 THERMAL INSULATION

2000°F High-Density-Insulation Test

At the completion of a 100-hour endurance test on the 2000°F insulation test tank, the decision was made to run the insulation test to the point of failure. During the quarter a total running time of 350 hours was accumulated at 2000°F and Mach 0.35. Inspection showed an increase in the buckling of the hot cover sheets around the fastening devices and along the seams between individual pads. Four of the 72 weld pins failed. Figure 76 shows the interior of the test tank after 300 hours of operation.

During the next quarter, the 2000°F pad insulation will be operated until the unit has reached complete failure.

Some data have been accumulated on the thermal conductivity of the high-density insulation used in this test tank. The sample tested has a density of 20 lb/ft^3. The thermal conductivity was 0.4 $Btu\text{-}in/ft^2\text{-}hr\text{-}^\circ F$ at 1000°F mean temperature.

Corrugated-Liner Insulation Design

The failure that occurred in the transition piece in the nose of the corrugated insulation liner has been thoroughly explained by stress analysis. The stress level on the 90-degree-bend transition piece was 16,894 psi. A redesign of the nose piece, so that the 90-degree bend in the transition piece is changed to a smaller angle, brings the stress level to within safe limits. This change in the transition piece is now being incorporated in the corrugated liner. Completion of this redesign and fabrication should be complete by the middle of the next quarter, and a 100-hour endurance test on this unit should be complete at the end of next quarter.

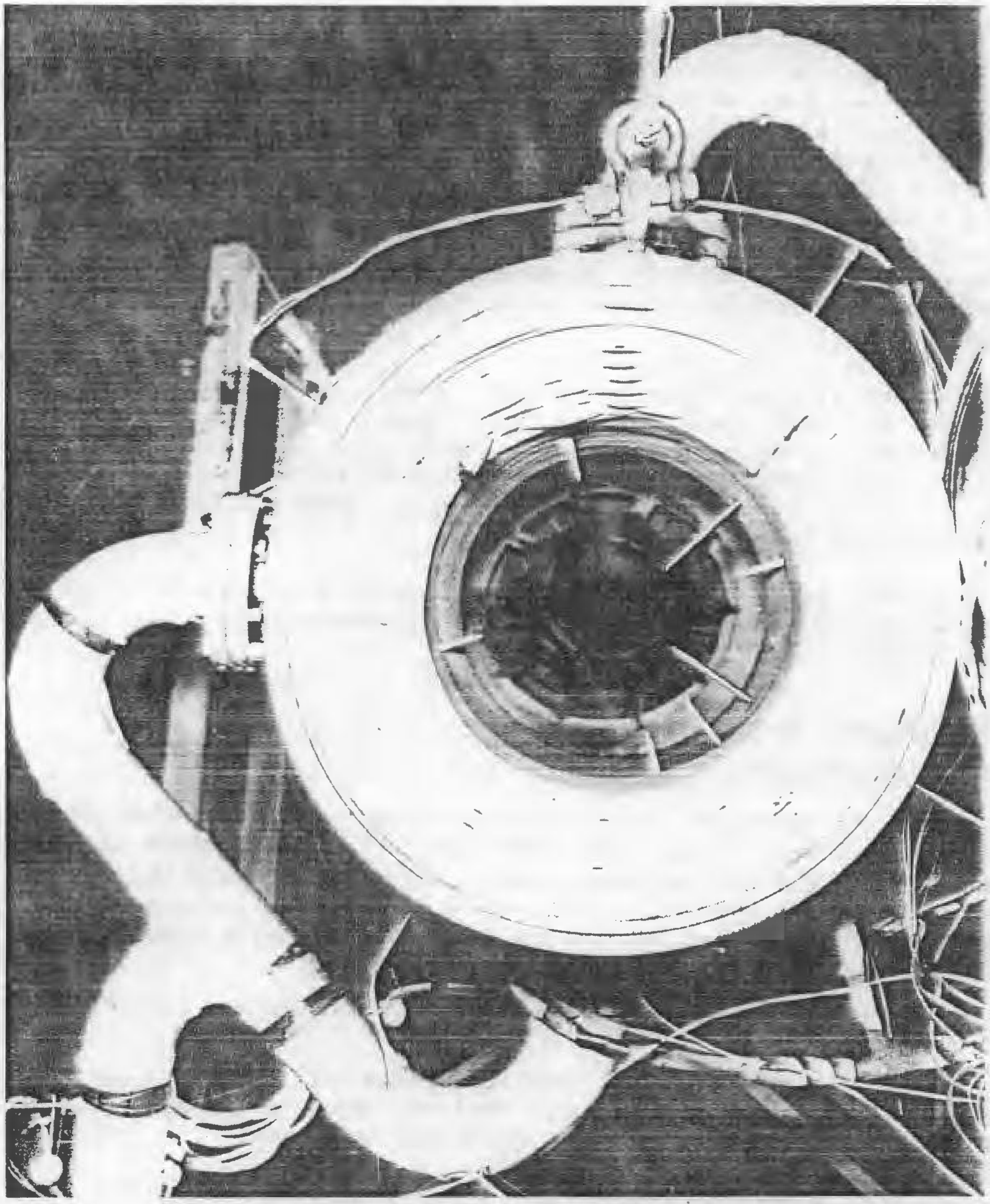

Fig. 76 – Interior of insulation test tank after 300 hours of operation

[redacted]

4.63 HIGH-TEMPERATURE BEARINGS AND LUBRICANTS

Bearings

Several screening tests on graphite - Ductile Ni-Resist No. 2 combinations were performed in a bearing test rig under various controlled temperature, speed, and load conditions. The results obtained in these tests indicate that a substantial increase in 56 HT grade graphite bearing life can be attained by decreasing the operating temperature from 1000°F to 750°F.

Preliminary tests were run at the General Engineering Laboratory on various plated coatings for Inconel X sliding against Inconel X. The following were tested at 1600°F: barium, cadmium, chromium, iron, nickel, silicon oxide, and silver. In addition, silver and chromic oxide were also tested as powders. The results indicated that only silver and nickel gave any significant improvement over Inconel X. The coefficient of friction with silver plate was initially 0.15, and then rose to the value obtained for Inconel X alone.

Screening tests were performed at 1300°F with porous stainless steel and porous Inconel impregnated with Cu_2O, PbO, CdO, and Be_2O_3. These test results indicate that all materials tested reduced wear and surface damage as compared to the porous material alone. The coefficient of friction was reduced for porous Inconel with PbO and Be_2O_3, and for porous stainless steel with Be_2O_3.

The same work was done with compresses using MgO and Cu_2O as the matrix and silver as the lubricant.

The Cu_2O compresses were too soft at 1600°F, and deformed under load.

Although the MgO-Ag mixture reduced the wear more than silver alone, the desired low friction was not obtained.

Tests were also run using WC-Ag and WC-Cu specimens that were obtained commercially. The WC-Ag compress had a coefficient of friction of 0.16 at 1000°F, but the value was higher at lower temperatures. The WC-Cu sample had high friction and showed little promise.

Lubricants

An experimental survey has been completed at GEL to determine the feasibility of using pretreated ball bearings in conjunction with a silane lubricant. All runs were made at a speed of 1800 rpm with thrust loads of 30 and 40 pounds. Triphenyl p-biphenylyl silane was used as the silane lubricant in this investigation. In the preliminary runs at 700°F, using untreated 52100 steel KP-4 bearings with the silane, it was found that friction was very high at the beginning of the test and decreased gradually with time. For comparison purposes, runs were also made at 350°F with the silane and with MIL-L-7808 oil. In order to round out the data on the effect of pretreatments, the bearings were coated with five different treatments and were run dry. These bearings were run for thirty minutes at 350°F, then the temperature was raised to 700°F, and the run was continued until a total running time of 65 minutes had been accumulated.

The pretreated bearings were also run with the silane under the same conditions at 700°F. With the exception of Electrofilm coating, severe wear occurred in every case in both the above tests.

The most important results of these tests may be summed up as follows:

1. The silanes, while not as good as MIL-L-7808, are, nevertheless, fair lubricants for ball bearings over a wide temperature range.

[redacted]

2. Pretreatment of the bearing races does not appear to be desirable under the conditions of these tests.
3. Clearances and the resulting changes in contact angle between the balls and the races have a considerable effect on bearing wear.
4. For short-time operation (50 to 100 hours) at temperatures up to 700°F, 52100 steel bearings may be satisfactory if the bearings are run in carefully and if critical speeds and loads are not exceeded.

Shell four-ball tests were run at 500°F and 700°F with three chain-type polynuclear hydrocarbons, two cyclic siloxanes, and five silanes.

All three of the polynuclear hydrocarbons - Pentalene 290, isopropyl biphenyl, and isopropyl m-terphenyl - were excessively volatile at 700°F. The best lubricant in this class was the Pentalene 290.

Both hexaphenyl cyclotrisiloxane and octaphenyl cyclotetrasiloxane were extremely poor lubricants.

The 2-thienyltriphenylsilane showed a decided improvement over the corresponding silane without the thienyl group, but the wear scars were still prohibitively large.

The tris (p-chlorophenyl) n-tetradecylsilane was found to be a good lubricant, especially at a 50-kilogram load. However, heavy resinous deposits were noted at 700°F.

All three of the silanes tested; i. e., n-octadecyltrioctylsilane, n-octadecyltridecylsilane, and di (n-octadecyl) diphenylsilane, have at least one long-chain alkyl group bonded to the silicon. These were all found to be excellent lubricants under light loads at both 500°F and 700°F. However, their lubricating effectiveness was found to be both load and temperature dependent.

The addition of 3 percent tricresyl phosphate to di (n-octadecyl) diphenylsilane resulted in a decided improvement in the critical-load-carrying capacity of the lubricant.

4.7 HAZARDS STUDIES

An opportunity to measure the whole-body radiation dose and its distribution over the body was afforded during disassembly of one of the panels which was irradiated during Systems Panel Test No. 2 at Convair.

The panel to be disassembled contained a J47 engine fuel control system, a J47 engine gear case, and a J79 engine gear case, all with associated accessories. All components were assembled in an aluminum alloy structure enclosed with 1/8-inch-thick aluminum alloy cover plates. Access to the components is provided by removal of the plates. Figure 77 is a view of the opened package showing the gear case end.

The fast-neutron dose rate incident on this test stand was calculated to be 0.2 rep-hr^{-1}-watt^{-1}.* The test stand was exposed to approximately 1.35×10^8 watt-hours of radiation during the experiment. The total integrated dose incident on the test stand was calculated to be 2.7×10^7 rep. This is about 70 times greater than the integrated fast-neutron dose at 5 feet from the side of one power plant for a 40-hour mission.

Isodose measurements were taken at the vertical midpoint of the package, and the isodose curves are shown in Figure 78. These measurements, taken approximately two

*Since the neutron constraint is currently reported in units of rep-hr^{-1}, the comparisons of various neutron environments on induced activity will also be based, to be consistent, on the same units.

months after exposure, defined the radiation environment of the work area around the package.

Activity within the package was investigated at various points. Figure 77 shows the dose rates, measured in milliroentgens per hour, and the locations of the measurements. The data show that the activity varies radically in all directions, both inside and outside the package. The lube oil system was the most active source in the package. Shortly after

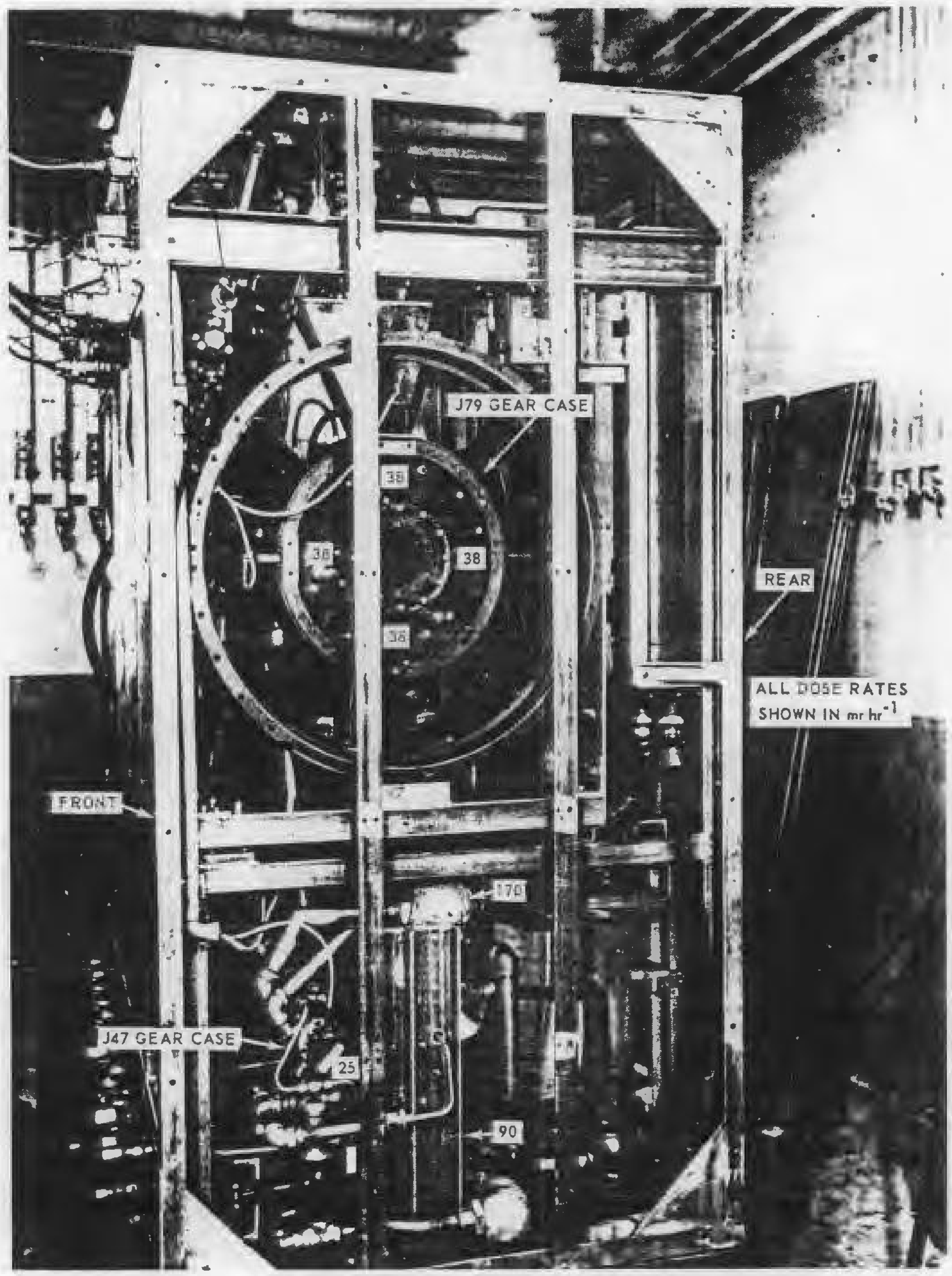

Fig. 77 – Dose rates, gear case end, for the hydraulic regulator control system and gear box and accessory test stand

[redacted]

CONFIDENTIAL

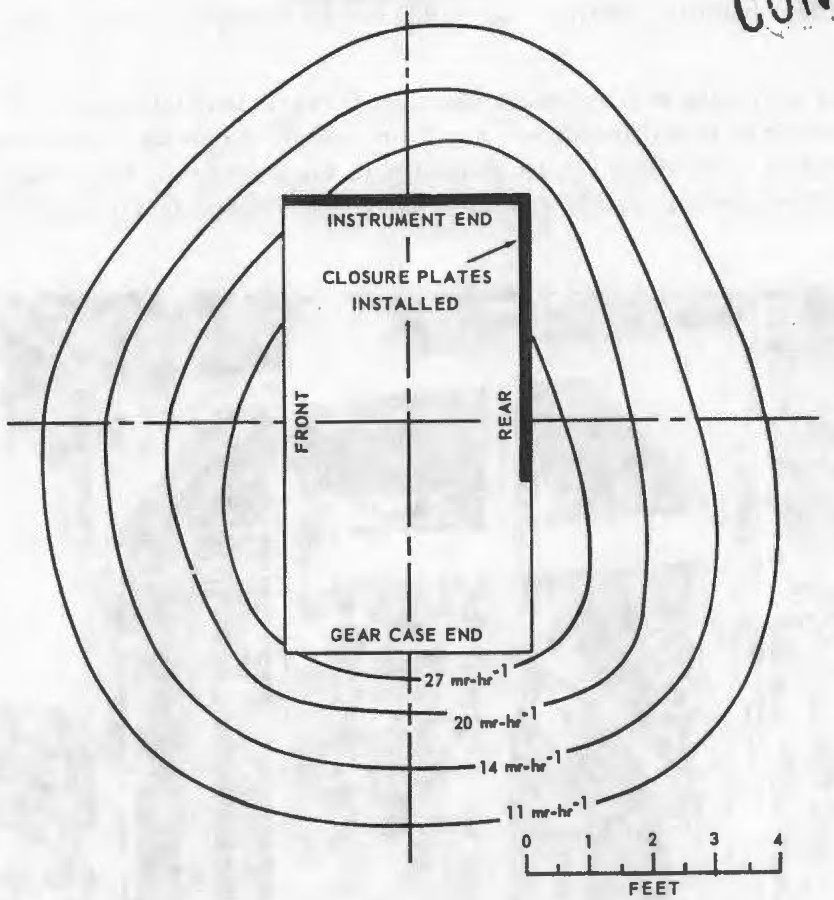

Fig. 78—Isodose curves about the hydraulic regulator control system, gear box, and accessory test stand

TABLE 8

BODY DOSES AND LOCATION

(1 hr 57 min Work Period)

Radiation monitor	Body Location	Measured Dose Worker No. 1	Measured Dose Worker No. 2
Film badge	Lower left trunk	0 mr beta 30 mr gamma	28 mr beta 0 mr gamma
Pocket chamber	Left chest	50 mr	50 mr
Finger ring film	Right hand	12 mr beta 28 mr gamma	0 mr beta 58 mr gamma
Finger ring film	Left hand	0 mr beta 28 mr gamma	0 mr beta 48 mr gamma
Pocket chamber	Right forearm	50 mr	
Pocket chamber	Left forearm	55 mr	
Pocket chamber	Mid front	40 mr	
Pocket chamber	Mid back	30 mr	
Pocket chamber	Right thigh	40 mr	
Pocket chamber	Left thigh	50 mr	

CONFIDENTIAL

[redacted]

irradiation a 3-r-per-hour dose rate was measured on the insulation covering the J79 lube oil filters. After several months a dose rate of 300 milliroentgens per hour was measured at the top of the lube oil filters. This was the highest dose rate found inside the package.

All work was performed within 2 to 3 feet of the package with the majority of the work performed at the package surface. Body penetration into the package was limited; it was impossible to gain full body entrance into the package.

Two men worked simultaneously on the package for 1 hour and 57 minutes. Both were equipped with protective clothing and various types of radiation monitors. The radiation field in the work area was thoroughly checked during and immediately after the disassembly work. The body doses received by the two workers and the monitoring equipment used are given in Table 8.

From the panel radiation measurements (Figure 78) a body dose of 50-60 milliroentgens could be predicted for an approximate 2-hour work period. From the measured doses it is apparent that this is a good estimate of the maximum possible dose, although the dose is not uniformly distributed over the body. It is possible to accumulate the least dose at the most unlikely location. Maximum possible doses are predictable when the radiation field is well known, but the distribution of dose is more difficult to define.

The immediate conclusion is that the whole body dose could be materially reduced by shielding localized hot spots with a lead blanket and by designating an order of work and procedure to be followed in order to take advantage of the shielding effect of low-activity-level components.

CONFIDENTIAL

CONFIDENTIAL

[redacted]

5. NEW TECHNICAL FACILITIES AND EQUIPMENT

Engineering Test Reactor (ETR)

It is expected that the Engineering Test Reactor will be completed late in the next quarter. At that time the prime contract expires and construction will be essentially complete. Operating personnel will then be responsible for completion of any remaining equipment checkouts and for normal reactor testing. It is estimated the reactor tests will extend two months from the date of completion. Experiment in-pile tubes will not be inserted into the reactor until such tests are completed. The first complete set of GE-ANPD in-pile tubes is scheduled to be delivered in the fall of 1957, and it is estimated that GE-ANPD samples will not be tested before October. The initial test program includes the following: one full-size HTRE No. 3 fuel cartridge in the 99 facility; one HTRE No. 3 moderator unit, one fuel cartridge or a combination fuel moderator assembly in the 66 facility; metallic Fe-Cr-Al - clad fuel samples, ceramic fuel samples and advanced solid moderator samples in the 33 facility.

Design of the experimental equipment is nearly complete. Orders have been placed for in-pile tubes, top cover plate, piping, control valves, block valves, orifice runs, filters, instrumentation and all injection water equipment except spray headers. Specifications have been completed on all other components except casks and shielding. Most of the pipe, fittings, and flanges have been received, and sections are now being welded in field shops.

The problem of top cap penetration was recently resolved. The operating contractor tentatively agreed that the three in-pile tubes could penetrate the reactor top cover on a trial basis. Early operations of the reactor will determine the extent of the sky-rights and refueling problems caused by penetrating the top cap. Momentum traps, which were intended to trap radioactive particles in the loop downstream from the sample, have been eliminated from the design.

High-Temperature Critical Experiment

Design and detailing of nearly all the basic solid moderator reactor structure for the high-temperature critical experiment facility was completed during the quarter. The structure assembly drawings are complete and many components are being fabricated. Parts for a checkout model of the proposed shim-scram actuators are fabricated so that assembly and test can occur in the near future. Components for the sensors to be used with the HOTCE control instrumentation are now being manufactured. A refinement in computations based on information gained in the operation of the HTRE No. 3 nuclear mockup has resulted in a minor change in the value of k as a function of fuel loading. If further checking confirms the new curve, a small increase in fuel loading may be required.

Ground Test Prototype Facility

An estimate of costs was prepared for converting the PUT Cell for chemically fueled testing of the ground test prototype power plant, and an outline of the test program objectives was developed.

[redacted]

[redacted]

The program envisions utilizing the converted cell for the following tests:

1. Tests of the shielding and X211 engine combination to demonstrate physical mating, structural integrity, and mechanical reliability of components.
2. Mechanical test of power-plant-mounted controls, accessories, and auxiliary systems to demonstrate functional suitability and environmental operating characteristics.
3. Instrument checkout of sensors, preamplifiers, insulation, etc., to demonstrate heat resistance, pressure sealing and vibration characteristics, and calibration requirements.
4. Testing of gas dynamics of shield plugs and shell to demonstrate full-scale airflow characteristics.
5. Tests of operational procedures to develop techniques for starting, for transfers between interburners and central heat source, and for shutdown and aftercooling.

2000°F Ducting Test Rig

The drawings for the 2000°F ducting loop were issued during the quarter, and fabrication is under way. Two phases of testing will be necessary with this ducting loop. The first phase will be a checkout of the loop with all of the water-jacketed, insulated, and water injection components installed. After a shakedown of the loop has been accomplished in this manner, the test component will be inserted and an endurance-type test conducted.

Because of the temperature limitation on the X39 engine, it will be necessary to use instream water injection to cool the combustion gases from 2000°F to 1400°F before the gases enter the engine. The design of this 1000-psig water-injection system has been completed and installation drawings will be issued during the quarter. All special components such as the high-pressure water pump and the pneumatically operated flow control valves are on hand.

[redacted]

[redacted]

6. APPENDIX

6.1 REPORTS ISSUED DURING THE QUARTER

APEX-290 - Administrative Report, January 27, 1957
APEX-291 - Reactor Controls Analysis
APEX-292 - Experimental Determination of the Reduction of Induced Activity in Metals
APEX-293 - Fast Neutron and Gamma Ray Point-Kernel Computer Program
APEX-294 - Reactor Thermodynamic Simulator
APEX-296 - Administrative Report, February 24, 1957
APEX-297 - Fabrication and Properties of Circular Fueled Wire

[redacted]